INCINERATION OF INDUSTRIAL ORGANIC WASTES IN A CIRCULATING FLUIDIZED BED COMBUSTOR

by

SIU CHING POLLY WONG

B.A.Sc. The University of British Columbia, 1990

A THESIS SUBMITTED IN PARTIAL FULFILLMENT OF THE REQUIREMENTS

FOR THE DEGREE OF MASTER OF APPLIED SCIENCE

in

THE FACULTY OF GRADUATE STUDIES

Department of Chemical Engineering

We accept this thesis as conforming

to the required standard

THE UNIVERSITY OF BRITISH COLUMBIA

November 1994

In presenting this thesis in partial fulfilment of the requirements for an advanced degree at the University of British Columbia, I agree that the Library shall make it freely available for reference and study. I further agree that permission for extensive copying of this thesis for scholarly purposes may be granted by the head of my department or by his or her representatives. It is understood that copying or publication of this thesis for financial gain shall not be allowed without my written permission.

Department of CHEMICAL ENGINEERING

The University of British Columbia
Vancouver, Canada

Date NOV. 21, 1994

DE-6 (2/88)

Abstract

The purpose of this study was to examine the feasibility of circulating fluidized bed incineration technology for solid organics wastes disposal. The study was divided into two parts: an applications study and a fundamental study. The applications study investigated the combustibility of selected industrial solid organic wastes and the effects of key operating parameters, i.e. temperature, excess air, primary-to-secondary air split ratio, suspension density and superficial gas velocity, on incineration performance of these wastes in a circulating fluidized bed incinerator. The fundamental study investigated the destruction of selected organics, i.e. chloroform and sulphur hexafluoride, as well as the hydrodynamic behaviour of gases and solids in the circulating fluidized bed incinerator. The incineration tests were carried out in the UBC pilot circulating fluidized bed combustor system.

Results from the applications study showed that increases in incineration temperature and in excess air tend to improve the combustion efficiency of the pilot CFB system, but tend to increase NO_X emissions. Increases in primary-to-secondary air split ratio, suspension density and superficial gas velocity tend to enhance the gas and solids mixing behaviour. As a result, combustion efficiency is improved while NO_X emissions are increased. The chemical nature, i.e. volatile, sulphur and ash contents, and the physical nature, i.e. particle size, of the wastes have a direct impact on their combustion behaviour and emissions. In general, the UBC pilot circulating fluidized bed combustor achieved high combustion efficiencies, in excess of 99.9 %, for the solid wastes, although high CO emissions were observed. CO emissions may be reduced by addition of an insulated afterchamber system to the pilot system. Limestone addition was effective for in-situ sulphur capture. Incineration of the solid wastes in general led to a substantial reduction in solids residue.

Results from the fundamental study showed that hydrodynamics within a circulating fluidized bed is very complex. Secondary air injection ports, baffles and reactor exit affect the hydrodynamic behaviour of solids and gases within the circulating fluidized bed. The UBC pilot circulating fluidized bed combustor system achieved destruction and removal efficiencies of essentially 100 % (at 870 ^{o}C) and 97.05 % (at 915 ^{o}C) for chloroform and sulphur hexafluoride respectively. The destruction of organics depends on both unimolecular and bimolecular reactions. Hence, the use of sulphur hexafluoride, a thermally stable compound, as a surrogate test burn compound results in a conservative prediction in the destruction efficiency of an incineration system. Thus, incineration temperature alone cannot ensure good combustion and destruction performance in an incinerator. The performance of an incineration system and its emissions are also affected by the nature of the wastes (chemical and physical) as well as by the operating conditions.

Table of Contents

Table of Contents (continued)

Table of Contents (continued)

List of Tables

List of Figures

List of Figures (continued)

List of Figures (continued)

Acknowledgments

There are many people who deserve thanks for helping me through this work. I would like to thank Dr. C. Brereton, Dr. J.R. Grace and Dr. C.J. Lim for their ideas, discussions, encouragement and support throughout this project. I am grateful to Mr. A. Mikkelsen, senior development engineer at Alcan Smelters and Chemicals Ltd., Kitimat, B.C., for his helpful discussions. I would also like to thank the people who made it possible for me to run the experiments, members of the UBC CFB group: Dr. C. Brereton, Dr. J. R. Grace, Dr. C.J. Lim, Dr. S. Julien, Dr. J. Chen, Dr. K.S. Lim, J. Muir, I. Hwang, W. Luan, F.L. Liu and L. Sung. I would like to thank the staff at the Chemical Engineering workshop and stores for their assistance. Finally, I would like to thank Alcan Smelters and Chemicals Limited, Kitimat, B.C. and the Natural Sciences and Engineering Research Council of Canada for their financial support.

1. INTRODUCTION

Industries generate vast quantities and a variety of wastes each year. These wastes may be in the form of sludges, metal wastes, chemical wastes, or organics. The wastes can occur in the forms of liquids, solids or slurries. Different disposal methods are needed for each different type or form of waste. Sludges, from primary wastewater treatment systems for example, are first dewatered and burned. Metal wastes, if in liquid or slurry form, are removed via chemical precipitation or pH adjustment. Solid forms of wastes contaminated with metals may be treated by stabilization/solidification processes in which the contaminants are chemically or physically encapsulated in the waste matrix. The matrix can be cement, lime or silicate based. The goal of stabilization/solidification processes is to reduce the leachable fraction of the waste, in particular, heavy metals in an ash, so that the waste matrix can be disposed of in a landfill [Exner, 1982]. The contaminants in the chemical wastes, depending on the nature of the wastes, can be removed by an extraction process, e.g. chemical precipitation or stabilization/solidification processes.

Organic wastes can be treated by biological treatment, land treatment or incineration. In biological treatment processes, the wastewater stream is brought into contact with a mixture of microorganisms which break down the organic contaminants in the waste stream. This treatment method is mainly applicable to aqueous media. The feed streams to processes such as activated sludge, aerated lagoon, trickling filter and waste stabilization ponds must be low in solids (< 1 %), free of oil and grease, and non-toxic to the active microorganisms (e.g. heavy metal content < 10 ppm) [Kiang and Metry, 1982]. The processes produce a biomass sludge which contains heavy metals and refractory organics not decomposed by the biologically active species present. Anaerobic digestion and composting processes are useful for more concentrated waste streams, tolerating solid contents of 5 to 7 % and 50 % respectively. Composting decomposes oils, greases and tars resulting in a concentrated metal

sludge and a leachate containing partially decomposed organics. However, halogenated aromatic hydrocarbons may inhibit the microbial population in the composting process [Kiang and Metry, 1982].

Land treatment relies on the dynamic physical, chemical, and biological processes occurring in the soil. Decomposition of waste constituents added to soil may occur by chemical reactions with the soil, as a result of biological degradation by soil microorganisms or as a result of photochemical degradation of organic wastes applied to surface soils. As a result, applied wastes are degraded, transformed to non detrimental by-products or immobilized. Land treatment technology can be applied to wastewaters, sludges, hazardous wastes and contaminated soils. With certain wastes, the total land requirement to treat these wastes may be very large and land treatment may not be an economic waste management alternative [Loehr and Malina Jr., 1986]. There is also concern with the transport and fate of the applied wastes in the ground, i.e. leaching and ground water contamination.

Incineration uses thermal decomposition via thermal oxidation at high temperatures (usually approx. 900 ^{o}C or greater) to destroy the organic fraction of the waste. Incineration technology is applicable to a wide variety of organic wastes of various physical forms. Combustible wastes or wastes with significant organic fraction are generally considered appropriate for incineration. The goal of incineration is to achieve complete destruction of organic constituents, which is related to, but not identical with, the complete combustion of the fuel and the combustible waste components. Incineration essentially destroys all hydrocarbon components, generating an ash residue. The need for further treatment of the resulting ash depends on the nature of the waste, in particular, the chemical composition and metal content. The volume reduction of the waste may be substantial for low ash and/or sulphur containing wastes. The focus of this thesis is to investigate circulating fluidized bed

(CFB) incineration as a potential treatment method for solid wastes having high organic contents.

1.1 Incineration

For good thermal destruction, the following parameters are important [Cheremisinoff, 1988] :

(1) Temperature - The temperature must be high enough to provide rapid pyrolysis and oxidation kinetics.

(2) Residence Time - There must be sufficient exposure of the waste to the high temperatures in the combustion chamber.

(3) Excess Air - The waste composition fixes the stoichiometric air requirements. Excess air is supplied to ensure adequate contact between waste and air and to enhance the kinetic reactions of the wastes.

(4) Turbulence - The degree of mixing between waste and air is important. Turbulence depends on the specific mechanical design of the incinerator as well as the air flow.

1.2 Incinerator Designs

There are four common incinerator designs which employ different combinations of the above parameters to achieve good thermal destruction. These are liquid injection incinerators, fixed hearth incinerators, rotary kiln incinerators and fluid bed incinerators, shown in Figures 1.1 to 1.4 respectively. Within each broad category there are many subdivisions. For example, fluid

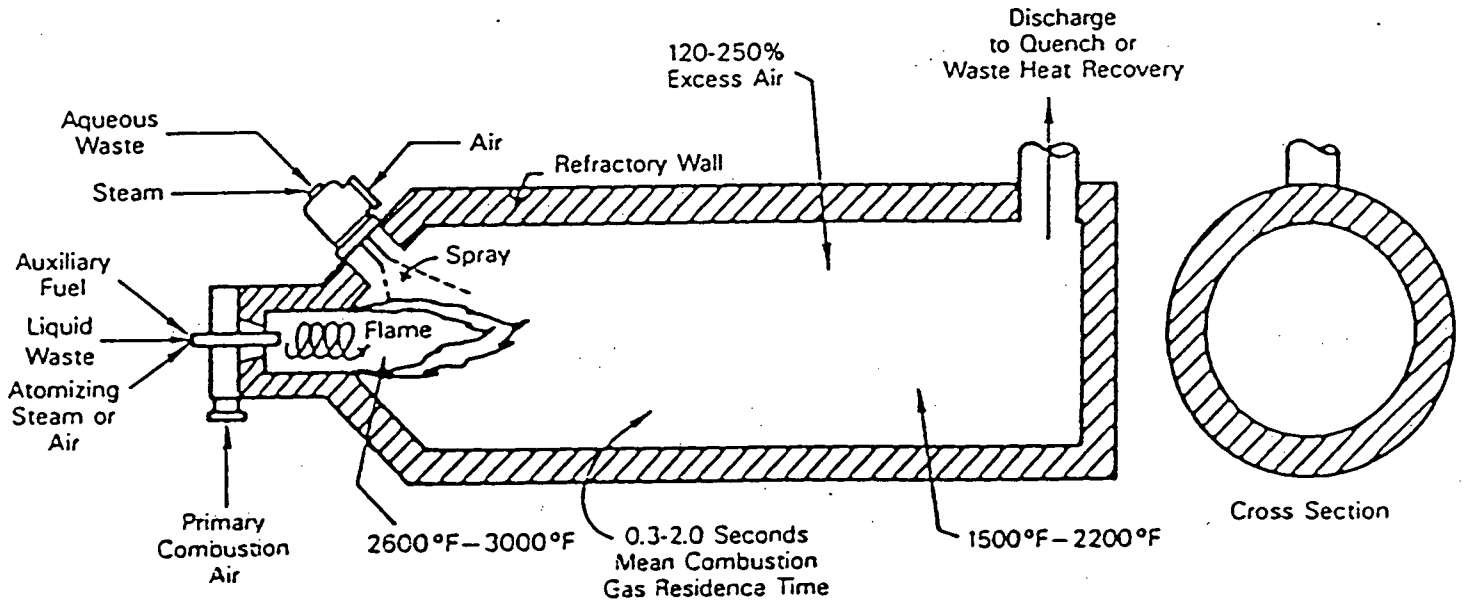

Figure 1.1 Liquid Injection Incineration System [Oppelt, 1987]

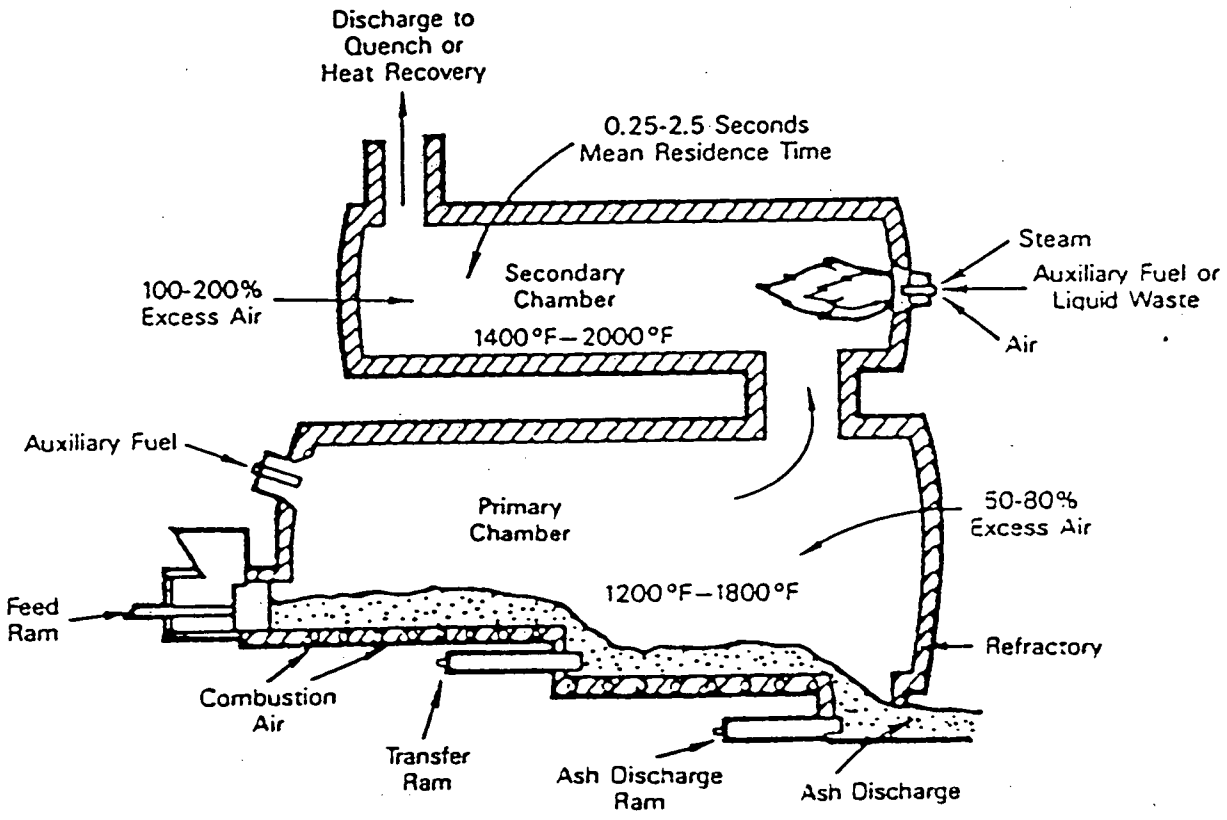

Figure 1.2 Fixed Hearth Incineration System [Oppelt, 1987]

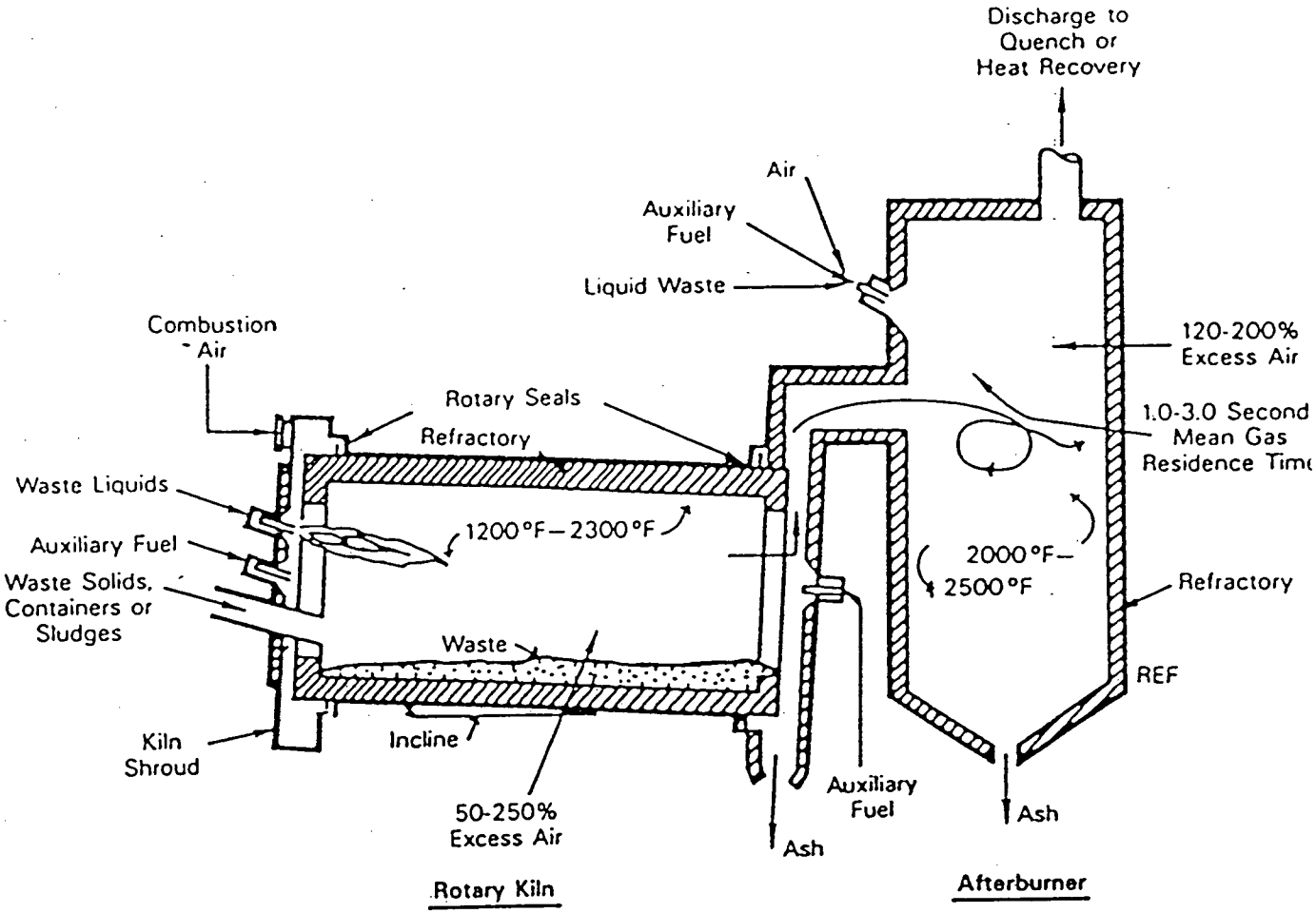

Figure 1.3 Rotary Kiln Incineration System [Oppelt, 1987]

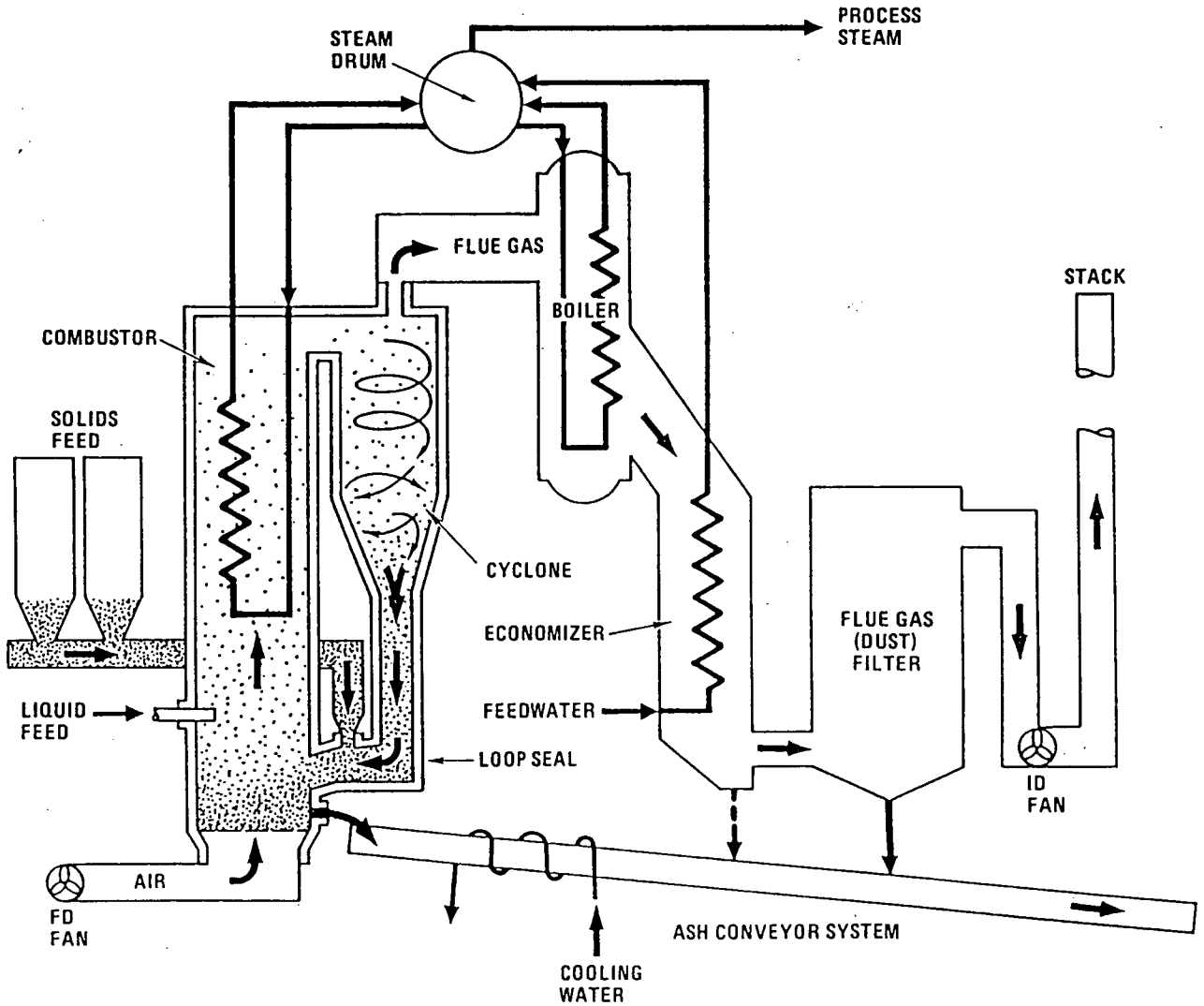

Figure 1.4 Circulating Fluidized Bed Incineration System
[Anderson and Wilbourn, 1989]

bed incinerators can be further categorized as bubbling bed or circulating fluidized bed incinerators. Which of the four major incineration systems is selected for a given application depends primarily on the form of the waste. Table 1.1 shows the applicability of incinerator types to wastes of various physical forms. The liquid injection and fixed hearth systems are limited in their ability to handle solids, slurries and sludges The feed flexibility of the rotary kiln and fluidized bed systems allows them to treat a broader variety of waste streams. Dempsey and Oppelt (1993) stated in their review of hazardous waste incineration that fluidized beds normally operate in the temperature range between 760 to 870 ^{o}C (1400 to 1600 ^{o}F); hence they excluded the applicability of fluidized bed incinerators to wastes containing halogenated aromatic compounds which require a minimum operating temperature of 1200 ^{o}C (2200 ^{o}F) for high degree of destruction (see Table 1.1). However, circulating fluidized bed incineration is applicable for treatment of polychlorinated biphenyl (PCB) contaminated soil (see section 2.1). Detailed descriptions of the rotary kiln and circulating fluidized bed are provided in the following sections.

1.2.1 Rotary Kiln

A rotary kiln is a cylindrical refractory-lined shell mounted on a slight incline (see Figure 1.3). Rotation of the shell transports the waste through the kiln while also enhancing mixing of the waste. The primary function of the kiln is to convert the combustible component of solid wastes to gases. This occurs through a series of volatilization, destructive distillation and partial combustion reactions. In many cases, the kiln operates in a pyrolysis mode. The waste is fed at one end and undergoes partial combustion reactions in the combustion chamber which operates at temperatures between 650 and 1260 ^{o}C. The residence time of waste solids in the kiln (generally 0.5 to 1.5 h) is controlled by the kiln rotation speed and the waste feed rate. The waste feed rate is also adjusted to limit the amount of waste being processed in the kiln to at most 20 % of the kiln volume.

Table 1.1 Applicability of Incinerator Types to Wastes of Various Physical Forms [Dempsey and Oppelt, 1993]

	Liquid Injection	Fixed Hearth	Rotary Kiln	Fluidized Bed
Solids:				
Granular, homogeneous		X	X	X
Irregular, bulky		X	X	
Low melting point (tar, etc.)	X	X	X	X
Organic compounds with fusible ash constituents		X	X	X
Unprepared, large, bulky material		X	X	
Gases:				
Organic vapour laden	X	X	X	X
Liquids:				
High organic strength aqueous wastes	X	X	X	X
Organic liquids	X	X	X	X
Solids/Liquids:				
Slurries			X	X
Aqueous organic sludge			X	X
Waste contains halogenated aromatic compounds (2200 ^{o}F min.)	X	X	X	

Flue gases leaving the kiln turn from a horizontal flow path upwards to the afterburner which may be oriented horizontally or vertically. An afterburner is needed to complete the gas phase combustion reactions. The temperature in the afterburner chamber is typically between 1090 and 1370 ^{o}C. Liquid waste can be fired through separate waste burners in the afterburner. Both the kiln and the afterburner are usually equipped with an auxiliary fuel firing system to bring the units up to and maintain the desired operating temperatures. Liquid waste streams

are sometimes fired into the afterburner as a temperature control measure [Dempsey and Oppelt, 1993].

1.2.2 Fluidized Bed - Circulating Fluidized Bed

A circulating fluidized bed is one type of fluidized bed system. When gas is passed upward through a bed of solid particles supported on a perforated plate, the gas pressure decreases across the bed. When the gas flow rate is increased sufficiently, the weight of the particles is supported by the flowing gas and the particles become fluidized. Further increases in the gas velocity lead to different regimes of fluidization as shown in Figure 1.5. The different fluidization regimes are described as [Grace, 1982] :

(a) Fixed Bed	- The particles are quiescent and gas flows through interstices.
(b) Expanded Bed	- Bed expands smoothly and there is some small scale particle motion.
(c) Bubbling	- The system behaves like a boiling liquid.
(d) Slugging	- Slugs of gas follow each other up the column with a regular frequency.
(e) Turbulent	- Darting tongues of gas and particles occur.
(f) Fast Fluidization	- Sheets of particles flow downwards at the wall, while there is dilute pneumatic conveying in the core; particles are transported out the top and must be replaced by adding solids at or near the bottom.

CFBs operate in the fast fluidization regime. They are distinct from conventional fluidized beds in that bubbling fluidized bed have a distinct upper bed surface and operate within a relatively narrow range of gas velocities typically from 0.5 to 2.5 m/s. In CFBs, higher gas velocities from 5 to 10 m/s are used and large fluxes of particles are transported out the top of the reactor. These particles are separated from the gas stream exiting the reactor by some

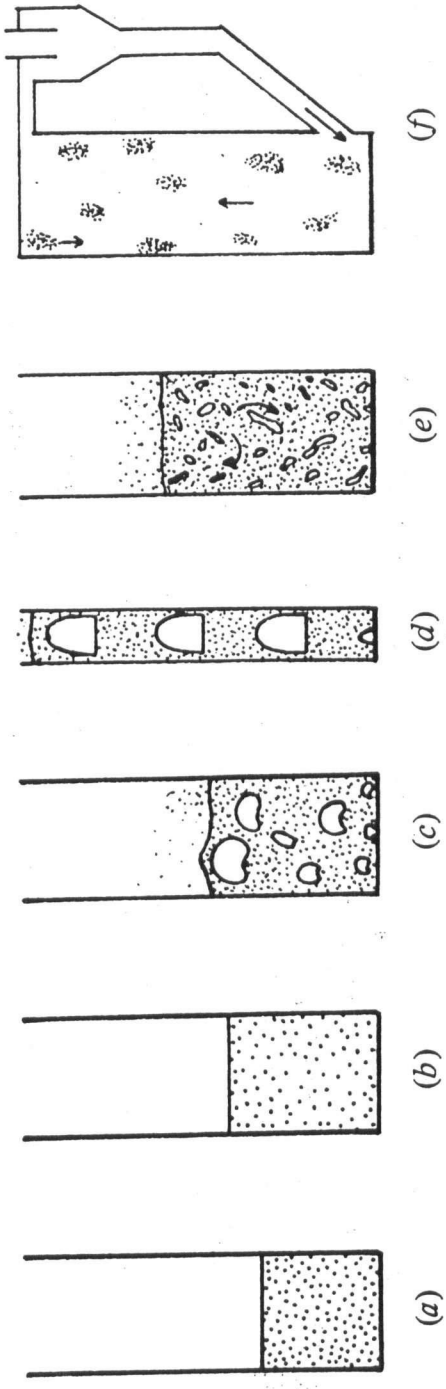

Figure 1.5 Fluidization Regimes [Grace, 1982]

form of separator and returned to the system, usually at the bottom of the reactor. In the core or centre section of the CFB riser, the gas stream, containing widely dispersed solids, moves upward while clusters or strands of particles move downward near the outer wall. There is no longer a clear interface between a dense bed and a more dilute freeboard region. Instead, there is a continuous, usually gradual decrease in solids content over most or all of the height of the riser.

A CFB incinerator is a refractory-lined combustion vessel (riser) partially filled with an inert bed material, usually sand, which acts as heat carrier in the system (see Figure 1.4). The combustible waste is fed into the bed together with the recirculated solids from the hot solids separator, usually a cyclone. Limestone can also be added with the waste for in-situ sulphur removal. High air velocities are used to transport both the bed material and the wastes through the reaction zone to the top of the combustion chamber and into the cyclone. The high gas velocities, high solids loading and internal solids flow patterns produce a high degree of solids circulation throughout the riser which quickly and uniformly mixes the waste and bed material. This gives the CFB the capability of using lower operating temperatures and lower excess air as compared to rotary kiln systems. The combination of lower temperatures and less excess air also leads to reduced NO_x emissions [Theodore and Reynolds, 1987]. The operating temperature in the CFB riser is usually between 800 and 1100 ^{o}C. The hot flue gas may be cooled before it enters the baghouse for particulate removal. The flue gas may then undergo further treatment for removal of other undesirable constituents from the gas stream prior to discharge through the stack. Ash can be removed periodically or continuously from the bottom of the reactor [Brunner, 1989].

Potential advantages of a CFB system over a rotary kiln include [Brunner, 1989]:

- a more compact design: less floor space but much taller
- fewer moving parts
- ability to handle viscous slurries without the need for atomization
- high combustion efficiency while operating at low temperatures (i.e. between 800 and 1100 ^{o}C)
- alleviation of slagging problems for some wastes due to lower combustion temperatures
- low NO_x emissions due to lower combustion temperature, reduced excess air requirements and staging of air injection
- ability to capture sulphur oxides in-situ using limestone or dolomite without the need for add-on scrubbers
- better control of excess air
- no need for expensive seals
- better heat transfer, useful if the incinerator is to act as a boiler

Potential disadvantages of a CFB system include:

- higher pressure drops over the system, requiring greater fan power
- less flexibility to handle future wastes which cannot be easily shredded to less than about 30 mm in maximum dimension and which contain large coarse inerts
- inability to operate in a slagging mode for wastes which are sticky at conventional temperatures, e.g. wastes which have high inorganic salt content and/or fusible ash content
- smaller experience base

Based on this simple comparison, CFB incineration technology appears to be a promising disposal method for certain organic streams; however, relatively little information is available

about performance with specific wastes. There is even less fundamental information on general organics destruction upon which designs can be based. In an attempt to address some of these issues, the objectives of this study were to assess the feasibility of CFB incineration for solid organic wastes disposal and to study the destruction behaviour of selected organics. The experimental work has been carried out in the UBC pilot CFB facility which is described in Chapter 4.

1.3 Source of Organic Wastes

Alcan Smelter and Chemicals in Kitimat, B.C. provided organic wastes used in this feasibility study. These solid wastes are typical of those found in the aluminum smelting industry. While there are no 'standard' organic wastes, the Alcan wastes represent a reasonable spectrum from the point of view of variability of physical and chemical characteristics (see Chapter 5). This study does not involve polychlorinated biphenyl (PCB) or pentachlorophenol (PCP) wastes.

Aluminum is produced by electrolysis of alumina, Al_2O_3, dissolved in a fused bath of cryolite, $AlF_3.3NaF$. The main electrochemical reaction at about 1000 ^oC is:

$$2Al_2O_3\ (\text{dissolved}) + 3C\ (s) \text{ ----- } 4Al\ (l) + 3CO_2\ (g)$$

The carbon needed for the electrochemical reaction is consumed from the anode. The anodes are prepared on-site in the anode paste plant. The paste consists mainly of coal tar pitch, which belongs to the chemical family of polycyclic hydrocarbons, and calcined delayed petroleum coke. Alcan uses prebaked anodes in their electrolytic cells. The prebaked anodes are made by bonding coke particles in a solid carbon mass with pitch binder in a separate baking oven before it is placed in the electrolytic cell. Table 1.2 shows the various waste

materials, most of which result from the anode manufacturing process, and their annual generation rates.

Table 1.2 Organic Wastes Generated by Alcan, Kitimat, B.C. [Alcan]

Material Description	Rate of Generation (tonne/year)
Stud Blast Fines, fines	250
Pitch Cones, solids	50
Miscellaneous Paste Waste, solids	25
D.C. Pitch Dust, fines	50
Total	375

When the anode is consumed, the residue is blasted from the steel studs used to suspend the anode. This residue is called stud blast fines and consists of petroleum coke, coal tar pitch and steel corrosion products. The other three materials originate from the on-site anode manufacture plant. The pitch cones and miscellaneous paste wastes constitute the residue of the anode paste manufacturing process. The pitch dust is collected from the air exhaust system. These wastes still retain the chemical properties of the raw materials used in the anode paste manufacturing process. Alcan has made good progress in decreasing waste generation and also in recycling the waste pitch and paste. The residual materials are stockpiled or sent off-site for disposal. This study makes use of the Alcan wastes as an example of typical high organic content industrial wastes to assess the feasibility of CFB incineration as a general technique for waste disposal.

2. LITERATURE REVIEW

Circulating fluidized bed technology has emerged as a leading technology for power generation from solid fuels. Many of the newly installed electrical generating facilities in North America and Europe are based upon circulating fluidized beds because of fuel flexibility, low emissions of CO, SO_2 and NO_x and high combustion and combined cycle efficiencies. Many of the features which make CFBs successful for power generation point positively toward its application in waste disposal. However, the growth of CFB technology for incineration and in waste management has been less than dramatic. As an incineration technology, CFB is still in its infancy. This is partly because CFB systems are poorly understood, but also because there is a lack of critical information needed for proper evaluation. The available pilot studies are generated by vendors for specific fuels under limited conditions. Information needed for generalization to other wastes is lacking. The information provided in this work, while still limited to relatively specific fuels, i.e. solid carbonaceous wastes, provides general trends showing the influence of key operating parameters on the performance of the CFB as an incinerator.

2.1 Applications of CFB Technology

In 1972, a study of fluidized bed incineration of industrial wastes was carried out in the Battelle Laboratories in Columbus, Ohio [Battelle, 1972]. The wastes included:

(1) paint wastes	- solvent recovery sludges
	- latex washout water
(2) plastic wastes	- primary treatment sludges
	- solid scraps
(3) rubber wastes	- primary treatment sludges

- wastes from reclamation of rubber from old tires

(4) textile wastes - wastes from viscose rayon production

These wastes were incinerated in a fluidized bed incinerator of inner diameter 0.254 m and height 1.83 m. The fluidized bed operated in the turbulent fluidization regime. The superficial gas velocity ranged from 0.5 to 1.0 m/s; the operating temperature ranged from 704 to 1010 ^{o}C and the oxygen content of the exhaust gas ranged from 2.2 to 16 % . The results of the study showed that fluidized bed incineration is a technically feasible treatment method. CFBs, as compared to conventional fluidized beds, offer the following advantages:

- further improvement in gas-solids contacting efficiency
- more uniform distribution of solids: little or no gas by-passing
- reduced axial gas and solids backmixing: approaches more nearly to plug flow
- higher production capacity (higher gas throughput)
- independent gas and solids retention time control
- higher turndown ratio
- excellent intraparticle and interparticle heat and mass transfer rate
- nearly uniform temperature distribution
- less particle segregation

As a result of these factors, circulating fluidized beds have been used in incineration applications for a variety of wastes shown in Table 2.1.

Table 2.1 CFB Incineration Applications

Waste	Description	Operating Conditions and Incinerator Performance
PCB contaminated soil	(a) PCB concentration in soil : 9800 - 11000 ppm (1)	(a) T : 982 ^{o}C % O_2 in flue gas 6.8 - 7.9 % CE : > 99.9 % DRE : > 99.9999 % dioxin/furan conc. in stack gas, bed ash and flyash : Not Detected
	(b) PCB concentration in soil : 289 - 801 ppm (2)	(b) T : 875 - 927 ^{o}C gas residence time : 1.47 - 1.68 s % O_2 in flue gas : 6.1 - 8.1 % dry basis CE : 99.98 - 99.99 % DRE : > 99.9999 %
Soil contaminated with No. 6 fuel oil (2)	naphthalene conc. : 4106 - 4730 ppm	T : 864 ^{o}C gas residence time : 1.8 s % O_2 in flue gas : 13.6 % dry basis CE : 99.99 % DRE : > 99.996 - > 99.99958 %
Refinery wastes (3) (a) an oily sludge (b) oil contaminated soil	(a) 31.5 wt. % oil, 55.5 wt. % water and 13.0 wt. % solids; Higher Heating Value (HHV) of 12.8 MJ/kg (b) 4.0 wt. % oil, 81.0 wt. % soil and 15.0 wt. % water; HHV of 1.73 MJ/kg	(a) T : 802 ^{o}C +/- 4 ^{o}C gas residence time : 1.3 s % O_2 in flue gas : 6 % wet basis
(a) Carbon tetrachloride; (b) Freon; (c) Malathion; (d) Dichlorobenzene; (e) Aromatic nitrile (f) Trichloroethane (4)	(a) liquid (b) liquid (c) liquid (d) sludge containing dichloro-benzene (e) tacky solid (f) liquid	(a) DRE : 99.9992 % (b) DRE : 99.9995 % (c) DRE : > 99.9999 % (d) DRE : 99.999 % (e) DRE : > 99.9999 % (f) DRE : 99.9999 %
(a) Cattle manure (b) Heavy metal waste (c) Chlorinated organic sludge (5)	(a) HHV of 13.9 MJ/kg (b) HHV of 28.6 MJ/kg (c) HHV of 32.6 MJ/kg	
Spent potliner from aluminum smelter (6)	40 wt. % fluoride salts; 30 wt. % refractory insulation; 30 wt. % carbon and 0.2 wt. % cyanide salts	T : 793 - 816 ^{o}C cyanide DRE : > 99.99 %
(a) Effluent treatment plant sludge (b) Extracted medicinal leaves (c) Agricultural liquid waste (d) Mixed plastics (7)		T : 900 - 1100 ^{o}C gas residence time : 1.5 - 2.0 s excess air level : 70 - 120 % CE : > 99.9 %

References:

(1) Jensen and Young, 1986
(2) Anderson and Wilbourn, 1989
(3) Wilbourn et al., 1986
(4) White et al., 1987
(5) Vrable et al., 1985
(6) Rickman, 1988
(7) Sethumadhaven et al., 1991

Note: CE denotes combustion efficiency and DRE denotes destruction and removal efficiency. CE and DRE are defined by equations 2.1 and 2.2 below respectively.

Ogden Environmental Services (OES) Inc. operates a 0.41 m ID pilot CFB test facility in San Diego for test trials of a variety of hazardous waste materials. OES has also developed transportable 0.91 m ID CFB units for waste remediation. Some of the applications mentioned above (i.e. 1 to 5) have been carried out in either the OES pilot facility or in OES transportable units.

An example of CFB incineration application involved the Superfund Innovative Technology Evaluation (SITE) demonstration test burn of McColl Superfund site soil. In March 1989, OES conducted incineration trials in their pilot 0.91 m ID CFB research facility. A total of 3400 kg of contaminated soil was processed through the CFB, of which 2100 kg was actual McColl waste. The materials processed included: waste blended with clean sand (Test 1), unblended waste (Test 2), and unblended waste spiked with carbon tetrachloride, CCl_4 (Test 3). The average combustion temperature was 937 ^{o}C. In all three tests, a combustion efficiency (CE) of 99.97 % was achieved, while the destruction and removal efficiency (DRE) of CCl_4 in test 3 was 99.9937 %. Both CE and DRE were consistently higher than the U.S. EPA (United States Environmental Protection Agency) regulatory limits (99.9 % and 99.99 %

respectively) [Anderson and Wilbourn, 1989]. The regulatory discharge limits vary from jurisdiction to jurisdiction. For example, in British Columbia the discharge criteria are set out in the Waste Management Act of B.C. The combustion efficiency and destruction and removal efficiency are calculated based on the following correlations [Waste Management Act of B.C., 1988]:

$$CE = \frac{C_{CO2}}{C_{CO2} + C_{CO}} * 100\ \% \qquad (2.1)$$

where

CE = combustion efficiency (%)

C_{CO2} = concentration of carbon dioxide in the exhaust emissions (ppm)

C_{CO} = concentration of carbon monoxide in the exhaust emissions (ppm)

$$DRE = \frac{W_{IN} - W_{OUT}}{W_{IN}} * 100\ \% \qquad (2.2)$$

where

DRE = destruction and removal efficiency (%)

W_{IN} = mass feed rate of one POHC in the waste feed stream (kg/h)

W_{OUT} = mass emission rate of the same POHC in the exhaust emissions (kg/h)

Principal Organic Hazardous Constituents (POHCs) are characterized as the most difficult compound to incinerate in the waste stream. A list of these compounds is presented in Appendix VIII of the U.S. Resource Conservation and Recovery Act (RCRA), which defines hazardous wastes and describes the methods needed for the control of these wastes. POHCs

are not defined in the B.C. Waste Management Act. The designation of POHC in a waste stream is decided by the Regional Director of the B.C. Ministry of Environment. POHC identification and incinerability ranking are discussed in detail in section 2.4.

The CO, NO_X, unburnt hydrocarbons (HCs), HCl and particulate emissions from the McColl test trials were well within U.S. federal, state and local requirements. Table 2.2 shows the emissions from Test # 3. These emissions also meet the B.C. Special Waste Regulation discharge limits. The operating conditions for Test # 3 were: Incineration temperature: 932 ^{o}C; Gas residence time: 1.55 s; Flue gas oxygen: 11.8 %, dry basis. The particulate emissions were lower than the U.S. federal limit of 0.08 gr/dscf (grains per dry standard cubic feet). Complete stack and ash analyses for volatiles, semi-volatiles and metals indicated no significant levels of hazardous compounds in the flue gas. Ash analysis indicated that no significant levels of hazardous organic compounds remained in the bed and fly ash material. A Toxicity Characteristic Leaching Procedure (TCLP) was performed on the McColl CFB ash. The leachabilities of contaminants such as arsenic, selenium, barium, cadmium, chromium, lead, mercury and silver were all found to be well below the federal requirements. As a result, the U.S. EPA concluded the test was successful and phase II of the SITE testing using a 0.91 m ID CFB reactor at the Fullerton site was proposed [Anderson and Wilbourn, 1989].

Table 2.2 Emissions from McColl Site Incineration Test # 3

	Raw Emissions	Emissions Corrected to 11 % O_2, 20 ^oC, 760 mm Hg, dry basis (mg/m^3)	B.C. Special Waste Regulation Limit (mg/m^3)
CO (ppm)	26	33	55
NO_x (ppm)	48	100	380
HC, hydrocarbon expressed as CH_4 (ppm)	2	1.5	32
HCl (lb/h)	< 0.0098	-	50
particulate (gr/dscf)	0.0035	5	-
particulate (mg/m^3)	8	-	20
CE (%)	99.97	-	≥ 99.9
DRE of CCl_4 (%)	99.9937	-	≥ 99.99

OES has also conducted incineration tests on PCB contaminated soil from Swanson River in Alaska. A transportable 0.91 m ID CFB unit was used to carry out six tests on the PCB contaminated gravel/silt soil (see Table 2.1, PCB contaminated soil (b)). In all cases, the combustion efficiency exceeded 99.9 % and DRE exceeded 99.99 %. No dioxins or furans were detected in the treated soil. The results met or exceeded all U.S. EPA Toxic Substance Control Act (TSCA) criteria for incineration of PCB contaminated soil. The TSCA addresses the control of PCBs in the environment.

In Canada, the Canadian Council of Ministers of the Environment, CCME, has developed national guidelines regarding the design and operating criteria for hazardous waste incineration facilities. These guidelines suggest that conventional incinerators, e.g., rotary kilns, operate at 1300 ^oC with a gas residence time of 2 s or at 1200 ^oC with a gas residence time of 3 s to ensure appropriate PCB destruction [National Guidelines, 1992]. CFBs do not meet these guidelines since they usually operate at lower temperatures (between 800 - 1100 ^oC) and have shorter residence times (less than 2 s) than conventional incinerators. Yet CFB

incineration technology, a low temperature process, is capable of achieving high degrees of organic destruction.

OES has developed a CFB waste treatment technology and demonstrated its applicability in private and government sponsored programs. Based on these development and testing programs, modular CFB units have been designed, manufactured and put to use in two large remediation projects [Anderson and Wilbourn, 1989].

Another example of fluid bed incineration application is the toxic waste incineration test facility in Trichy, India. More than ten different types of wastes have been incinerated successfully at this facility including effluent treatment plant sludge, extracted medicinal leaves, mixed plastics and agricultural liquid wastes. The fluid bed facility achieved combustion efficiencies exceeding 99.9 %, and the residual ash was found to be non-toxic [Sethumadhaven et al., 1991]. Consequently, Sandoz (India) proposed installation of a pilot incinerator (capacity of approximately 200 tonnes per year) near Bombay in order to conduct extensive trials and to obtain quantitative data for full-scale design.

The UBC pilot circulating fluidized bed combustion facility, in operation since 1986, has been used to burn a variety of coals and wastes efficiently with low pollutant emissions. The work performed to date has included study of the influence of such factors as temperature, excess air, staged combustion, suspension density, gas velocity, limestone addition and fuel type on the emissions. Profiles of gaseous component concentrations in the combustor have been obtained via a stationary multi-point sampling system. The combustion tests [Grace and Lim, 1987; Grace et al., 1989; Brereton et al., 1991] have generated practical data for the design and operation of commercial equipment. Work is also being carried out on heat transfer, systems control and modeling of pollutant formation.

In previous combustion studies, the UBC pilot CFB unit operated as a combustor rather than an incinerator. For a combustion system, the objective is to generate and recover energy by the burning of fuels, whereas for an incineration system, the objective is to achieve the highest degree of destruction possible for the wastes in question. Consequently, the operating conditions for a combustor may differ from those for an incinerator. For example, in combustion systems, it is necessary to minimize the heat carried away with the flue gas by operating at minimal excess air. On the other hand, in incineration systems, where emissions regulations for unburnt gaseous hydrocarbons are typically orders of magnitude lower than for power generation systems, it may be necessary to operate at higher temperatures and with higher excess air. A detailed discussion of the operating conditions for the UBC pilot CFB unit operating as an incinerator is given in section 6.1.

2.2 Evaluation of Incinerator Performance

Two main performance indicators for an incineration system are its combustion efficiency, CE, and destruction and removal efficiency, DRE. Regulatory bodies require continuous monitoring of CO emissions. Consequently, CE can be determined by continuous monitoring of CO and CO_2 emissions. It would be useful to continuously monitor DRE; however, there is no simple low cost continuous monitoring method for this. Sevon and Cooper (1990) tried to correlate operating conditions, i.e. excess oxygen, gas phase residence time and temperature, to combustion efficiencies of incinerators. Chang et al. (1987) tried to correlate operating conditions as well as concentrations of CO and total hydrocarbon (THC), in the flue gas with the destruction efficiency of organic compounds in incinerators. However, there is no single parameter which can be used to accurately predict the performance of an incinerator.

Sevon and Cooper (1990) investigated the effects of operating parameters on combustion efficiency of a two-stage CFB liquid organic incinerator. The CFB unit had an internal

diameter of 0.13 m and a total height of 2.4 m. The operating parameters included excess air, mean operating temperature, average particle size of the bed material, and ratio of primary air to total air. Propanol was the test fuel burned. The authors concluded that the CFB was incapable of achieving a 99.9 % combustion efficiency because the incinerator height resulted in short residence times, approximately 1.0 to 1.6 s as compared to 2 s for commercial units. Gas velocities for the various operating conditions were not provided. However, calculations based on the total volumetric flowrate of air at the operating temperatures and the cross-sectional area of the column show that the gas velocities were typically less than 2 m/s. The fluidization regime map [Grace, 1986] which shows the various hydrodynamic fluidization regimes as a function of dimensionless superficial gas velocities versus dimensionless particle diameter, indicate that the pilot unit operated in the turbulent regime rather than the fast fluidization regime. Consequently, these results are probably applicable for fluid bed incinerators operating in the turbulent regime.

Chang et al. (1987) evaluated the potential of a pilot CFB unit as a hazardous waste incinerator burning a fuel mixture composed of Freon 113 (trichlorotrifluoroethane), trichlorobenzene, hexachlorobenzene, ethylbenzene, carbon tetrachloride (CCl_4), toluene and xylene under non-optimum conditions. Both POHCs and PICs (products of incomplete combustion) were measured. Details on PICs are presented in section 2.3. The pilot CFB operated under intermittent fuel-rich conditions which resulted in surges of fuel-rich plugs of gas passing through the bed. The results showed that the fraction of PICs remaining seemed to increase with increases in CO and THC emissions. However, there were instances where high CO emissions were observed without a corresponding increase in PIC concentrations. DREs of POHCs, i.e. Freon 113, CCl_4, exceeding 99.99 % were observed. The DREs did not appear to correlate well with either CO or THC emissions.

2.3 Products of Incomplete Combustion

POHCs are defined in the RCRA regulations while PICs are not. In general, PICs are organic compounds generated by burning of organic materials but were not present in the original waste feed stream [Brunner, 1989]. In the EPA's test program, compounds were considered to be PICs if they were regulated organic compounds, i.e. those listed in Appendix VIII of the RCRA, and if they were detected in the stack emissions but not in the feed waste stream at concentrations greater than 100 ppm. PICs may result from [Dempsey and Oppelt, 1993]:

(1) incomplete destruction of POHCs

(2) formation in the combustion zone and downstream as the result of partial destruction followed by radical-molecule reactions with other compounds or compound fragments

(3) Appendix VIII compounds present in the feed but not specifically identified as a POHC and

(4) other sources such as ambient air pollutants in the combustion air

At the present time, there are no reliable techniques to predict the generation of PICs. No specific control technology exists for these organics, although, it has been found that with good combustion (> 99.9 % CE or less than 100 ppm CO in the flue gas stream) the generation of PICs is extremely small [Brunner, 1989]. There is limited regulation regarding the issue of PIC generation and control. Recent proposed amendments to the U.S. hazardous waste incineration regulation (RCRA) included a provision to control PICs by setting limits on parameters such as CO and hydrocarbon emissions to ensure that the thermal facility is operating under favourable combustion conditions. While these amendments have not been made official, this approach is being implemented on a national basis by permit writers using the "omnibus" authority (40 CFR 270.32, Title 40 of the Code of Federal Regulations, Part 270.32,) [Dempsey and Oppelt, 1993].

The B.C. Special Waste Regulation does not specify or limit PIC emissions. Instead there are emission limits on CO and total hydrocarbon (THC) in the stack gas. However, there is concern regarding the possible impact of potentially hazardous PIC emissions on human health and the environment. The greatest amount of scientific and pubic attention has been given to dioxins and furans. Dioxins are members of a family of organic compounds known chemically as dibenzo-p-dioxins. This family is characterized by a three-ring nucleus consisting of two benzene rings interconnected by a pair of oxygen atoms. Furans are members of a family of organic compounds known chemically as dibenzofurans. They have a similar structure to the dibenzo-p-dioxins except that the two benzene rings in the nucleus are interconnected with a five-member ring containing only one oxygen atom. From a human health hazard viewpoint, the 'tetra' and 'penta' forms of polychlorinated dibenzo-p-dioxins (PCDDs) i.e. 2,3,7,8-tetrachlorodibenzo-p-dioxin (2,3,7,8-TCDD) and polychlorinated dibenzofurans (PCDFs) compounds are the most significant [Dempsey and Oppelt, 1993]. In the U.S. and in B.C., the incineration of wastes containing polychlorinated biphenyls (PCBs), PCDFs or PCDDs requires 99.9999 % DRE of these compounds as compared to 99.99 % DRE for POHCs.

2.4 POHC Identification and Incinerability Ranking

Before an operating permit is granted for a hazardous wastes incinerator, trial burns must be conducted to demonstrate the ability of the incinerator to achieve 99.99 % DRE of the POHCs identified in the waste stream and to also achieve 99.9 % CE. In the United States, POHCs are selected from RCRA Appendix VIII constituents present in the wastes. The compounds likely to be chosen are those with the highest concentration in the waste stream and are the most difficult to incinerate. The U.S. EPA uses the heat of combustion of a compound as a ranking index of compound incinerability. This ranking method is based on the assumption that the lower the heat of combustion, the more difficult the compound is to

incinerate. The appropriateness of this ranking method has been the subject of considerable debate. The main reasons are [Lee et al., 1990]:

(1) The destruction of POHCs in a flame zone is caused by temperature, time and turbulence. The heat of combustion is related somewhat to temperature but does not relate to the residence time and turbulence in an incineration system.

(2) The heat of combustion does not include combustion chemistry factors such as kinetics and radical attack, which dominate POHC destruction in the post-flame zone.

(3) The heat of combustion does not include combustion physical factors such as mixing which have great impact on POHC destruction efficiency in both the flame and post-flame zones.

Other ranking methods which have been proposed include autoignition temperature, oxidative stability of pure compounds, a theoretical ranking based on in-flame oxidation rates, theoretical flame mode kinetics, experimental flame failure modes, ignition delay time, and gas phase (nonflame) thermal stability [Taylor et al., 1990; Lee et al., 1990; Dempsey and Oppelt, 1993; Dellinger et al., 1993]. Dellinger et al., (1985) compared the rankings of compounds by each of the indices mentioned above to their observed incinerability in ten pilot and field scale incineration units. The nonflame thermal stability incinerability index was the only one which showed a statistically significant correlation for the compounds evaluated. Engineering analysis of thermal destruction of hazardous wastes showed that more than 95 % of the compounds entering the flame zone of an incinerator are destroyed in a very short time, of the order of microseconds. The remaining compounds enter the post-flame zone for further thermal decomposition which takes place in the order of 1 to 2 s. The gas phase thermal decomposition kinetics control the rate of POHC destruction in the post-flame zone. The compounds which escape post-flame decomposition are emitted from the incineration facility if they are not captured by the downstream pollution control equipment. Thus, the post-flame

environment determines the fraction of the remaining compounds which escape and affect the DRE of the incineration system. Emissions data from full-scale incinerators are several orders of magnitude higher than those calculated using oxidation kinetics and residence times together with mean temperatures in the post-flame zone [Lee et al., 1990]. Lee et al. (1990) suggested that oxygen-depleted pathways in an incinerator may be responsible for most POHC emissions since pyrolysis is associated with slower POHC destruction. Although an incinerator may be operating under nominally excess air conditions, poor mixing can result in oxygen deficient pockets where the rate of POHC destruction is low. Hence, most emissions are due to pyrolysis reaction pathways. Lee et al. (1990) proposed and developed an incinerability ranking based on the concept of gas phase (nonflame) thermal stability under sub-stoichiometric oxygen conditions.

Incineration is a process of intensive thermal oxidation accompanied by pyrolysis and radical processes. The decomposition of a molecule can be initiated by either internal redistribution of energy such that the molecule decomposes or is rearranged, i.e. unimolecular pathways or by radical attack (a bimolecular pathway). Unimolecular reactions can be classified into bond homolysis and concerted molecular elimination. The bond homolysis process involves the breaking of the weakest bond in a compound. The concerted molecular elimination process involves an internal molecular rearrangement and elimination of a stable species such as HCl, H_2O or CO_2. Bimolecular reaction pathways involving radical attack can be subdivided into four classes: atom metathesis, electrophilic addition, hydrogen abstraction and displacement [Lee et al., 1990]. Taylor et al., (1990) ranked 320 hazardous organic compounds based on the thermal stability concept using experimental results and thermochemical reaction kinetic theory. The thermal stability ranking was divided into three groups based on the type of dominant decomposition mechanism of the compound. The first group consisted of the 77 most stable compounds (with cyanogen (ethanedinitrile) and SF_6 ranking 1st and 4th respectively), and these may be characterized by bimolecular decomposition reactions which

are believed to dominate decomposition. This group of compounds is the hardest of the three to assess because there is a lack of high temperature bimolecular reaction rate data and because of the multiplicity of reaction pathways. The second group of compounds (ranking 78 to 125) may be characterized by decomposition dominated by mixed unimolecular and bimolecular reactions. The third group of compounds (ranking 126 to 320) are characterized by decomposition dominated by unimolecular reactions. The experimental decomposition curves for the organic compounds burned in the tests were compared to the theoretical thermal decomposition curves, and there was good agreement between theory and experiment. A kinetic expression which incorporated all known reaction pathways (unimolecular and bimolecular) for chemical changes of the POHC was used to generate the theoretical thermal decomposition curves. The kinetic expression used for bimolecular reactions incorporated terms which accounted for the temperature-dependent radical concentration and the chain length for radicals. Free radicals are generated during the combustion process. At temperatures greater than 725 ^{o}C, H, O, and OH radicals are responsible for chain branching. As a result, the combustion process is dominated by reactions with free radicals [Anthony, 1994] The radical concentrations used by Taylor et al., (1990) were estimated by applying the partial equilibrium hypothesis, which assumes that the concentrations of highly reactive species, e.g. OH radicals and H, O and Cl atoms, achieve equilibrium with each other via fast bimolecular reactions, even though the overall system is not at chemical equilibrium.

Dellinger et al. (1993) presented the results of a full-scale evaluation of the thermal stability-based incinerability ranking based on tests performed at the Kodak chemical waste incinerator in Rochester, New York. The incinerator consists of a rotary kiln, mixing chamber and secondary combustion chamber, followed by a quench chamber and venturi scrubber. The total thermal capacity of the unit is 95 kJ/h. A mixture containing sulphur hexafluoride, chlorobenzene, toluene, tetrachloroethene, methylene chloride, 2-chloropropene and 1,1,1-

trichloroethane were burned under nominal incinerator operating conditions. Based on median DREs of the compounds tested, the results showed that the pyrolytic ranking was statistically significant at the 90 % confidence level while the oxidative ranking level was statistically significant at the 97.5 % confidence level. The heat of combustion ranking failed to provide a statistically significant correlation at the 90 % confidence level. The statistical success of the pyrolysis and oxidative thermal stability rankings and the failure of the heat of combustion ranking suggests that chemical reaction kinetics controlled the relative emission rates of organic compounds during these tests. This seems to suggest that reaction kinetic considerations can be used to predict relative POHC destruction efficiencies. Although the oxidation kinetics ranking was slightly better than the pyrolysis-based ranking for this system, the authors warn that there is insignificant statistical difference in the degree of correlation of the two kinetic-based rankings with the emissions data. Consequently, slight variation in the two rankings should not be given much weight.

There are few bench-scale data available for approximately half of the Appendix VIII compounds even though this thermal stability ranking method seems promising. In order to determine POHC destruction efficiencies, a numerical model encompassing the temperature, exact time and reaction atmosphere (e.g. total reactant concentration, molecular waste composition, elemental waste composition and waste/oxygen equivalence ratio) of all molecules in an incinerator is required [Taylor et al., 1990]. Researchers [Chang et al., 1987; Chang and Senkan, 1989; Weissman and Benson, 1984; Senser et al., 1986] are in the process of developing detailed chemical kinetic models of the thermal degradation of some simple chlorinated hydrocarbons such as chloromethane, dichloromethane, and trichloroethylene. Computer codes are also being developed to model incinerator conditions [Clark et al., 1988]. However, a sufficiently detailed understanding of this complex chemical and physical process is not currently available.

2.5 Use of Surrogate Compounds to Determine Incinerator Performance

Identification of POHCs in a waste stream is difficult, time consuming and expensive due to the complex nature of the waste streams. This, combined with the uncertainty over incinerability rankings, has led to the use of surrogate compounds to demonstrate the DRE capabilities of an incinerator. It is commonly assumed that if an incinerator is capable of achieving a DRE of 99.99 % for a surrogate, e.g. a thermally stable compound such as SF_6, then it is capable of destroying other organic materials to at least the same extent. In practice, this assumption is often flawed since destruction of SF_6 is related primarily to temperature due to the strength of the SF bond [Bott and Jacobs, 1969] while incineration of organics not only depends on temperature, but also on turbulence, residence times and excess air. A detailed discussion of possible SF_6 decomposition mechanisms is provided in Section 2.5.1.

Selection criteria for a surrogate compound includes low toxicity, high thermal stability, unlikelihood of being formed as a PIC, chemical similarity to the wastes in question, commercial availability at relatively low cost, and ease of analysis of the compound. Gaseous SF_6 is a commonly used surrogate compound. It is non-toxic, highly thermally and chemically stable, not usually present in wastes and commercially available at relative low cost. Gaseous SF_6 cannot be easily added to liquid or solid hazardous wastes but it can be easily added continuously to the combustion air. Therefore, the drawback in using SF_6 is that it may not simulate the combustion dynamics, mixing effects or waste form that a POHC experiences.

Feasibility studies [Mournighan and Olexsey, 1985] on SF_6 as a surrogate have been carried out in a CFB, a dry-process cement kiln and an asphalt plant. DREs of SF_6 (90 to 99.99 %) in a CFB appears to be a function of temperature (790 to 850 ^{o}C). SF_6 was not detected in the stack gas from the cement kiln. Consequently, the DRE of SF_6 (> 99.999 % at 1500 ^{o}C) was calculated based on the detection limit of the GC/ECD used for the analysis. Typically,

cement kilns operate between 1300 and 1500 ^{o}C [Brunner, 1989]. The DRE of SF_6 was not very high in the asphalt plant (99.3 to 99.8 % at a stack temperature of 190 ^{o}C). However, DREs for the POHCs were not available in that test and further studies are needed to develop the relationship between POHC and SF_6 destruction [Mournighan and Olexsey, 1985]. A study of SF_6 as a tracer for verification of waste destruction levels in an incineration process had been carried out at the University of Florida [Proctor et al., 1987]. SF_6 was mixed with natural gas and burned in a turbulent diffusion flame, typical of industrial boiler flames. The DREs of benzene and trichloroethylene, when burned in the same environment as the SF_6, were greater than the DRE of SF_6. This shows that SF_6 is more difficult to destroy than benzene and trichloroethylene and that SF_6 would be a good tracer for these waste compounds.

2.5.1 SF_6 Destruction Mechanisms

As previously mentioned, the choice of SF_6 as a surrogate compound in the present study is largely based on its high thermal stability. It is thought that high temperatures and sufficient exposure time are responsible for its destruction. Taylor and Chadbourne (1987) believe that unimolecular reactions are the dominant destruction mechanism. As a result, the stability of SF_6 is thought to be independent of the reaction environment. However, Graham et al. (1986) have found that bimolecular reactions (i.e. reactions with reactive free radical species such as the hydroxyl, oxygen and hydrogen radicals) and the reaction environment (e.g. oxidative rather than pyrolytic) are important for destruction of organics. In developing the thermal ranking of compounds, Taylor et al. (1990) included both unimolecular and bimolecular reactions data in predicting the destruction of various organic compounds. There was good agreement between the theoretical and the experimental destruction curves. It is likely that the destruction of SF_6 may also depend on bimolecular reactions and the reaction environment [Khare, 1989; Reider 1990].

Bott and Jacobs (1969) performed shock-tube kinetic studies of SF_6 dissociation in an argon mixture. The tests were carried out in the temperature range of 1377 to 1777 ^{o}C (1650 to 2050 K) and pressures from 13 to 3000 kPa (0.13 to 30 atm). The resulting dissociation rate constants were found to be explainable by unimolecular reaction kinetics. Wilkins (1969) studied the decomposition products of a SF_6 mixture (1 mole % SF_6 and 99 mole % Argon). He found that at temperatures below approximately 1127 ^{o}C (1400 K) there is relatively little thermal decomposition of SF_6 (15 to 30 %). It is only at higher temperatures i.e. between approximately 1127 and 1827 ^{o}C (1400 and 2100 K), that there is rapid thermal decomposition of SF_6. Taylor and Chadbourne (1987) found that SF_6 stability was independent of the oxygen concentration in the incineration system over the temperature range between 200 and 1050 ^{o}C, and thus concluded that SF_6 stability was primarily dependent on the exposure residence time and temperature within a given incinerator.

Graham et al. (1986) studied the effect of oxygen concentration on the thermal stability of an organic mixture composed of carbon tetrachloride, monochlorobenzene, Freon 113, trichloroethylene, and toluene. The tests were carried out over a temperature range of 300 to 1000 ^{o}C with a gas residence time of 2 s. The results showed that the thermal stabilities of the components in the mixture varied with reaction atmosphere. The stability of the mixture components with the exception of Freon 113 increased with decreasing oxygen concentration. Under oxidative or stoichiometric oxygen conditions, the components in the mixture are subject to attack by high concentrations of reactive hydroxyl oxygen radicals; hence resulting in a decrease in the stability of the organic components. Under pyrolytic conditions, the components in the mixture degrade due to the attack of hydrogen radicals or via unimolecular decomposition. The hydrogen radicals, which are present under reducing conditions, are less reactive and occur at lower concentrations than the hydroxyl or oxygen radicals which are

present under oxidative conditions. Consequently, there is an increase in the stability of the organic components.

Khare (1989) and Reider (1990) suggested that reactions with hydrogen and hydroxyl radicals may be important for decomposition of SF_6. Khare performed incineration experiments (at a temperature of 1000 ^oC and gas residence time of 0.234 s) without a hydrogen source and obtained a SF_6 DRE of 79.31 %. When methanol was added as a hydrogen source (at the same operating conditions), a DRE of 99.999986 % was achieved. Reider also investigated the effect of hydrogen on SF_6 destruction. He used methane as a source for hydrogen and performed experiments introducing a wide range of hydrogen concentrations with a constant SF_6 concentration (435 ppm). The amount of hydrogen added was reported in terms of the ratio of moles of hydrogen to moles of fluorine (H/F). Reider found that DRE increased with increased molar H/F ratio (at a temperature of 1000 ^oC and gas residence time of 0.234 s). Although the exact reason for this observation was not known, he suggested that hydroxyl radical, OH*, formation was important for SF_6 destruction. The OH* reacts very rapidly with SF_6, breaking it down into HF and various sulphur oxides. Since SF_6 destruction is believed to be improved by the presence of OH* formed during methane combustion, Reider predicted the maximum DRE should occur at stoichiometric proportions for the oxidation of methane in air. This translated into a H/F ratio of approximately 170. The DRE increased rapidly as the H/F ratio approached 170. However, there was a great deal of experimental scatter near H/F = 170. This may be due to added reactivity provided by the increasing presence of OH*. Hence, at fluid bed combustion temperatures and at the temperatures of most incineration systems, bimolecular reactions with free radicals may affect the stability of SF_6 as it does for other organics.

2.6 Hydrodynamics in CFBs

Although pilot plant studies have shown that CFB technology shows promise as a viable waste incineration process and that larger commercial units can be designed and implemented, there are still many unknowns. For example, the mixing behaviour of gas and solids in the CFB is not well understood. Previous work in the UBC pilot unit has shown the importance of understanding hydrodynamic issues for interpretation of the formation and destruction of NO_X in CFBs [Zhao, 1992].

Low velocity fluidized beds have been studied extensively. Simple two-phase models have been moderately successful in predicting the main features of small scale fluidized bed reactors operating in the bubbling and slugging fluidization regimes. This is in contrast to a more limited knowledge of the hydrodynamics of high velocity fluidized beds. It is generally accepted that circulating fluidized bed reactors have strong lateral gradients of solids with a higher concentration of solids near the outer wall than in the interior. This has led to the hydrodynamics being characterized by a simple core-annulus model where the core region is assumed to consist of a high velocity gas stream with entrained solids traveling upwards, while the annulus region consists of dense streams or clusters of solids flowing downwards at or near the outer wall of the reactor. The gas moves either upwards or downwards much more slowly in the annulus region than in the central dilute core. A simplified version of flows in the CFB is shown by Figure 2.1 [Grace, 1990]. The actual flow patterns of gases and solids are much more complex since the interface between the two regions is not well defined and the interface is diffuse and changes with time. The dilute core region for a dilute suspension can sometimes reach the wall. The solids at or near the wall have a wide range of local voidages and velocities. Disturbances in the lower regions of the reactor due to solids feed ports, solids recycle port and secondary air entry nozzles affect the gas and solids flow patterns. The geometry of the reactor exit also affects the flow pattern of solids. A smooth

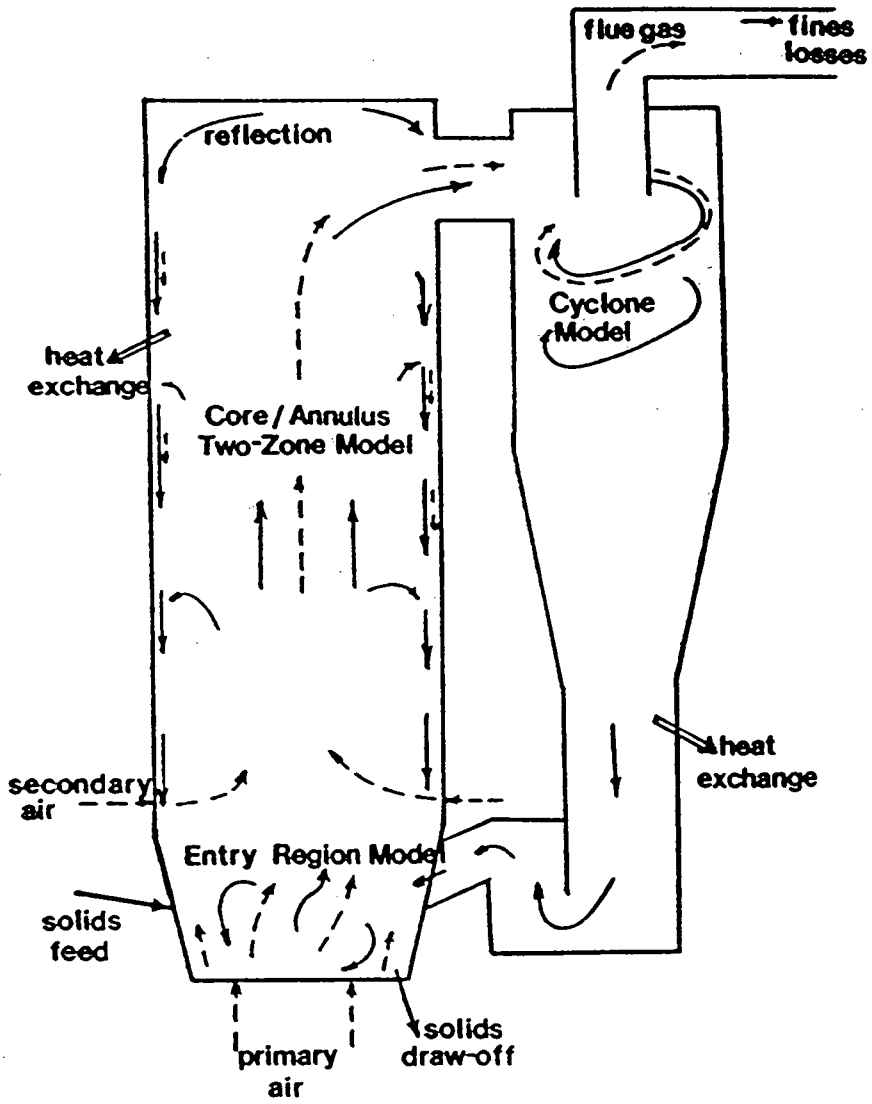

Figure 2.1 Schematic Diagram Showing Flow Patterns of Solids (solid arrows) and Gas (dashed arrows) and Showing Elements which Need to be Included in CFB Reactor Models [Grace, 1990]

tapered exit geometry results in minimal internal separation of solids at the top of the reactor and more solids are carried out of the reactor to be externally recirculated. An abrupt 90 degree exit geometry results in substantial internal separation of entrained solids at the top of the reactor causing fewer particles to be entrained from the top of the reactor [Brereton et al., 1988; Grace, 1990]. Consequently, it is very difficult to characterize the complex micro and macro mixing behaviour of solids and gas in a CFB. There are few experimental results which allow the evaluation of gas-solids contact in CFBs having well-characterized hydrodynamics. From previous hydrodynamics studies carried out in the UBC pilot CFB unit, there is some basic understanding of the movements and interactions between the gas and solids in the unit [Brereton, 1987; Senior, 1992]. It is hoped that the results from this study will add to the database.

3. RESEARCH OBJECTIVES

A feasibility study on CFB incineration of solid carbonaceous wastes was carried out in the UBC pilot CFB combustor. The objectives of this study were:

1) to study the combustibility of solid wastes and to carry out a systematic study of the effects of operating parameters, in particular temperature and excess air, on the flue gas emissions for each of the wastes

2) to gain a basic understanding of where and how an organic compound such as chloroform and a common surrogate compound, sulphur hexafluoride, are destroyed in CFBs

The feasibility study is comprised of two parts: an applications study and a fundamental study.

3.1 Applications Study

In this study, the focus was on the applicability of CFB incineration technology for solid carbonaceous wastes. These wastes included pitch cones, miscellaneous paste wastes, pitch dust and stud blast fines. There was no designation of POHCs in the waste streams due to the complex nature of the wastes. Initially, brief incineration tests on these materials were carried out. These tests served as a preliminary indicator of the combustibility of the different materials and of specific operating problems, especially feed problems due to coking tendencies of pitches which required modification of the feed system. These tests involved monitoring of flue gas emissions. Concentrations of O_2, CO, CO_2, NO, SO_2, and THC (total hydrocarbons expressed as CH_4) were analyzed and measured continuously by on-line

analyzers, while N_2O and NO_2 were measured periodically by a Fourier Transform InfraRed detector, FTIR. There was no solids residue sampling due to the short test periods.

A second set of tests was carried out after resolving the feed problems encountered during the initial incineration tests. These tests focused on a systematic study of the effects of incineration temperature and excess air on the exhaust gas emissions for each of the wastes. Exhaust gas emissions were monitored and measured. The performance standards for CE and DRE, and emission criteria specified in the Special Waste Regulations of the Waste Management Act of B.C. for a thermal facility, were used to assess the performance of the pilot CFB unit. The data generated from the incineration tests can be used in modeling work and for designing a full size CFB incinerator.

3.2 Fundamental Study

The fundamental study focused on gaining a basic understanding of the destruction tendencies of organics and more specifically, POHCs in CFBs. A well-defined fuel, chloroform ($CHCl_3$) and a tracer compound, sulphur hexafluoride (SF_6) were burned separately in the pilot CFB plant. The destruction profiles of $CHCl_3$ and SF_6 under steady state conditions were followed through the riser, the cyclones and the baghouse. Their concentrations were measured at different lateral locations between the riser wall and its centreline at four axial positions along the riser, as well as at the flue gas filter and at the exit of the baghouse. Simultaneous with the $CHCl_3$ or SF_6 measurements, O_2, CO, CO_2, NO, SO_2, and THC emissions were also monitored. At each sampling point, a sample of the gases was collected and analyzed for $CHCl_3$ or SF_6. A map of all the measured fuel, tracer and emissions concentration generated a picture of the incineration progress and of the gas mixing behaviour in the pilot CFB combustor. As part of the fundamental study, a simple incineration model was developed to predict the destruction profiles of sulphur hexafluoride. The computer

model may be a useful tool for interpreting experimental results. The details of the model are provided in the following sections.

3.3 Development of a Simple Model for a CFB Incinerator

Models for coal combustion processes in fluidized beds have been used as a tool for understanding and to some extent, for designing large scale commercial combustion systems. Models may include hydrodynamics and heat transfer aspects of CFBs, and they have different degrees of complexities depending on their objectives. The details of the various fluidized bed coal combustion models are beyond the scope of this thesis, but can be found in papers by Rajan and Wen (1980); Wells et al.; Gordon et al. (1978); Park et al. (1981); Tomita et al.; and Smoot (1984). However, there are no models for CFBs incineration systems. As part of this thesis, a simple numerical model was developed to investigate the destruction of selected compounds, chloroform and sulphur hexafluoride, within the UBC pilot CFB. The objective of the computer simulation is to predict the destruction profiles of the compounds as a function of axial and lateral position within the UBC pilot CFB using a simple hydrodynamic and a simple kinetic model. The destruction (concentration) profiles of chloroform and sulphur hexafluoride, will provide a picture of the progress of the incineration process and also the gas mixing behaviour inside the CFB. The details of the program are described in the following sections.

3.3.1 Kinetics Considerations

The kinetics of chloroform and sulphur hexafluoride destruction are described by assuming a first order reaction with respect to their respective concentrations. The decomposition of chloroform and sulphur hexafluoride is also assumed to be a function of the partial pressure of oxygen, P_{O2}, in the riser since oxidation reactions are also important. The bulk of the gas,

which contains the various organic compounds, comes into contact with oxygen and decomposes. However, small packet of gas may not contact oxygen and hence the destruction of the organic compounds will rely on thermal means. The partial pressure of oxygen is derived from previous experimental data [Zhao, 1992]. The reaction rate constant, K_R, can be written [Brunner, 1989] as:

$$K_R = V \exp\left(\frac{-E_A}{RT}\right) \tag{3.1}$$

where

K_R = reaction rate constant (1/s)

V = frequency factor (1/s)

E_A = activation energy (calories/mole)

R = universal gas constant (1.987 calories/mol.K)

T = incineration temperature (K)

For chloroform [Taylor et al., 1990],

$$K_R = 1.6E16\exp\left(\frac{-77000}{RT}\right) + 2.0E14\exp\left(\frac{-54500}{RT}\right) \tag{3.2}$$

The decomposition of chloroform is largely unimolecular in nature. The first term in the above expression represents the bond homolysis process, while the second term represents the concerted three-center elimination process,

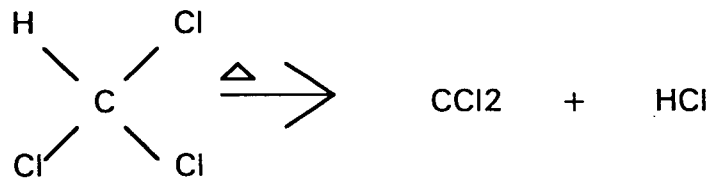

The kinetic rate constant expression for sulphur hexafluoride based on an unimolecular pathway [Lyman, 1977] is:

$$K_R = 1.2E15\exp(\frac{-92000}{RT}) \tag{3.3}$$

Hence, the reaction rate, $R(C)$, is expressed as:

$$R(C) = -K_R P_{O2} C \tag{3.4}$$

where

C = concentration of compound (mol/m^3)

P_{O2} = partial pressure of oxygen (mole fraction)

3.3.2 Hydrodynamic Considerations

Extrapolation of kinetic data from plug flow reactors to industrial circulating fluidized bed, CFB, reactors requires an understanding of the gas mixing behaviour. The CFB reactor is affected by complex solids and gas micro and macro-mixing parameters which determine the degree of non-isothermality and deviation from plug flow. A core-annulus model was used to describe the flow patterns within the UBC pilot CFB unit. The hydrodynamics are based on the work by Brereton et al. (1988) where gas mixing in a CFB reactor was described by a simple two-phase model (see Figure 3.1). The gas flow in the core region is characterized by axially dispersed plug flow, and there is assumed to be no gas flow through the annulus region.

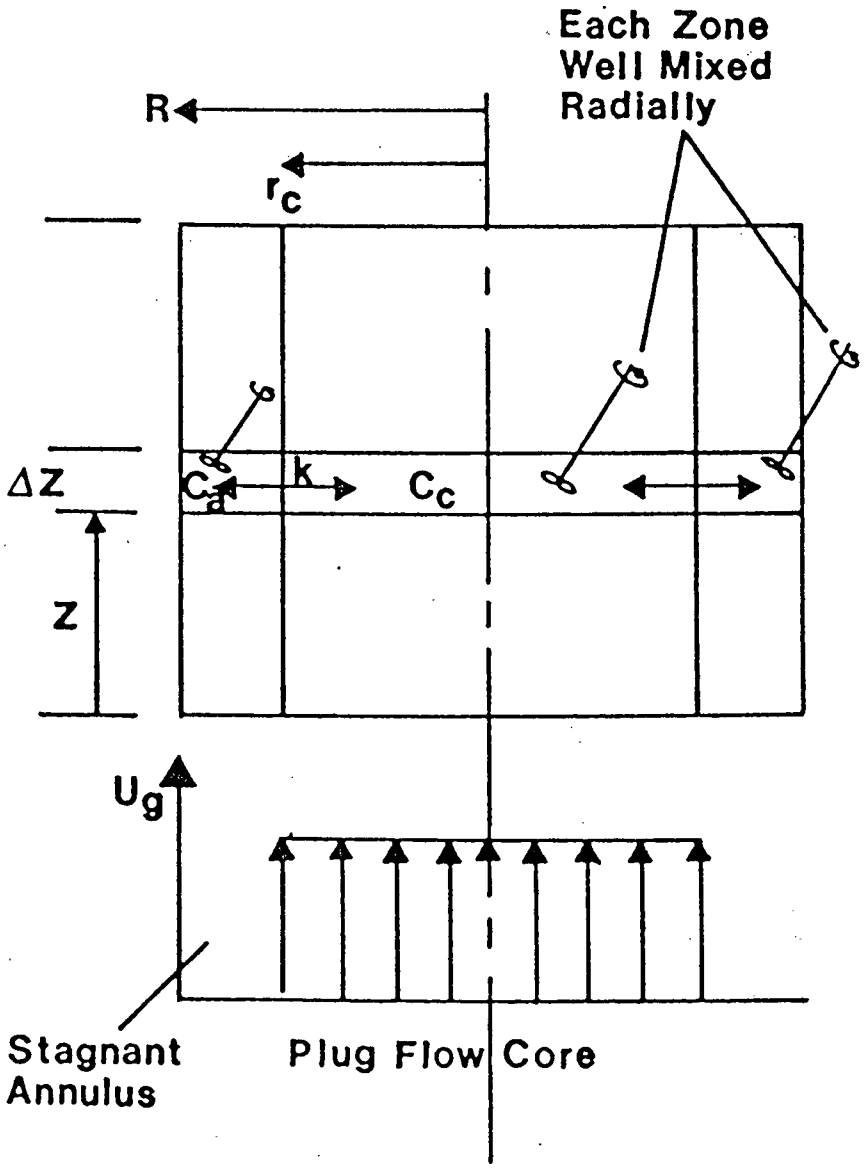

Figure 3.1 Two Zone Model for Gas Mixing in a CFB.
Ca=conc. in annulus; Cc=conc. in core;
rc=core radius; R=column radius;
k=mass (crossflow) coefficient. [Brereton, 1987]

The key assumptions made in the incineration model regarding the hydrodynamic characteristics of a CFB are:

(1) The CFB riser is a circular column.

(2) A core-annulus flow pattern exists in the riser.

(3) The gas flow in the core region is described by a dispersed plug flow model, in which axial dispersion is imposed on plug flow of gases.

(4) There is no gas flow through the annulus region.

(5) The thickness of the annulus does not vary with height in the riser.

(6) The core and annulus are well mixed radially and there is radial mass transfer from the core to the surrounding annulus.

(7) There is negligible axial dispersion in the annulus.

(8) The mass transfer coefficient, K_M, does not vary with height.

(9) Radial dispersion is negligible.

(10) The riser is an isothermal reactor.

Radial dispersion can be neglected in comparison with axial dispersion when the reactor diameter-to-length ratio is very small and the flow is turbulent [Wen and Fan, 1975]. The CFB riser diameter-to-length ratio is 0.021 and the flow is turbulent as shown by the Reynolds number (e.g., for a temperature of 900 ^{o}C and superficial gas velocity of 7.5 m/s, Re = 7300). Hence, the radial dispersion was neglected. All of the combustion air is considered to enter from the bottom of the riser. The effects of staged combustion air, i.e. secondary air injection, are not considered.

A correlation for the axial dispersion coefficient, D, for single phase flow of fluids through an empty tube or pipe and for $N_{Re} > 2000$ is [Wen and Fan, 1975]:

$$\frac{1}{N_{Pea}} = \frac{3.0E7}{N_{Re}^{2.1}} + \frac{1.35}{N_{Re}} \tag{3.5}$$

where

$$N_{Pea} = \frac{Ud}{D} \qquad \text{(Peclet number)} \tag{3.6}$$

$$N_{Re} = \frac{Ud\rho}{\mu} \qquad \text{(Reynolds number)} \tag{3.7}$$

where

U = average fluid velocity (m/s)

d = pipe diameter (m)

ρ = fluid density (kg/m^3)

μ = fluid viscosity (kg/ms)

D = axial dispersion coefficient (m^2/s)

At low Reynolds number corresponding to laminar flow, dispersion is mainly due to molecular diffusion whereas at high Reynolds number corresponding to turbulent flow, dispersion is mainly due to turbulent fluctuations [Wen and Fan, 1975].

The differential equations governing flow, reaction and dispersion for the riser core and annulus during steady state are as follows:

Core:

$$D\frac{\partial^2 C_C}{\partial z^2} - U_C\frac{\partial C_C}{\partial z} - \frac{2K_M(C_C - C_A)}{R_C} - K_R P_{O2} C_C = 0 \qquad (3.8)$$

Annulus:

$$-\frac{U_A \partial C_A}{\partial z} + \frac{2K_M R_C (C_C - C_A)}{R_R^2 - R_C^2} - K_R P_{O2} C_A = 0 \qquad (3.9)$$

where

C_A = concentration of compound in the annulus (mol/m^3)

C_C = concentration of compound in the core (mol/m^3)

D = axial dispersion coefficient (m^2/s)

K_M = mass transfer (crossflow) coefficient (m/s)

K_R = reaction rate constant (1/s)

P_{O2} = partial pressure of oxygen (mole fraction)

R_R = radius of the riser column (m)

R_C = radius of the core (m)

U_A = superficial gas velocity in the annulus (m/s)

U_C = superficial gas velocity in the core (m/s)

z = height coordinate (m)

Wen and Fan (1975) suggested that suitable boundary condition for a dispersion model reactor must be such that the computations under isothermal steady state conditions should be consistent with the limits of maximum and minimum conversion attainable for the first order

reaction corresponding to D approaching 0 for plug flow and D approaching infinity for complete mixing conditions, respectively. A boundary condition consistent with this criterion is equivalent to what is classified as a 'closed-closed' system, where there is no dispersion of material in and out of the system. The boundary conditions are shown below.

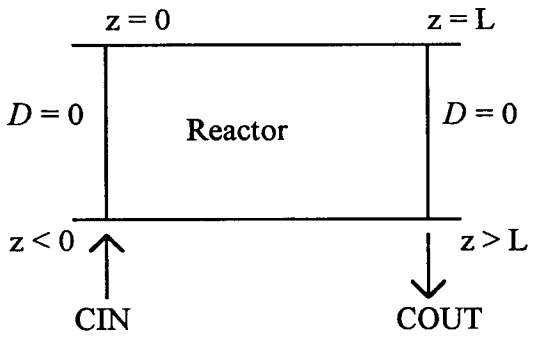

At z = 0,

$$UC_{z\to 0+} - UC_{IN} = D\left(\frac{\partial C}{\partial z}\right)_{z\to 0+} \qquad (3.10)$$

At z = L,

$$\frac{\partial C}{\partial z} = 0 \qquad (3.11)$$

Equations (3.8) and (3.9) were solved for the case of a stagnant annulus (i.e. U_A = 0 m/s) and the boundary conditions given above. Numerical integration was performed using the finite difference method with forward sweep. The computer code was written in FORTRAN and solved on the UBC mainframe computer system. The program code is provided in Appendix A.

The experimentally determined destruction profiles of SF_6 were compared to those predicted by the computer model. The experimental and computer-generated results are discussed in section 7.3.

4. UBC PILOT CFB FACILITIES

A simplified schematic description of the UBC pilot CFB combustor unit is shown in Figure 4.1. Detailed description of each of the key reactor and return system components follow.

4.1 Reactor Shaft

The principal reactor shaft or riser is composed of five refractory-lined flanged sections providing a chamber of 152 mm square cross-section with an overall height of 7.32 m. A view of the reactor is shown in Figure 4.2. The refractory is erosion resistant and held in place by pins welded to the outside steel walls. The bottom section, which has stainless steel walls, is tapered gradually on the inside from a 51 mm by 152 mm cross-section at the bottom to 152 mm by 152 mm over its 1.22 m height. This feature is to provide a high velocity region which helps to prevent agglomeration and sintering. Pressure taps and thermocouples are located at 610 mm maximum intervals along opposite east and west faces of the column. In addition, there are twelve regularly spaced 41 mm diameter ports which can be used as viewing ports, for withdrawal of gas/or solids samples or for insertion of probes and feed nozzles.

The distributor and plenum chamber are suspended from the bottom of the reactor for easy removal. Primary air is introduced to the bottom of the reactor through a novel distributor shown in Figure 4.3. This distributor has twenty 9.5 mm diameter orifices drilled at 30 to 50 degrees to the horizontal axis. Located at the centre of the base is a 38 mm tube which allows for easy removal of small agglomerates of sintered solids and other oversize material. The plenum chamber is also equipped with a drain pipe for removal of solids that might flow back through the distributor during shut-down. For start-up of the unit, the primary air is preheated in an external burner by combustion of natural gas. Secondary air is introduced at

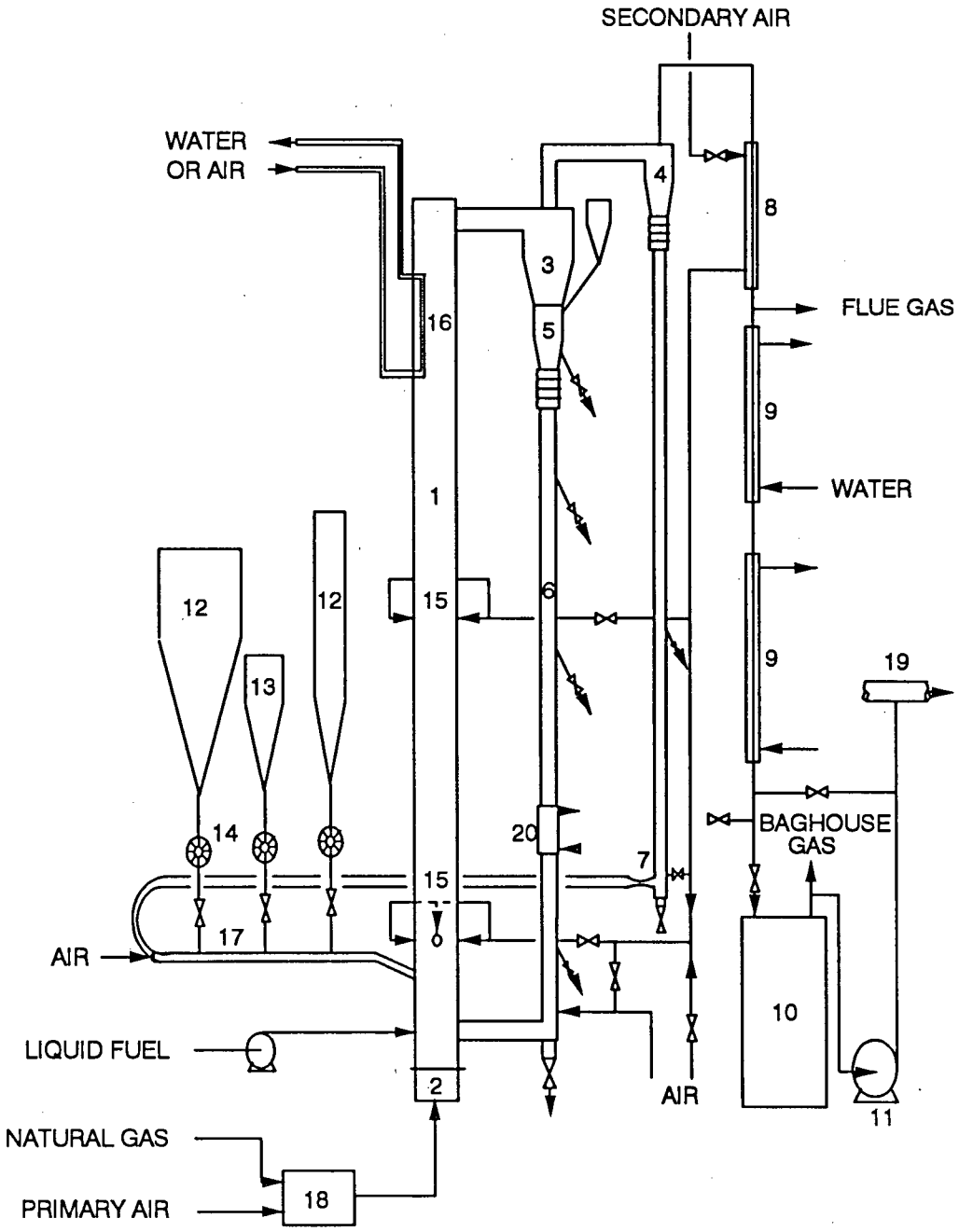

1. Reactor; 2. Windbox; 3. Primary cyclone; 4. Secondary cyclone; 5. Recycle hopper; 6. Standpipe; 7. Eductor; 8. Secondary air preheater; 9. Flue gas cooler 10. Baghouse; 11. Induced draught fan; 12. Fuel hopper; 13. Sorbent hopper; 14. Rotary values; 15. Secondary air ports; 16. Membrane wall; 17. Pneumatic feed line; 18. External burner; 19. Ventilation; 20. Calorimetric section;

Figure 4.1 Simplified Schematic Diagram of Circulating Fluidized Bed Combustion Facility (UBC)

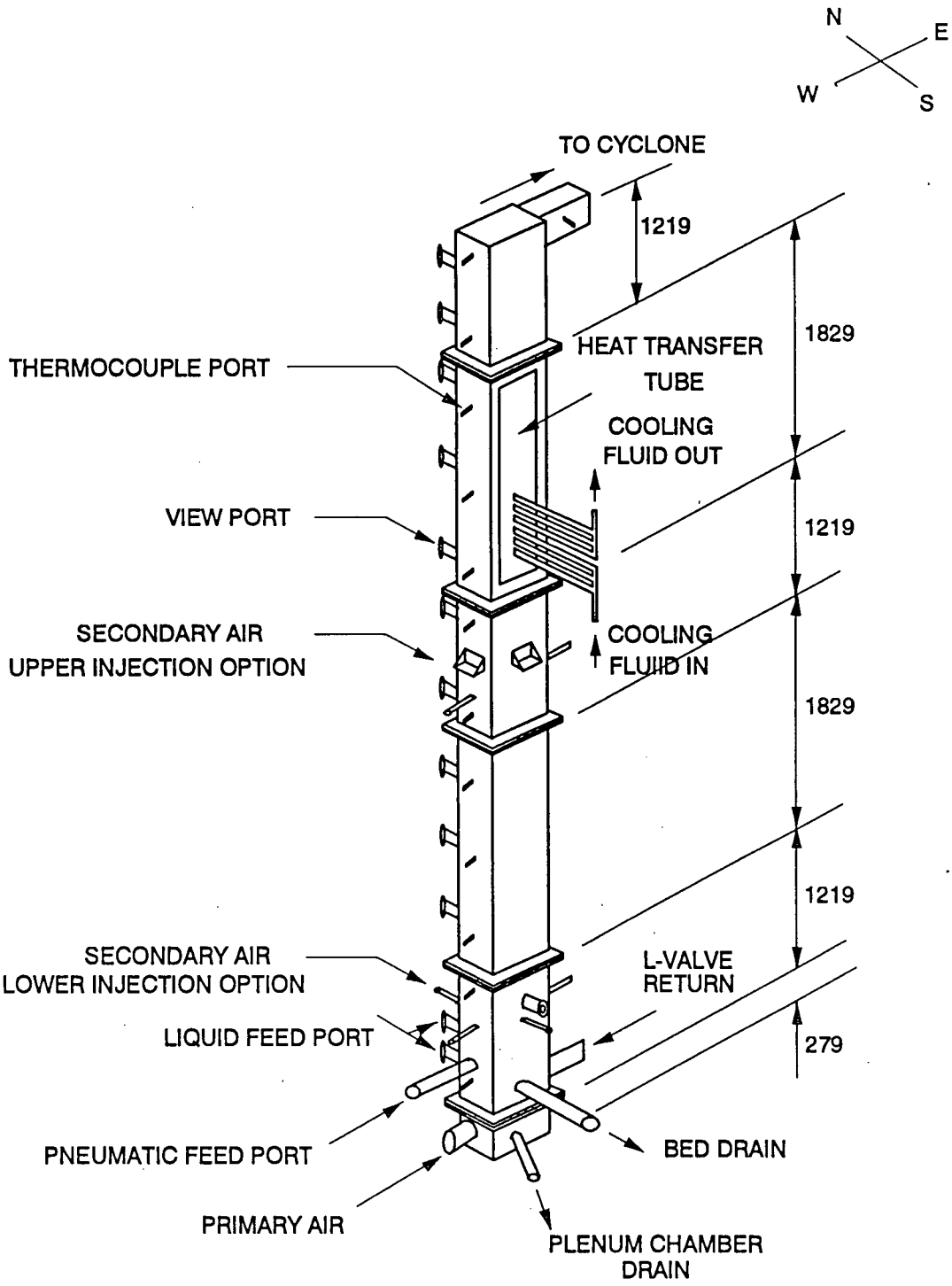

Figure 4.2 View of Principal Refractory-lined Reactor Column
(All dimensions are in mm)

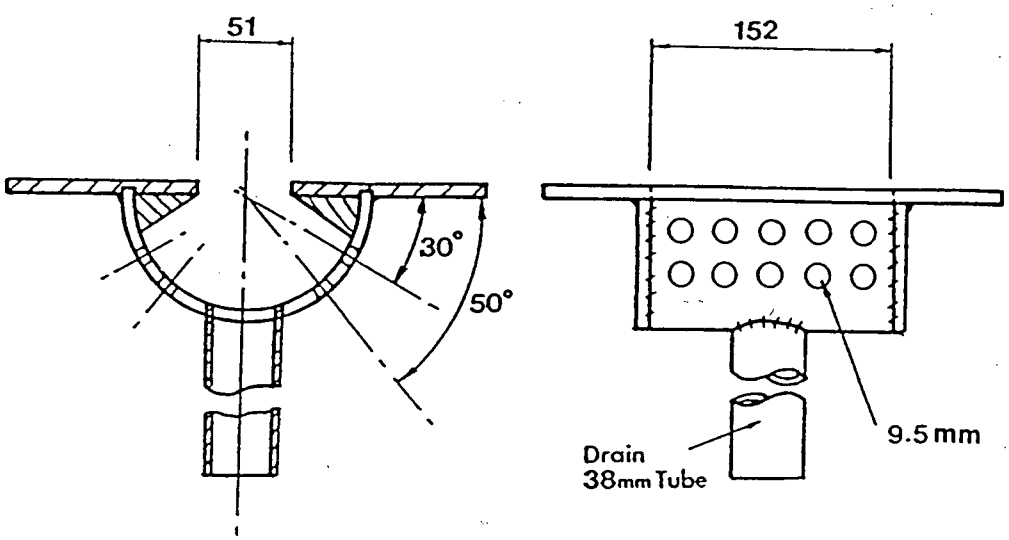

(a) Front view (b) Side view

Figure 4.3 Primary Air Distributor

0.9 m above the distributor plate. Air introduction at a height of 3.4 m above the distributor level was further added because NO_x emissions were insensitive to the primary-to-secondary air split when the secondary air was introduced at 0.9 m above the distributor plate. It was believed that introduction at such a low level was eliminating a true staging effect. By introducing secondary air at a higher level, there was some improvement in the sensitivity of NO_x emissions to staging [Zhao, 1992]. However, for high volatile fuels, the effect of introducing secondary air at a higher level was to increase the total NO_x emissions. The secondary air was introduced at 3.4 m above the distributor for this work.

4.2 Fuel Feed Systems

4.2.1 Solids Feed System

The feed system varies according to the type of fuel burned. For solid fuel feeding, the system consists of up to three sealed hoppers (one for a high reactivity start-up coal, the second for the fuel to be studied and a third for sorbent). In previous work, only two hoppers were available, and it was more convenient to premix the test fuel/sorbent to the specified Ca:S ratio. Interest in control studies, which would require continuous variation in limestone feed rate, and improved flexibility prompted the addition of the third hopper. The capacities are 2 drums of solid fuel (approx. 360 kg) for the large hopper, 1 drum (approx. 180 kg) for the smaller start up hopper and approximately 20 kg for the limestone hopper. The solid fuel or fuel/sorbent mixture is fed pneumatically through a 38 mm diameter pipe entering the reactor at an angle of 15 degrees downward to the horizontal. Generally, the pneumatic conveying air is first used to pick up secondary cyclone solids; it then entrains the feed fuel and limestone. If it is not desirable to recycle the secondary cyclone catch, it is possible to bypass this pick-up and take fuel feed air directly from the main compressed air line. The solids feed rates are controlled by means of rotary valves, one per hopper, with rubber impellers and a transparent

front to allow visual verification that the feeder is operating properly at all times. All three hoppers are mounted on load cells which allow the feed rates to be determined by weight loss over a period of approximately 5 minutes.

4.2.1.1 Alcan Solids Feed System

In the existing solids feed system, the feed solids are entrained with the fine solids recycled from the secondary cyclone return via a pneumatic transport loop. Data from previous combustion runs showed that the temperature of the solids at the secondary cyclone return (before the eductor) varies between 60 and 200 ^{o}C depending on the combustion temperature inside the combustor. The pitch cones have a softening point of 125 ^{o}C [Alcan]. Hence, potential plugging problems may occur in the feed line. Consequently, samples of the solid waste materials were subjected to bench scale heating tests in order to determine their softening and melting points. The results of these tests showed that only the stud blast fines did not soften at all between 80 and 180 ^{o}C. The other solid waste materials, i.e. pitch cones, miscellaneous paste waste and the pitch dust, have softening points ranging from 100 to 125 ^{o}C.

As a result of the bench scale heating test, modifications to the existing solids feed system were made. The solids from the secondary cyclone return were recycled back into the combustor via the existing pneumatic conveying air loop, but the feed solids were no longer entrained using this feed loop. A new feeding system for the temperature sensitive solids was designed and implemented. The key components of the new solids feeding system consist of a separate pneumatic air line, two flowmeters, a pressure gauge, a 50.8 mm carbon steel inverted Y-piece and a water-cooled feeder probe (see Figure 4.4). The pneumatic air flow rate is controlled by two flowmeters connected in parallel for a maximum flow rate of approximately 34 m^3/h (20 SCFM). The calibration curves for these two flowmeters are

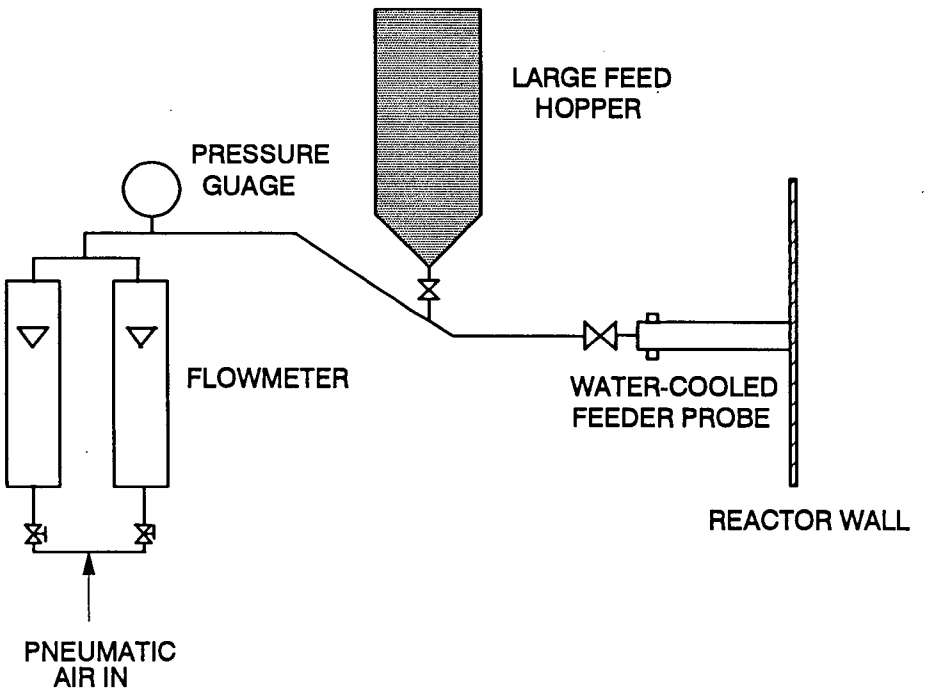

Figure 4.4 Schematic Diagram of Alcan Solids Feed System

provided in Appendix B. The solids from the large feed hopper are dropped into the inverted Y-piece, entrained by the pneumatic air into the water-cooled feeder probe and fed into the reactor from the north face. The feeder probe, which can be air or water cooled, consists of two concentric stainless steel tubes, baffles on the outer surface of the inner stainless steel tube and a ram-rod for removal of solids build-up in the inner tube (See Figure 4.5). The solids travel through the inner tube while cooling water travels past the baffles to maintain the temperature of the solids below their softening point temperature. The feeder probe is inserted into the liquid feed port (on the north face of the riser) shown in Figure 4.2 and projects 10 mm into the riser. Care was taken to ensure that the pneumatic air velocity was low enough (between 10 to 12 m/s) that the solids do not shoot out through the probe and impinge on the opposite refractory wall surface, and at the same time high enough to prevent solids from settling in the feed line. This pneumatic air flow is accounted for as part of the total primary air flow rate.

4.2.2 Chloroform Feed System

A liquid feed system was designed and implemented to introduce chloroform into the pilot CFB. A schematic of the chloroform feed system is shown in Figure 4.6. The key components of the feed system consist of a chloroform feed tank, a peristaltic pump with a variable speed controller, a compressed air line with a control valve and a 6.35 mm 316 stainless steel feed tube. Compressed air was used to provide atomization of chloroform instead of using a spray nozzle. The feed tube is inserted into a thermocouple port on the north face of the riser located 1067 mm above the distributor plate and 13 mm into the riser. The flow rate of chloroform is provided by the calibration curve of the pump and also by the weight loss in the chloroform feed tank over the duration of the test.

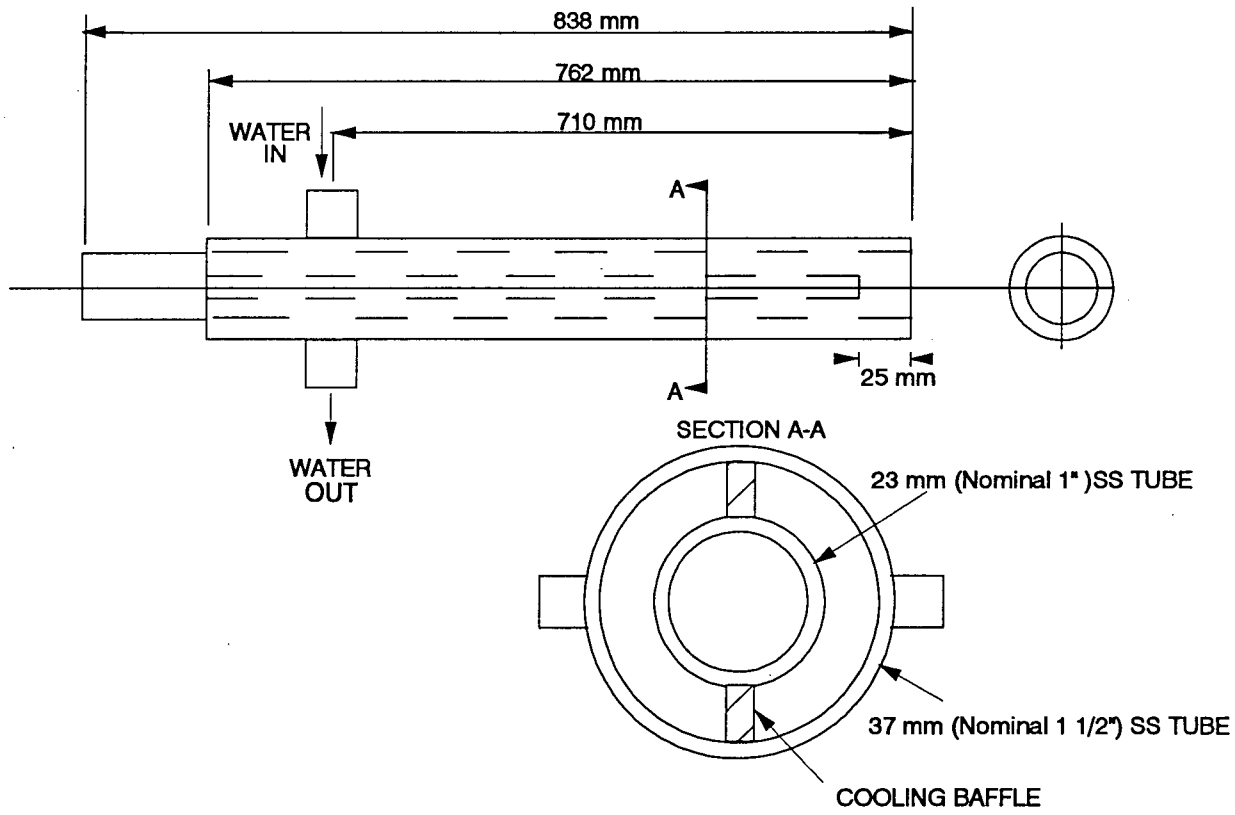

Figure 4.5 Water-Cooled Feeder Probe

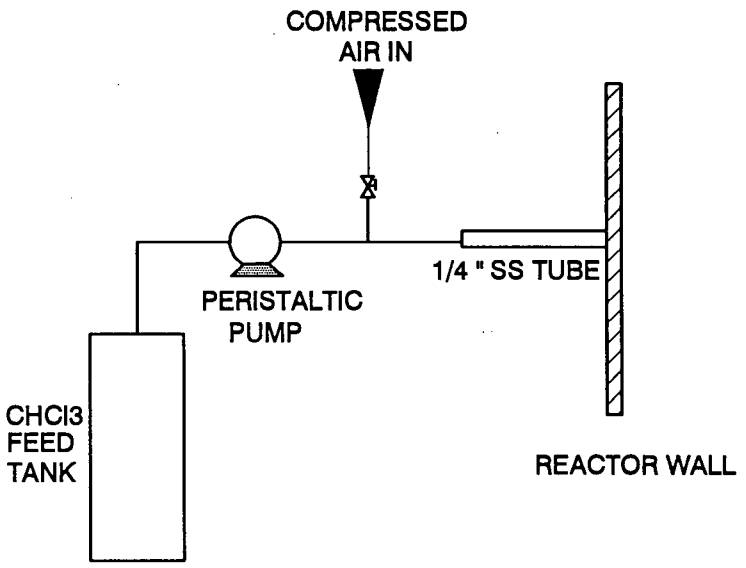

Figure 4.6 Schematic Diagram of Chloroform Feed System

4.2.3 Sulphur Hexaflouride Feed System

A gas feed system was designed and implemented to introduce sulphur hexafluoride into the pilot CFB. A schematic of the SF_6 feed system is shown in Figure 4.7. The key components of the feed system consist of a SF_6 gas cylinder and regulator, a digital balance, a flowmeter, a pressure gauge and a 6.35 mm 316 stainless steel feed tube. The feed tube was inserted into a thermocouple port located after the natural gas burner. The SF_6 was pre-mixed with the primary combustion air entering the plenum chamber. The flow rate of SF_6 was measured by the weight loss of the SF_6 cylinder over 10 minute intervals and by the flowmeter.

4.3 Heat Transfer Surface

The heat transfer section, located in the upper section of the combustor as shown in Figure 4.2, contains three heavy-wall stainless steel tubes of 12.7 mm OD and 9.4 mm ID, in a hairpin configuration as shown in Figure 4.8. This surface reasonably approximates a superheater plate. Water or air can be used as cooling fluid in one, two or three tubes at a time. This allows heat removal rates to be varied from 0 to approximately 20 kW, without problems due to thermal expansion since the tube bundle can expand freely inside the reactor. The heat transfer surface has a total exposed area of 0.34 m^2.

4.4 Solids Recycle Systems

Gas and entrained solids leaving the top of the reactor enter a refractory-lined medium-efficiency primary cyclone of inside diameter 305 mm. Solids captured in the primary cyclone drop into a conical recycle hopper. Make-up inert particles can also be added into this vessel from a small external hopper. From the bottom of the vessel, the solids descend in moving

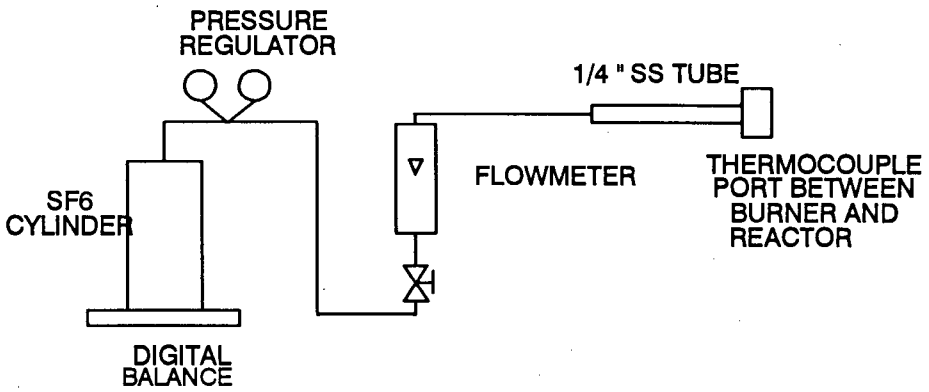

Figure 4.7 Schematic Diagram of Sulphur Hexafluoride Feed System

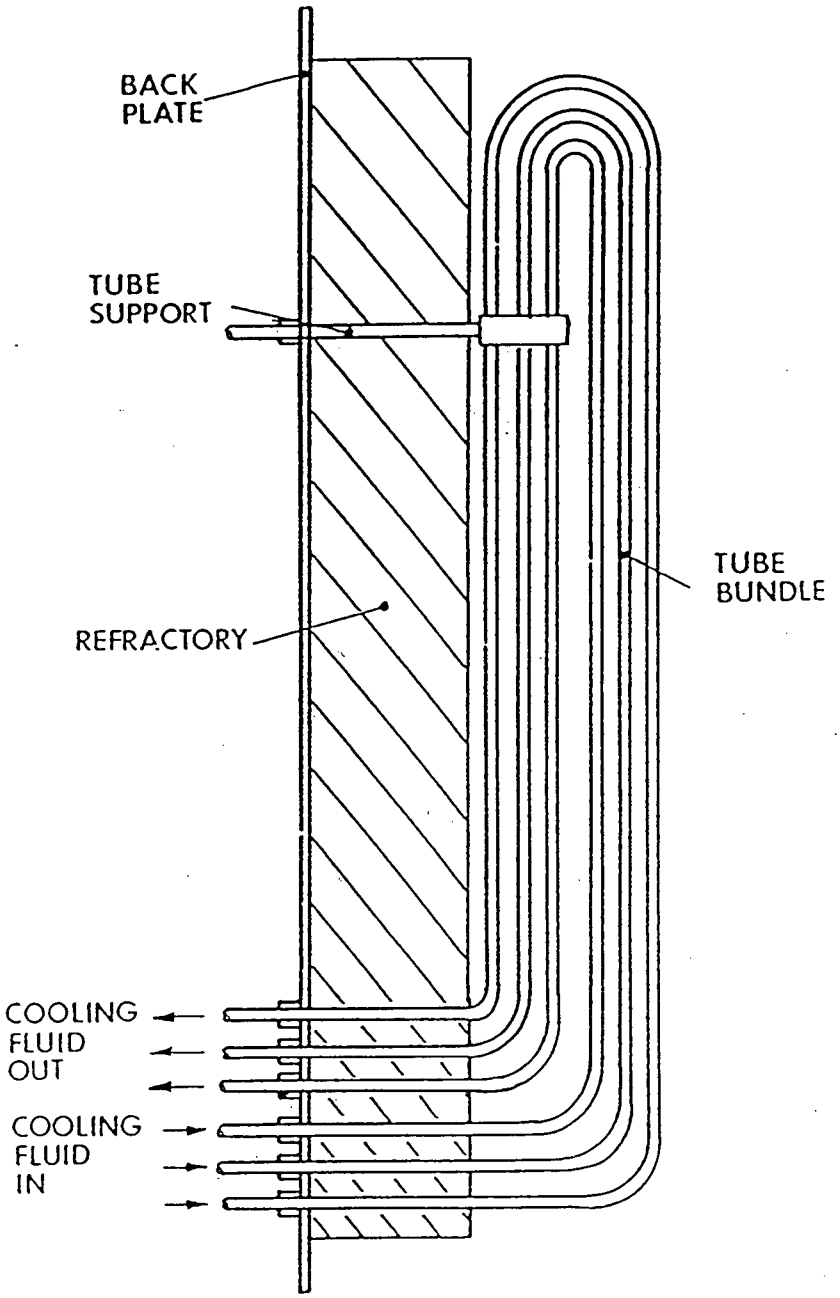

Figure 4.8 Hairpin Configuration Heat Transfer Surface

packed bed or fully fluidized flow in a 102 mm ID, 4.72 m long externally insulated stainless steel standpipe, forming the vertical leg of an L-valve. There is a bellows-type expansion joint between the top of the standpipe and the bottom of the recycle hopper to allow for thermal expansion. The solids are returned to the reactor 152 mm above the primary air distributor through the horizontal section of the L-valve which is 790 mm long and 102 mm ID.

The circulation rate is controlled by the amount of aeration air fed to the L-valve at a single point, 102 mm above the horizontal axis of the L-valve. The circulation rate of solids can be measured by calorimetry. The calorimetric section, shown in Figure 4.9, consists of a 584 mm long jacketed section of the standpipe beginning 1.06 m above the bottom of the L-valve. Cooling air is passed through the jacket which is insulated on the outside. Determination of the coolant flow rate and its inlet and outlet temperatures allows the total heat exchange to be calculated. By measuring the solids temperature entering and leaving the jacketed section of the pipe and ignoring the contribution of interstitial gas to the energy loss, it is then possible to estimate the mass flow rate of solids (Burkell et al., 1988). The solids temperature is measured at four radial positions (at 0, 25, 37.5 and 50 mm from the wall) at two levels across half the diameter of the standpipe. Numerical integration then provides a measure of the average solids temperature.

Gas and entrained solids leaving the primary cyclone are directed to a 203 mm ID, high-efficiency secondary cyclone made of stainless steel and insulated externally. Solids captured in the secondary cyclone fall into a 76 mm diameter dipleg and are returned to the bottom of the reactor by the jet eductor shown in Figure 4.10. The purpose of the eductor is to enable

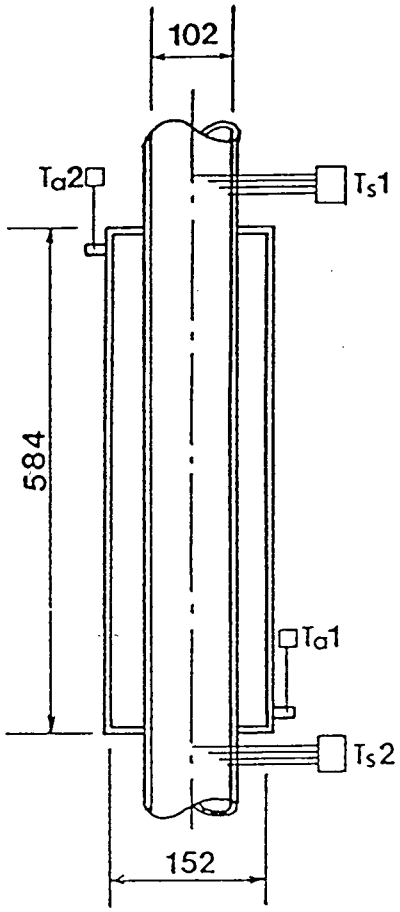

Figure 4.9 Calorific Section for Measuring Solids Circulation Rate (All dimensions are in mm) (Tai: air temperature; Tsi: average solid temperature)

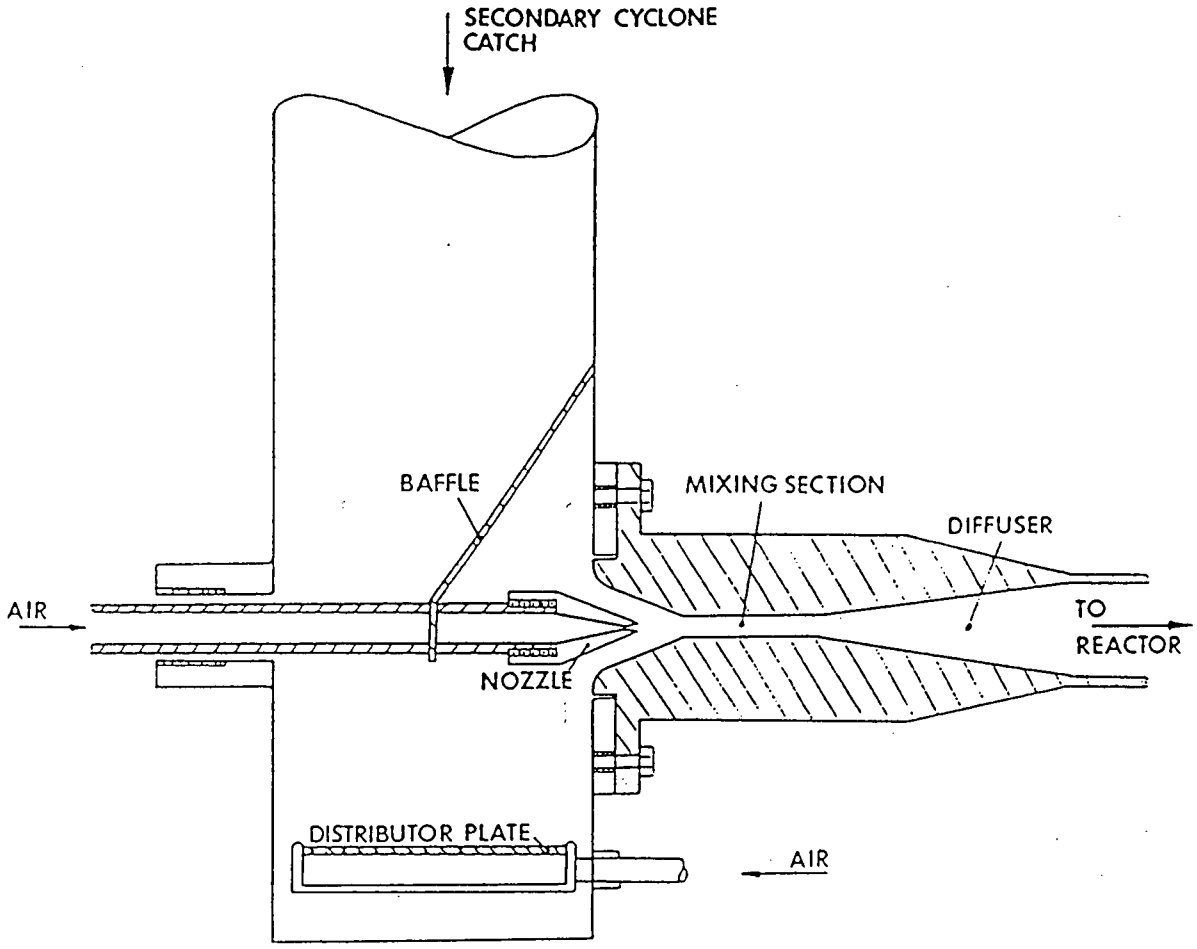

Figure 4.10 Eductor Configuration for Secondary Solids Return

the solids from the secondary cyclone, together with a small amount of gas, to be returned to the reactor bottom which is at a higher pressure. A small amount of air is fed to the distributor (see Figure 4.10) to keep the solids fluidized. Larger particles, which might obstruct the venturi section, fall onto the distributor. The distributor can be rotated to allow removal of solids through a ball valve below. The air fed to the eductor nozzle, together with that entrained from the base of the cyclone, is then used as pneumatic gas flow for solid fuel feeding. The oxygen or carbon dioxide concentration can be measured in the dipleg to ensure that the air introduced in the eductor and by the distributor are drawn downward so that the performance of the secondary cyclone is not adversely affected by air rising from below.

4.5 Gas Cooling and Analysis

Gas leaving the secondary cyclone is cooled on the inside of three double-pipe heat exchangers in series. The first of these heat exchangers may be used as the secondary air preheater, while the other two are water-cooled. The third heat exchanger offers the possibility of further cooling with three independently controlled internal water-cooled coils. Particulate solids are removed from the flue gas in the baghouse before the flue gas enters an exhaust duct connected to an induced draught (I.D.) fan. The flue gas is then directed into the building ventilation duct. The I.D. fan creates a negative pressure in the baghouse eliminating the risk of flue gas leaking into the laboratory.

Gas samples taken from five axial positions along the reactor, from between the two cyclones and from the flue gas after the first heat exchanger can be monitored continuously to determine concentrations of O_2, CO_2, CO, SO_2, NO and unburned hydrocarbons (as CH_4). A sampling point after the baghouse filter was added to the existing sampling points and a portable multipoint sampling system was developed and implemented. The details of these additions and the analytical instruments are described in more detail below.

4.6 Solids Sampling System

Solids samples can be withdrawn from seven positions in the reactor system (Figure 4.11):

(1) from the bottom of the reactor shaft through a ball valve;

(2) from the top of the reactor

(3) obliquely from the recycle hopper below the primary cyclone;

(4) from one of the three positions on the standpipe: near the top, in the middle or just above the L-valve aeration air port;

(5) from the L-valve corner below the aeration point;

(6) from the secondary cyclone return leg by rotating the distributor plate below the eductor and

(7) from the baghouse.

4.7 Instrumentation and Data Acquisition

The system instrumentation consists of the following:

(a) flowmeters for measuring all air, water and SF_6 flow rates;

(b) thermocouples throughout the entire system to allow measurement of temperature profiles (see Figure 4.12);

(c) pressure transducers connected to pressure taps on the main reactor to allow measurement of pressure profiles and of the overall pressure drop;

(d) load cells supporting all three hoppers to determine the solid and sorbent feed rates;

(e) digital balance to determine the average chloroform and SF_6 feed rates over time; and

(f) gas analyzers, as described below.

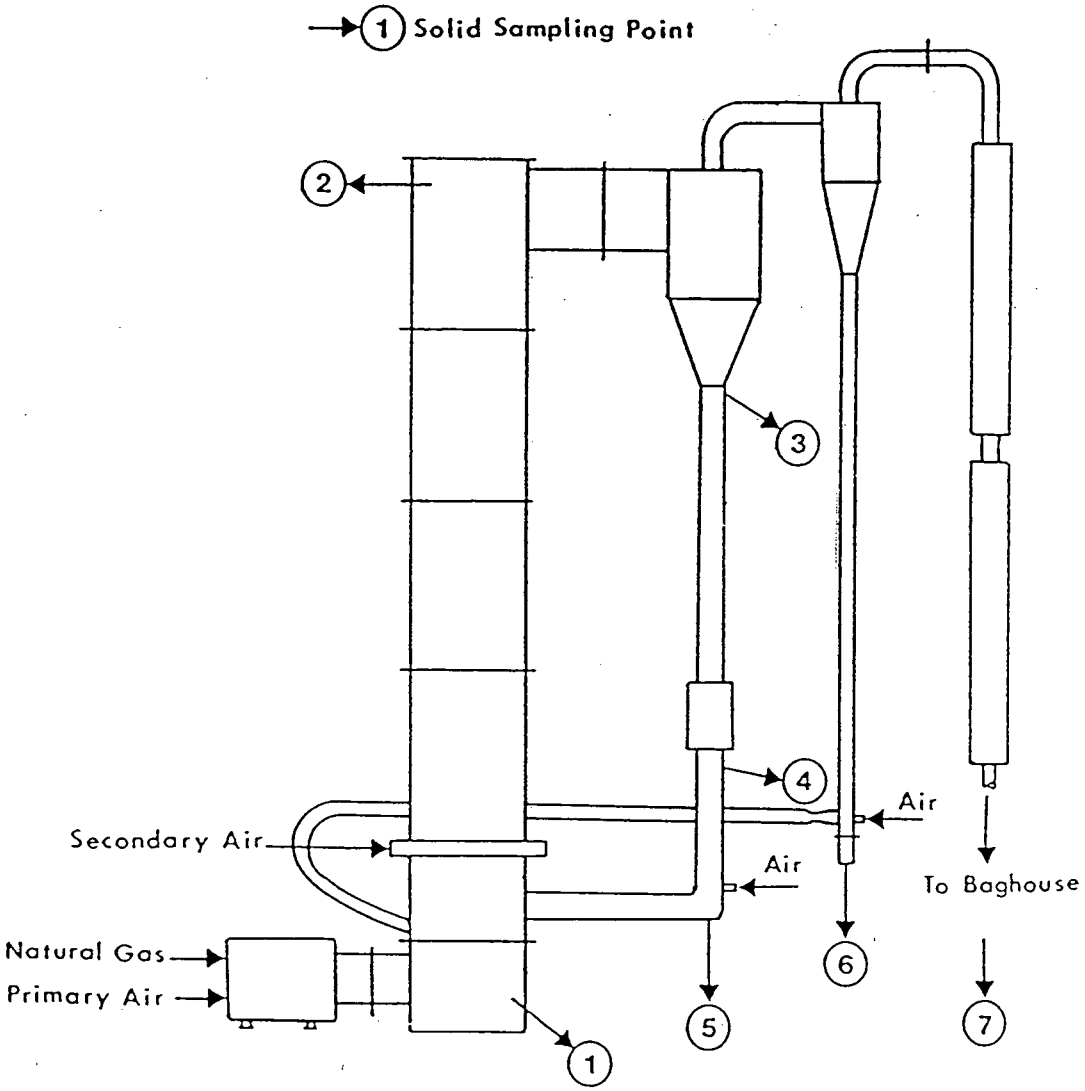

Figure 4.11 Locations of Solids Sampling Ports

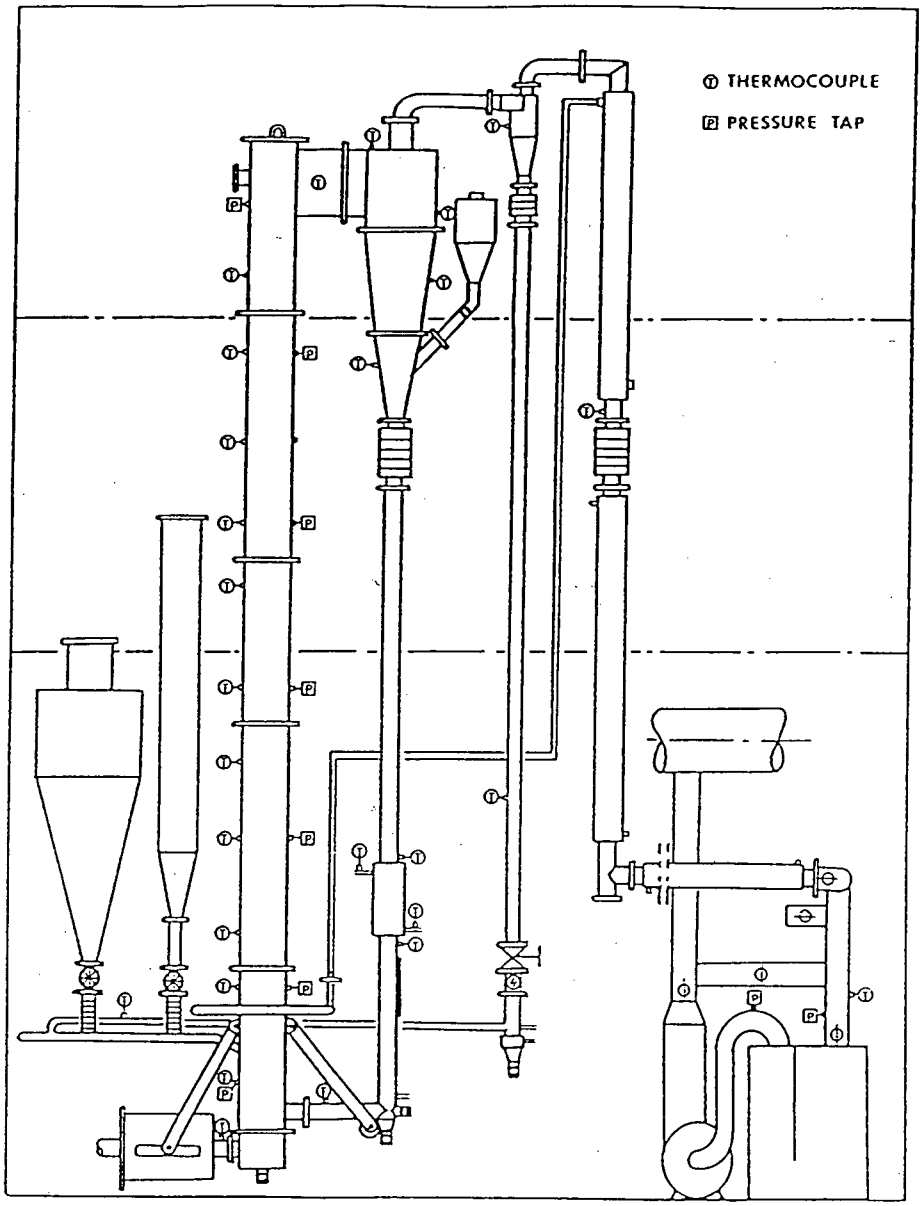

Figure 4.12 Thermocouple and Pressure Tap Locations
in CFBC Reactor System

Data acquisition is provided by an AT&T 6300 PC equipped with a Metrabyte interface permitting up to 4000 samples per second using BASIC language. It may be expanded with up to eight multiplexer boards with 16 channels on each board. Electrical outputs from thermocouples, pressure transducers and gas analyzers can be stored and processed in the computer. The load cells are connected through summation boxes to digital readouts. Air, water and SF_6 flow rates are read from calibrated flowmeters. An Optomux system is used for automatic control and for transient testing work. This utilizes a different set of A/D converters than the Metrabyte system. Using its D/A capability it can also be used to send signals to automatic control valves on the primary, secondary and L-valve air lines, and to the rotary valves on the fuel and limestone feed systems.

4.8 Gas Sampling System

A portable multipoint gas sampling system was developed and used to withdraw gas samples from different axial and radial locations in the combustor. Analysis of the samples allows construction of concentration profiles which help to provide information on formation and destruction mechanisms of various gaseous species.

Sample gas can be withdrawn at five different heights along the combustor (see Figure 4.13) as well as between the two cyclones and from the flue gas conduit. A new gas sampling point located after the baghouse filter, which would be equivalent to the stack discharge in an industrial setting, was added in order to have a more accurate representation of the gas composition. A vacuum pump was used to draw the gases leaving the baghouse filter through the sampling train shown in Figure 4.14. Approximately 1000 cm^3/min. (1 litre per minute) of gas flowed through the analyzers while the excess was vented. An electrochemical oxygen analyzer was used to measure the oxygen concentration in the gas stream leaving the flue gas

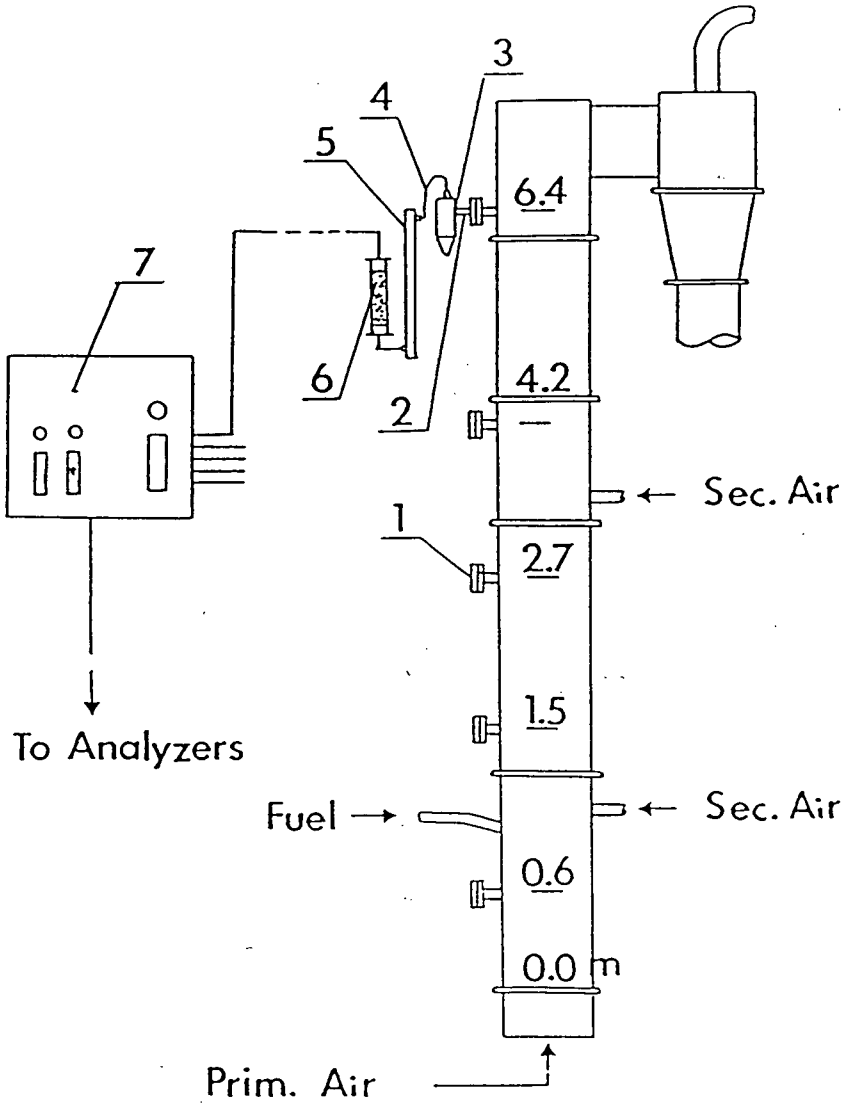

1. Sampling port;
2. Sampling probe extending into reactor;
3. Gas filter; 4. Flexible Stainless steel tubing;
5. Heat exchanger; 6. Dryer; 7. Control panel.
(Note that only one of the five sampling trains is shown.)

Figure 4.13 Vertical Gas Sampling Positions and Sampling Train

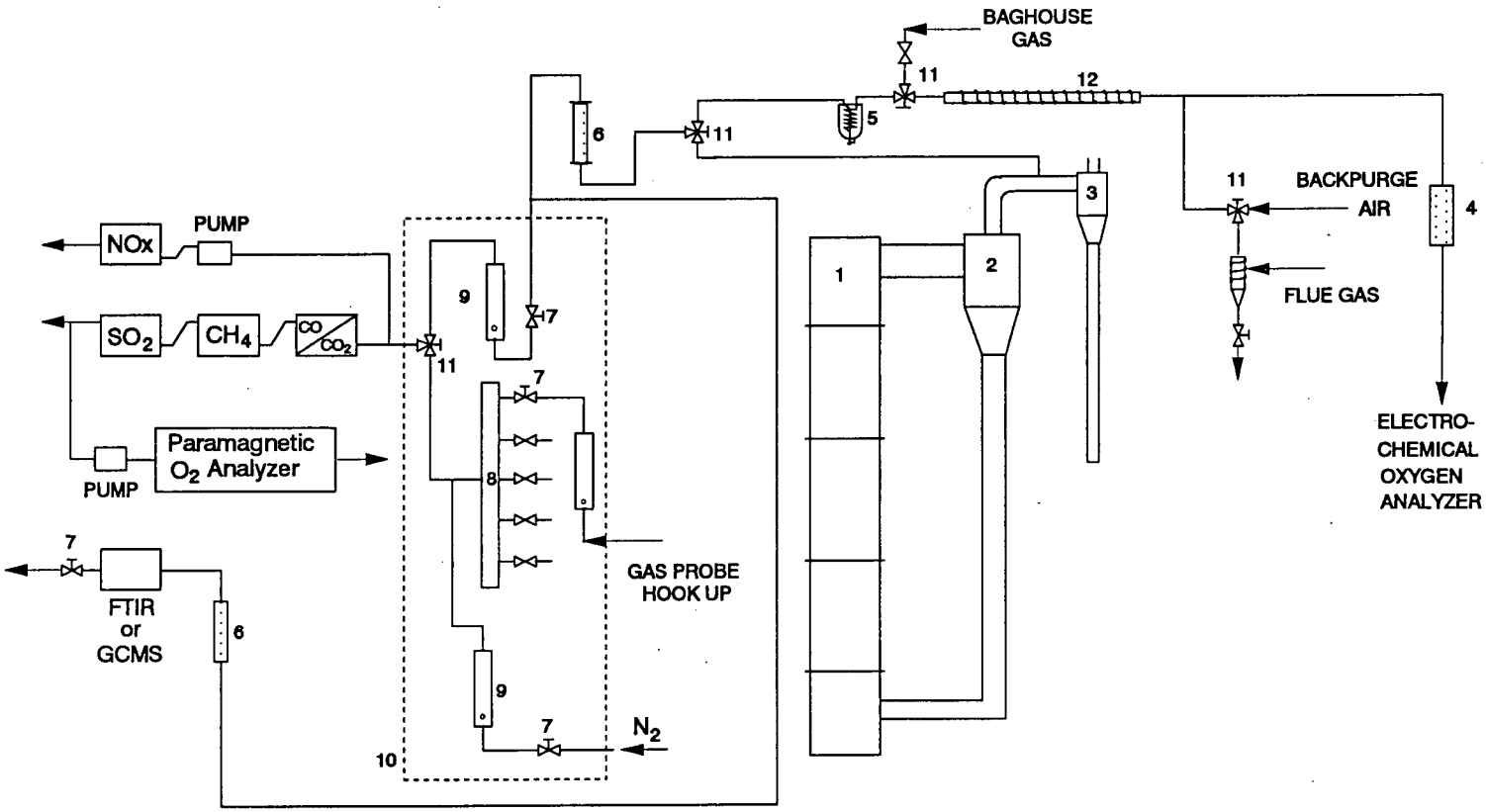

1. Reactor; 2. Primary cyclone; 3. Secondary cyclone;
4. Gas filter; 5. Water trap; 6. Dryer; 7. Control valve;
8. Manifold; 9. Rotamter; 10. Control panel; 11. Three-way valve;
12. Electrically heated gas sampling line

Figure 4.14 Gas Sampling System

filter. A paramagnetic oxygen analyzer was used to measure the oxygen concentration in the gas stream leaving the flue gas filter or the baghouse filter, depending on the sampling point. The portable multipoint sampling system can be used to withdraw gas from any of the five vertical locations along the riser. At a given vertical location, gas samples were obtained at one of the three points along a horizontal line between the back (north) and front (south) walls: (a) on the riser axis; (b) at the middle position 75 mm from the wall; (c) the wall position (flush with the wall surface).

4.8.1 Portable Multipoint Gas Sampling System

In the old stationary multipoint gas sampling system, a gas sample probe was inserted into the reactor at the desired location. These probes were connected to their respective filters by flexible stainless steel tubing, allowing them to be moved to different radial positions. The sample gas flowed through a porous stainless steel filter in which the gas and solids were separated. The gas was then cooled in a water-cooled heat exchanger. Condensed water was drained from the bottom of the exchanger. A drying tube filled with magnesium perchlorate, $Mg(ClO_4)_2$, was used to remove any residual moisture before the sample gas reached a manifold on the analyzer control panel (see Figure 4.13). The stationary system resulted in five gas probes and their corresponding sets of filter, heat exchanger and drier systems. This sampling strategy was very time consuming. The large quantities of solids collected in the probe as well as in the stainless steel filter tended to cause blockages. Hence, compressed air was used to purge the filter to remove the solids but then one had to wait for the system to re-equilibrate before taking measurements.

A portable multipoint gas sampling system was developed to replace the five sampling trains with just one sampling train for ease of portability and to reduce the solids blockage problem. The key components of the new system consist of a gas sample probe, a 19 mm (3/4 inch)

diameter uncooled stainless steel tube with a ram-rod for solids removal, a solids knock-out chamber, a porous stainless steel filter, an ice bath, a drier system containing silica gel to remove moisture from the sample gas, flexible stainless steel tubing and quick connectors (see Figure 4.15). This system is contained within an angle-iron frame structure for portability. Solids were purged from each sample port by compressed air before insertion of the probe. The compressed air line was connected by a quick connector, which allowed the line to be clicked in and out of position. The process of solids purging using compressed air before gas sampling makes it easier to insert the probe and also reduces solids blockage. The majority of the solids were collected in the probe and in the solids knock-out chamber. The knock-out chamber is a modified porous stainless steel filter in which the filter was removed and holes were drilled on opposite sides to allow insertion of the ram-rod. The ram-rod, inserted through the solids knock-out chamber into the probe, allows solids to be removed without the use of compressed air. The larger particulates were removed from the gas stream in the knock-out chamber. As a result, fewer particles passed through the stainless steel filter, reducing solids blockages in the filter and allowing ample gas flow to the analyzers. The ram-rod and the solids knock-out chamber allows the sampling time to be reduced to approximately 3 to 4 hours for the 12 sampling positions (3 lateral positions at each of the 4 axial levels) as compared to 6 to 8 hours previously required with the stationary sampling system.

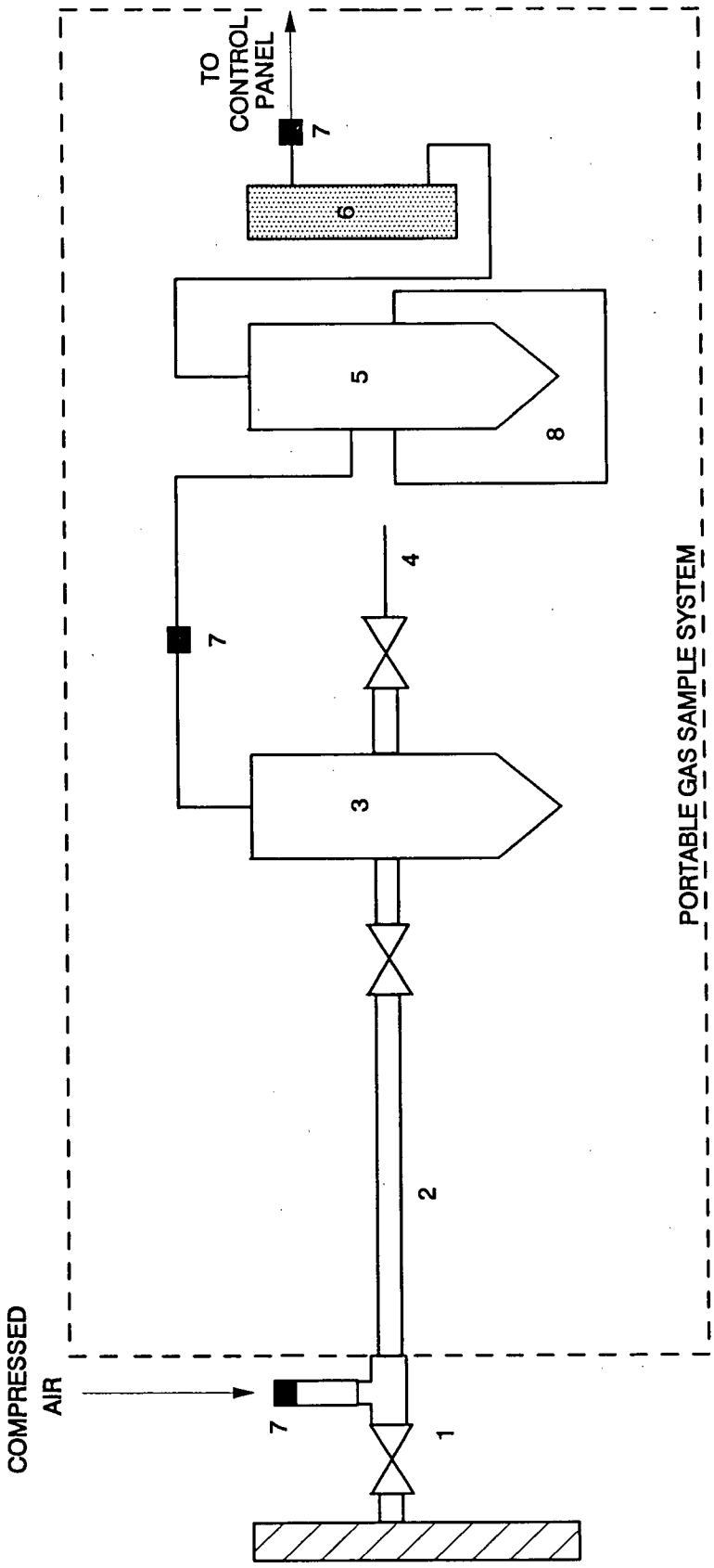

1. Reactor wall sample port; 2. Gas sample probe; 3. Solids knock-out chamber; 4. 1/4 " SS ram-rod; 5. Filter; 6. Dryer; 7. Quick connector; 8. Ice bath

Figure 4.15 Portable Multipoint Gas Sampling System

Different types of sampling probes have been used at different times (Zhao, 1992) including bare stainless steel tubes, outer-cooled double pipe heat exchanger probes and an inner-cooled probe. Quartz-lined probes have also been developed to eliminate any potential effect of catalytic NO_x reduction on high temperature stainless steel surfaces. The design of the externally-cooled probe is shown in Figure 4.16. This is probably the best overall probe from a point of view of immediately quenching any gas phase reactions. However, because of the high moisture contents of some of the flue gases, water-cooled probes tend to cause condensation, in turn resulting in blockage of the sampling tube by wet solids. Some gas concentration profiles were obtained using uncooled sampling elements. A series of calibration tests using these probes showed minimal burnout of hydrocarbons and CO along the probes due to very poor mixing at low suction velocities [Zhao, 1992]. NO_x reduction was also found to be minimal. Hence, profiles obtained with the uncooled probes are considered to provide a satisfactory representation of the true profiles within the combustor.

To minimize the possibility of reactions in the sampling lines, all sampling lines were made of stainless steel or Teflon. Air purge was used periodically to back-flush solids from the filters and sample lines. To ensure accuracy of gas sampling, the combustor was controlled at a small positive pressure using a damper on the flue gas line just upstream of the baghouse. Hence, no vacuum pump was needed on the sample line and there was no possibility of dilution due to air leakage into the sampling lines. A schematic of the complete sampling system is provided in Figure 4.14.

Continuous on-line gas analyzers used for emissions measurements include:

(1) a Horiba (Model PMA-200) paramagnetic O_2 analyzer,

(2) a Teledyne electrochemical O_2 analyzer,

(3) a Whittaker (Model Fuji 732) infrared CO/CO_2 analyzer,

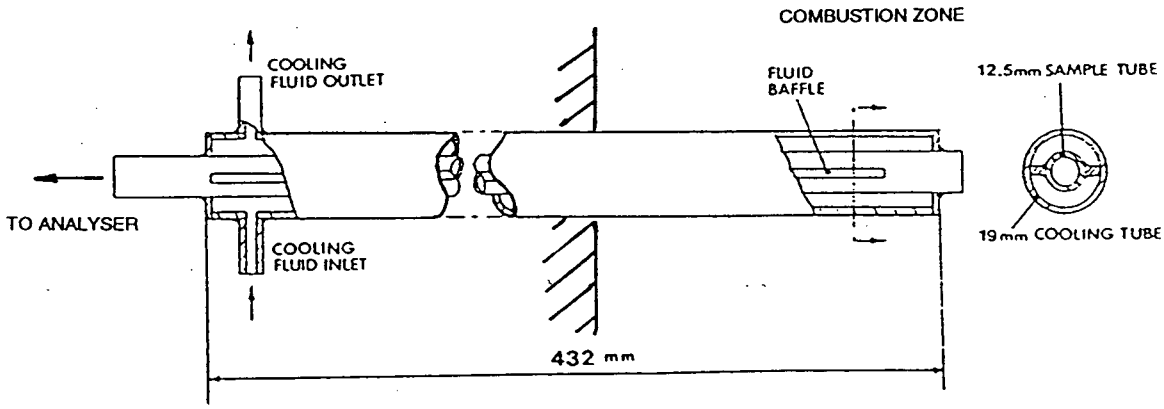

Figure 4.16 Gas Probe with Outer Water-Cooling

(4) a Whittaker (Model Fuji 730) infrared CH_4 analyzer,

(5) a Monitor Lab (Model 8840) chemiluminescence NO_x (NO and NO_2) analyzer and

(6) a Horiba (Model PIR-2000) infrared SO_2 analyzer.

The details of the analyzers are given in Table 4.1. A MIDAC high resolution FTIR spectrometer was used for periodic N_2O and NO_2 measurements. This has been found to give unambiguous and reproducible measurements for N_2O except in the presence of very high concentrations of volatile hydrocarbons such as at the bottom of the reactor [Brereton et al., 1991]. The FTIR spectrometer has the following specifications:

(1) A liquid nitrogen cooled Mercury Cadmium Telluride (MCT) detector with a resolution of up to 0.5 cm^{-1}(in terms of wavenumber)

(2) A gas cell with a 3.2 m optical path length

(3) Potassium bromide (KBr) windows.

The spectrometer uses "Spectra Calc" software for data acquisition and analysis. All the N_2O data were taken with the following parameters:

- resolution = 0.5 cm^{-1}
- co-added scans =15
- gain = 1
- ZPD = 256
- laser wavenumber = 7899 cm^{-1}

Table 4.1 Key Features of Gas Analyzers

Gas Species	Principle	Range	Response Time	Accuracy
O_2	Paramagnetic	0 - 10 %	20 s.	1 %
		0 - 25 %		
O_2	Electrochemical	0 - 5 %	10 s	5 %
		0 - 10 %		
		0 - 25 %		
CO	NDIR *	0 - 1000 ppm	5 s	1 %
CO_2	NDIR *	0 - 20 %	5 s	1 %
CH_4	NDIR *	0 - 0.2 %	5 s	1 %
		0 - 0.5 %		
NO	Chemiluminescence	0 - 250 ppm	3 min	1 %
		0 - 500 ppm		
NO_2	FTIR +	0 - 10 ppm	3 min	1 %
		0 - 50 ppm		
N_2O	FTIR +	0 - 1000 ppm	1 min	5 ppm
SO_2	NDIR *	0 - 1000 ppm	5 s	1 %
		0 - 3000 ppm		
		0 - 5000 ppm		

* Non-Dispersive Infrared
+ Fourier Transform Infrared.

Nitrogen was used to provide a reference spectrum and a 99 ppm N_2O standard gas was used for calibration. The infrared absorbance for N_2O has two characteristic peaks. One is found in the wavenumber range of 2260 - 2180 cm^{-1} and the other at 1320 - 1240 cm^{-1}. The peak at 2260 - 2180 cm^{-1} is masked by carbon dioxide and carbon monoxide peaks and thus cannot be used for analysis. The peak at 1320 - 1240 cm^{-1} has some overlap with sulphur dioxide peak; however, this can be resolved by selecting a narrower waveband for the analysis (see Figure 4.17).

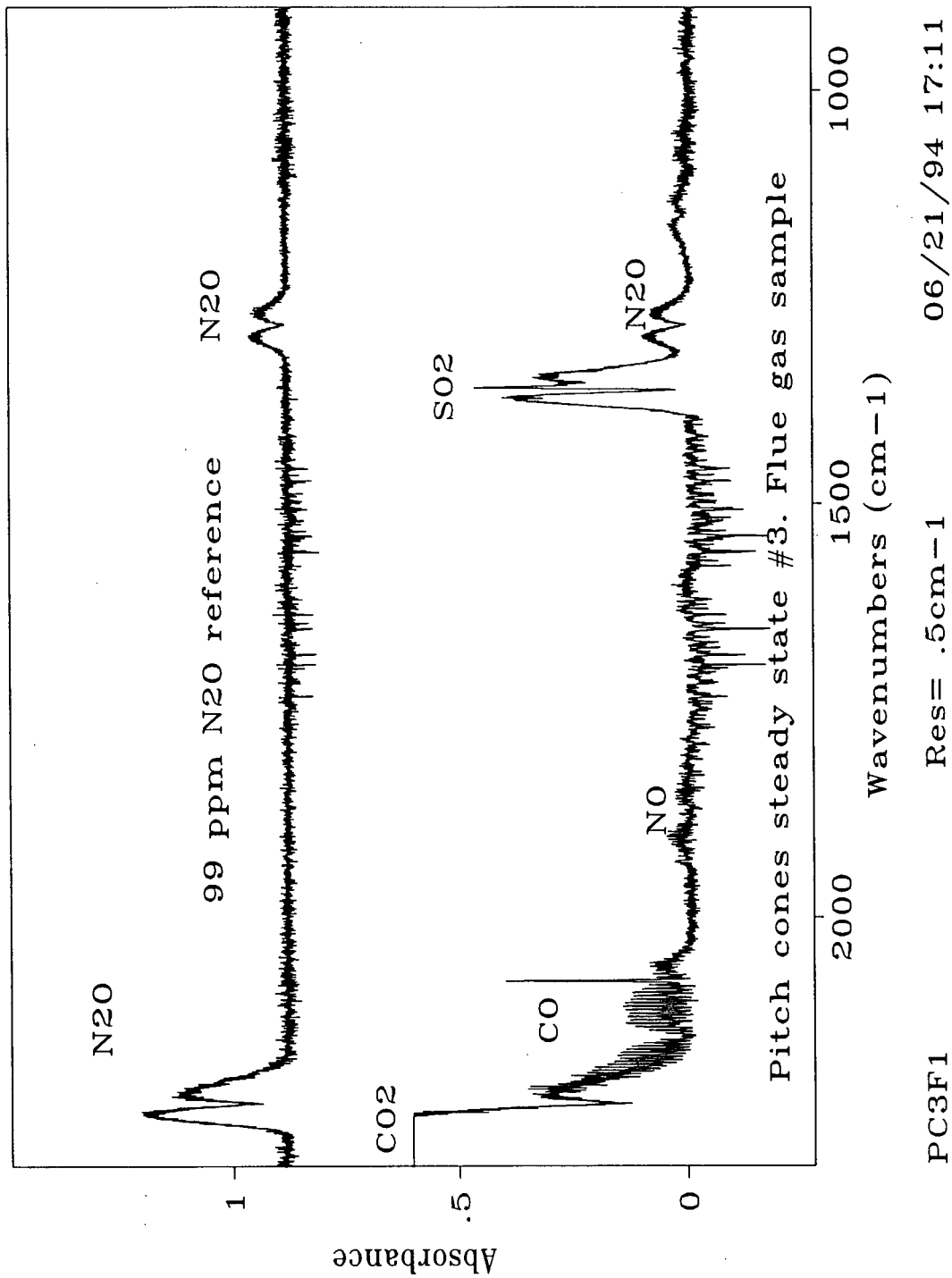

Figure 4.17 FTIR Spectra of Calibration Gas and Flue Gas

The chloroform and sulphur hexafluoride analyses were carried out on-site by Sheraton Manufacturing, B.C. The chromatographic conditions for the analyses were as follows:

Chloroform Analysis

- performed on a HP 401 Gas Chromatograph
- detection on a pulsed electron capture detector
- column: 0.61 m Chromosorb 102, 6.35 mm outside diameter SS
- detector temperature: 240 ^{o}C
- column temperature: 200 ^{o}C
- carrier gas: argon-5% methane at flow of 3 on rotameter scale
- purge rate: argon/methane at flow of 4 on rotameter scale

Sulphur Hexafluoride Analysis

- performed on a HP 401 GC
- detection on a pulsed electron capture detector
- column: 1.8 m molecular sieve 5A, 6.35 mm outside diameter glass
- detector temperature: 220 ^{o}C
- column temperature: 40 ^{o}C

The samples were diluted in bottled air by a factor between 1/2000 and 1/20000 to achieve a concentration which could be analyzed.

4.9 Additional Insulation

Following the preliminary incineration test on the stud blast fines, 63.5 mm of Basalt insulation was added on top of the existing 25.4 mm Fiberfrax insulation layer on the reactor

column, the primary and secondary cyclones and standpipe. The Basalt insulation is covered by an aluminum cladding. It is estimated that this additional insulation reduced the heat loss from the pilot CFB unit to the surroundings by approximately 30 %. As a result, higher operating temperatures could be attained.

5. PROPERTIES OF FUELS, SORBENT AND INERT PARTICLES

The fuels burned in the feasibility study included stud blast fines, pitch cones, miscellaneous paste waste, pitch dust, British Coal gasification char fines, Highvale coal, chloroform and sulphur hexafluoride. The pitch dust and stud blast fines are fine particulates and did not require pretreatment for feeding purposes. However, the size of the pitch cones ranged from powder to chunks as large as 50 mm long. The miscellaneous paste wastes are slag-like jagged pieces with irregular shapes and various sizes. Their lengths ranged from 5 to 70 mm, widths from 5 to 50 mm and thicknesses from 20 to 50 mm. The pitch cones and the miscellaneous paste waste were crushed to less than 6.35 mm using a hammer mill in order to reduce the size of the solids for feeding purposes. Such pretreatment would not be necessary for a commercial unit. Particle size distributions for the pitch cones (as received), miscellaneous paste waste (as received) and (crushed), pitch dust and the stud blast fines were determined by sieving and are reported in Table 5.1. The particle size distribution for the crushed pitch cones was not available, but it may be similar to the particle size distribution for the crushed miscellaneous paste waste.

Random samples of the solid materials were analyzed for their composition (ultimate analysis), higher heating value and metals content. The ultimate analysis provides the average composition of the waste: % moisture content, % carbon, % hydrogen, % nitrogen, % chlorine, % sulphur, % ash and % oxygen by difference. The higher heating value analysis determines whether co-firing of auxiliary fuel is necessary for combustion. The metals analysis provides information on the types of metals and their concentrations present in the ash of the solid materials. This gives an indication of the expected metals content in the ash residue. The ultimate and higher heating value analyses were performed by CT & E Testing Corporation in Vancouver. Results of the ultimate and heating value analyses for the solid fuels are shown in Tables 5.2 and 5.3. The heating values reported are the higher heating

values of the fuels The ash metals analyses were performed by Acme Analytical Laboratories in Vancouver. The results of the metals analysis are provided in Appendix C. Total sulphur analyses for the four Alcan fuels were determined using the LECO analyzer at UBC. The total sulphur content of these fuels are shown in Table 5.4. The properties of the liquid/gaseous fuels: chloroform and sulphur hexafluoride, as provided by the suppliers, are shown in Table 5.5. The physical properties of sand and sorbent used in the incineration tests are shown in Table 5.6.

Table 5.1 Particle Size Analyses for the Alcan Solid Fuels

Size (mm)	Pitch cones (as is) % non-cumulative	Misc. paste waste (as is) % non-cumulative	Misc. paste waste (crushed) % non-cumulative	Pitch dust (as is) % non-cumulative	Stud blast fines (as is) % non-cumulative
+ 5.60	59.47	99.15	-	-	-
+ 2.80	-	0.52	37.90	-	-
+ 2.00	18.78	0.06	18.08	-	-
+ 1.00	12.79	0.04	20.91	-	-
- 1.00	-	0.06	-	-	-
+ 0.500	5.72	-	8.86	0.05	1.86
+ 0.250	2.75	-	4.32	0.10	11.08
+ 0.180	-	-	-	4.82	12.14
+ 0.125	-	-	-	1.32	16.17
+ 0.090	0.23	-	-	39.23	13.30
- 0.090	0.12	-	-	-	-
+ 0.053	-	-	5.94	40.55	21.61
- 0.053	-	-	3.64	13.50	23.58

Table 5.2 Ultimate Analysis and Heating Values of Alcan Solid Fuels

	Stud blast fines	Pitch cones	Misc. paste waste	Pitch dust
% moisture	0.60	0.37	0.35	0.34
C	47.01	93.60	84.25	93.60
H	0.87	2.96	2.48	2.96
N	0.53	1.24	1.05	1.24
Cl	0.01	0.01	0.00	0.01
S	12.17	0.50	1.34	1.38
Ash	39.41**	1.06	9.54	0.25
O (by diff.)	0 **	0.63	1.34	0.56
Total (wt. % dry)	100	100	100	100
Higher heating value (Btu/lb, dry basis)	8555	15935	14836	15321
Higher heating value (MJ/kg, dry basis)	19.9	37.0	34.5	35.6

Table 5.3 Ultimate Analysis and Heating Values of Solid Fuels

	British Coal Gasification Char Fines	Highvale Coal [Brereton et al., 1991]
% moisture	0.72	15.2
C	62.61	62.4
H	0.27	3.6
N	1.09	0.8
Cl	0.37	0
S	1.88	0.2
Ash	34.15 **	14.3
O (by diff.)	0 **	18.7
Total (wt. % dry)	100	100
Higher heating value (Btu/lb, dry basis)	9509	10325
Higher heating value (MJ/kg, dry basis)	22.1	24.0

** In the ultimate analysis, the percent of C, H, N, Cl, S and ash are determined via ASTM methods. The percent of oxygen is obtained by difference. From the metals analysis for stud blast fines ash, the stud blast fines contain approximately 68 % Fe. The iron in the ash had oxidized to form FeO and Fe_2O_3; hence the mass of the ash is higher than if the iron had not oxidized. As a result, the ash was in a higher state of oxidation and resulted in a negative value for oxygen. Consequently, the oxygen was adjusted from -8.30 % to 0 % while the ash was adjusted from 47.54 % to 39.41 %. The ash for the British Coal Gasification Char fines was also in a higher state of oxidation. Thus, the oxygen was adjusted from -0.91 % to 0 % while the ash was adjusted from 35.06 % to 34.15 %.

Table 5.4 Total Sulphur Content of the Alcan Solid Fuels

	Pitch cones	Misc. paste waste	Pitch dust	Stud blast fines
Total sulphur (%, wet basis)	0.59	1.61	1.52	13.34

Table 5.5 Properties of Chloroform and Sulphur Hexafluoride

Fuel	Chloroform
Boiling Point :	61 ^{o}C
Vapour Pressure :	100 mm Hg @ 10.4 ^{o}C
Vapour Density :	4.12 (AIR = 1)
Specific Gravity :	1.48 (H_2O = 1)
Percent Volatile :	100
Appearance and Odour :	Colourless volatile liquid with a sweet odour
Fuel	**Sulphur Hexafluoride**
Boiling Point :	-63.9 ^{o}C, sublimation point @ 1 atm
Freezing Point :	-50.5 ^{o}C @ 1 atm
Vapour Pressure :	2200 kPa @ 21.1 ^{o}C
Solubility in Water :	Negligible
Gas Density :	6.15 kg/m^3 @ 1 atm and 21.1 ^{o}C
Specific Gravity :	5.105 @ 1 atm and 21.1 ^{o}C (AIR = 1)
Liquid Density :	1439 kg/m^3, liquid at vapour equilibrium @ 15 ^{o}C
Appearance and Odour :	Colourless, odourless gas

Table 5.6 Physical Properties of Sand and Sorbent

Sand [Brereton et al., 1991]	F 70 Silica Sand
Particle Density :	2650 kg/m^3
Mean Particle Diameter :	148 micrometers
Voidage at minimum fluidization :	0.43
Minimum fluidization velocity at (i) room temperature : (ii) 850 ^{o}C	 0.021 m/s 0.0094 m/s
Sorbent	British Coal Limestone
Mean Particle Diameter :	0.5 mm
Density Packed : Loose : $CaCO_3$ content :	 1548 kg/m^3 1280 kg/m^3 98 wt. % (dry basis)

The minimum fluidization velocity of the F70 silica sand at 850 ^{o}C is calculated using the following equations [Grace, 1982]:

$$Ar = \frac{\rho_f(\rho_s - \rho_f)gd_s^3}{\mu_f^2} \tag{5.1}$$

where

Ar = Archimedes number

ρ_f = density of air (kg/m^3)

ρ_s = density of sand (kg/m^3)

g = gravitational constant (9.8 m/s^2)

d_s = mean particle diameter (m)

μ_f = viscosity of air (kg/ms)

For Ar < 1000,

$$U_{mf} = \frac{0.0075(\rho_s - \rho_f)gd_s^2}{\mu_f} \tag{5.2}$$

where

U_{mf} = minimum fluidization velocity (m/s)

6. FURTHER EXPERIMENTAL DETAILS

6.1 Operating Conditions

As noted in Section 2.1, the operating conditions for an incineration system may differ from those for a combustion system. In combustion systems (e.g. combustors and boilers), the purpose is to generate and recover energy by burning fuels. By increasing the amount of excess air, the heat loss associated with unburnt combustibles (e.g. carbon) decreases. At the same time, the amount of heat loss associated with the flue gas, a major source of heat loss, increases. Therefore, in order to achieve efficient energy recovery, it is necessary to minimize the heat loss associated with the flue gas by operating at minimal excess air. For the destruction of organic wastes, the objective is to achieve the highest possible degree of destruction of organic material. This is achieved by operating the combustion system as an incinerator in which the material is burned at a higher temperature and excess air level. However, there are limitations on the operating temperature of a circulating fluidized bed system which result in a compromise between the operating temperature and the amount of excess air added. At high operating temperatures and low excess air, the inert sand may react with additives present in the wastes, e.g. sodium salts, to form low melting eutectics with ash at high temperatures ($T > 950 - 1000\ ^{o}C$) and slagging may occur. NO_x and SO_2 emissions also tend to increase with increasing temperature.

In a fluidized bed, in-situ sulphur capture is achieved by addition of limestone. SO_2 is converted to $CaSO_4$ by the reaction:

$$CaO + SO_2 + 1/2\ O_2 = CaSO_4$$

However, at high temperatures, the reverse reaction becomes significant and $CaSO_4$ decomposes back to SO_2. At low operating temperatures and high excess air, there is an increase in carbon loss due to unburned carbon which results in decreased combustion efficiency and reduced destruction and removal efficiency, and lower NO_x emission. In view of these factors, the operating temperature in a CFB combustor/incinerator is traditionally limited to between 800 - 1000 ^{o}C. The high heat losses in the UBC pilot CFB system tend to restrict the excess air addition and hence the oxygen content in the flue gas is limited to approximately 5 mole percent (dry basis) or less. However, the amount of heat loss decreases with increasing reactor scale due to the decrease in the surface area-to-volume ratio of the combustor. Thus it is likely that higher excess air (excess oxygen) levels will be employed in commercial systems.

A Lotus 123 spreadsheet was used to perform the mass balance around the CFB combustor in order to estimate feasible operating conditions for the combustion tests. The parameters which may be varied include:

(a) the waste feed rate,
(b) the moisture content of the waste,
(c) the combustion efficiency,
(d) the sulphur capture efficiency,
(e) the limestone feed rate,
(f) the primary and secondary air flow rates,
(g) the temperature of the reactor and
(h) the composition of the wastes (from ultimate analysis).

Given the moisture content of the waste, the combustion efficiency, the sulphur capture efficiency, the limestone feed rate, the incineration temperature, and the composition of the

waste material, the feed rate of the waste is determined by varying the feed rate of the waste and the flow rates of the combustion air (primary and secondary) until:

(1) the primary to secondary air flow ratio is approx. 2:1,
(2) the superficial velocity inside the combustor is approx. 7.0 m/s and
(3) the mole percent oxygen in the gas stream exiting the flue gas filter (dry basis) is 3.5 %, 4.5 or 5.5 % (level of excess air).

The incineration test matrix for the second set of incineration tests for the Alcan solid materials is shown in Table 6.1. The ranges for the two parameters were chosen based on previous combustion experience with the pilot CFB combustor.

Table 6.1 Incineration Test Matrix

	T1 = 900 ^{O}C	T2 = 875 ^{O}C	T3 = 850 ^{O}C
O_2 = 3.5 %	1	2	3
O_2 = 4.5 %	4	5	6
O_2 = 5.5 %	7	8	9

The nine test conditions shown in this test matrix provide a systematic means of studying the effects of incineration temperature and excess air (expressed as % oxygen) on the exhaust gas emissions. The constant parameters were the total air flow rate, the primary-to-secondary air split ratio and the suspension density. Primary air is defined as the sum of combustion air flowing through the distributor plate, the air flowing through the eductor and the pneumatic air flow for solids feed transport. The variable parameters were the air cooling rate through the hairpin heat exchanger, the secondary air preheat by-pass (ON/OFF) and the fuel feed rate. For the test condition(s) which resulted in acceptable levels of emissions, the parameters which were kept constant were varied to note their effects on emissions. As a result, a maximum of twelve test conditions may be performed for each waste material.

6.2 Experimental Protocol

The sequence of incineration tests performed was as follows:

(1) short preliminary tests for the stud blast fines and the pitch cones;
(2) longer tests for the pitch cones, the miscellaneous paste wastes and the pitch dust;
(3) chloroform co-fired with British Coal gasification char;
(4) sulphur hexafluoride co-fired with Highvale coal.

Details of the data acquisition, solids sampling and gas sampling procedures are presented in the following paragraphs. The results of the incineration tests are presented in chapter 7.

6.2.1 Data Acquisition

During the tests, the following parameters were measured:

(1) the solid fuel feed rate, chloroform feed rate and SF_6 feed rate,
(2) the air and water flow rates,
(3) pressure profiles and the overall pressure drop across the reactor,
(4) the temperature at various locations in the CFB system and
(5) gas composition profiles.

Temperature measurements were obtained from thermocouples located at various levels along the wall of the primary combustor chamber and in the primary and secondary cyclones. The average incineration temperature reported is the arithmetic average of the temperatures measured within the CFB riser. In the UBC pilot CFB combustion system, the combustion

and destruction of the organic waste not only takes place in the combustor itself, but also in the primary and secondary cyclones (where reactions include the conversion of CO to CO_2 and burnout of the carbon fines). Hence, temperatures in the primary and secondary cyclones were also measured and reported.

6.2.2 Solids Residue Sampling and Analysis

Solids residue (e.g. flyash, bottom ash) were generated in the incineration process. During the short preliminary incineration tests for stud blast fines and pitch cones, only a small amount of ash was generated. As a result, there was no solids sampling. If low ash fuels or fine powder fuels were to be incinerated for long test periods, sand, may have to be added periodically to replace the loss of coarse solids while some ash may have to be withdrawn from the CFB. For the second set of tests on the Alcan solid wastes involving pitch cones, miscellaneous paste wastes and pitch dust, as well as for the chloroform and SF_6 tests, a sample of baghouse ash was removed at the end of each test and stored for future analysis. The baghouse was cleaned at the end of each test.

6.2.3 Gas Sampling and Analysis

For the stud blast fines and pitch cones tests, the "flue gas" (combustion gases which has passed through the secondary cyclone and the first heat exchanger) was monitored continuously by on-line gas analyzers to determine the concentrations of O_2, CO, CO_2, SO_2, NO, and unburned hydrocarbons (expressed as CH_4). N_2O, nitrous oxide and NO_2 were also measured periodically. N_2O is a gas which contributes to the greenhouse effect. It is 200 times as effective as CO_2 on a molar basis in absorbing infra-red radiation and has a high capacity for destroying ozone in the upper atmosphere. This gas is a concern for those doing research on CFBs and other low temperature combustion techniques where N_2O formation is

significant [Brereton et al., 1991]. Therefore, although there are no regulations on N_2O emissions in B.C., N_2O emissions were also measured and analyzed using an on-line FTIR detector.

It was anticipated that fluorine would not be present in the solid organic wastes; therefore, hydrogen fluoride was not monitored. Only 0.01 weight percent (dry basis) of chlorine was present in the stud blast fines, the pitch cones and pitch dust; hence hydrogen chloride was also not monitored. Since there is no metals sampling train for the flue gas in the CFB reactor system, the trace metals content in the flue gas could not be monitored. If necessary, a metals sampling train could be set up in the future to measure the metals concentration in the flue gas.

For the second set of incineration tests on the Alcan solid wastes, the flue gas composition was monitored and measured as for the trial test. The baghouse emissions at a new gas sampling point situated downstream from the baghouse filter were also measured. Details of this new sampling point are provided in section 7.1.2. In the fundamental study, chloroform was co-fired with British Coal gasification char and SF_6 was co-fired with Highvale coal. The flue gas and baghouse emissions were measured for the chloroform and SF_6 incineration tests. A portable multipoint gas sampling system was used to determine emissions at different radial positions, i.e. wall, middle and centreline, and at four different axial positions along the riser: 1.5 , 2.7 , 4.2 and 6.4 m. This resulted in a total of 14 gas sampling points. At each sampling point in the riser, a gas sample was collected for analysis of chloroform or SF_6.

7. EXPERIMENTAL RESULTS

7.1 Preliminary Results and Discussion

7.1.1 Stud Blast Fines

A brief incineration test on the stud blast fines was carried out in the UBC pilot CFB unit using the solids feed system described in Section 4.2.1. The ultimate analysis was not available prior to the test and it was assumed that the stud blast fines contained approximately 7% sulphur on a dry, ash free, basis. However, it was later determined that the stud blast fines contained approximately 13.2 weight percent (13.1 wt. % dry basis) sulphur by performing a total sulphur analysis (via the LECO analyzer). The operating condition and the resulting emissions measured after the flue gas filter are shown in Tables 7.1 and 7.2, respectively. The experimental emissions in Table 7.2 have been corrected to 11% O_2, 20 ^{o}C, 760 mm Hg and dry basis and are expressed in terms of mg/m^3 for comparison with the Special Waste Regulation (SWR) permitted discharge levels.

A detailed mass balance for this run is provided in Appendix D. Plots of O_2, CO, CO_2, CH_4, NO_x, SO_2 emissions are plotted versus time in Appendix E. Temperature profiles evolving over time are provided in Appendix F. The average incineration temperature is the arithmetic average of the temperatures measured at z = 0.305, 1.067, 2.743, 3.962, 4.572, 5.75 and 6.041 m above the base. Steady state was not achieved during the one hour test duration because the stud blast fines are not reactive due to the lack of volatiles. During the total sulphur analysis, the stud blast fines samples were heated to a temperature of 1351 ^{o}C in an oxidizing environment. No flames, which would indicate that volatiles are being burned off, were observed. The test was stopped due to the high SO_2 concentration detected in the flue

gas, since there is potential damage to the gas analyzers for such high SO_2 concentrations as well as SO_2 leakage from the pilot system to the surrounding work area.

Table 7.1 Operating Condition for Stud Blast Fines

Avg. Incineration Temp. (^oC)	861
Excess Air (% O_2)	4.2
Fuel Feed Rate (kg/h)	24.4
P : S Air Split Ratio	2.1
Total Air Flow Rate (SCFM)	85
Total Air Flow Rate (m^3/h)	145
Superficial Gas Velocity (m/s)	7.3
Suspension Density (kg/m^3)	120

Table 7.2 Stud Blast Fines Flue Gas Emissions

Species	Flue Gas Emissions	Corrected Average Flue Gas Emissions (mg/m^3)	SWR Limit (mg/m^3)
O_2 (%)	4.2	11 %	11
CO_2 (%)	13.8	-	-
CH_4 (%) *	0	0	32
CO (ppm)	981	680	55
NO_x (ppm)	252	287	380
SO_2 (ppm) **	> 14000	>22000	180
N_2O (ppm)	-	-	N/A
CE (%)	99.3	99.3	≥ 99.9

* High CH_4 emissions were observed (0.0034 vol. %, or 135 mg/m^3) because of interference resulting from the high SO_2 concentration (since the absorption peaks for sulphur dioxide and methane overlap). There is probably little or no total hydrocarbon, expressed as methane, since there is no volatile matter to generate this. Thus, the true quantity of methane may be assumed to be essentially zero.

** This calculated SO_2 emission is based on the sulphur content of the stud blast fines at the operating conditions given in Table 7.1 (see mass balance in Appendix D). No limestone was added in this test and the amount of SO_2 measured in the flue gas exceeded 8000 ppm. However, the actual SO_2 concentration was probably higher since the reading was well beyond the linear calibration range (> 4570 ppm) of the analyzer. As a result, the calculated SO_2 emission assuming complete oxidation of sulphur is reported in Table 7.2.

The UBC pilot CFB was unable to achieve an operating temperature higher than about 860 ^{o}C when burning the stud blast fines. In order to improve the combustion efficiency of the system, it would be necessary to operate the system at a higher temperature (e.g. at 900 ^{o}C by adding insulation to the system) and to raise the excess air to 6% oxygen in the flue gas.

This preliminary incineration test demonstrated that the stud blast fines with a higher heating value of 19.9 MJ/kg was able to sustain combustion without addition of auxiliary fuel. However, incineration may not be the most appropriate disposal solution for the stud blast fines due to their high sulphur and ash content. In general, the use of limestone for in-situ sulphur capture in a CFB unit becomes unattractive if the sulphur content of the fuel is too high. In the best case, 95 % sulphur capture may be obtained at a molar calcium to sulphur ratio of 2 to 1. Under these circumstances (assuming limestone with 95.5 % calcium carbonate and operating at the conditions in Table 7.1), the sulphur dioxide emission would be approximately 680 ppm, and approximately 1.14 kg of solid wastes would be generated per kg of stud blast fines incinerated (see mass balance in Appendix D). Hence, the sulphur emission would still be high, and there would be a volume increase of the solids after incineration so that ash management would become problematic. A wet scrubber preceded by a baghouse is generally preferred in such a case since it generates a sewerable sodium sulphate/sulphite mixture solution. Yet, there will still be ash management problems since the stud blast fines have approximately 47 wt. % ash. Of the waste materials analyzed thus far, only the stud blast fines have an unusually high sulphur content (approx. 13 wt. %, dry basis). The other three materials have sulphur contents from 0.50 to 1.4 wt. %, dry basis. As a result, the wet scrubber would be overdesigned for the other waste materials. Consequently, it may be more viable to look at other disposal alternatives rather than to design a system which focuses so much effort on a single waste.

Disposal alternatives for the stud blast fines may include usage as a heavy metals precipitation reagent for wastewater treatment and as a flyash stabilization reagent. Sulphide precipitation is used in wastewater treatment primarily for the removal of soluble heavy metal ions from water as shown by the reaction below :

$$M^{2+}_{(aq)} + HS^{-}_{(aq)} = MS_{(s)} \quad H^{+}_{(aq)}$$

where

M = heavy metal (i.e. cadmium, chromium, etc.)

The solubilities of some heavy metal sulphides are low compared to their hydroxides. Sulphide precipitation can be a very effective means of treatment for removal of metals whose hydroxides are more soluble. Sources of sulphide ion include sodium sulphide, Na_2S, sodium hydrosulphide, NaHS, hydrogen sulphide, H_2S and iron (II) sulphide, FeS. Hydrogen sulphide is a toxic gas and is considered to be a hazardous waste itself. Iron (II) sulphide can be used as a safe source of sulphide ion to produce sulphide precipitates with other metals that are less soluble then FeS. Since iron (II) sulphide is only slightly soluble itself, it presents a relatively low hazard [Manahan, 1990]. Two sulphide precipitation processes are used. In the first process, the sulphide is added in a liquid form (as sodium sulphide) to the wastewater, and the metal precipitate is removed by a conventional filter. In the second process, the wastewater is passed through a column of sparingly soluble metal sulphide (iron (II) sulphide). Precipitation and filtration then occur in a single step with the column acting as a granular filter [Attalla, 1991].

Simple chemistry experiments (see Appendix H) carried out at UBC have shown that the dominant form of sulphur in the stud blast fines is ferrous sulphide, FeS; therefore, the stud blast fines may have potential application in the second sulphide precipitation process. Further

work in this area is needed to confirm this. The stud blast fines also have approximately 47 wt. % carbon (dry basis) which may be converted to activated carbon for the removal of organics from the liquid waste stream. Currently, there is no evidence that the carbon can be activated. If the carbon can be activated, there is still the concern that the polycyclic aromatic hydrocarbons, PAHs, in the stud blast fines may contaminate the liquid waste stream being treated. If the issues regarding carbon activation and PAHs can be resolved, the stud blast fines may be suitable for removal of both organics and heavy metals from wastewater streams.

Bench scale tests were performed to study the effect of pH on the solubilities of metal precipitates and to compare the effectiveness of using pure FeS versus stud blast fines as a means for metal sulphide precipitation. A solution containing 40 mg/L of copper, 20 mg/L of lead and 50 mg/L of zinc was prepared. The results showed that by increasing the pH alone from 5 to 7, the concentration of soluble metals decreased due to the decrease in solubility of metal hydroxides. At a pH of 5, the soluble copper, lead and zinc concentrations were 36 mg/L, 16 mg/L and 50 mg/L, respectively. At a pH of 7, the soluble copper, lead and zinc concentrations were 3 mg/L, 3 mg/L and 40 mg/L, respectively. Significant reduction in soluble metals concentration was achieved by using pure FeS for metal sulphide precipitation at a given pH. At a pH of 5, the soluble copper, lead and zinc concentrations were 2 mg/L, 8 mg/L and 50 mg/L, respectively. At a pH of 7, the soluble copper, lead and zinc concentrations were 1 mg/L, 1 mg/L and 37 mg/L, respectively. Significant reduction in soluble metals concentration was also achieved by using stud blast fines for metal sulphide precipitation at a given pH. At a pH of 5, the soluble copper, lead and zinc concentrations were 0.67 mg/L, 0.07 mg/L and 24 mg/L, respectively. At a pH of 7, the soluble copper, lead and zinc concentrations were 0.67 mg/L, 0.07 mg/L and 21 mg/L, respectively. Stud blast fines appear to be more effective as a precipitation reagent compared to pure FeS since it resulted in lower soluble metals concentrations and the solubility of metals in the solution is less sensitive to pH changes .

Flyash from incinerators may contain heavy metals, depending on the nature of the waste materials incinerated. In some cases, these heavy metals may be leachable, and the ash is blended with cement to form flyash/cement blocks which are disposed of in landfills. The mass ratio of ash to cement is about 1 to 0.3 and may vary. When cement is added to the ash, hydration reactions occur with water adding to the weight of the waste matrix. The large quantity of cement used contributes to high reagent costs and the increase in the weight of the waste matrix contributes to high disposal costs. There is environmental concern regarding leaching potential of heavy metals in the flyash/cement matrix. Thus, the metals in the flyash may require stabilization against leaching prior to landfilling. Bench scale tests were performed to study the feasibility of using stud blast fines as a flyash stabilization reagent. Concrete samples containing Highvale coal flyash, Portland cement, 120 mg/kg of lead and 33000 mg/kg of zinc were prepared with pure FeS and varying concentrations of stud blast fines as the stabilization reagent. Following a curing period of 28 days, the concrete samples were subjected to the Sequential Chemical Extraction test, a rigorous leaching test. The results showed that increasing the quantity of excess sulphide ions did not significantly change the concentration of the soluble metal ions in solution, and that stud blast fines were as effective as pure FeS in reducing the solubilities of lead, but the results for zinc were inconclusive. The work by Clemente (1994) showed that stud blast fines have potential as a flyash stabilization agent. If the amount of cement added can be reduced by replacing it with additives such as the stud blast fines, there would be a saving in chemical and disposal costs.

7.1.2 Pitch Cones

After the stud blast fines incineration test, insulation was added to the pilot CFB system as described in section 4.9, and the solids feed system was modified as described in section 4.2.1.1 (but without the ram-rod) before the pitch cones incineration test was carried out.

The objectives of this test were to test the modified solids feed system with the water-cooled feeder probe and to study the combustibility of the pitch cones.

Two operating conditions were achieved. The first operating condition and the resulting emissions are shown in Table 7.3. The average incineration temperature is the arithmetic average of the temperatures measured at z = 1.067, 5.791 and 6.401 m above the base. Flue gas emission plots of O_2, CO, CO_2, NO and CH_4 are shown in Figures 7.1 to 7.5. The NO_x emissions reported in Table 7.3 and in all subsequent emissions tables are the sum of the equivalent NO_2 emissions (calculated based on continuous NO emissions) and the NO_2 emissions measured periodically by the FTIR. In condition 2, the primary air to secondary air split ratio was reduced from 2.05 : 1 to 1.14 : 1, while the total air flow rate remained unchanged. This was to study the influence of primary-to-secondary air split ratio on flue gas emissions. The operating condition and the resulting emissions are shown in Table 7.4. Emission plots of O_2, CO, CO_2, NO_x and CH_4 are shown in Figures 7.6 to 7.10. Detailed mass balances for both operating conditions are provided in Appendix D.

Table 7.3 Pitch Cones Flue Gas Emissions: Condition # 1

Parameter	Test Condition 1	Corrected Emissions (mg/m^3)	SWR Limit (mg/m^3)
Avg. Incineration Temperature (^oC)	897	-	-
Fuel Feed Rate (kg/h)	10.3	-	-
Superficial Gas Velocity (m/s)	7.10	-	-
Primary-to-Secondary Air Ratio	2.05	-	-
O_2 (%)	6.5	-	-
CO_2 (%)	13.5	-	-
THC (expressed as CH_4) (%)	0.000244	1	32
CO (ppm) *	155	125	55
NO_x (ppm)	156	206	380
SO_2 (ppm) **	270	290	180
CE (%)	99.88	-	≥ 99.9

Table 7.4 Pitch Cones Flue Gas Emissions: Condition # 2

Parameter	Test Condition 2	Corrected Emissions (mg/m^3)	SWR Limit (mg/m^3)
Avg. Incineration Temperature (^oC)	893	-	-
Fuel Feed Rate (kg/h)	10.4	-	-
Superficial Gas Velocity (m/s)	7.09	-	-
Primary-to-Secondary Air Ratio	1.14	-	-
O_2 (%)	6.5	-	-
CO_2 (%)	13.2	-	-
THC (expressed as CH_4) (%)	0.0073	34	32
CO (ppm) *	200	160	55
NO_x (ppm)	130	172	380
SO_2 (ppm) **	272	290	180
CE (%)	99.86	-	≥ 99.9

* An apparent CO emission rather than the true emission.
** Estimated SO_2 emission based on the sulphur content in the pitch cones.

During condition 1, the flue gas CO emission was constant at approximately 155 ppm before the flue gas filter was purged with compressed air (see Figure 7.2). After the air purge, the O_2, CO_2, NO and CH_4 emissions returned to their steady state levels prior to the purge (at t = 100 minutes). One would expect that the CO emission would also return to its steady state value. However, the CO emission at 100 min was only 130 ppm and it continued to increase while all other emissions remained steady. It is believed that prior to the air purge, there may have been a build-up of a layer of Highvale coal ash (from start-up of system) on the flue gas filter which may have a buffering effect on the unburned carbon deposits, soot. When the filter was purged, the Highvale coal ash layer was removed and the unburned carbon was deposited directly onto the filter surface. As the carbon deposit accumulated over time, reactions take place on the surface of the filter, resulting in CO production from soot. Each time the filter was back-purged with compressed air, the CO emission would first decrease (due to purging) and then would increase over time. It was difficult to obtain a representative CO concentration. When the filter was disassembled at the end of the test, a layer of black

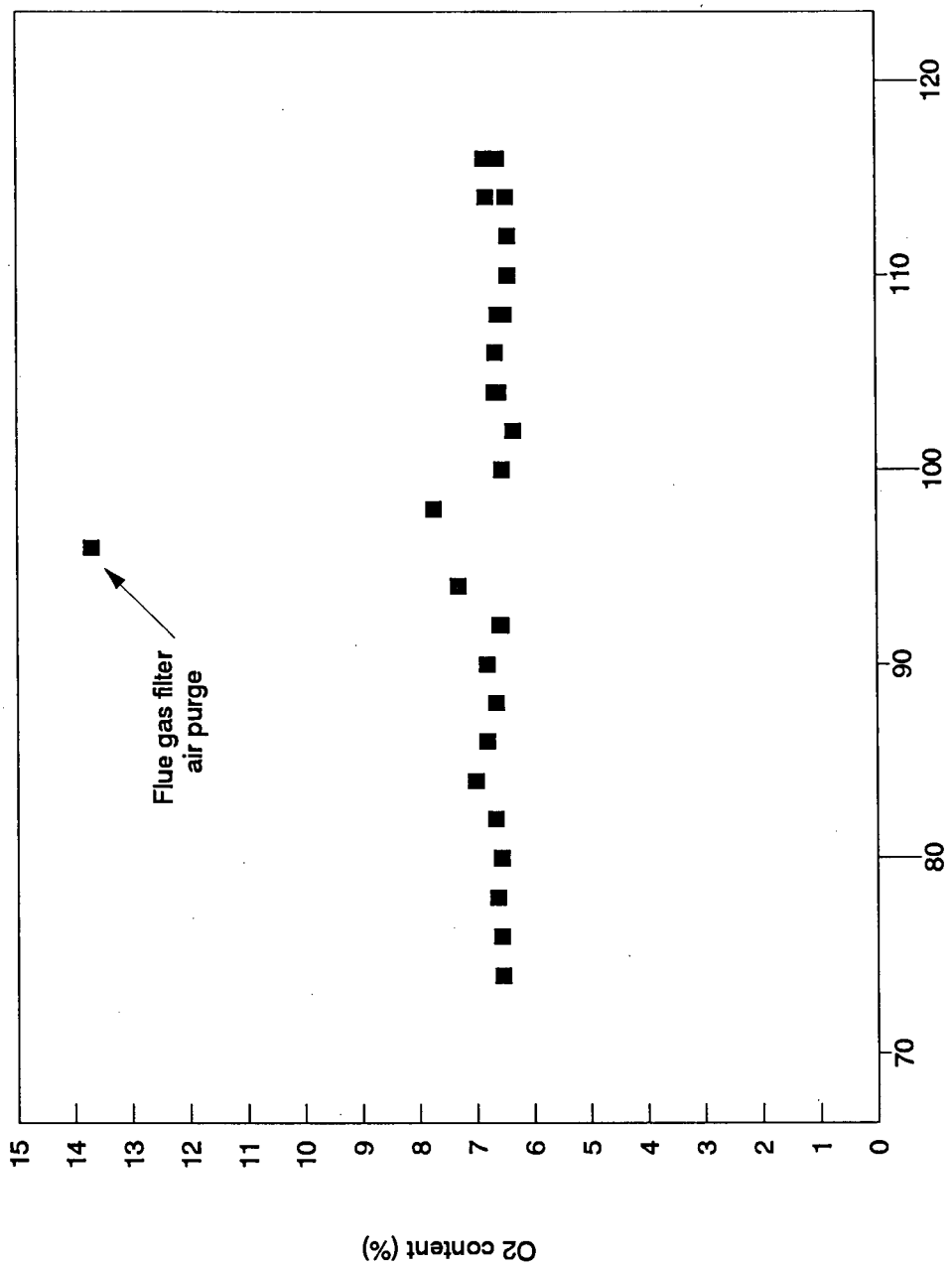

Figure 7.1 Flue Gas O2 Content for Pitch Cones : Condition 1.
(See Table 7.3 for details).

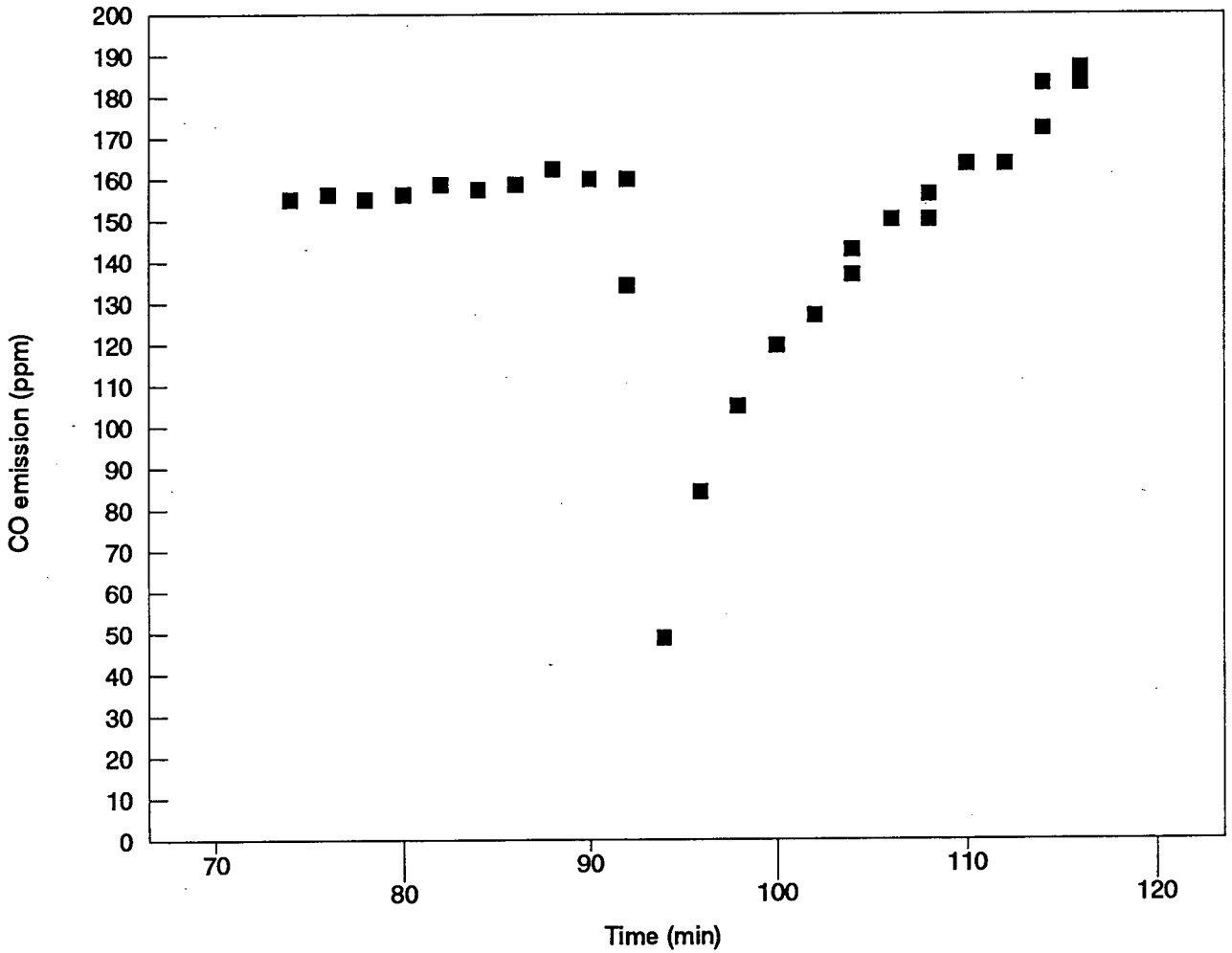

Figure 7.2 Flue Gas CO Emission for Pitch Cones : Condition 1.
(See Table 7.3 for details).

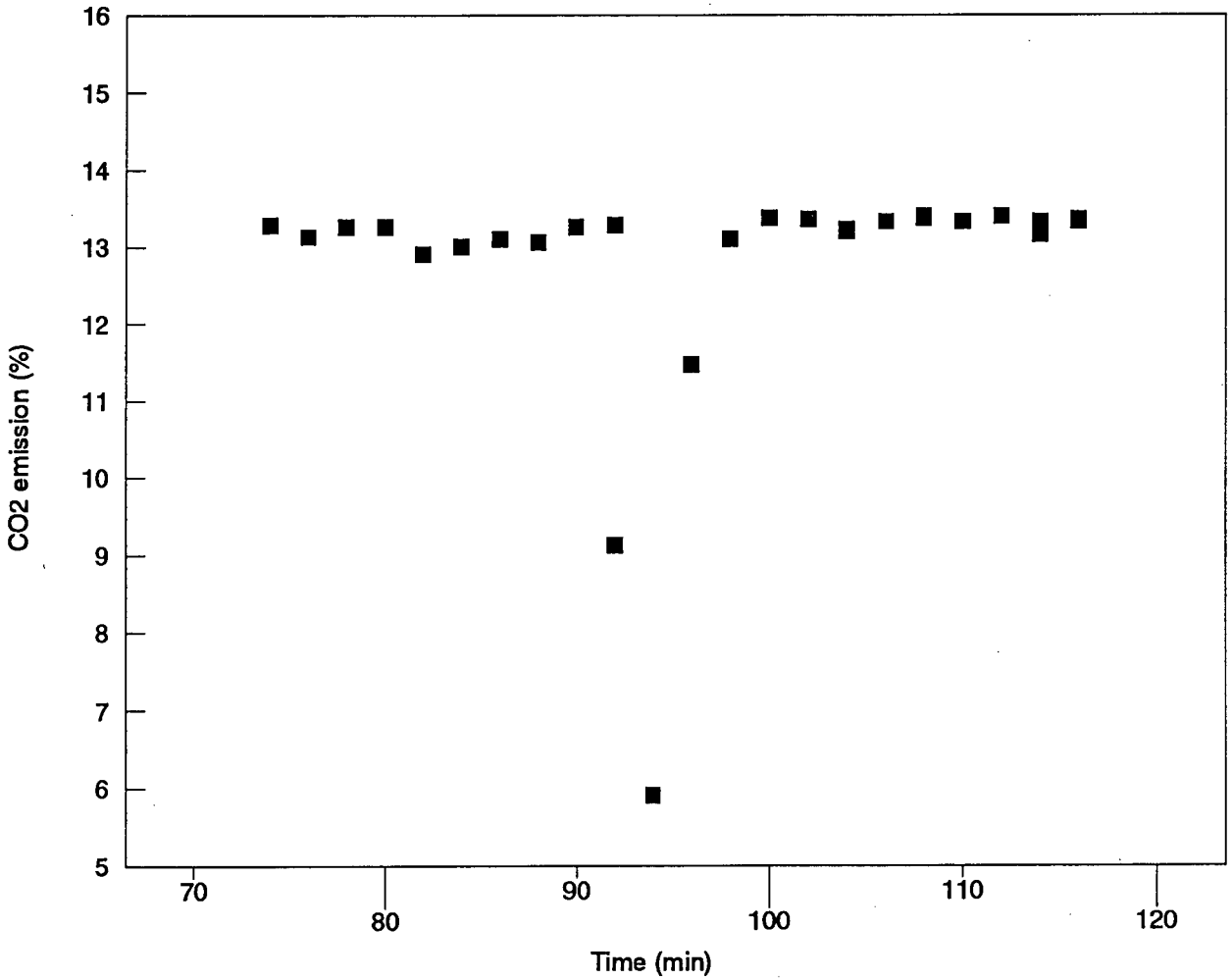

Figure 7.3 Flue Gas CO2 Emission for Pitch Cones : Condition 1.
(See Table 7.3 for details).

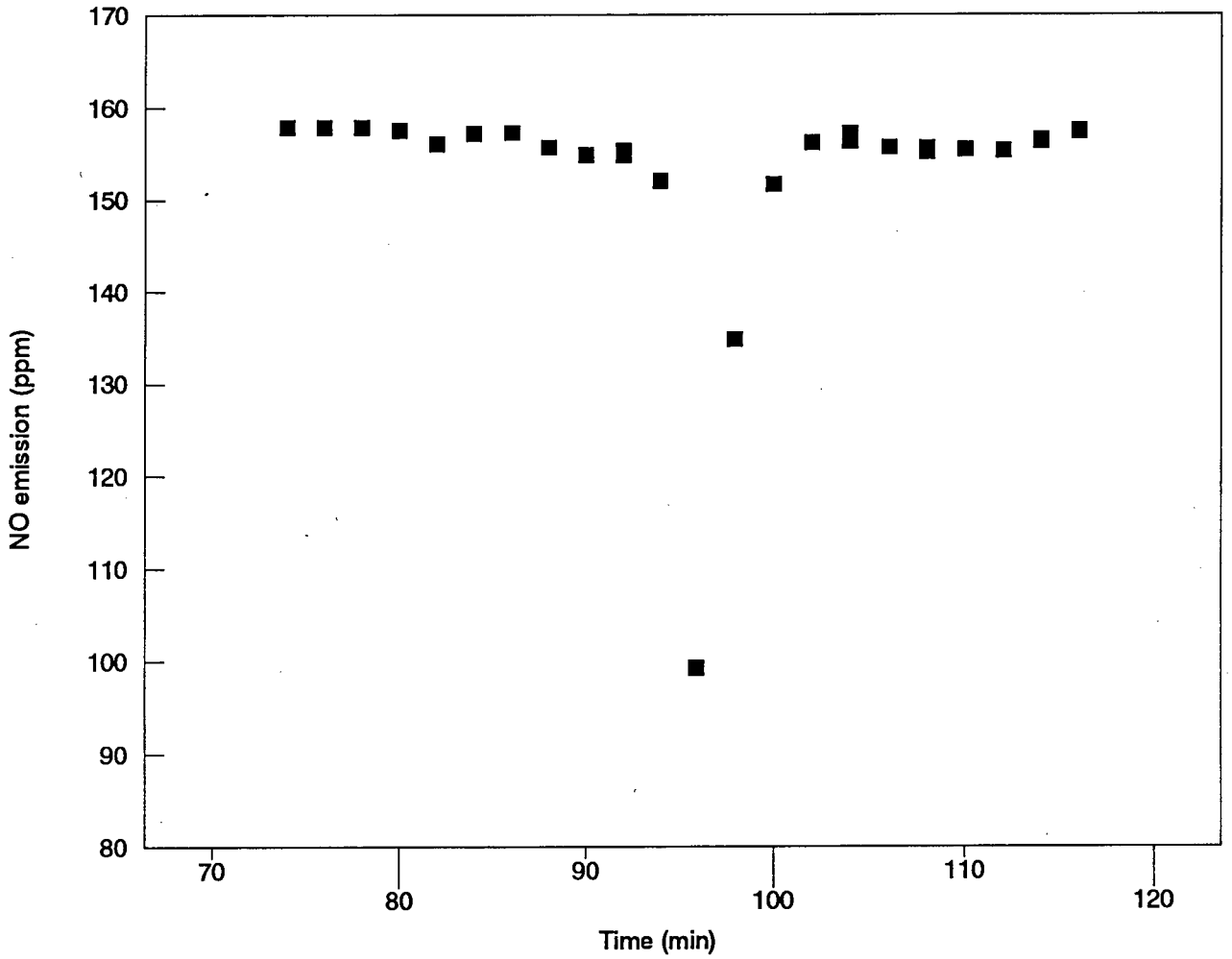

Figure 7.4 Flue Gas NO Emission for Pitch Cones : Condition 1.
(See Table 7.3 for details).

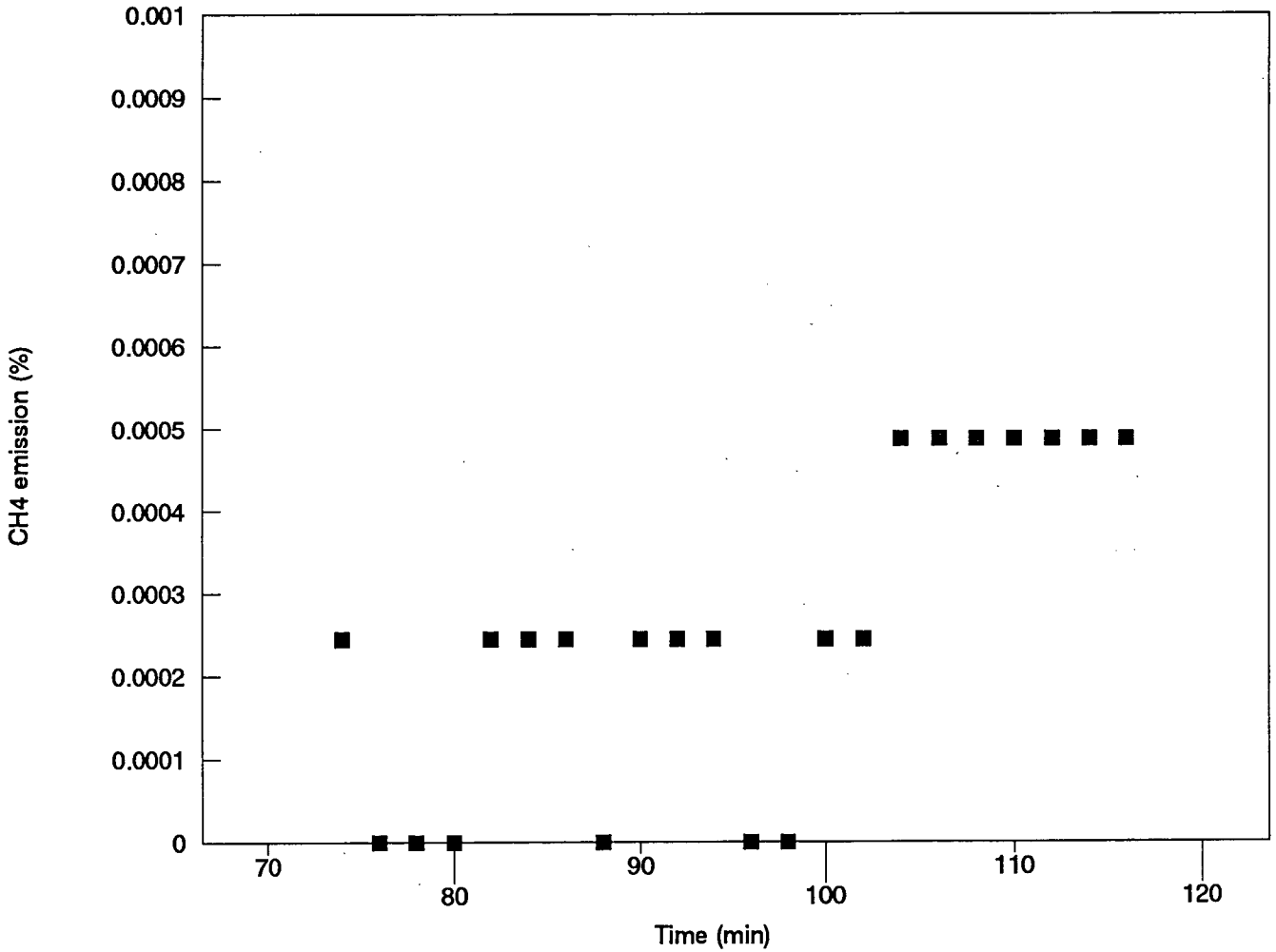

Figure 7.5 Flue Gas CH4 Emission for Pitch Cones : Condition 1.
(See Table 7.3 for details).

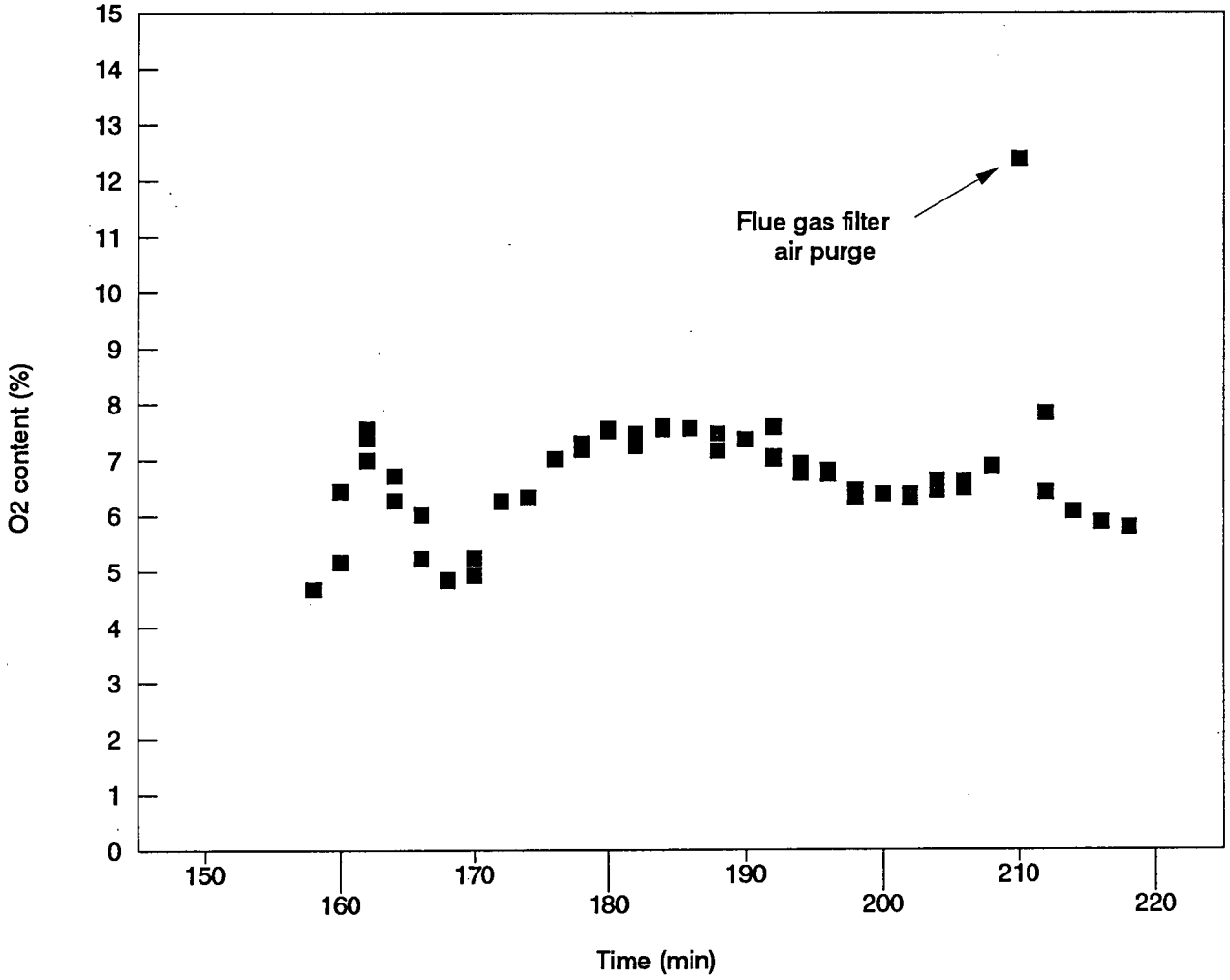

Figure 7.6 Flue Gas O2 Content for Pitch Cones : Condition 2.
(See Table 7.4 for details).

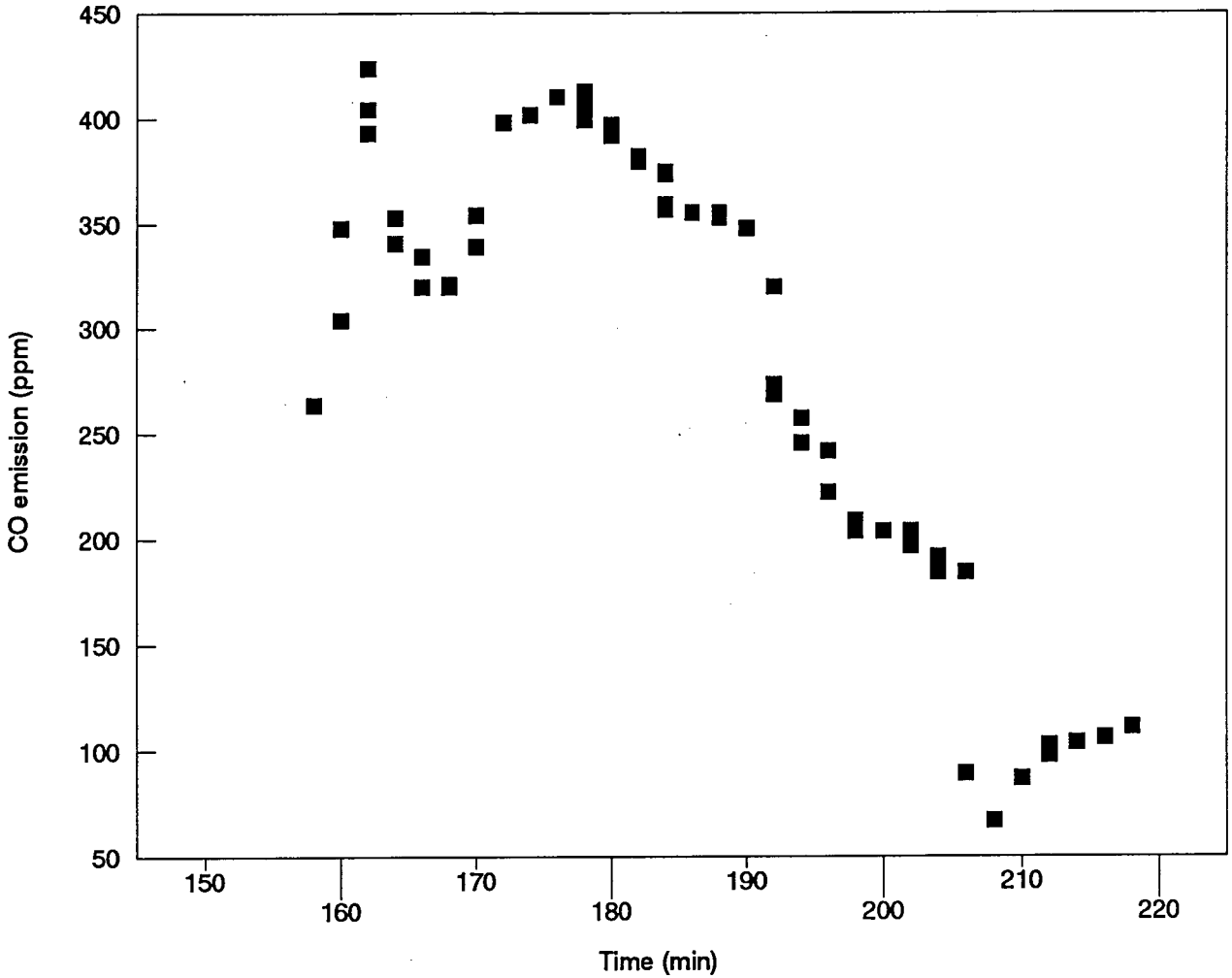

Figure 7.7 Flue Gas CO Emission for Pitch Cones : Condition 2.
(See Table 7.4 for details).

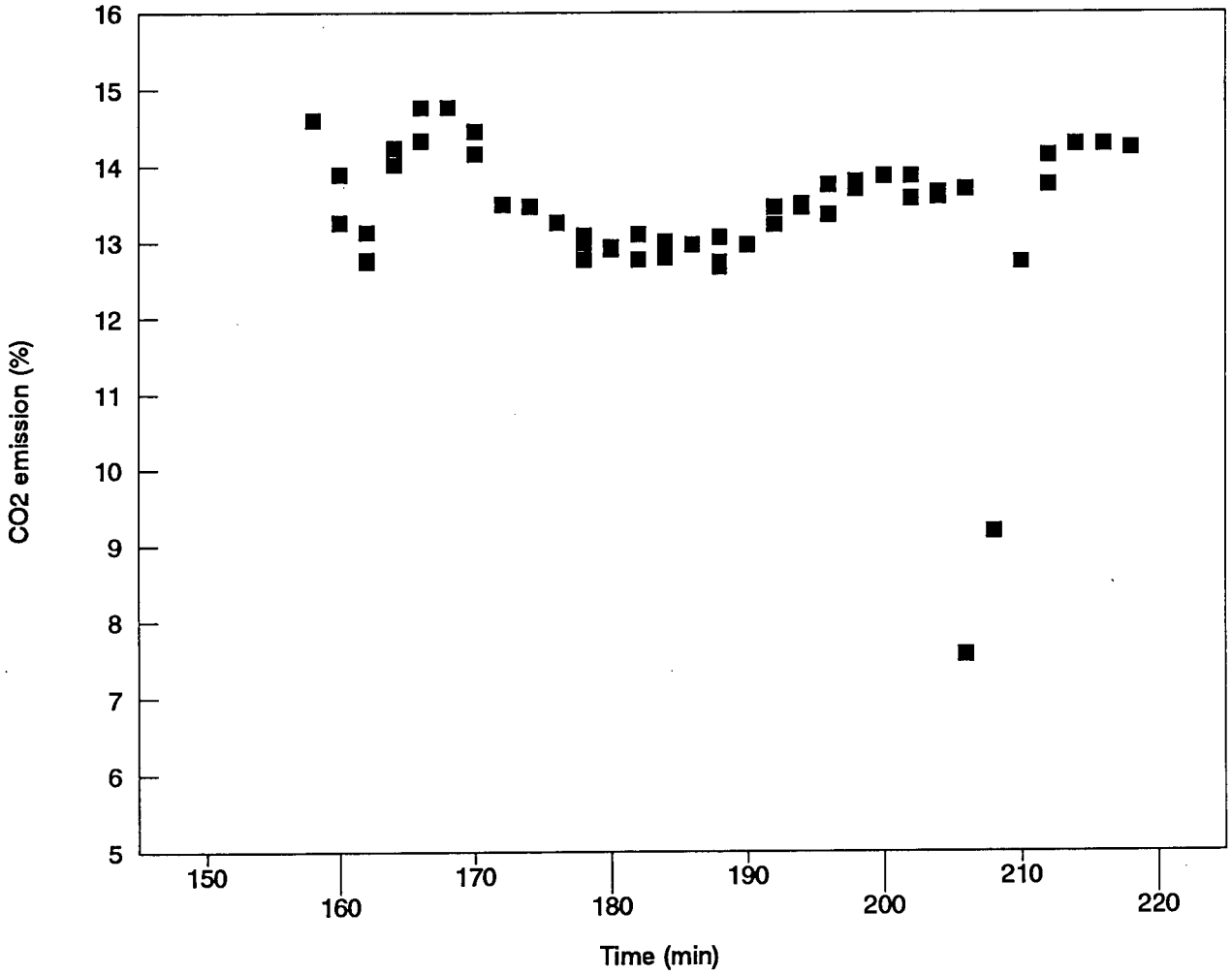

Figure 7.8 Flue Gas CO2 Emission for Pitch Cones : Condition 2.
(See Table 7.4 for details).

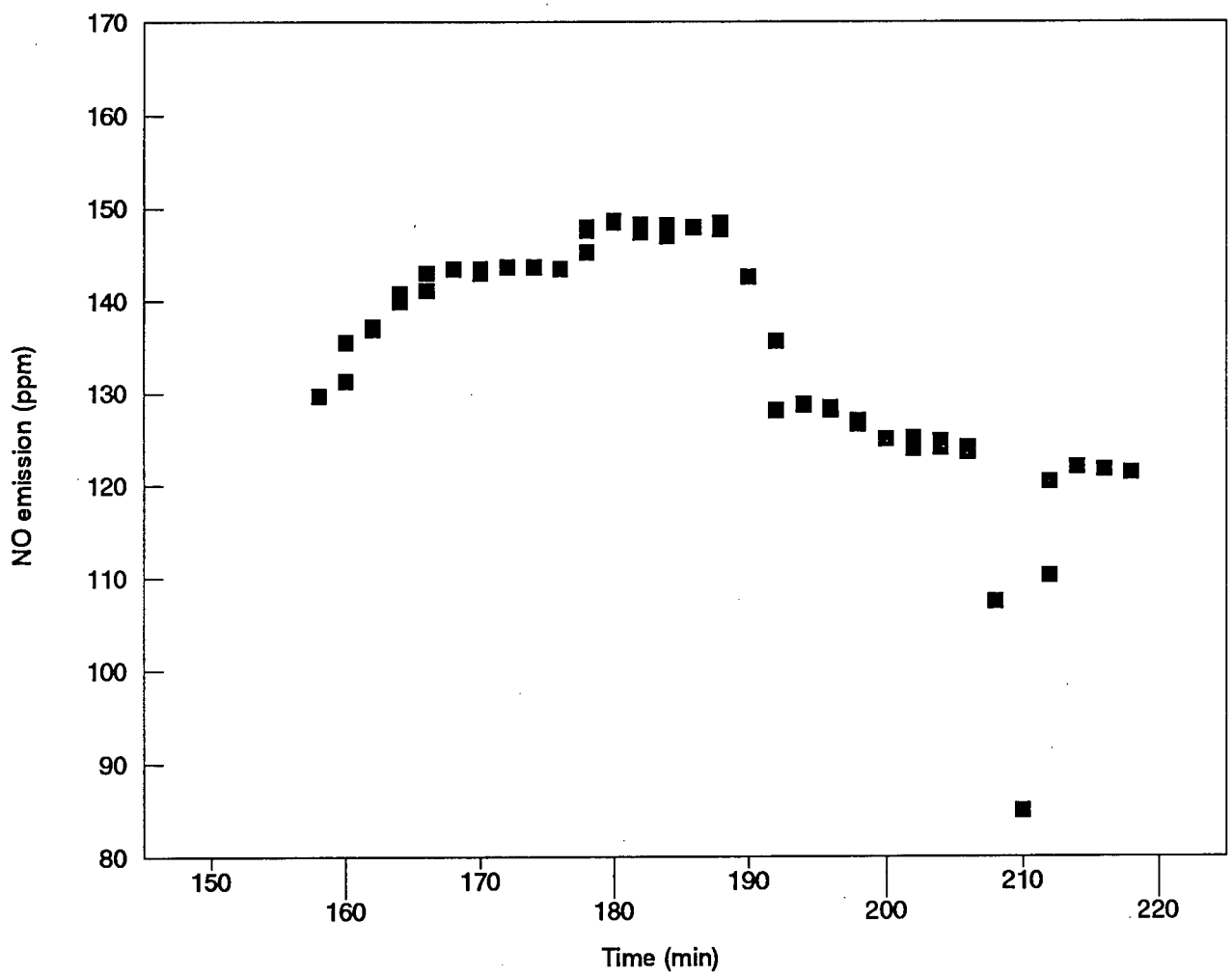

Figure 7.9 Flue Gas NO Emission for Pitch Cones : Condition 2.
(See Table 7.4 for details).

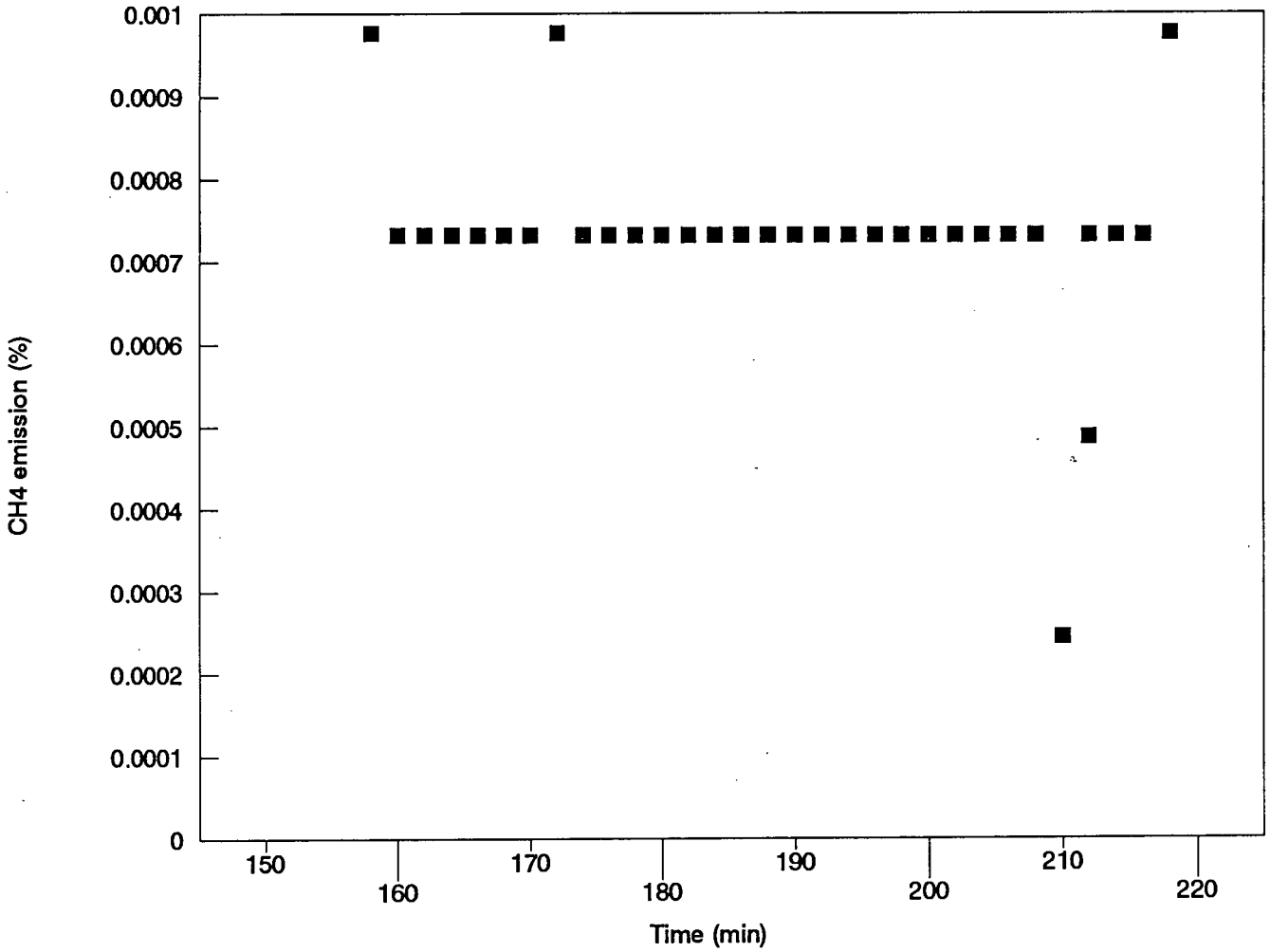

Figure 7.10 Flue Gas CH4 Emission for Pitch Cones : Condition 2.
(See Table 7.4 for details).

fine solids was found on the filter surface. This may suggest that the soot deposited on the filter surface may have some effect on CO production in the flue gas filter. Consequently, it seems clear that the true CO emission was lower than what was measured (an apparent CO emission). The high CO emissions are unlikely to represent a problem for larger units which provide much longer gas and solids residence times.

In condition 2, the CO emission continued to decrease from 360 ppm to 200 ppm (see Figure 7.7) although the oxygen level was steady in the same time interval. The continual decrease in CO emission may be due to variation in the size of the pitch cones fed into the combustor. Segregation of the pitch cones solids occurred in the feed hopper. At the beginning of the test, i.e. during condition 1, it was observed via the rotary valve window that fine solids were being fed into the combustor, while near the end of the test, i.e. during condition 2, coarser solids were being fed into the reactor. The coarser particles are captured by the primary and secondary cyclones and are returned to the riser. They may go through this cycle a few times, whereas the finer particles tend to pass through the riser and the cyclones only once. Thus, the longer time spent by the coarser particles in the CFB loop leads to an improvement in combustion and lower CO emissions are observed.

The SO_2 emissions reported in Tables 7.3 an 7.4 were estimated based on the sulphur content of the pitch cones. There were negligible flue gas SO_2 emissions for both operating conditions due to SO_2 condensation in the flue gas filter. It was later found that when the flue gas filter was heated with heating tape so that the temperature in the filter increased between 150 and 200 ^{o}C, the concentration of SO_2 increased to over 500 ppm. At the same time, the concentration of CO also increased drastically (to > 1000 ppm). When the heating tape was removed, the CO concentration decreased to 200 ppm over time. This further supports the postulate that soot deposited on the filter surface may be reacting to form CO.

The pitch cones burned readily in the pilot circulating fluidized bed unit. In view of the higher heating value of 37 MJ/kg, there were no problems with attaining a combustion temperature of 900 ^{o}C. During the total sulphur content analysis via the LECO analyzer, small flames were observed when the pitch cones were subjected to a temperature of 1351 ^{o}C in an oxidizing environment. The flames indicate the presence of volatiles. As a consequence, this fuel is much more reactive than the stud blast fines which had little or no volatiles. The segregation of pitch cones solids showed that fuel particle size affects the burning behaviour of the fuel. The modified solids feed system worked well in introducing the pitch cones which have a softening point at approximately 125 ^{o}C into the combustor. There were minor instances where the feeder probe became plugged, but it became unplugged as the softened pitch cones burned off. Despite the high apparent CO emissions, the pilot CFB achieved good combustion efficiency.

These preliminary results led to the following recommendations for the pilot CFB system.

1. There were instances where blockage did occur in the water-cooled solids feeder probe. The solids which softened in the probe did burn out and the probe became unplugged. However, at one point, there was partial blockage in the probe and the solids failed to burn off. Consequently, the test was terminated at that point. When the probe was removed from the combustor, it was observed that a hardened layer of solids (a mixture of pitch cones and sand) had penetrated a few centimetres into the probe. To reduce plugging problems in later incineration tests, a 6.35 mm 316 stainless steel tube (ram-rod) was inserted into the probe to remove the solids in the feeder.

2. It was observed that SO_2 condensed in the flue gas filter. A temperature regulated heating tape was wrapped around the flue gas filter for later tests. The temperature of

the flue gas filter should be maintained between 160 and 170 ^{o}C because at temperatures lower than 160 ^{o}C, SO_2 reacts with the $Ca(OH)_2$ in the ash layer on the surface of the filter.

3. Combustion efficiency is a major performance indicator of an incinerator. It is important to determine the CO emission accurately. However, with the existing flue gas sampling point, an apparent CO emission is obtained because it is difficult to prevent soot build up on the surface of the flue gas filter. In industrial applications, the emissions are sampled at the stack discharge point. Therefore, modifications to the gas sampling system were made to allow gas sampling immediately downstream of the baghouse filter (baghouse emissions). This better simulates the stack gas discharge conditions of an industrial unit. The gas residence time between these two sampling points is important for further reaction of the species in the gas stream, i.e. oxidation of CO to CO_2.

7.2 Incineration Results for Alcan Solid Waste Materials

Following the adjustments made to the UBC pilot CFB system after the preliminary incineration tests for stud blast fines and pitch cones, a second set of incineration tests was performed to study the effects of operating parameters on the emissions. The incineration results for the pitch cones, miscellaneous paste wastes and pitch dust are discussed in the following sections. For each waste material, the operating conditions are presented, followed by the flue gas and baghouse emissions. Then a discussion is presented of the effects of the operating parameters on the baghouse emissions. Finally, general comments are made regarding incineration of each of the waste materials.

7.2.1 Pitch Cones

The operating conditions for the incineration of the pitch cones are shown in Table 7.5. A steady state is characterized by stable operating temperature and flue gas emissions of O_2, SO_2, CO_2 and NO but not by the solids balance around the CFB system.. In order to have meaningful results on the solids balance around the system, the inert bed material, sand, in the combustor must be displaced by the ash generated during the combustion process. This would require over 48 hours of steady combustion. Seven steady state conditions were achieved for incineration of pitch cones, as compared to the proposed twelve conditions set out in section 6.1. In between steady states, there is a transition period during which the pilot CFB adjusts to the changes in operating parameter(s). In the transition period, the temperature (measured at 1.067 m above the base) is sampled at two minute intervals and the concentration of the flue gas constituents is measured continuously and recorded on the chart recorder. When both the temperature (i.e. typically +/- 5 ^{o}C) and the flue gas emissions become stable as observed over a time interval between 10 to 15 minutes, a steady state is deemed to have been achieved. Then, sampling of flue gas and baghouse emissions begins and the steady state is maintained until sampling has been completed (typically between 30 to 40 minutes).

The order of the steady states achieved differed from that proposed. The starting point depended on which of the steady states could be achieved quickly. For example, instead of starting with condition 1 (at T = 850 ^{o}C with 3.5 % O_2, see Table 6.1), the CFB achieved steady operation at T = 895 ^{o}C with 6.2 % O_2. Hence, the first steady state condition achieved corresponded to condition 7 in Table 6.1. For operating control purposes, it was easiest, for example, to change the temperature by changing the fuel feed rate, the degree of secondary air preheat and/or the rate of cooling via the hairpin heat exchanger while holding the excess air level constant. It would have been too time consuming and impractical to run at

the exact operating conditions proposed in section 6.1. Instead it was better to go with what the system is capable of achieving as long as it was within or near the values of the experimental parameters.

For steady states 1 to 3, the objective was to study the effect of decreasing operating temperature while trying to keep the excess air level at about 5.5 % oxygen. The total air flow rate, the primary-to-secondary air split ratio and the suspension density were kept constant. The change in temperature was achieved by adjusting the fuel feed rate and/or the cooling rate via the heat transfer surface. The secondary air fed into the riser was preheated during steady states 1 and 2, but not during steady state 3. Based on the observed emissions during these three steady states, it was clear that operating the CFB at a high temperature, 890 ^{o}C, and at an excess air level such that there was 5.5 % oxygen in the flue gas yielded the best emissions. Thus, steady state 1 was chosen as the base case.

In steady state 4, the objective was to study the effect of the primary-to-secondary air split ratio while trying to keep the operating condition similar to that of steady state 1. Although the primary-to-secondary to air split ratio was adjusted to 1.27, the total air flow rate remained constant so that the average gas residence time through the riser was still 7.6 m/s. During steady states 4 to 7, the secondary air was preheated before it was fed into the riser and there was no cooling via the hairpin heat exchanger. The fuel feed rate was adjusted during these steady states to maintain a temperature of 890 ^{o}C. In steady state 5, the objective was to study the effect of suspension density while trying to keep the operating condition similar to that of steady state 1. In steady state 6, the objective was to study the effect of operating the CFB at 890 ^{o}C, but at a lower excess air level of 3.2 % oxygen while trying to keep the other operating parameters at the same values as for steady state 1. In steady state 7, the objective was to study the effect of superficial gas velocity (gas residence time) while trying to keep the other operating conditions similar to those in steady state 1.

Table 7.5 Operating Conditions for Pitch Cones

	SS # 1	SS # 2	SS # 3	SS # 4	SS # 5	SS # 6	SS # 7
Avg. Incineration Temp. (^{o}C)	895	856	833	887	887	889	890
Avg. Primary Cyclone Temp. (^{o}C)	861	836	804	857	858	866	864
Avg. Secondary Cyclone Temp. (^{o}C)	868	840	821	865	863	873	865
Excess Air (% O_2)	6.1	5.5	5.2	5	5.4	3.2	5
Fuel Feed Rate (kg/h)	11.3	11.9	12	12.3	12	13.6	10.4
P : S Air Split Ratio	2.01	1.96	1.96	1.27	1.96	1.95	2.02
Total Air Flow Rate (SCFM)	85	86	85	86	86	86	72
Total Air Flow Rate (m^3/h)	145	146	145	146	146	146	123
Superficial Gas Velocity (m/s)	7.6	7.4	7.2	7.6	7.6	7.6	6.4
Suspension Density (kg/m^3)	120	120	120	120	140	120	120

The average incineration temperature is the arithmetic average of the temperatures measured at z = 0.305, 1.067, 2.134, 2.743, 3.962, 4.572, 5.182, 5.791 and 6.041 m above the base. The average primary cyclone temperature is the arithmetic average of the temperatures measured at the top, the middle and the bottom of the cyclone. The average secondary cyclone temperature is the arithmetic average of the temperatures measured there. The excess air is the percent of oxygen present in the flue gas prior to dilution with air in the baghouse. The temperature in the baghouse was maintained at approximately 150 ^{o}C by addition of dilution air.

Raw flue gas emissions and their corresponding corrected emissions are shown in Tables 7.6 and 7.7. Raw baghouse emissions and their corresponding corrected emissions are shown in Tables 7.8 and 7.9. The raw emissions are expressed on a volume basis, i.e. % by volume or ppm by volume. The average gas residence times reported in Tables 7. 7 and 7.9 are based on the total air flow rate through the riser with the CFB operating at the average incineration temperature. A detailed mass balance for each steady state is given in Appendix D. Sample

calculations for the correction of flue gas and baghouse emissions are provided in Appendix E. Plots of the flue gas and baghouse emissions (raw data) as a function of time for each steady state are also provided in Appendix E. Plots of axial temperature profiles for each steady state are provided in Appendix F.

Table 7.6 Pitch Cones Flue Gas Emissions

Species	SS # 1	SS # 2	SS # 3	SS # 4	SS # 5	SS # 6	SS # 7
O_2 (%)	6.1	5.5	5.2	5	5.4	3.2	5
CO_2 (%)	14.6	14.9	14.5	14.7	14.2	16.1	14.3
CH_4 (%)	0.0010	0.0017	0.0030	0.0029	0.0029	0.0038	0.0033
CO(ppm)	137	240	363	116	145	237	123
NO_x (ppm)	150	113	135	172	190	166	205
SO_2 (ppm)	149	178	171	182	182	248	195
N_2O (ppm)	75	99	114	84	83	84	72

Table 7.7 Pitch Cones Corrected Flue Gas Emissions

Species	SS # 1	SS # 2	SS # 3	SS # 4	SS # 5	SS # 6	SS # 7	SWR Limit
O_2 (% in flue gas)	6.1	5.5	5.2	5	5.4	3.2	5	-
Avg. Incin. Temp. (^oC)	895	856	833	887	887	889	890	-
Avg. Gas Residence Time (s)	0.96	0.99	1.02	0.96	0.96	0.96	1.14	-
O_2 (%)	11	11	11	11	11	11	11	11
CO_2 (%)	9.8	9.6	9.2	9.2	9.1	9	8.9	N/A
CH_4 (mg/m^3)	4	7	13	12	12	14	14	32
CO (mg/m^3)	107	180	268	84	108	155	90	55
NO_x (mg/m^3)	193	139	163	206	233	178	245	380
SO_2 (mg/m^3)	266	306	288	303	311	371	325	180
N_2O (mg/m^3)	92	122	132	96	97	86	82	N/A
CE (%)	99.91	99.84	99.75	99.92	99.90	99.85	99.91	≥ 99.9

Table 7.8 Pitch Cones Baghouse Emissions

Species	SS # 1	SS # 2	SS # 3	SS # 4	SS # 5	SS # 6	SS # 7
O_2 (%)	15.2	14.8	13.5	14	14.5	13	16.3
CO_2 (%)	7	7.2	8.1	7.9	7	8.5	7.3
CH_4 (%)	0	0.0004	0.0017	0.0017	0.0014	0.0022	0.0020
CO(ppm)	47	55	69	36	36	38	21
NO_x (ppm)	60	55	89	96	107	91	100
SO_2 (ppm)	75	76	95	89	76	119	82
N_2O (ppm)	28	43	56	39	37	37	33

Table 7.9 Pitch Cones Corrected Baghouse Emissions

Species	SS # 1	SS # 2	SS # 3	SS # 4	SS # 5	SS # 6	SS # 7	SWR Limit
O_2 (% in flue gas)	6.1	5.5	5.2	5	5.4	3.2	5	-
Avg. Incin. Temp. (^oC)	895	856	833	887	887	889	890	-
Avg. Gas Residence Time (s)	0.96	0.99	1.02	0.96	0.96	0.96	1.14	-
O_2 (%)	11	11	11	11	11	11	11	11
CO_2 (%)	12.1	11.6	10.8	11.3	10.8	10.6	15.5	N/A
CH_4 (mg/m^3)	0	4	15	16	14	18	28	32
CO (mg/m^3)	94	103	107	60	64	55	52	55
NO_x (mg/m^3)	198	170	227	262	315	218	407	380
SO_2 (mg/m^3)	344	326	337	339	311	396	465	180
N_2O (mg/m^3)	88	127	137	102	104	85	128	N/A
CE (%)	99.93	99.92	99.91	99.95	99.95	99.96	99.97	≥ 99.9

In the UBC pilot CFB unit, combustion reactions take place in the combustor and the primary and secondary cyclones. The decrease in the CO emission between the flue gas filter and the baghouse for all steady states showed that reactions continue to take place between these two

sampling locations (see corrected flue gas and baghouse emissions). The NO emission tended to decrease, while NO_2 emission tended to increase between these sampling points. This is due to continual NO oxidation to NO_2. The CFB riser and its two cyclones provide good initial combustion. After the majority of the particulates have been removed by the two cyclones, the components in the gas stream continue to undergo reactions. This is similar to the afterburner effect for the completion of gas phase combustion reactions. There is a reduction in CO emissions due to the gas phase residence time between the flue gas filter and the baghouse filter. With such a small unit; however, an afterburning chamber, i.e. an insulated section after the cyclones, is needed to decrease the CO emissions to acceptable levels. The CFB system can be designed for any desired residence time after the cyclone systems to bring down the CO emissions.

The extent of reactions in CFBs is a function of the incineration temperature, excess air, suspension density and residence time (a function of superficial gas velocity). The effects of these operating parameters on the corrected baghouse emissions are discussed in the following sections. As mentioned before, the temperature in the baghouse is maintained at approximately 150 ^{o}C by addition of dilution air. However, the amount of dilution air added was not measured and the oxygen content in the baghouse varied for each steady state. Hence, it is necessary to correct the baghouse emissions to the same basis, i.e. 11% O_2, 20 ^{o}C, 760 mm Hg and dry basis, for comparison analysis.

7.2.1.1 Effect of Incineration Temperature

A decrease in the incineration temperature from 898 to 835 ^{o}C (SS # 1 - 3) resulted in an increase in CO emissions from 94 to 107 mg/m^3. The total hydrocarbons expressed as methane, CH_4, also increased from 0 to 15 mg/m^3. This shows that high temperatures are required to achieve higher degrees of combustion. However, there are limitations imposed on

the incineration temperature (see section 6.1). The temperature of the preheated secondary air in steady states 1 and 2 may also have helped to enhance the oxidation of CO to CO_2; hence, resulting in lower CO emissions compared to steady state 3. NO_x emissions generally tend to decrease with decreasing incineration temperature at a given excess air level. The NO_x emission decreased from 198 to 170 mg/m^3 when the incineration temperature was decreased from 895 to 856 ^oC. However, the NO_x emission increased from 170 to 227 mg/m^3 when the incineration temperature was further decreased from 856 to 833 ^oC. It is unclear why this happened. For combustors operating at low incineration temperatures, N_2O formation is significant. This is shown by the increase in N_2O emissions from 88 to 137 mg/m^3 as the incineration temperature was decreased from 895 to 833 ^oC.

7.2.1.2 Effect of Excess Air

A decrease in the amount of excess air from 6.1 to 3.2 % O_2 (cf. SS # 1 and 6) resulted in more unburned carbon; CH_4 emission increased from 0 to 18 mg/m^3. However, the combustion efficiency at 3.2 % O_2 still exceeded 99.9 %. NO_x formation generally tends to increase with increasing excess air levels at a given temperature. However, the NO_x emission increased from 198 to 218 mg/m^3 as the excess air decreased from 6.1 to 3.2 % O_2. It is unclear why this occurred. Operating at 895 ^oC and 6.1 % O_2 yielded the best emissions for the pitch cones. Hence, using this operating condition (SS # 1) as the base condition, the effects of air split ratio, suspension density and superficial gas velocity on emissions are presented in the following paragraphs.

7.2.1.3 Effect of Primary-to-Secondary Air Split Ratio

In general, CFBs have good solids mixing but poor radial gas mixing behaviour. A high secondary air flow stream into the CFB may affect the radial mixing patterns and hence

improve the radial gas mixing. The primary-to-secondary air split ratio was decreased from 2.0 to 1.27 (SS # 4) while maintaining a constant total air flow rate. The average gas residence time remained at 0.96 s, but, the residence time of the primary air stream increased from 0.67 to 0.80 s in the bottom 3.4 m of the riser. The increase in secondary air flow rate 3.4 m above the distributor during steady state # 4 improved radial gas mixing and increased the local oxygen concentration. Consequently, the CO emission decreased from 94 to 60 mg/m^3 and the NO_X emission increased from 198 to 262 mg/m^3.

7.2.1.4 Effect of Suspension Density

By increasing the suspension density from 120 to 140 kg/m^3 (SS # 5), the degree of air/waste contact and gas mixing is enhanced. As a result, the CO emission decreased from 94 to 64 mg/m^3 and the NO_X emission increased from 198 to 315 mg/m^3.

7.2.1.5 Effect of Superficial Gas Velocity

The superficial gas velocity was decreased from 7.6 to 6.5 m/s (SS # 7) by decreasing the total air flow rate. As a result, the average gas residence time was increased from 0.96 to 1.14 s and the residence time of the pitch cones in the CFB riser increased at the same time. The resulting increases in the gas and waste solids residence times led to improved combustion, with the CO emission decreasing from 94 to 52 mg/m^3. The longer gas and solids residence time also increased the NO_X emission from 198 to 407 mg/m^3.

7.2.1.6 General Comments

The pitch cones containing 0.5 weight percent sulphur (dry basis) were incinerated without limestone addition. The measured flue gas SO_2 emissions were approximately 100 ppm lower

than calculated (see mass balances). The calculated values were based on the assumption that all the sulphur in the pitch cones would be oxidized to form sulphur dioxide. Possible explanations for the discrepancy include: (i) some portion of the sulphur measured in the ultimate analysis is not converted to SO_2 during combustion and (ii) catalytic effects of vanadium in the ash causing oxidation of SO_2 to SO_3 which is not detected by the SO_2 analyzer. There is approximately 1000 ppm vanadium in the pitch cones ash and previous pilot [Brereton et al., 1992] and bench-scale tests [Brereton et al., 1993] at UBC have shown that vanadium in the form of vanadium pentoxide, V_2O_5, in coke ashes acts as a catalyst for oxidation of SO_2 to SO_3. More work is needed to resolve the SO_2 balance.

These tests demonstrate that CFB combustion technology is suitable for the incineration of pitch cones with a low sulphur and ash content, 0.50 wt % and 1.06 wt. % respectively, while having a higher heating value of 37 MJ/kg, dry basis. Although SO_2 emissions were high in all steady states, this problem can be readily remedied by limestone addition. At steady state operating condition # 6, approximately 330 ppm (494 mg/m^3) of SO_2 would be generated as provided by the mass balance. At the same time approximately 0.012 kg of solid wastes would be generated per kg of pitch cones incinerated. With limestone addition, (at a molar Ca:S ratio of 0.68, assuming limestone with 95.5 wt. % $CaCO_3$ and 63 % sulphur capture efficiency) approximately 122 ppm (182 mg/m^3) of SO_2 would result, and approximately 0.026 kg of solid wastes would be generated per kg of pitch cones incinerated (see mass balance). This would still result in a substantial reduction in solids residue. The pilot CFB unit consistently achieved combustion efficiencies exceeding 99.9 %. The high CO emissions can be reduced by adding an afterburner chamber after the cyclone systems. It is anticipated that with suitable operating conditions and limestone addition, the UBC pilot CFB unit could meet all the B.C. Special Waste Regulations emission discharge criteria.

7.2.2 Miscellaneous Paste Waste

The operating conditions for the incineration of the miscellaneous paste waste are shown in Table 7.10 Four steady state conditions were achieved. The miscellaneous paste waste was incinerated without limestone addition during the first two steady states, with the incineration temperature decreased from 877 to 819 ^{o}C. It was anticipated that the miscellaneous paste waste would exhibit behaviour similar to the pitch cones under similar steady state conditions since they are similar in chemical composition and they may have similar particle size distributions. However, the miscellaneous paste waste, which contained 1.34 weight percent sulphur (dry basis), resulted in much higher baghouse SO_2 emissions. There was also a sulphurous odour in the area surrounding the pilot plant. With approximately 60 kg of miscellaneous paste waste remaining in the feed hopper, corresponding to about 4.5 hours of operation, a decision was made to study the effect of sulphur capture by limestone addition since it would take several hours for the SO_2 emissions to stabilize after limestone addition. Hence, the incineration temperature was increased from 820 to 870 ^{o}C (SS # 3) and when the system became stable, British Coal Limestone with approximately 98 weight percent calcium carbonate, $CaCO_3$, was added at a molar Ca:S ratio of 2.5 : 1 (SS # 4). The secondary air was preheated in steady states 1, 3 and 4 in order to maintain the temperature. The objectives of the incineration tests for the miscellaneous paste wastes were therefore to study the effects of incineration temperature on emissions and limestone addition on sulphur capture.

Table 7.10 Operating Conditions for Miscellaneous Paste Waste

	SS # 1	SS # 2	SS # 3	SS # 4
Avg. Incineration Temp. (^{o}C)	877	819	870	871
Avg. Primary Cyclone Temp. (^{o}C)	855 *	818	860	852
Avg. Secondary Cyclone Temp.(^{o}C)	871	824	869	869
Excess Air (% O_2)	5.6	5.3	5.2	5.2
Fuel Feed Rate (kg/h)	13.2	13.5	13.6	13.5
P : S Air Split Ratio	1.96	1.96	1.96	1.96
Total Air Flow Rate (SCFM)	86	86	86	86
Total Air Flow Rate (m^3/h)	146	146	146	146
Superficial Gas Velocity (m/s)	7.5	7.2	7.5	7.5
Suspension Density (kg/m^3)	120	120	120	120
Limestone Feed Rate (kg/h)	-	-	-	1.44
Molar Ca: S ratio	-	-	-	2.5 : 1

* This is the temperature at the top of the primary cyclone during the steady state.

The flue gas emissions and their corresponding corrected emissions are shown in Tables 7.11 and 7.12, while baghouse emissions and their corresponding corrected emissions are shown in Tables 7.13 and 7.14. A detailed mass balance for each steady state is shown in Appendix D. The combustion efficiencies used in the mass balances are based on the flue gas emissions. Plots of the flue gas and baghouse emissions (raw data) as functions of time for each steady state are provided in Appendix E. Axial temperature profiles are provided in Appendix F for each steady state.

Table 7.11 Miscellaneous Paste Waste Flue Gas Emissions

	SS # 1	SS # 2	SS # 3	SS # 4
O_2 (%)	5.6	5.3	5.2	5.2
CO_2 (%)	14.6	14.7	14.9	14.7
CH_4 (%)	0.0078	0.0076	0.0085	0.0021
CO(ppm)	140	311	156	95
NO_x (ppm)	166	115	179	162
SO_2 (ppm)	711	757	812	107
N_2O (ppm)	87	109	98	76

Table 7.12 Miscellaneous Paste Waste Corrected Flue Gas Emissions

Species	SS # 1	SS # 2	SS # 3	SS # 4	SWR Limit
O_2 (% in flue gas)	5.6	5.3	5.2	5.2	-
Avg. Incin. Temp. (^oC)	877	819	870	871	-
Avg. Gas Residence Time (s)	0.98	1.02	0.98	0.98	-
O_2 (%)	11	11	11	11	11
CO_2 (%)	9.5	9.4	9.4	9.3	-
CH_4 (mg/m^3)	34	32	36	9	3232
CO (mg/m^3)	106	231	115	70	55
NO_x (mg/m^3)	206	140	217	196	380
SO_2 (mg/m^3)	1230	1284	1369	180	180
N_2O (mg/m^3)	103	127	113	88	N/A
CE (%)	99.90	99.79	99.90	99.94	≥ 99.9

Table 7.13 Miscellaneous Paste Waste Baghouse Emissions

Species	SS # 1	SS # 2	SS # 3	SS # 4
O_2 (%)	15	16	16	15.5
CO_2 (%)	6.9	7.8	6	6.7
CH_4 (%)	0.0037	0.0038	0.0034	0.0010
CO(ppm)	27	69	22	18
NO_x (ppm)	83	80	87	87
SO_2 (ppm)	235	303	220	38
N_2O (ppm)	32	59	35	24

Table 7.14 Miscellaneous Paste Waste Corrected Baghouse Emissions

Species	SS # 1	SS # 2	SS # 3	SS # 4	SWR Limit
O_2 (% in flue gas)	5.6	5.3	5.2	5.2	-
Avg. Incin. Temp. (^oC)	877	819	870	871	-
Avg. Gas Residence Time (s)	0.98	1.02	0.98	0.98	-
O_2 (%)	11	11	11	11	11
CO_2 (%)	11.5	15.6	12	12.2	-
CH_4 (mg/m^3)	41	51	45	12	32
CO (mg/m^3)	52	161	51	38	55
NO_x (mg/m^3)	265	306	333	303	380
SO_2 (mg/m^3)	1043	1614	1172	184	180
N_2O (mg/m^3)	98	216	128	80	N/A
CE (%)	99.96	99.91	99.96	99.97	≥ 99.9

7.2.2.1 Effect of Incineration Temperature

A decrease in the incineration temperature from 877 to 819 ^oC resulted in an increase in baghouse CO emission from 52 to 161 mg/m^3 and a decrease in the combustion efficiency from 99.96 to 99.91 %. Operating at 819 ^oC, the temperature was too low to provide complete combustion. By changing the incineration temperature, the volumetric flow of gas through the riser changes and this also changes the average gas residence time. In this case, the decrease in temperature increased the average gas residence time by only 0.03 s. The

temperature of the preheated secondary air in steady state 1 may have helped to enhance the oxidation of CO to CO_2; hence, resulting in lower CO emissions.

7.2.2.2 Effect of Limestone Addition on Sulphur Capture

Figures 7.11 to 7.16 show the flue gas O_2, CO, CO_2, NO, CH_4 and SO_2 emissions and the incineration temperature as a function of time for steady states # 3 and 4, respectively. During steady state # 3, flue gas emissions were measured at t = 22 min and baghouse emissions were measured at t = 28 min. Limestone was then fed into the pilot CFB at 1.44 kg/h beginning at t = 40 min, and this operating condition was maintained for 4 hours due to the length of time required for the SO_2 emission to stabilize. The flue gas SO_2 emission was continuously monitored to provide a conservative SO_2 emission value. The transition period from steady state # 3 to # 4 took approximately 2.3 hours. Steady state # 4 started at approximately t = 180 min and ended at t = 286 min. The SO_2 emission was fairly steady during this period but began to drift near the end (see Figure 7.16). At t = 272 min, baghouse emissions were measured. The flue gas SO_2 emissions with and without limestone addition were 180 mg/m^3 and 1369 mg/m^3 respectively. This corresponds to 87 % sulphur capture efficiency with molar Ca:S = 2.5 with the SO_2 emission meeting the SWR discharge limit of 180 mg/m^3. The baghouse SO_2 emissions with and without limestone addition were 184 mg/m^3 and 1172 mg/m^3 respectively, corresponding to 83 % sulphur capture efficiency, with the SO_2 emission close to meeting the SWR discharge limit of 180 mg/m^3. Without limestone addition as in steady state 3, approximately 0.096 kg of solids wastes would be generated per kg of misc. paste waste incinerated (see mass balance). With limestone addition at a molar Ca:S of 2.5:1 as in steady state 4, and assuming 83 % sulphur capture, approximately 0.185 kg of solid wastes would be generated per kg of misc. paste waste incinerated (see mass balance). With limestone addition, there is still a substantial reduction in solids residue.

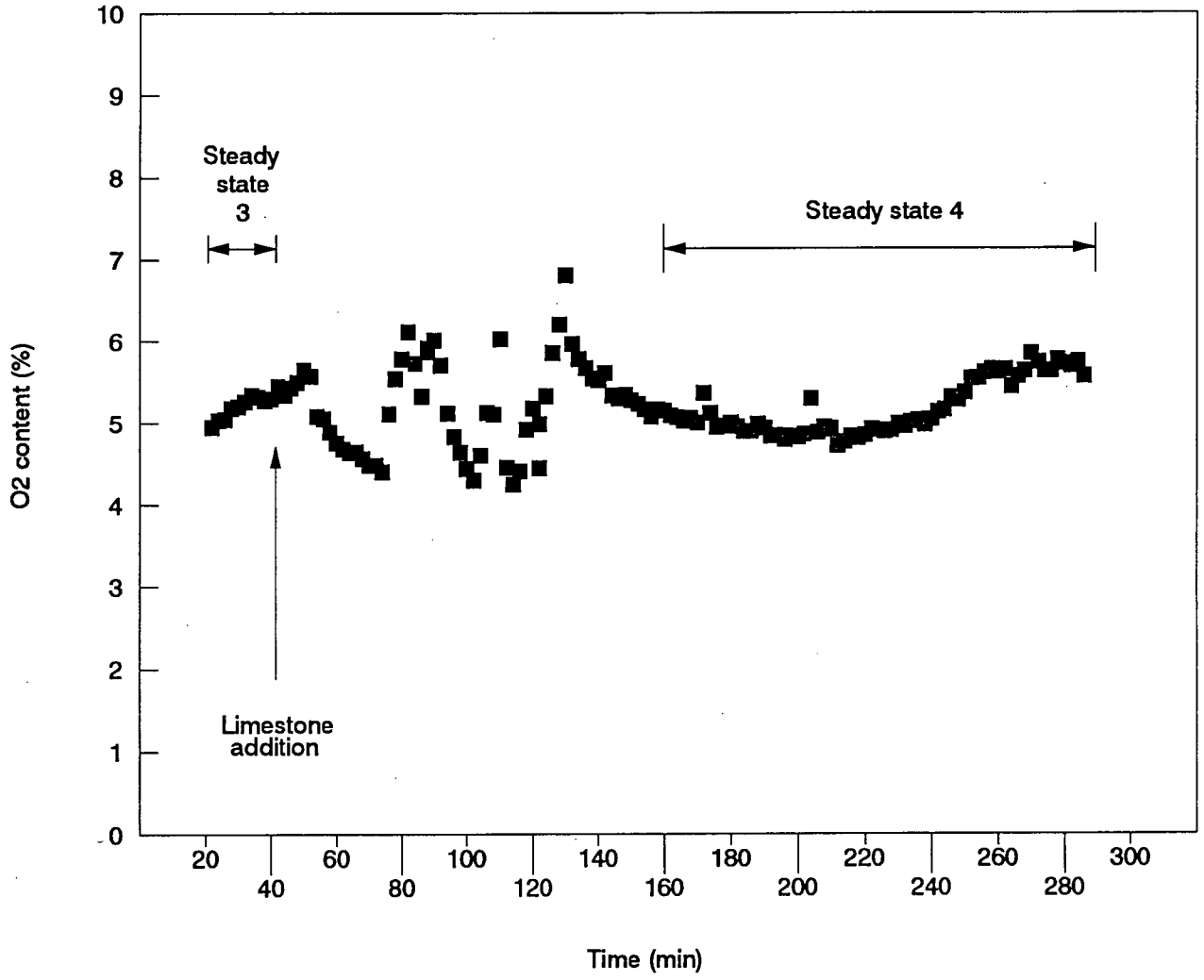

Figure 7.11 Flue Gas O2 Content for Misc. Paste Waste : Steady States 3 and 4. (See Table 7.10 for details).

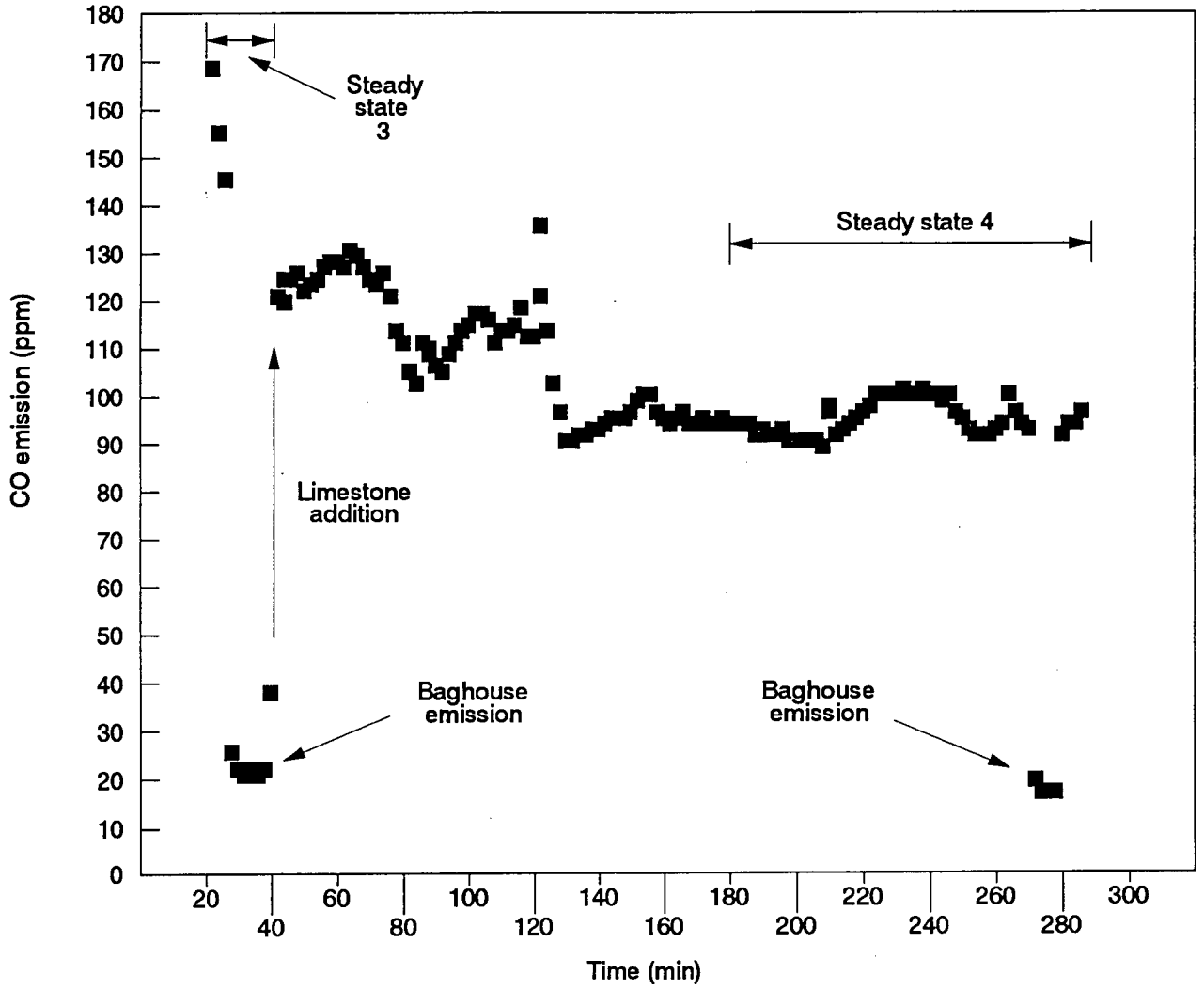

Figure 7.12 Flue Gas CO Emission for Misc. Paste Waste : Steady States 3 and 4. (See Table 7.10 for details).

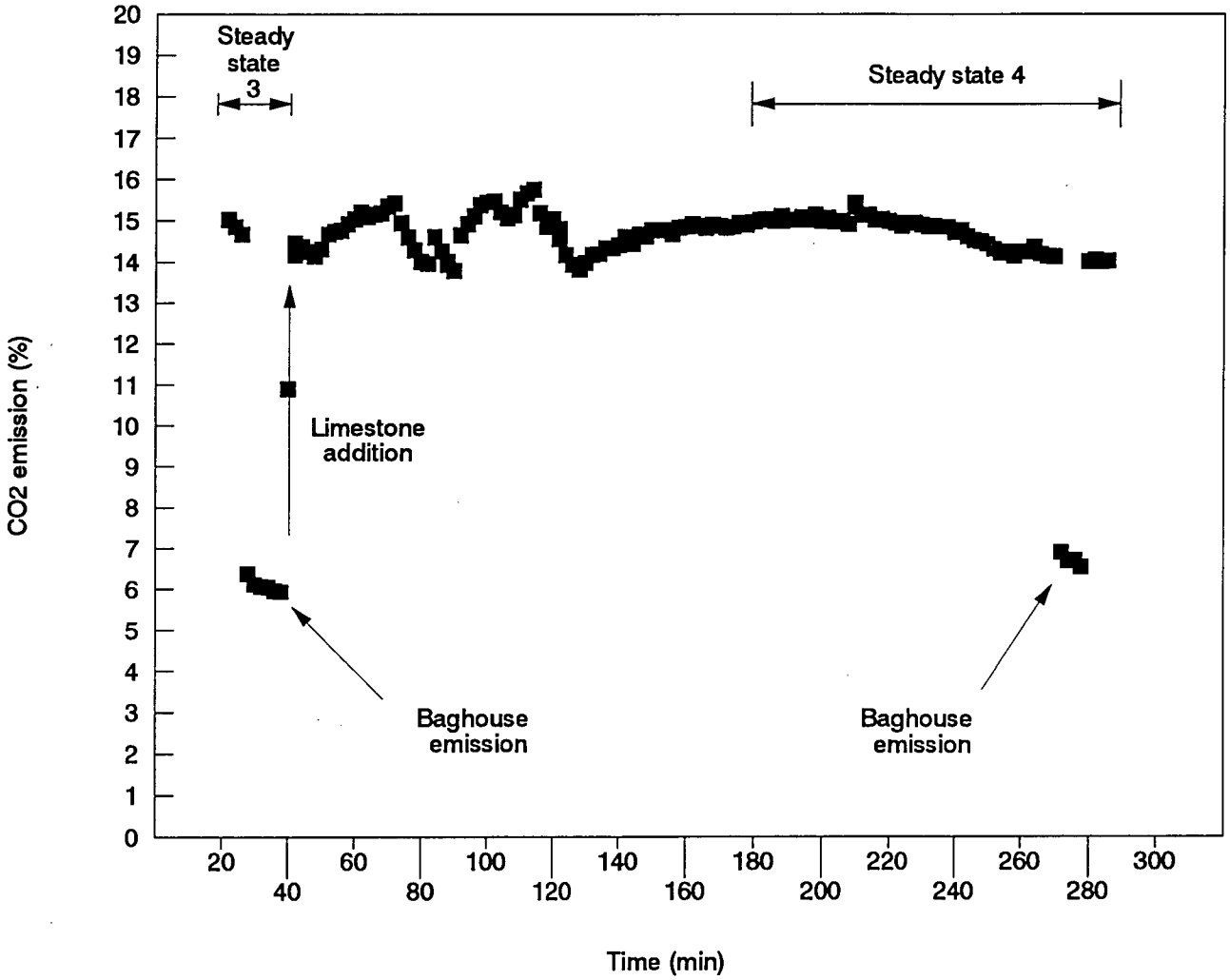

Figure 7.13 Flue Gas CO2 Emission for Misc. Paste Waste : Steady States 3 and 4.
(See Table 7.10 for details).

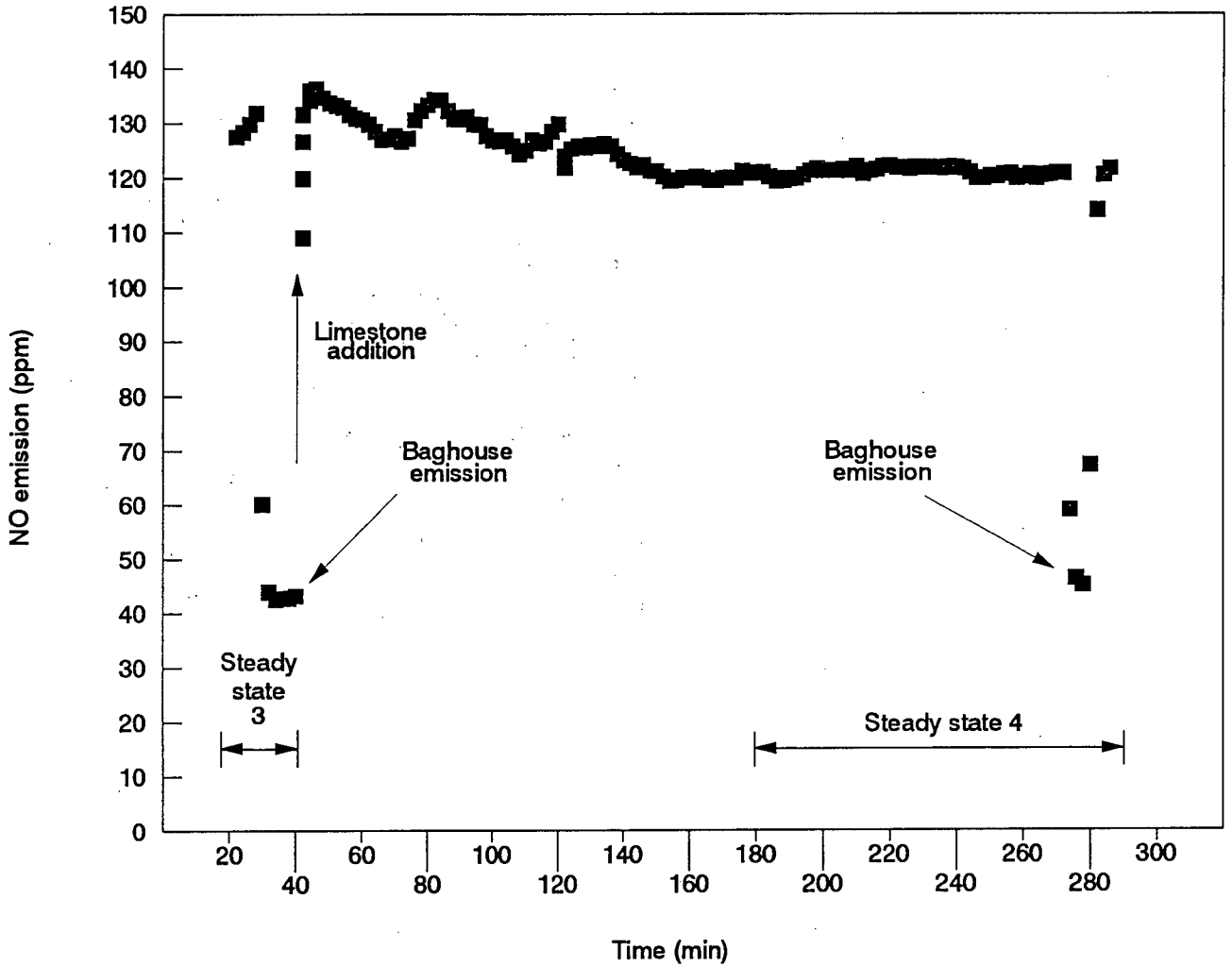

Figure 7.14 Flue Gas NO Emission for Misc. Paste Waste : Steady States 3 and 4. (See Table 7.10 for details).

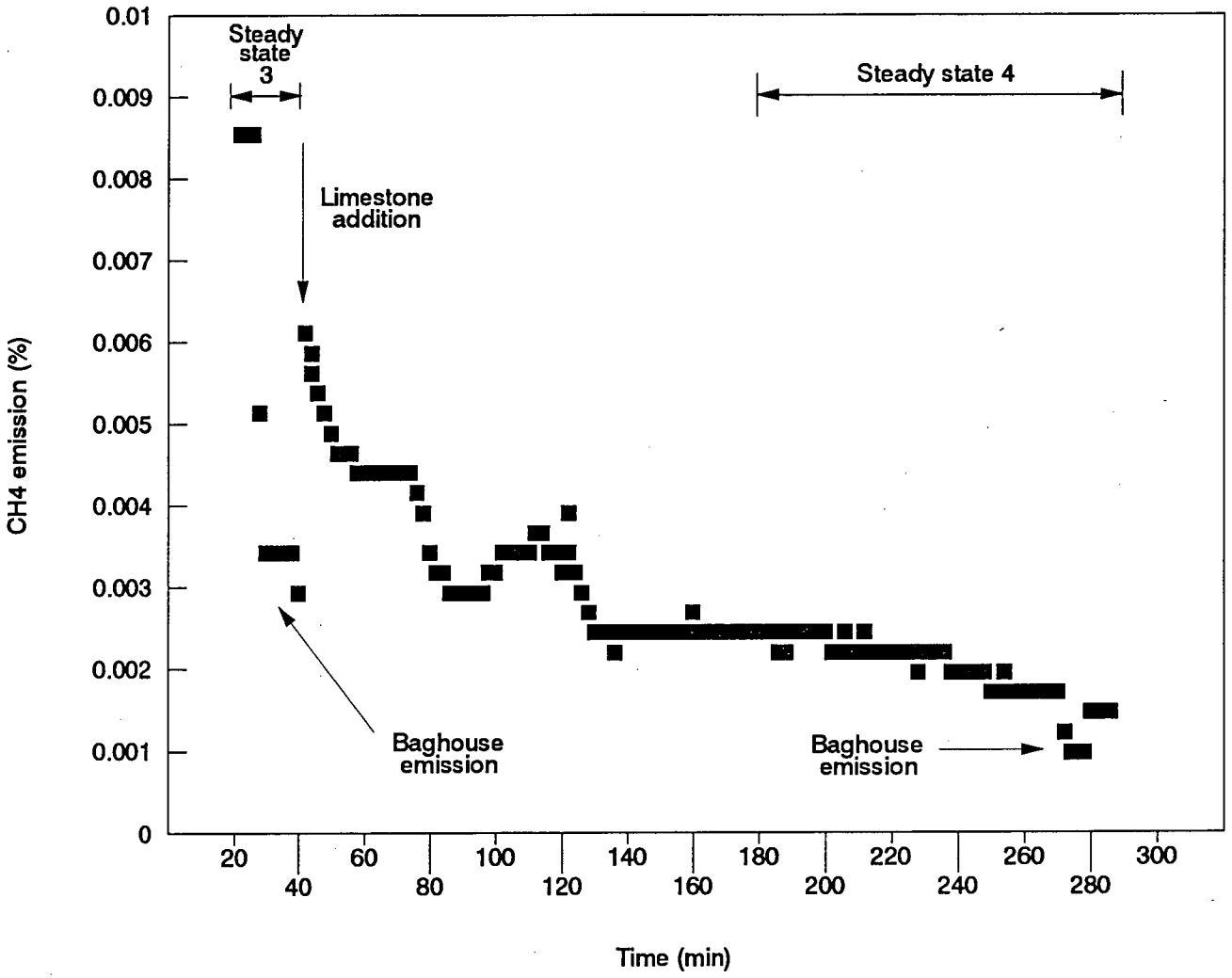

Figure 7.15 Flue Gas CH4 Emission for Misc. Paste Waste : Steady States 3 and 4. (See Table 7.10 for details).

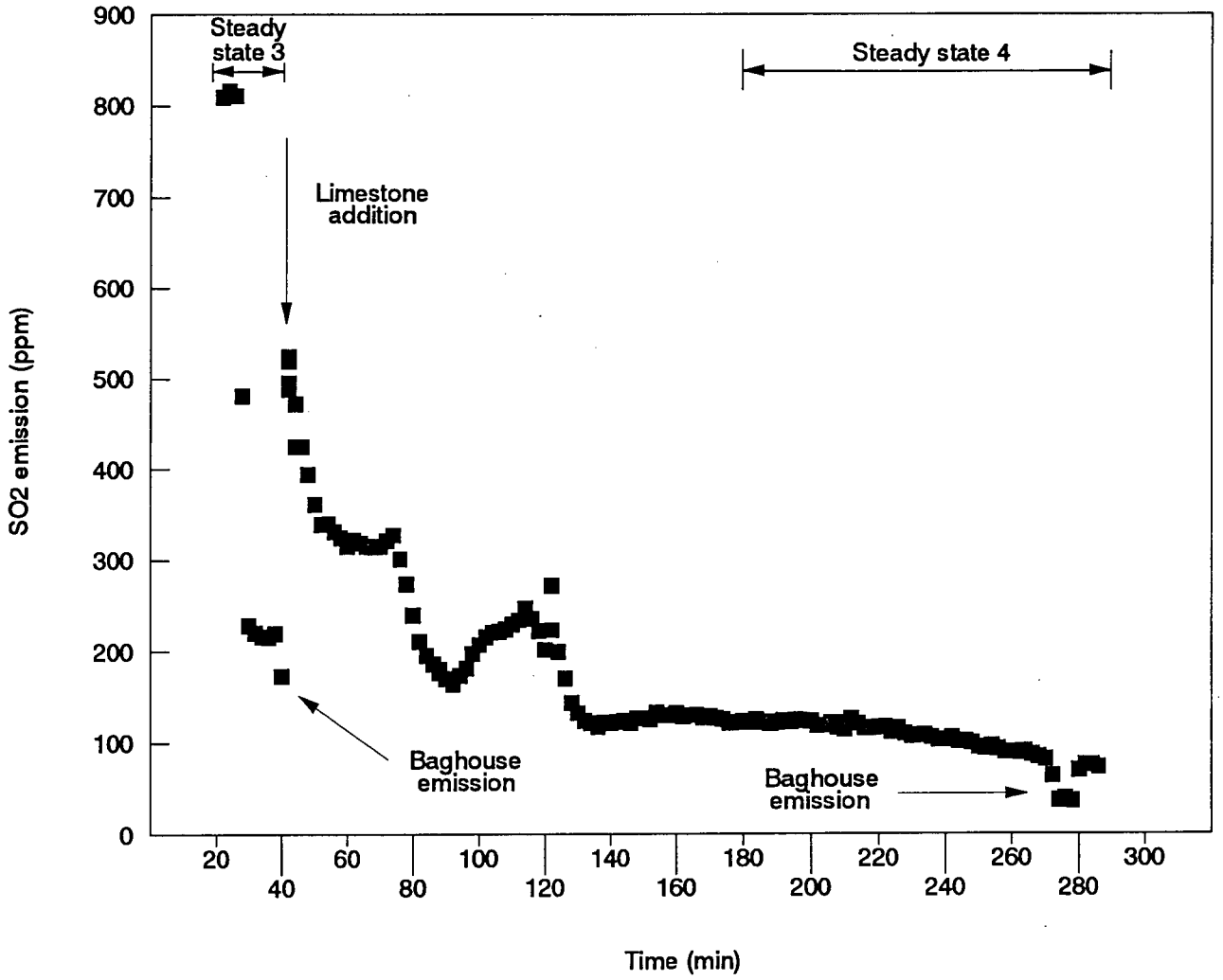

Figure 7.16 Flue Gas SO2 Emission for Misc. Paste Waste : Steady States 3 and 4. (See Table 7.10 for details).

7.2.2.3 General Comments

The miscellaneous paste waste with a higher heating value of 34.5 MJ/kg burned readily in the pilot CFB. In-situ sulphur capture by limestone addition was effective in reducing the SO_2 emission. Incineration of miscellaneous paste waste at operating conditions corresponding to steady state condition # 4 resulted in emissions which meet the SWR discharge limits except for SO_2 emissions. The SO_2 emissions may be further decreased to meet the discharge criteria by increasing the molar Ca:S ratio.

7.2.3 Pitch Dust

Pitch dust was incinerated with limestone addition immediately after the miscellaneous paste waste because (i) the pitch dust contains approximately 1.38 weight percent sulphur (dry basis) and would result in high SO_2 emissions as in the case of the miscellaneous paste waste, and (ii) it would take several hours for the limestone already in the pilot CFB to exit the system. Hence, the pitch dust was burned with limestone in the first operating condition. Then, the limestone feed would be stopped while holding all other parameters constant to obtain baseline emissions. However, there were problems with the solids feeding system during the first operating condition. The solids feed probe became plugged approximately every 10 minutes which made it difficult to achieve steady state conditions. This is evident in Figure 7.18 which shows the baghouse CO emission over time. Following the cleaning of the probe with the ram-rod, high CO peaks resulted due to a sudden surge of the carbon mass which had been lodged in the probe. However, between the periods of cleaning, there was a brief period in which stable CO emission was achieved. Two such periods are between t = 158 and 162 min and between t = 170 and 174 min. These two periods are designated t1 and t2 respectively but they are not steady states. The operating conditions, baghouse emissions and corrected baghouse emissions during these two periods are shown in Tables 7.15, 7.16

and 7.17, respectively. Plots of oxygen content in the flue gas and baghouse emissions of CO, CO_2, NO, CH_4 and SO_2 are shown in Figures 7.17 to 7.22, respectively. An axial temperature profile (over the time interval between t = 84 and 176 min) is shown in Figure 7.23. The variation of temperature 0.305 m above the distributor with time is shown in Figure 7.24.

Table 7.15 Operating Conditions for Pitch Dust

	t1	t2
Incineration Temp. (^oC)	877	885
Excess Air (% O_2)	3.9	6.8
Fuel Feed Rate (kg/h)	13.1	10.9
P : S Air Split Ratio	1.97	1.97
Total Air Flow Rate (SCFM)	86	86
Total Air Flow Rate (m^3/h)	146	146
Superficial Gas Velocity (m/s)	7.6	7.6
Suspension Density (kg/m^3)	120	120
Limestone Feed Rate (kg/h)	1.4	1.4
Molar Ca: S ratio	2.37 : 1	2.85 : 1

Table 7.16 Pitch Dust Baghouse Emissions

Species	t1	t2
O_2 (%)	16.8	16.3
CO_2 (%)	5.7	6.2
CH_4 (%)	0.0016	0.0022
CO(ppm)	27	29
NO_x (ppm)	101	93
SO_2 (ppm)	46	91
N_2O (ppm)	18	17
CE (%)	99.95	99.95

Table 7.17 Pitch Dust Corrected Baghouse Emissions

Species	t1	t2	SWR Limit
O_2 (%)	11	11	11
CO_2 (%)	13.6	13.2	-
CH_4 (mg/m^3)	25	31	32
CO (mg/m^3)	75	72	55
NO_x (mg/m^3)	460	378	380
SO_2 (mg/m^3)	292	516	180
N_2O (mg/m^3)	78	66	N/A
CE (%)	99.95	99.95	≥ 99.9

The flue gas oxygen level as well as the baghouse CO_2 and SO_2 concentrations were quite stable during the brief intervals. Figure 7.23, shows that the temperature profile was non-uniform within the riser. This is due to a non-uniform fuel feed rate and failure to achieve steady state. The effects of stopping the feed system briefly and cleaning the feeder are evident in Figure 7.24. When the fuel feed was stopped and the feeder cleaned, a corresponding decrease in temperature was measured below the fuel feed point.

7.2.3.1 General Comments

During the incineration of the pitch dust, tar was deposited in the magnesium perchlorate drier (part of the gas sampling train). Tar production is an indication of incomplete combustion. From the viewport on the south face of the riser, approx. 1 m above the base of the riser, it was observed that when the pitch dust was burned, it was generating big flashing yellow flames in this region of the riser. The pitch dust and pitch cones are similar in chemical composition; however due to its particle size (the pitch dust is a fine powder with the majority of particulates in the 53 to 90 micron range), the burning behaviour of the pitch cones and pitch dust appears to be quite different. The pitch cones burns as solid particulates in which the volatiles are first burned at the surface of the particulate. The top layer of the particulate

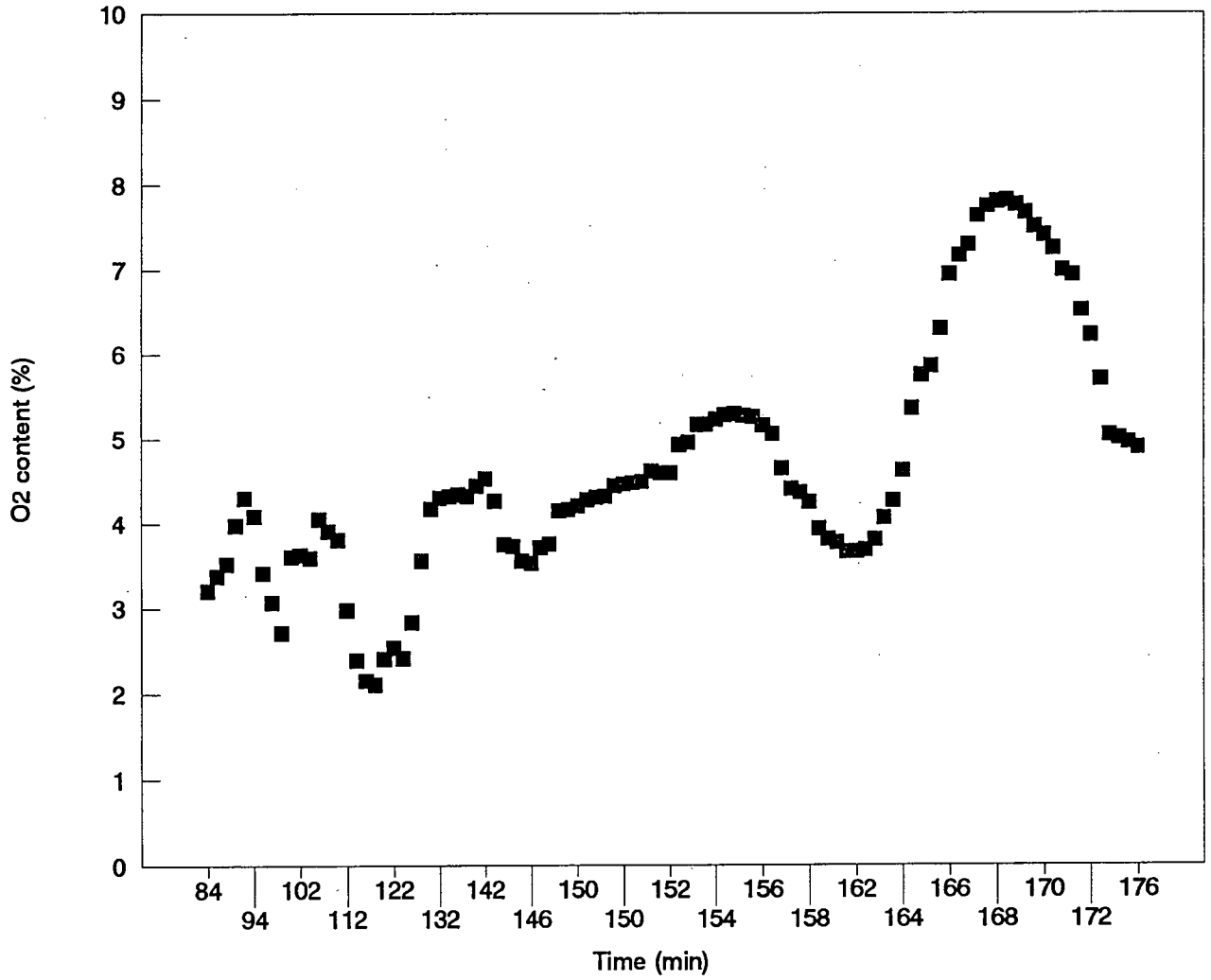

Figure 7.17 Flue Gas O2 Content for Pitch Dust.
(See Table 7.15 for operating conditions).

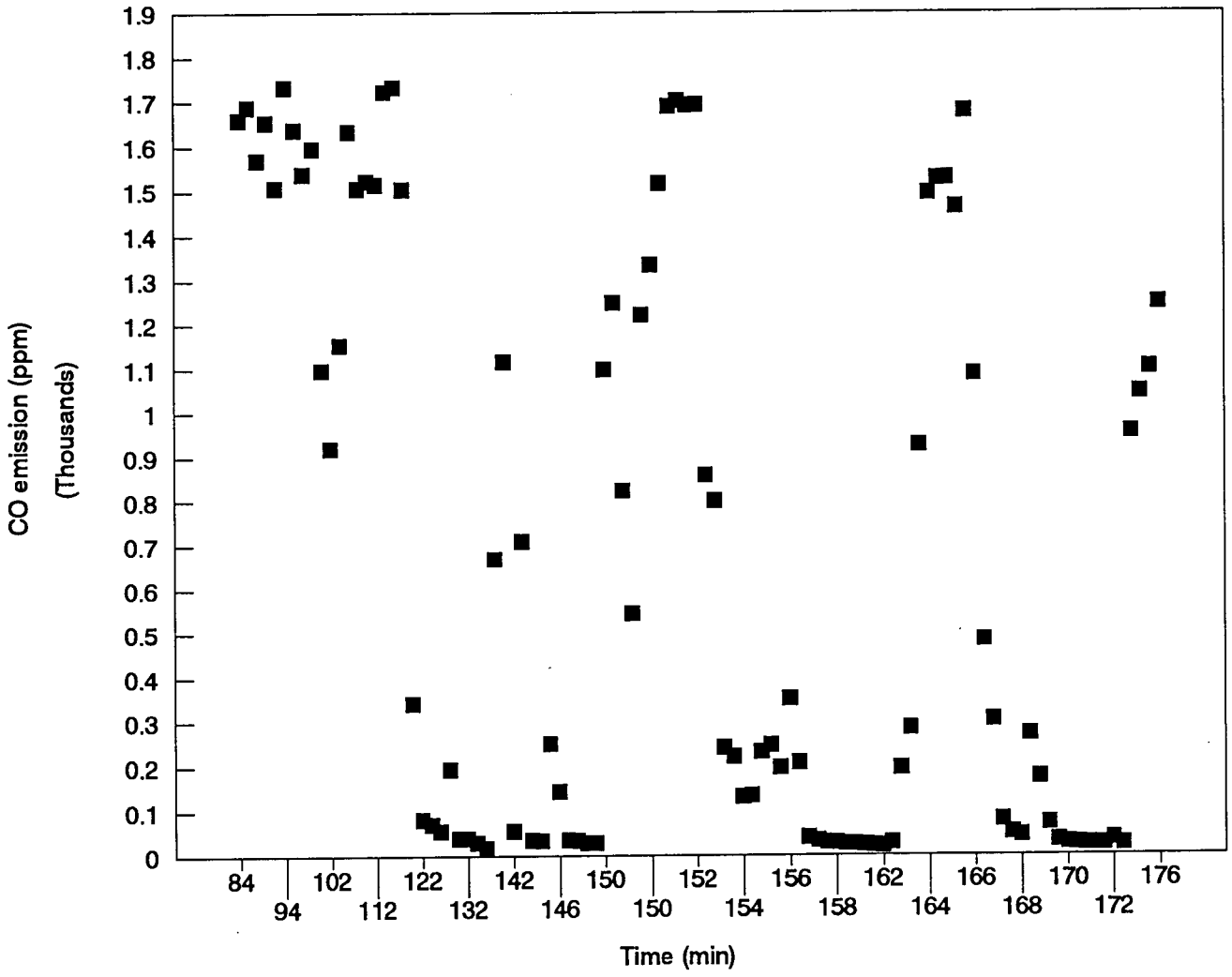

Figure 7.18 Baghouse CO Emission for Pitch Dust.
(See Table 7.15 for operating conditions).

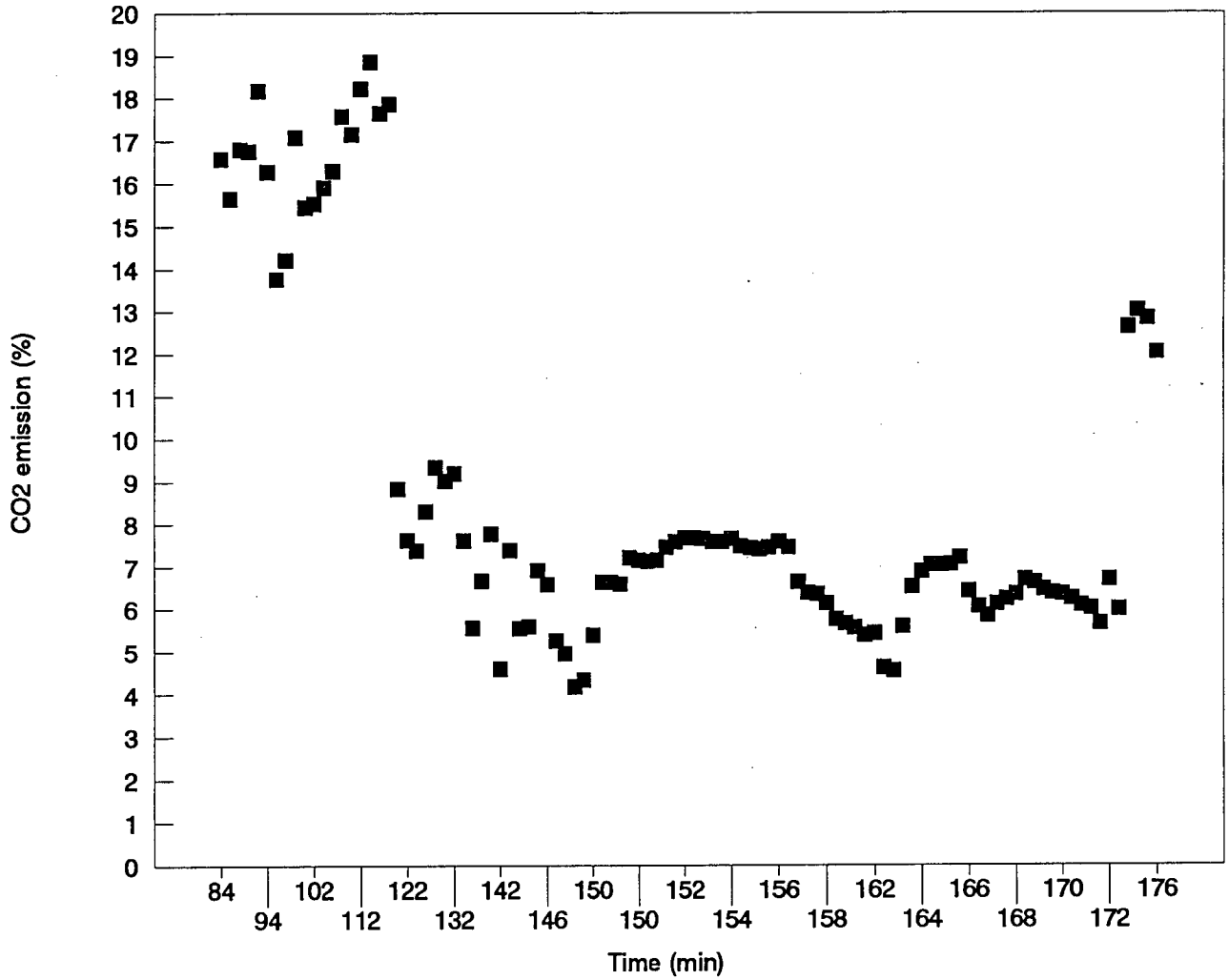

Figure 7.19 Baghouse CO2 Emission for Pitch Dust.
(See Table 7.15 for operating conditions).

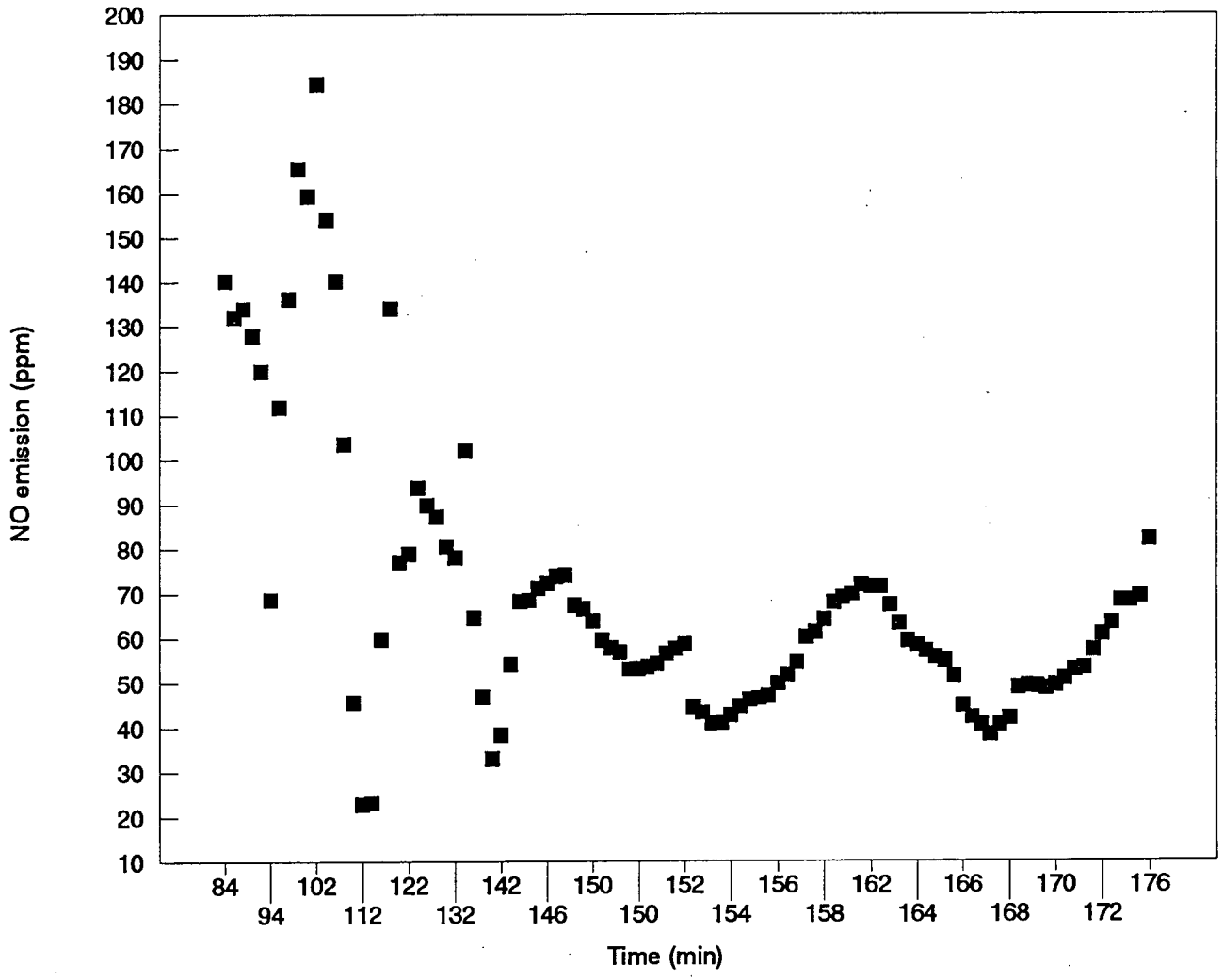

Figure 7.20 Baghouse NO Emission for Pitch Dust.
(See Table 7.15 for operating conditions).

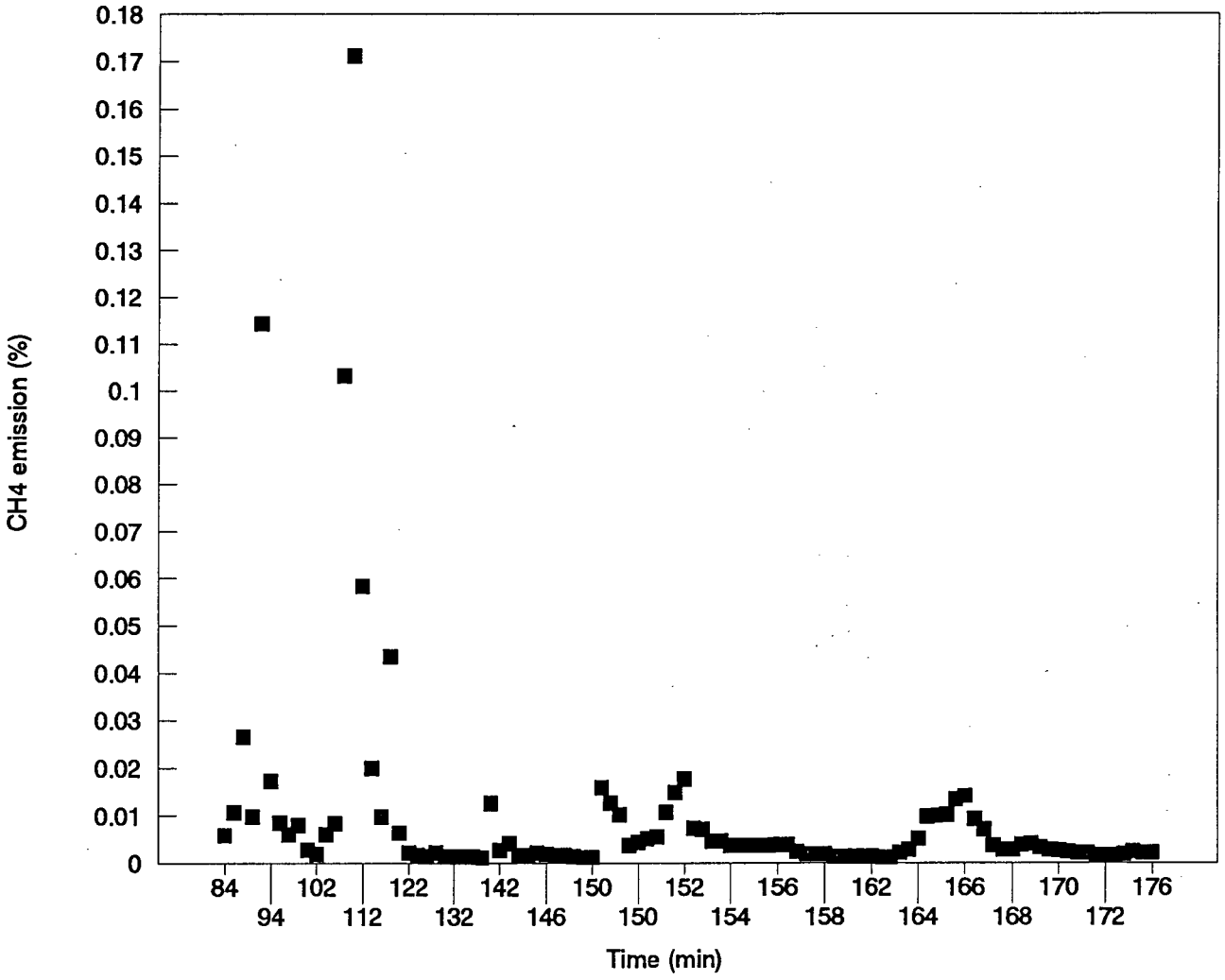

Figure 7.21 Baghouse CH4 Emission for Pitch Dust.
(See Table 7.15 for operating conditions).

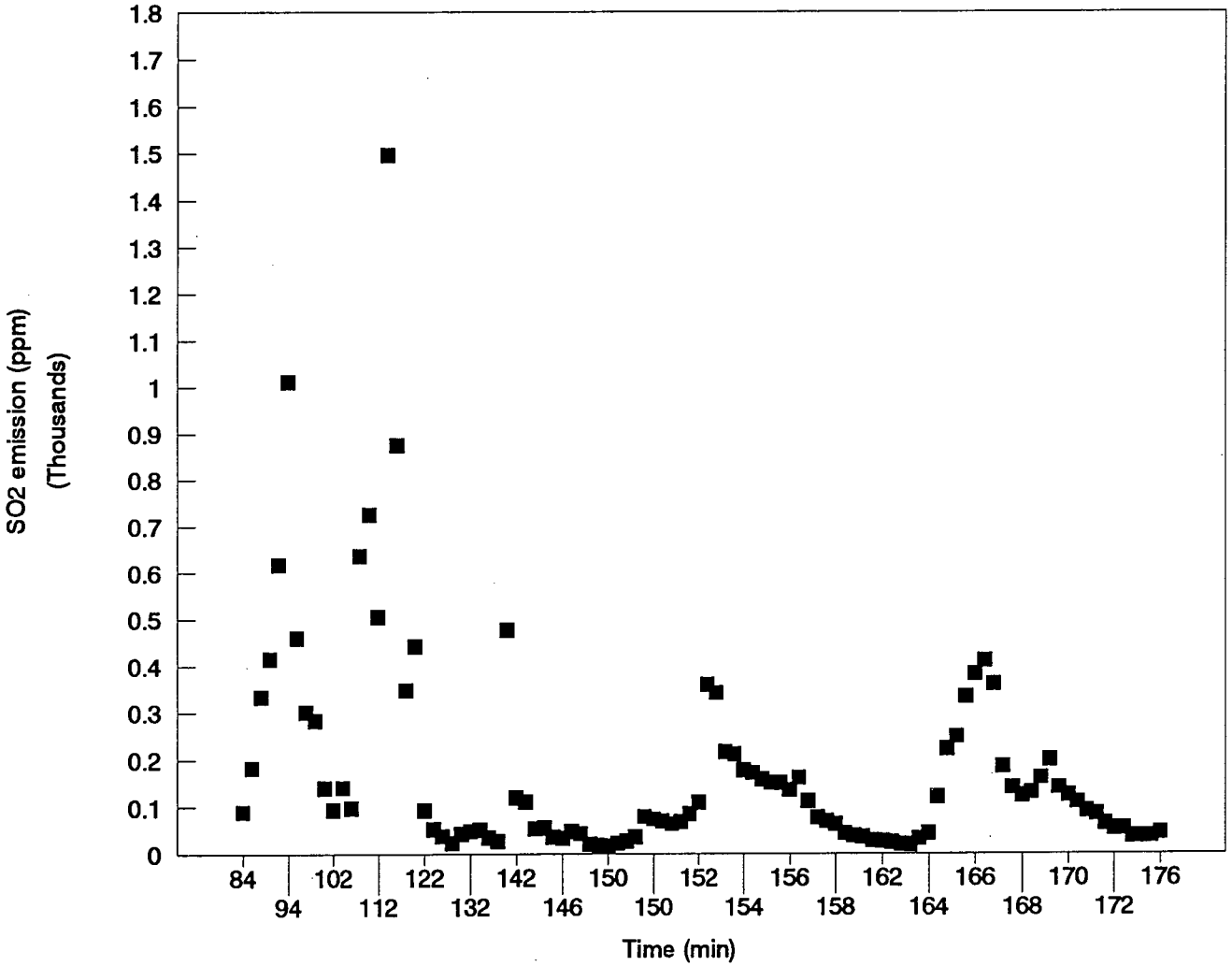

Figure 7.22 Baghouse SO2 Emission for Pitch Dust.
(See Table 7.15 for operating conditions).

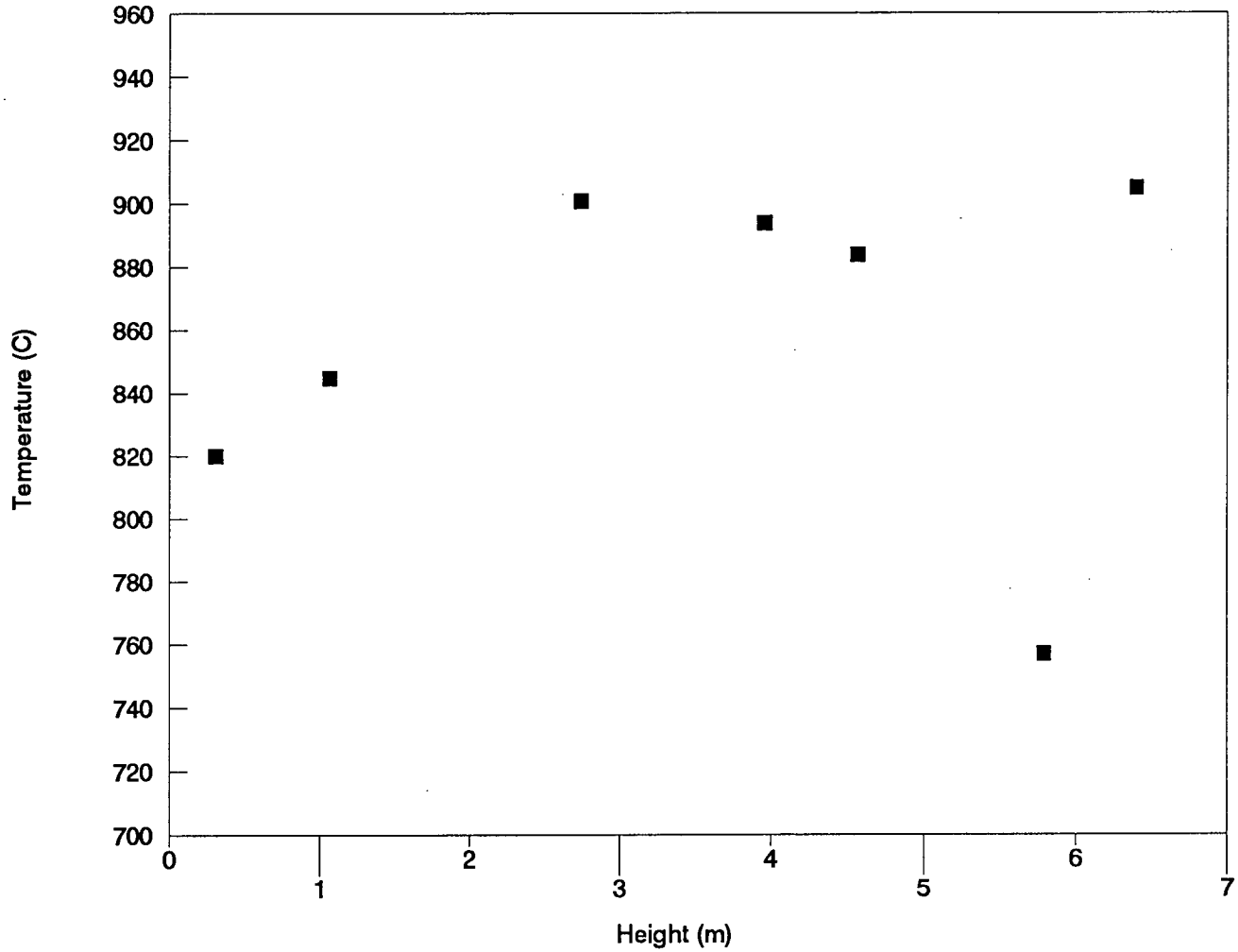

Figure 7.23 Axial Temperature Profile for Pitch Dust.
(See Table 7.15 for operating conditions).

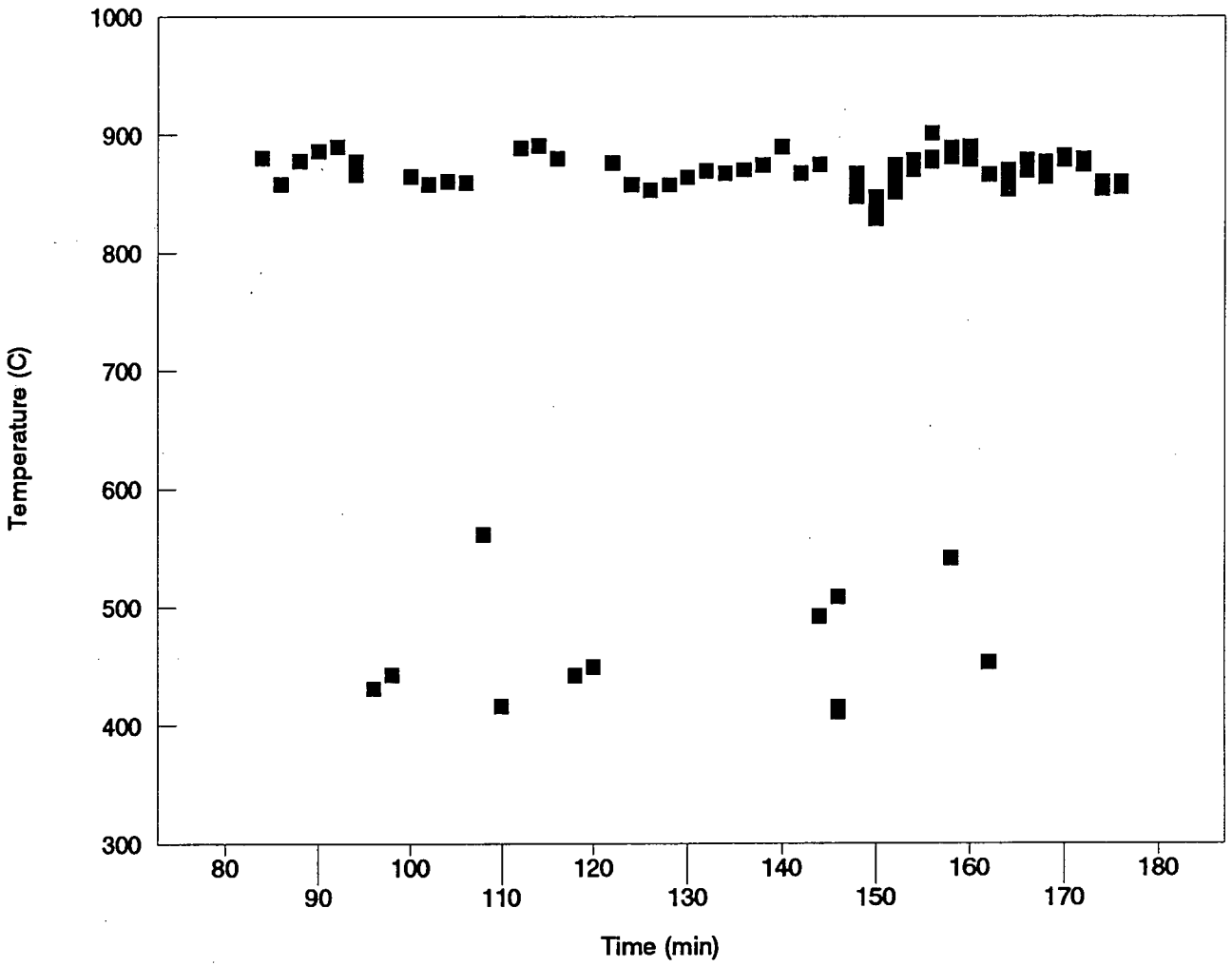

Figure 7.24 Temperature Profile Measured at 0.305 m along Riser.
(See Table 7.15 for operating conditions).

continues to burn at the higher temperature of the particulate surface, generating emissions and an ash layer. As the combustion progresses, the particulate continues to diminish in size. The combustion process continues until the combustible fraction of the particulate has been burned. The combustion pattern of the pitch dust is somewhat like a liquid in that the solids are so fine that they follow the path of the gas rather than that of the bulk bed solids. In this way, they behave more like a liquid fuel than a coarse solid fuel. The pitch dust is a reactive fuel, as shown by the big flames observed as the fuel burned during the run and the dramatic temperature increase with a small increase in the pitch dust feed rate. The secondary air was not preheated in this test and heat removal by the hairpin heat exchanger was needed to maintain the temperature below 900 ^{o}C. The pitch dust, with its higher heating value of 35.6 MJ/kg, burned readily in the UBC pilot CFB unit; however, more work is needed to achieve steady waste feeding.

7.3 Incineration Results for Chloroform and Sulphur Hexafluoride

Incineration tests with chloroform and SF_6 were carried out in the pilot CFB. In the first test, chloroform was co-fired with British Coal Gasification char fines, while in the second test, SF_6 was co-fired with Highvale coal. Multipoint gas sampling was performed at 14 locations throughout the pilot system for each test. The operating conditions for the two tests are shown in Table 7.18. The average incineration temperature is the arithmetic average of the temperatures measured at z = 2.134, 2.743, 5.182 and 6.401 m above the base. The species concentrations in the combustion gas at the various sampling locations for the two tests are provided in Tables 7.19 and 7.20, respectively. These emissions have not been corrected to 11 % O_2, 20 ^{o}C, 760 mm Hg and dry basis. The pilot CFB unit achieved DREs of 100 % and 97.05 % for chloroform and SF_6 respectively. Figures 7.25 and 7.26 present the O_2 and CO_2 concentration profiles for chloroform incineration. Figures 7.27, 7.28 and 7.29 present the O_2, CO_2 and SF_6 concentration profiles for SF_6 incineration. These concentration profiles

provide valuable information regarding the gas mixing and gas-solids mixing behaviour in the CFB, as well as showing the destruction behaviour of the organics. Figure 7.30 shows temperature profiles in the riser for both chloroform and sulphur hexafluoride incineration.

Table 7.18 Operating Conditions for $CHCl_3$ and SF_6 Incineration Tests

	$CHCl_3$ Test	SF_6 Test
Avg. Incineration Temp. (^oC)	870	915
Avg. 1' Cyclone Temp. (^oC)	871	886
Avg. 2' Cyclone Temp. (^oC)	912	885
Baghouse Temp. (^oC)	151	79
Excess Air (%)	4.7	5.7
BCGC Fines Feed Rate (kg/h)	21.1	-
Highvale Coal Feed Rate (kg/h)	-	21.4
$CHCl_3$ Feed Rate (kg/h)	2.45	-
$CHCl_3$ Inlet Conc. (ppm)	3429	-
SF_6 Feed Rate (kg/h)	-	0.20
SF_6 Inlet Conc. (ppm)	-	210
P : S Air Split Ratio	2.12	2.09
Total Air Flow Rate (SCFM)	87.7	86.4
Total Air Flow Rate (m^3/h)	149	147
Avg. Gas Velocity (m/s)	7.60	8.27
Avg. Gas Residence Time (s)	0.96	0.89
Suspension Density (kg/m^3)	120	120
CE (%)	96.7	100
DRE (%)	100	97.05

Table 7.19 Summary of Results for Multipoint Gas Profiling for $CHCl_3$

Position (Ht. above distr.)	Radial Position	O_2 (%)	CO (ppm)	CO_2 (%)	SO_2 (ppm)	CH_4 (%)	NO (ppm)	$CHCl_3$ (ppm)
2	w	1.3	> 1500	16.8	16	0.002	245	ND
(1.5 m)	m	6	> 1500	13.7	21	0.002	215	ND
	c	11	> 1500	9.5	21	0.002	165	ND
3	w	1.0	> 1500	17.5	26	0.002	270	ND
(2.7 m)	m	3.5	> 1500	15.7	26	0.002	290	ND
	c	9.0	> 1500	10.8	21	0.004	190	ND
4	w	11.5	> 1500	8.4	26	0.0	215	ND
(4.2 m)	m	10.2	>1500	8.8	26	0.002	215	ND
	c	5.8	>1500	12.2	26	0.001	350	ND
5	w	3.0	> 1500	16.8	26	0.003	250	ND
(6.4 m)	m	6.0	> 1500	14.1	26	0.003	230	< 0.153
	c	7.5	> 1500	12.4	26	0.001	230	ND
Flue gas		5.0	> 1500	14.5	691	0.012	275	ND
Baghouse		16.5	> 1600	4.9	203	0.003	70	ND

Note: ND denotes Not Detected; w = wall; c = centreline; m = midway between wall and centreline

Table 7.20 Summary of Results for Multipoint Gas Profiling for SF_6

Position (Ht. above distr.)	Radial Position	O_2 (%)	CO (ppm)	CO_2 (%)	SO_2 (ppm)	CH_4 (%)	NO (ppm)	SF_6 (ppm)
2	w	2.5	> 1600	17.7	47	0.01	215	11.5
(1.5 m)	m	8.5	> 1100	13.0	47	0.004	175	38
	c	13.5	98	7.9	47	0	120	30
3	w	2.8	> 1000	17.3	47	0.003	170	10.5
(2.7 m)	m	7.5	398	13.7	47	0	175	30.0
	c	10	428	11.3	47	0	170	30.0
4	w	12.3	215	8.4	57	0.002	120	23.0
(4.2 m)	m	5.3	> 1700	12.4	62	0.002	170	24.0
	c	5.0	131	14.2	62	0.001	200	21.6
5	w	4.5	351	14.7	47	0.004	175	14.4
(6.4 m)	m	7.5	590	12.4	57	0.002	140	16.0
	c	9.0	> 1100	10.7	57	0.002	130	23.2
Flue gas		5.0	ND	14.9	265	0.004	150	6.2
Baghouse		17.5	ND	3.5	16	0.002	35	4.2

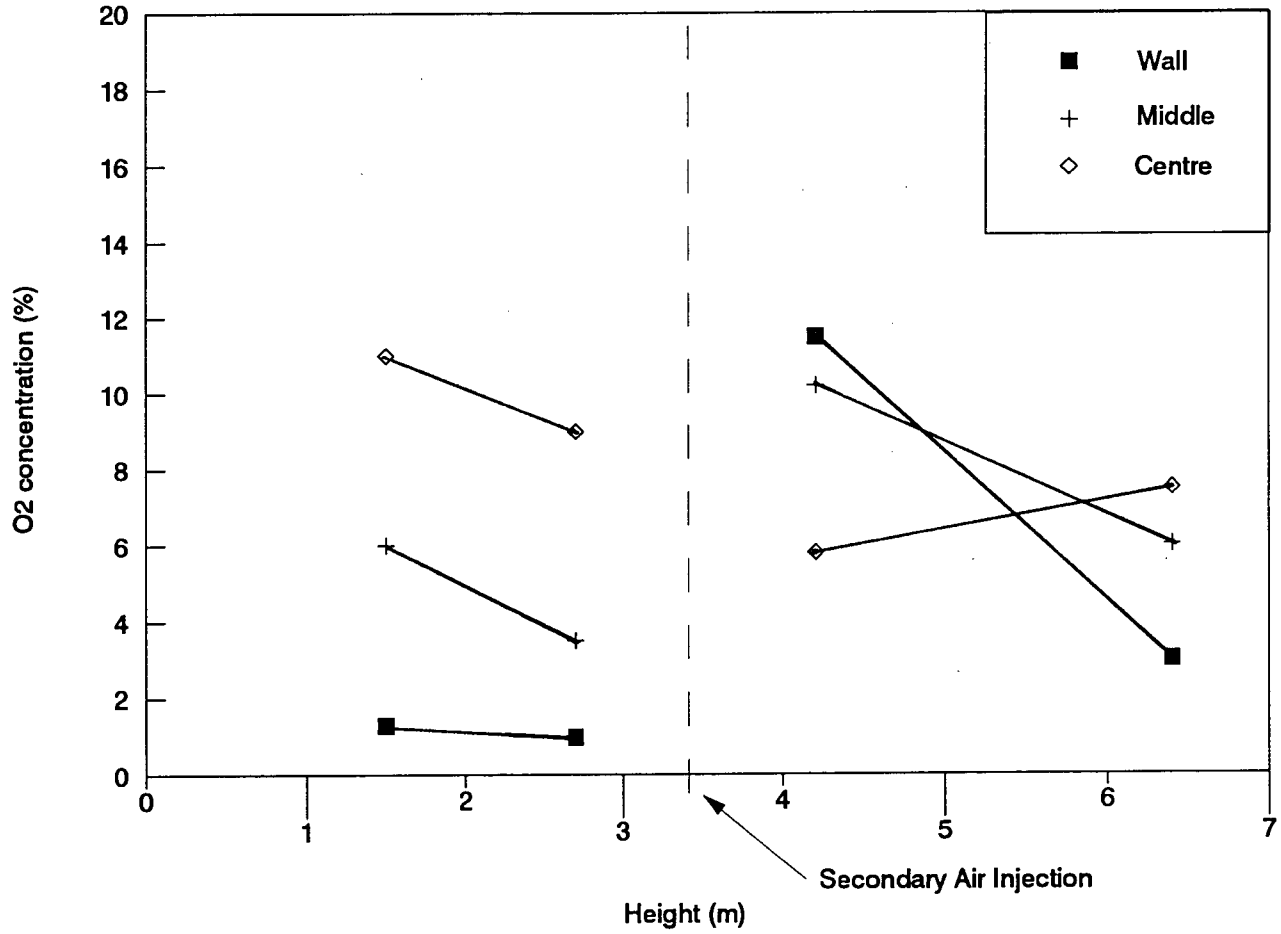

Figure 7.25 Axial O2 Concentration Profiles for Chloroform.
(See Table 7.18 for operating conditions).

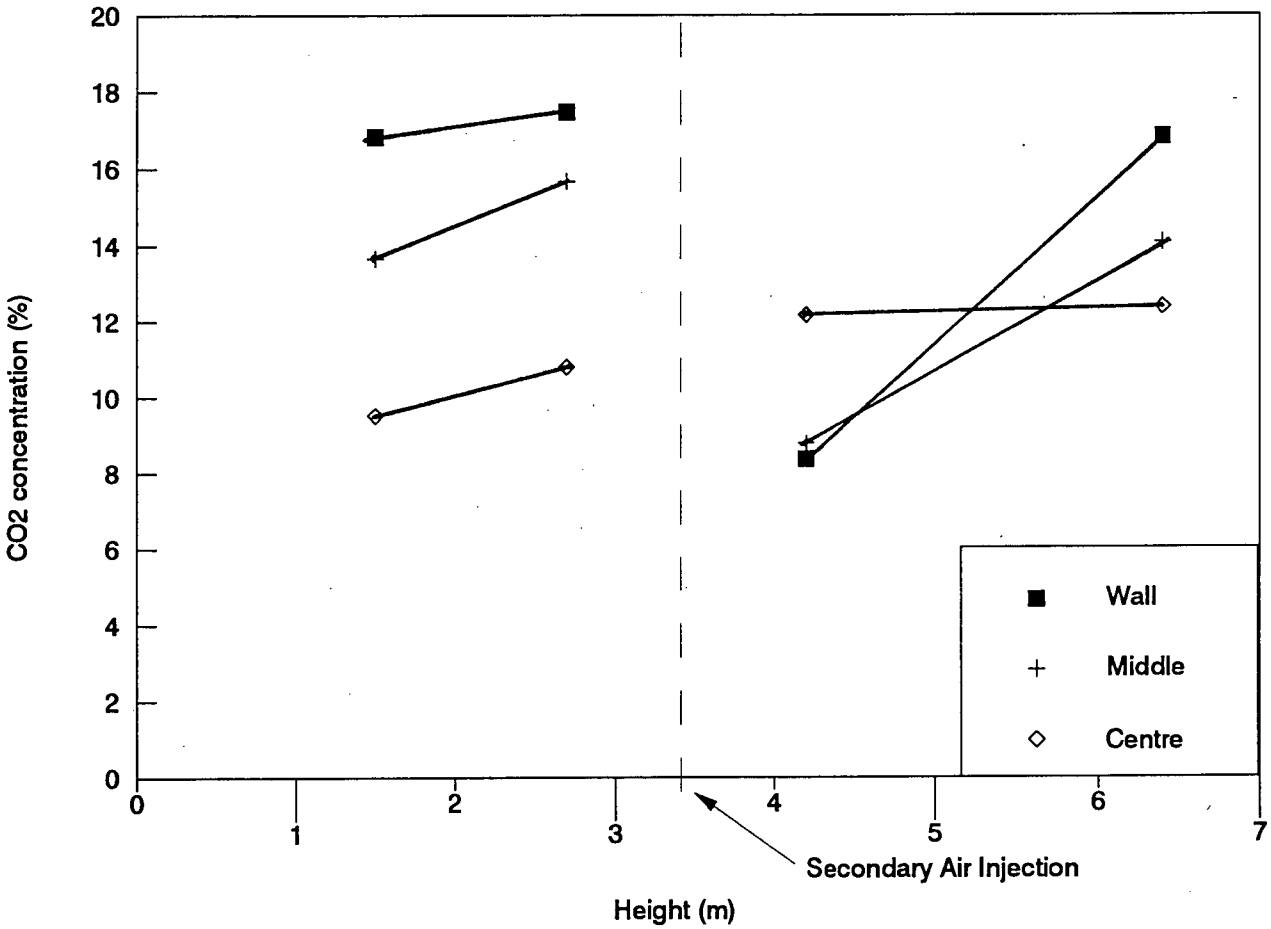

Figure 7.26 Axial CO2 Concentration Profiles for Chloroform.
(See Table 7.18 for operating conditions).

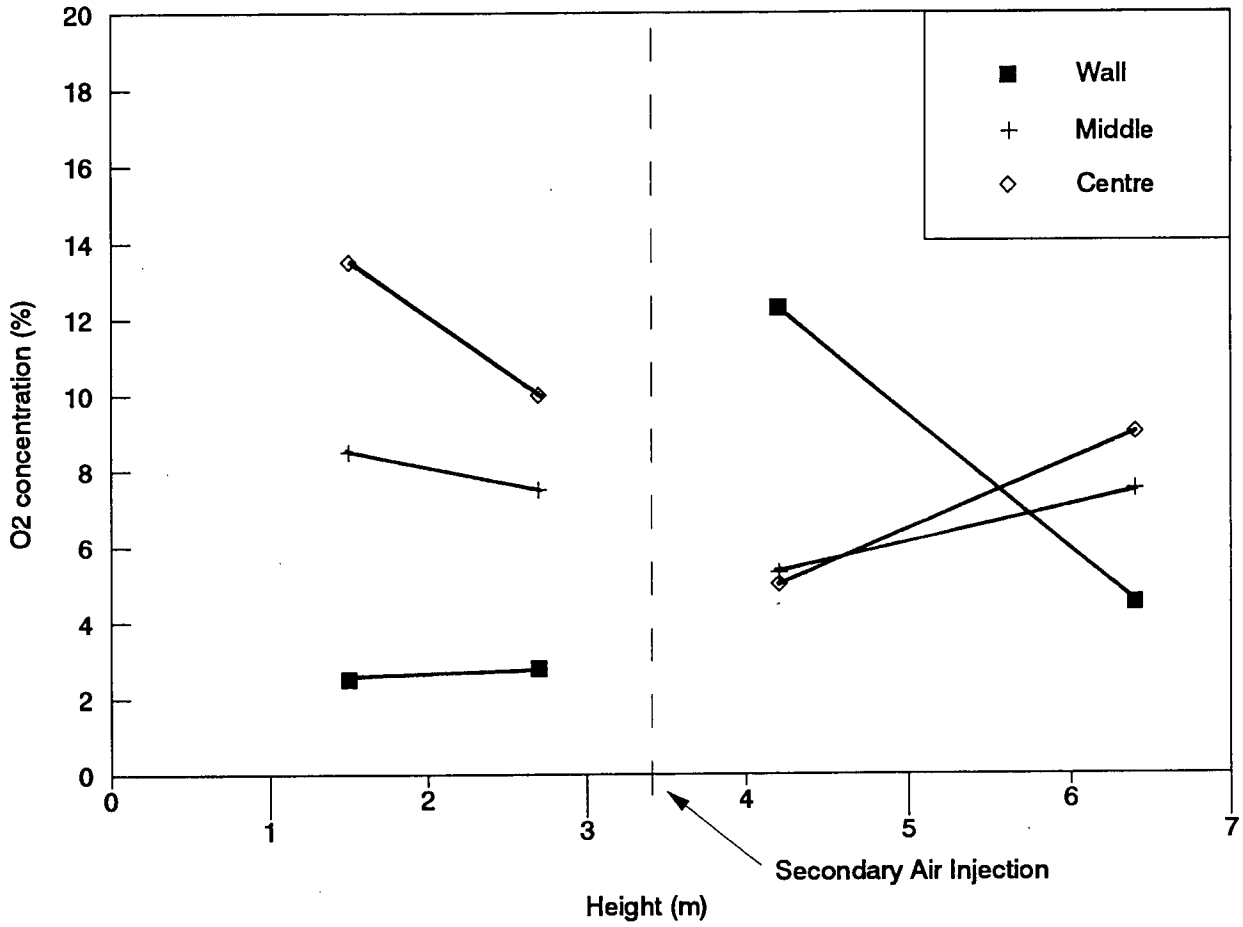

Figure 7.27 Axial O2 Concentration Profiles for SF6.
(See Table 7.18 for operating conditions).

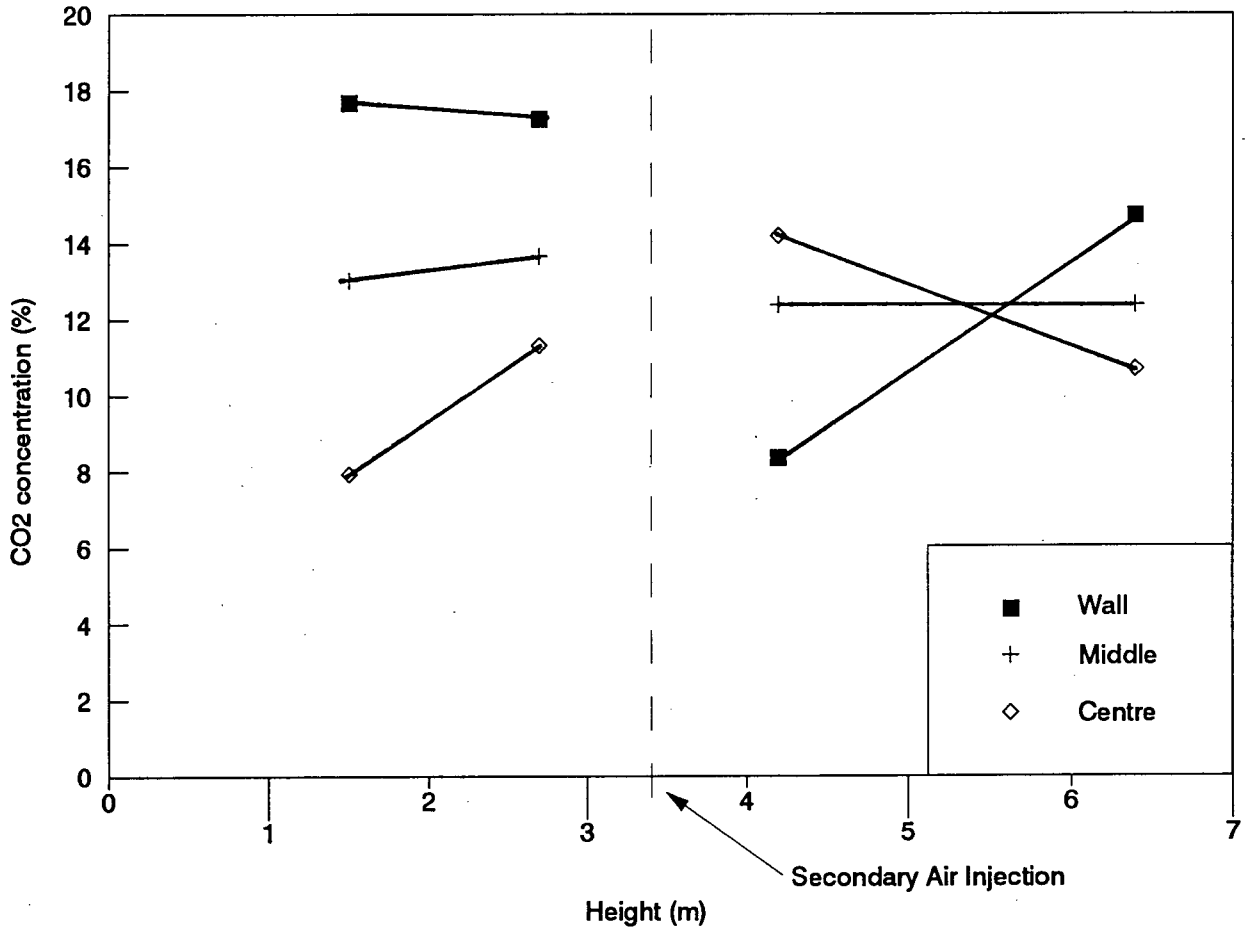

Figure 7.28 Axial CO2 Concentration Profiles for SF6.
(See Table 7.18 for operating conditions).

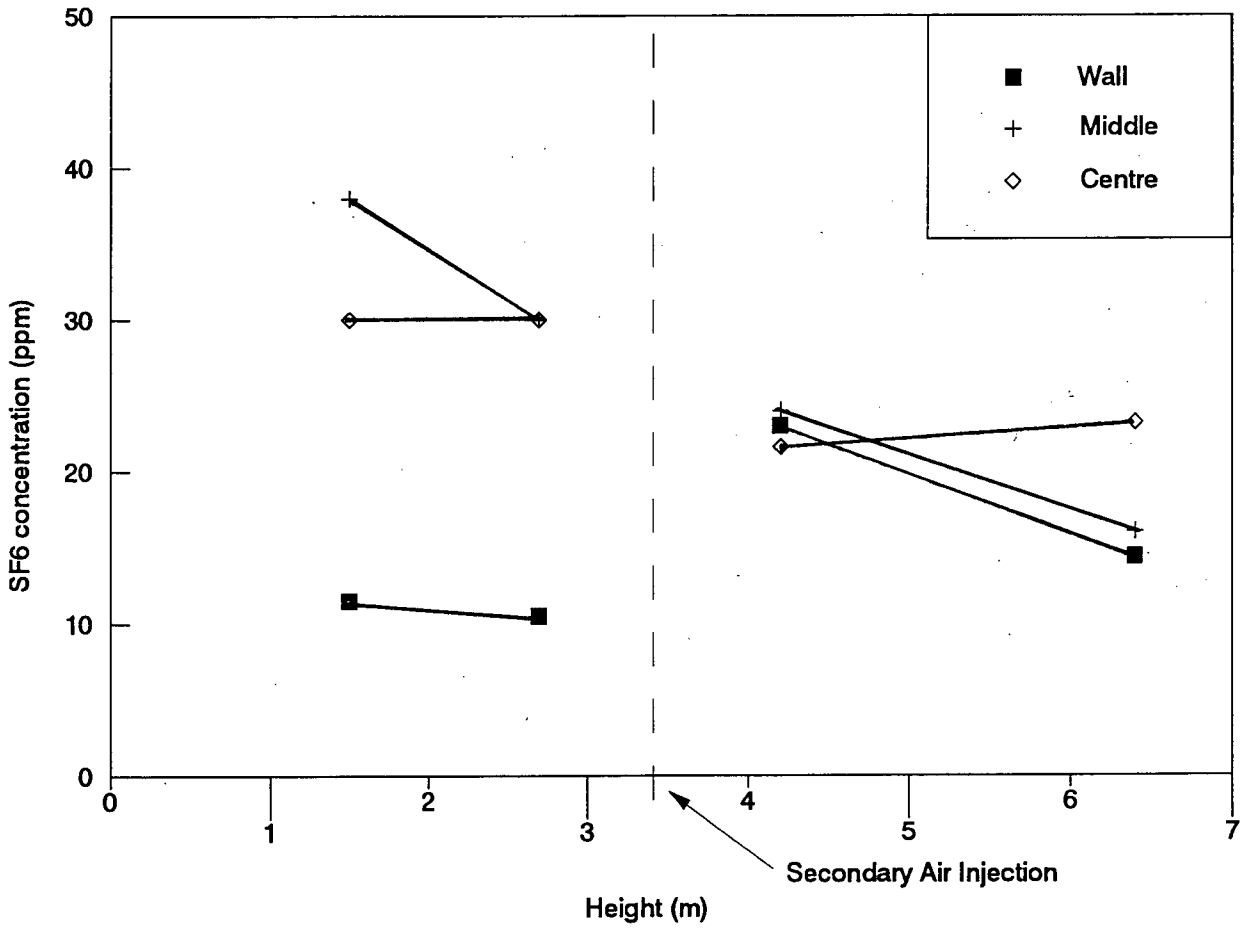

Figure 7.29 Axial SF6 Concentration Profiles.
(See Table 7.18 for operating conditions).

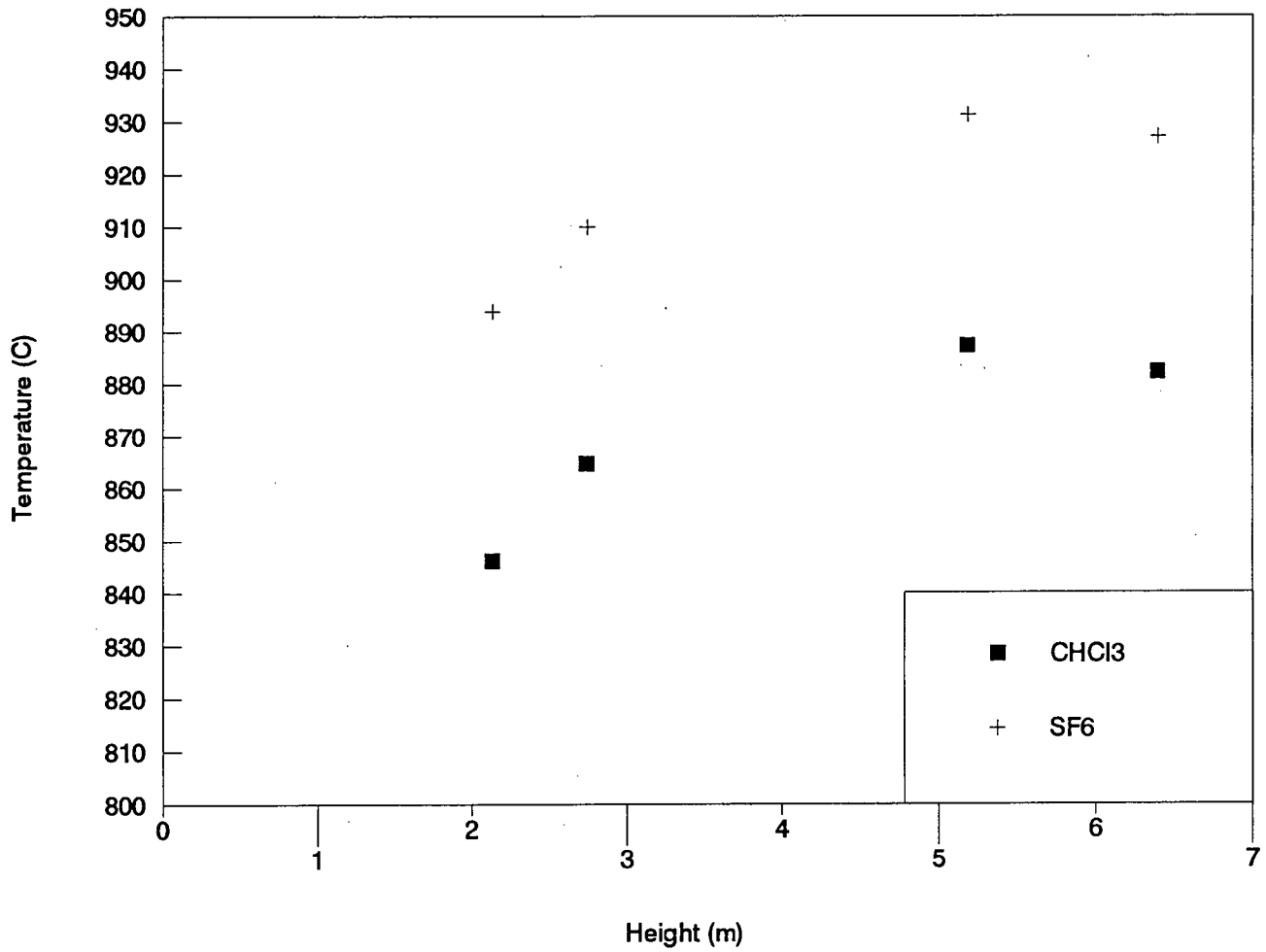

Figure 7.30 Axial Temperature Profiles for CHCl3 and SF6 Incineration.
(See Table 7.18 for operating conditions).

7.3.1 Gas Mixing and Gas-Solids Mixing in UBC Pilot CFB

In order to interpret the gas mixing and gas-solids mixing behaviour in the pilot CFB system, it is necessary to view the CFB riser in three dimensions (see Figure 7.31). There are five gas sampling ports on the north face of the riser: 0.6, 1.5, 2.7, 4.2 and 6.4 m above the distributor plate. Gas samples were obtained at three radial positions from sample ports 2, 3, 4 and 5. The secondary air injection ports are located on the north and south faces of the riser, 3.4 m above the distributor plate (between sample ports 3 and 4). Figure 7.32 shows a top view of the injection ports. The hairpin heat transfer surface (see Figure 7.31) is situated between sample ports 4 and 5 and extends from the south wall into the riser.

The effects of secondary air injection and the presence of the heat transfer surface are shown by the concentration profiles of O_2, CO_2 and SF_6 presented above. In the bottom portion of the riser ($z < 3$ m), there is radial variation as well as axial variation in the O_2, CO_2 and SF_6 concentrations. The low O_2 concentrations and high CO_2 concentrations at the wall occur for the combustion of the solid fuels, i.e. British Coal Gasification char (chloroform incineration) and Highvale coal (SF_6 incineration) due to the dense wall layer of particulates. The high O_2 concentrations and low CO_2 concentrations at the centreline shows that there is less combustion taking place in this region because fewer solids are present. Consequently, the bottom 3 metres of the riser can be described as having a core-annulus structure. At approximately 3.4 m above the distributor plate, there is a sharp rise in the O_2 concentrations with a corresponding sharp drop in the CO_2 concentrations at the wall. At the centreline, the opposite occurs. The increase in O_2 concentrations at the wall is due to secondary air injection. A simple momentum flux balance on the secondary air jets and the solids downflow along the wall was performed. Details of the momentum calculation are provided in Appendix G. The results show that the momentum of the solids downflow, 0.212 kgm/s^2, is greater than the momentum of each of the two secondary air jets, 0.0752 kgm/s^2. Hence, it is

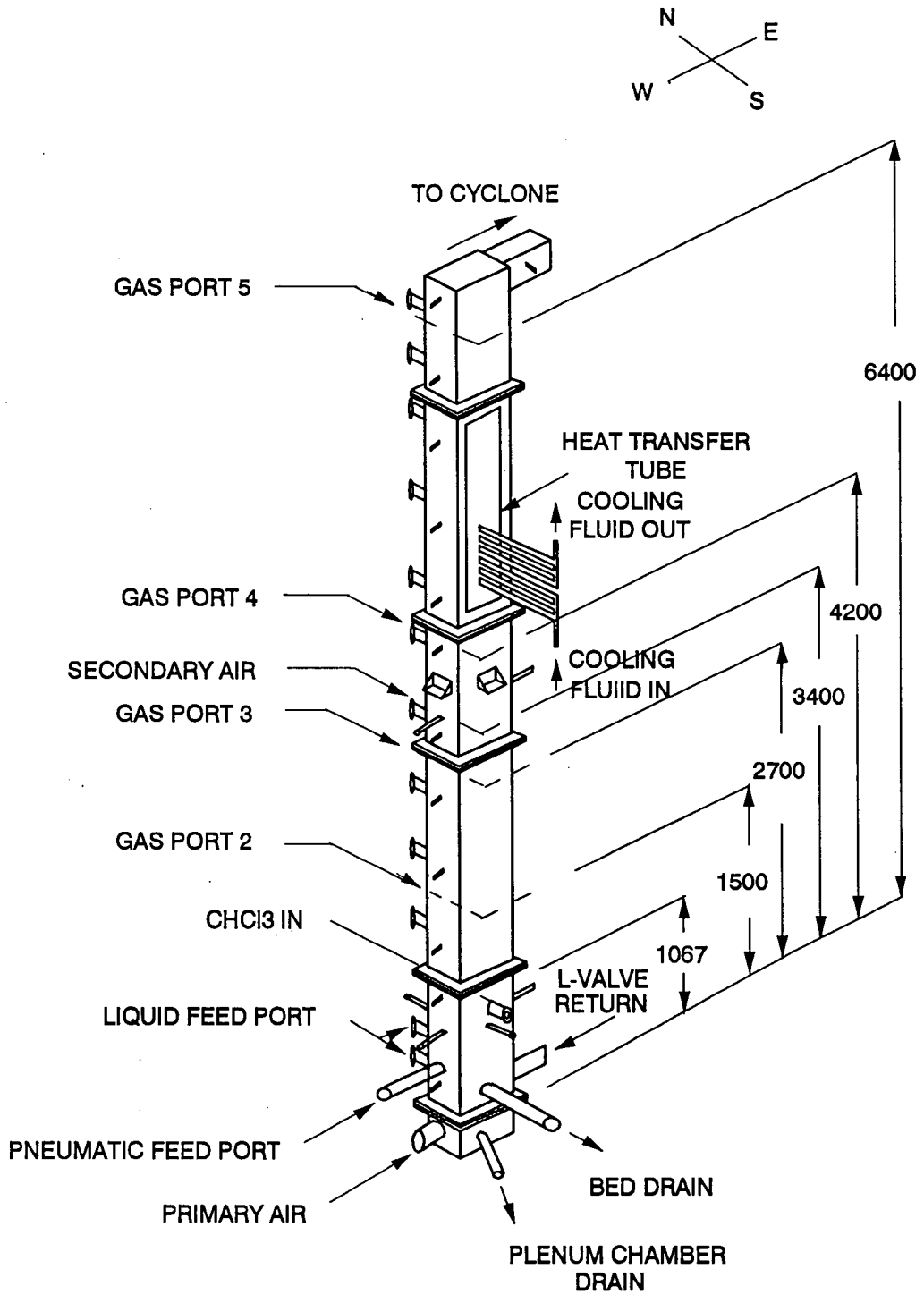

Figure 7.31 View of Principal Refractory-lined Reactor Column with Feed Ports and Gas Sampling Ports (All dimensions are in mm)

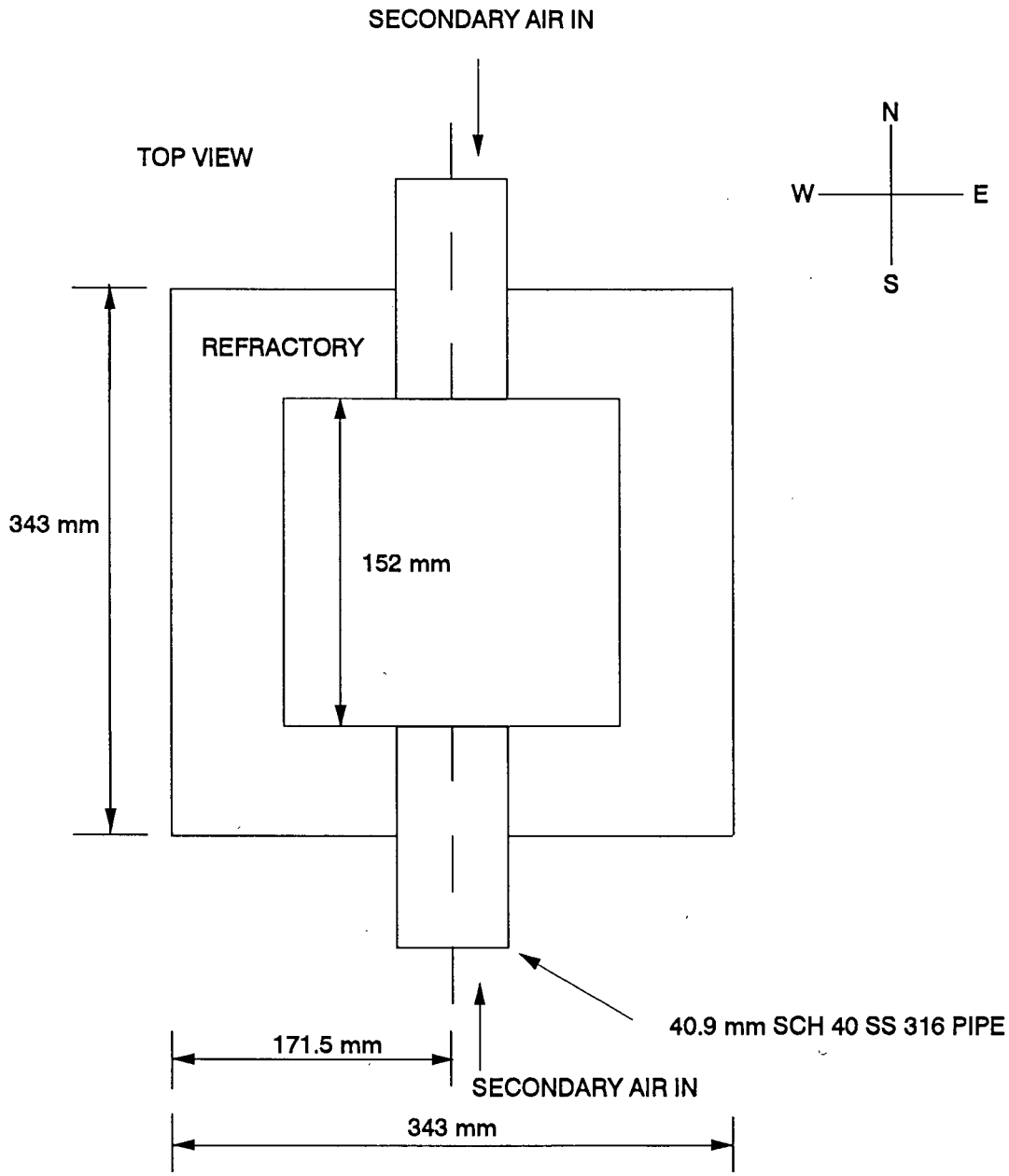

Figure 7.32 Cross-sectional Sketch Showing the Secondary Air Injection Ports

believed that the secondary air diffuses and disperses in the dense solids layer, causing displacement of gases within the solids layer, thereby leading to improved gas mixing in this region of the riser. Figure 7.33 shows the gas and solids mixing between gas sample port 3 to the top of the riser (two-dimensional view). The heat transfer surface approximately 4.3 m above the distributor plate acts as a vertical baffle and deflects some of the solids traveling upwards in the riser downwards. The combination of this solids reflux and gas mixing created by the secondary air jets resulted in a zone with good gas-solids contact as well as gas mixing. The combustion reactions are rapid compared to the decomposition reactions of SF_6; therefore, the O_2 and CO_2 concentrations reach equilibrium faster than SF_6. The slow SF_6 decomposition reactions resulted in a fairly uniform SF_6 concentration as compared to the O_2 or CO_2 concentrations in this well-mixed region. Having passed through this well-mixed region (between approximately 4.3 and 5 m above the distributor plate), the concentration profiles readjust themselves and try to re-establish the same trend as in the bottom 3 m of the riser. Near the top of the riser, the concentration profiles are affected by solids refluxing as a consequence of the riser exit effect.

The experimental oxygen concentration profiles are vastly different from that assumed in the computer model. The oxygen profile used in the model (see Figure 7.34) did not show the effect of secondary air injection. This oxygen profile was obtained experimentally by combustion of Minto coal (Run # 16, condition 6) with temperature = 895 ^{o}C; superficial gas velocity = 7.6 m/s; P:S = 1; Ca:S = 3; and 3.1 % O_2 in the flue gas; hairpin heat transfer surface present [Brereton et al., 1991]. The experimental concentration profiles have shown that the assumptions of gases traveling in plug flow through a CFB and of a core and annulus structure may not be representative of the actual gas and solids flow patterns. Consideration must be given for the fluctuations due to secondary air entry nozzles, heat transfer surfaces and the riser exit when modeling the hydrodynamic behaviour of the system. It may be more

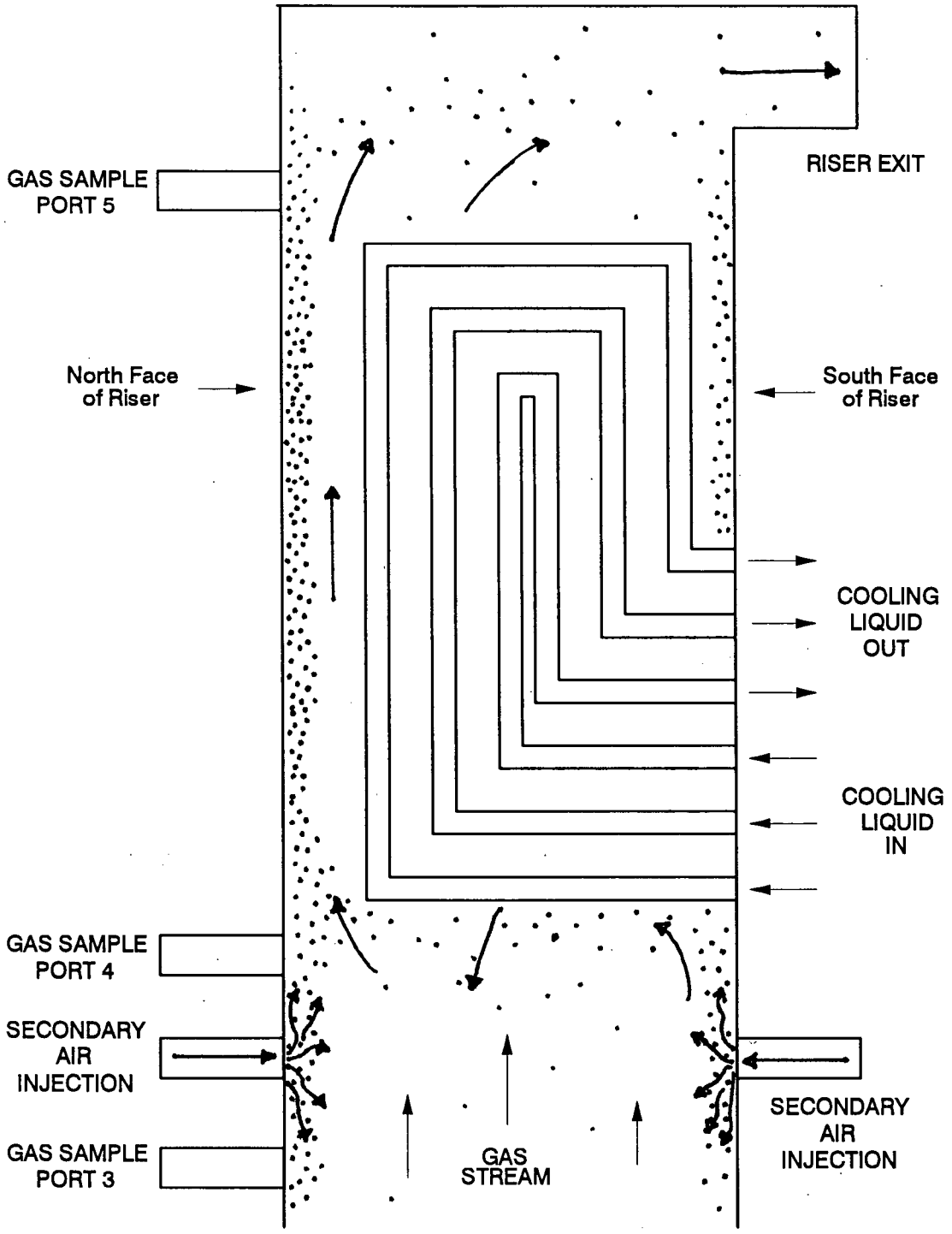

Figure 7.33 Schematic Showing Gas and Solids Contacting Behaviour in Riser

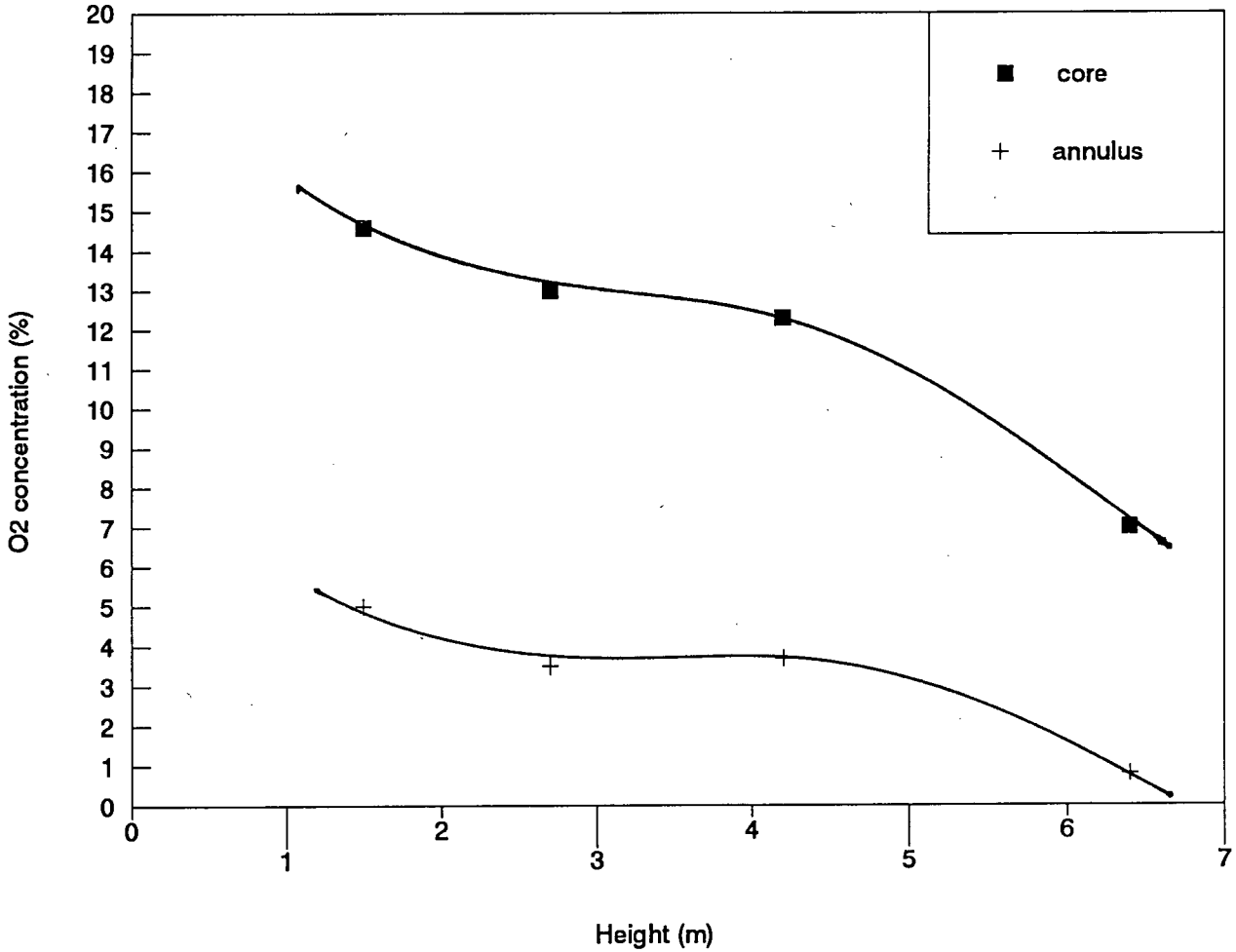

Figure 7.34 Axial O2 Concentration Profiles from Run # 16 : Minto Coal.
(See section 7.3.1 for operating conditions).

appropriate to divide the CFB into different zones characterized by different gas and solids mixing behaviour.

7.3.2 Chloroform Destruction

The UBC pilot CFB unit operating at 870 ^{o}C achieved 100 % DRE for chloroform. This is in good agreement with the theoretical and experimental results obtained by Taylor et al. (1990). The temperature needed for a 99 % DRE at a gas phase residence time of 2 s is approximately 635 ^{o}C. Chloroform is ranked 158 to 161 in the thermal stability ranking developed by Taylor et al. (1990) and the dominant reaction is the concerted three-center HCl elimination reaction. The destruction of chloroform led to high CO emissions throughout the CFB system. Before chloroform addition into the system, the baghouse CO emission was 103 ppm. After chloroform was added, the CO emission throughout the CFB system exceeded 1500 ppm. The baghouse CO emission was greater than 1600 ppm. In fact the actual CO emissions may be even higher since the CO reading was well beyond the linear calibration range of 1000 ppm. The high CO emissions are the results of halogen inhibition of CO oxidation. Bulewicz et al. (1989) found that halogens inhibit CO oxidation during coal combustion in a fluidized bed. The CO concentration in the flue gas was found to increase when coal was burned in a fluid bed combustor in the presence of small quantities of alkali halides. Halogens and halogen halides are well known flame inhibitors, while halogenated hydrocarbons have been used as flame extinguishants. The magnitude of the effects with chemically similar inhibitors is in the order of F << Cl < Br < I. The presence of HCl (decomposition product of chloroform) inhibits the oxidation of CO to CO_2 by competing for hydroxyl radical, OH*, formed during combustion reactions. For every mole of chloroform decomposed, one mole of HCl is formed to compete with CO for the hydroxyl radical.

The HCl and CO reactions with hydroxyl radical are as follows:

$$HCl + OH^* \quad \text{-----} > \quad H_2O + Cl$$

$$CO + OH^* \quad \text{-----} > \quad CO_2 + H$$

HCl inhibition of CO oxidation greatly affects the combustion efficiency of an incinerator. Prior to chloroform addition, the pilot CFB achieved 99.8 % CE as compare to 97.0 % CE after chloroform addition. Inhibition of CO oxidation was also observed during SF_6 incineration. The baghouse CO emissions before and after SF_6 addition were both approximately 0 ppm. However, the CO emissions measured at different axial and radial positions in the riser varied between approximately 100 ppm and 1700 ppm. Consequently, one must not only consider the effects of incineration temperature, excess air, degree of turbulence and residence time have on the combustion efficiency of an incineration system, but also the effect of halogenated compounds in the waste feed stream. The molar hydrogen-to-halogen ratio for the chloroform test was 1.5 : 1. In general, a ratio of 4 : 1 is recommended to ensure that there is excess hydrogen to form HCl, the complete combustion product of chlorine. Otherwise, chlorine gas, Cl_2 will form by the reaction:

$$2\ HCl + 1/2\ O_2 \text{ ------} > H_2O + Cl_2$$

The CO emission may be affected if the quantity of hydrogen in the fuel is small. CO is oxidized by the hydroxyl radical produced from the moisture and hydrogen contents in the fuel. If the fuel has a low moisture and/or hydrogen content, then a high CO emission will result because not enough hydroxyl radicals are being generated to oxidize the CO.

7.3.3 SF_6 Destruction

The UBC pilot CFB unit operating at 915 ^{o}C achieved 97.05 % DRE (based on the flue gas emission) for SF_6. Figure 7.35, in which the SF_6 concentration at z = 0 m is assumed to be the inlet SF_6 concentration, 210 ppm, shows a steep axial profile for SF_6 in the bottom 1.5 m of the riser. The average SF_6 concentration (based on experimental results) at z = 1.5 m was approximately 27 ppm, corresponding to approximately 87 % DRE. Taylor and Chadbourne (1987) stated that SF_6 destruction depends mainly on temperature and residence time for the thermal decomposition of the strong S-F bond and is independent of the oxygen concentration in the incinerator. However, the high degree of SF_6 destruction achieved in this study cannot be attributed to temperature or residence time effects because SF_6 decomposes rapidly only at temperatures exceeding 1400 K (1127 ^{o}C) [Bott and Jacobs, 1969; Wilkins, 1969] not at 915 ^{o}C, and the average gas residence time corresponding to z = 1.5 m is only 0.18 s. The experimental SF_6 concentration profiles were compared with those generated by the computer simulation. The computer simulation assumes that SF_6 decomposition is independent of the partial pressure of oxygen, and with the incinerator operating conditions similar to the SF_6 experimental test condition (see Appendix A for computer program code and results).

At 915 ^{o}C, the computer-generated SF_6 concentration profiles shown in Figure 7.36 predict SF_6 DREs of only 1.43 % and 1.90 % in the core and annulus regions respectively. At 1200 ^{o}C, overall SF_6 DREs of 100 % were predicted in both the core and annulus regions (see Figure 7.36.).

Figure 7.37 shows the computer-generated SF_6 concentration profiles with the assumption that SF_6 decomposition is a function of the partial pressure of oxygen (using the oxygen profile from Minto run). Once again, at 915 ^{o}C, little SF_6 decomposition is predicted. At 1200 ^{o}C, there is significant SF_6 decomposition but not as much as for just thermal

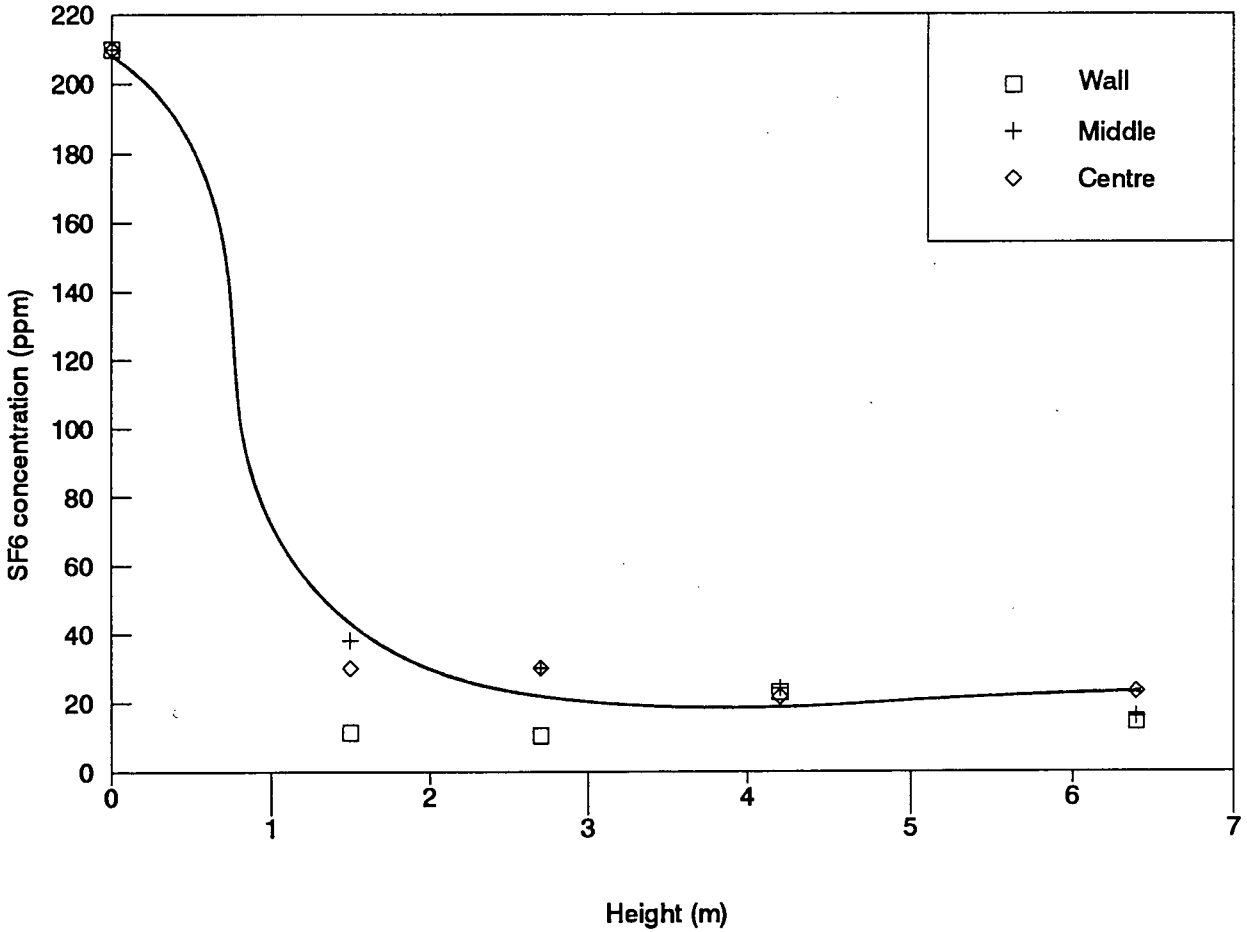

Figure 7.35 Axial SF6 Concentration Proflies (210 ppm of SF6 at Inlet)
(See Table 7.18 for operating conditions).

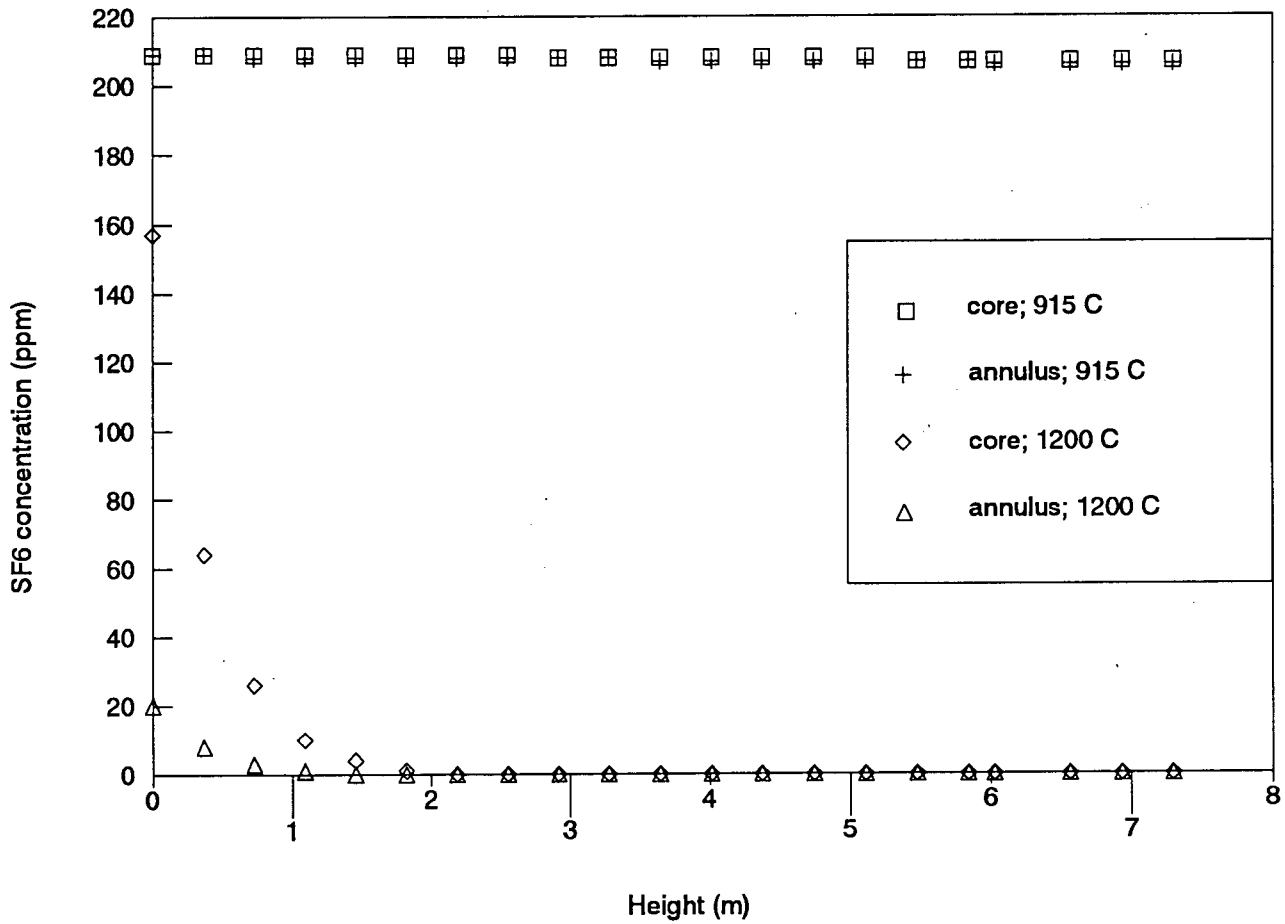

Figure 7.36 Axial SF6 Concentration Profiles from Computer Simulation at 915 C and 1200 C; SF6 Decomposition Is Assumed to be Independent of Oxygen Concentration within the Riser

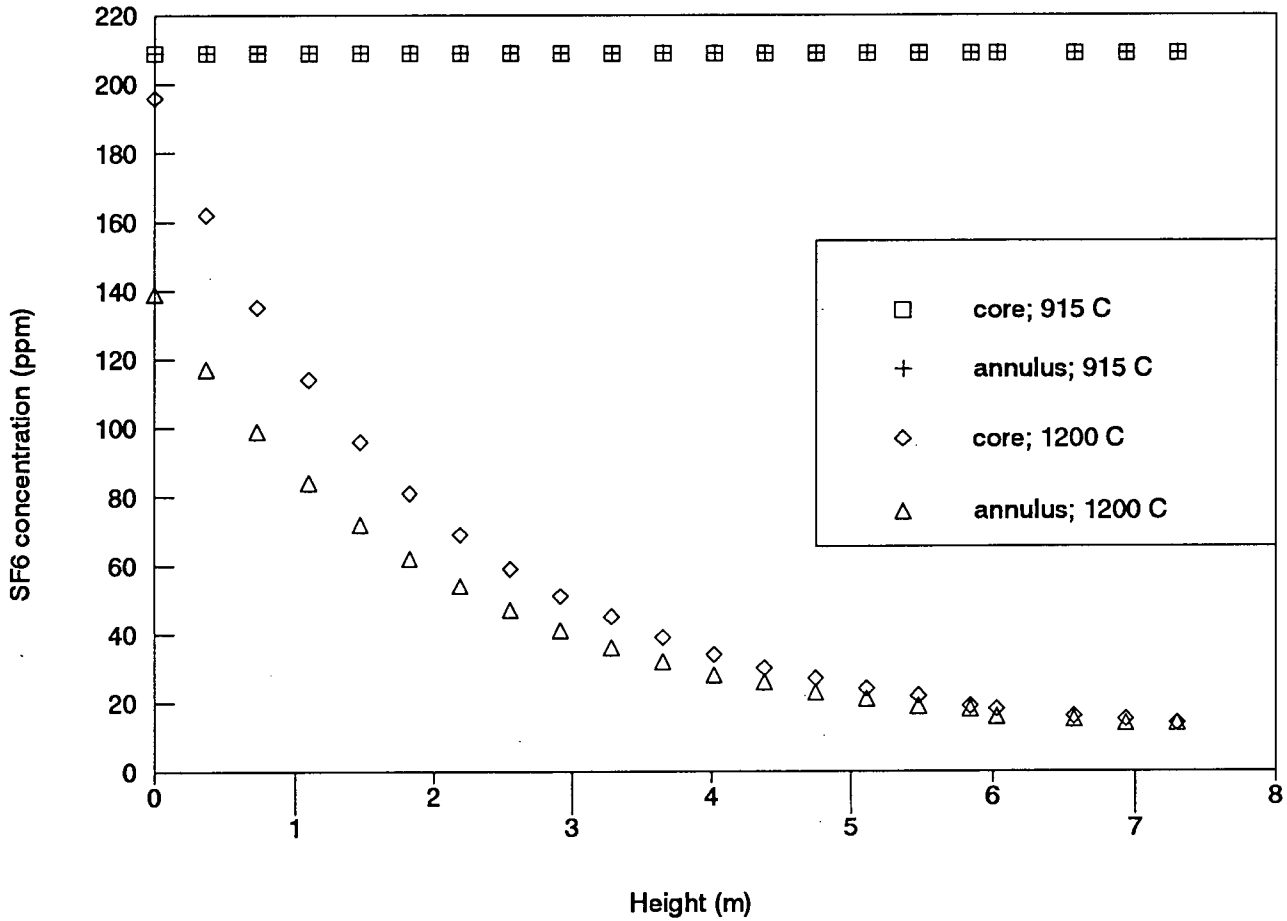

Figure 7.37 Axial SF6 Concentration Profiles from Computer Simulation at 915 C and 1200 C; SF6 Decomposition is Assumed to be 1st Order with Respect to Oxygen Concentration within the Riser

decomposition (Figure 7.36). It is clear that at high temperatures, SF_6 destruction depends mainly on thermal decomposition. There is relatively little thermal decomposition of SF_6 at low temperatures. Yet, the pilot CFB operating at only 915 ^{o}C with a gas phase residence time of only 0.18 s. (at z = 1.5 m) achieved an average SF_6 DRE of approximately 87 %. Thus, other mechanisms, e.g. reactions with free radicals, must be responsible for SF_6 decomposition at low temperatures. The computer prediction may be improved by incorporating the experimental oxygen concentration profile and reactions involving radicals, i.e. OH, and dividing the riser into zones characterized by different gas mixing behaviour, i.e. plug flow and perfect mixing.

Although decomposition of SF_6 may not be directly affected by the oxygen concentration in the reactor, there may be an indirect effect. During combustion processes, hydroxyl, oxygen, hydrogen and chlorine (depending on the fuel type and combustion temperature) free radicals are generated as intermediate products before forming complete combustion products of combustion, i.e. CO_2 and H_2O. The free radicals are released when the volatile portion of the fuel is vapourized. It is possible that the CFB produces super-equilibrium concentrations of radicals. The temperature of the outer layer of the burning fuel particle is higher than the bulk temperature of the gas/solids stream. Hence, higher radical concentrations may be generated due to the higher surface temperature of the fuel particle compared to the radical concentration generated due to the bulk temperature. Therefore, it is reasonable to assume that reactions with free radicals may also be responsible for the decomposition of SF_6 since the experimental results show that thermal destruction of SF_6 is not the dominant decomposition mechanism at low temperatures. However, it would be difficult to measure the free radical concentrations in a thermal system to confirm the depletion of free radicals during SF_6 destruction. Low temperature incineration systems such as CFBs can also achieve high degrees of SF_6 destruction. Consequently, incineration temperature should not be the sole

parameter used to ensure good combustion and destruction characteristics in an incineration system.

8. CONCLUSIONS

The results of this study show that CFB incineration technology is suitable for disposal of solid organic wastes. Increases in incineration temperature and excess air tend to increase the combustion efficiency of the system, but also tend to increase the NO_x emissions. Increases in primary-to-secondary air split ratio, suspension density and superficial gas velocity tend to enhance gas and solids contacting behaviour, thereby leading to improved combustion efficiency and higher NO_x emissions.

The composition of the solid wastes, in particular the volatile, sulphur and ash contents, has significant impact on the incineration performance and emissions of the incinerator. Wastes with low volatile contents are less reactive and tend to burn at slower rates; resulting in high CO emissions. For wastes with low sulphur content, i.e. approx. 1.5 wt. % and low ash content, there is significant solids residue reduction upon incineration and in-situ sulphur capture via limestone is effective in reducing SO_2 emissions. For wastes with high sulphur content, approx. 13 wt. %, with high ash content in one case, high SO_2 emissions result even with limestone addition and the large quantity of limestone added leads to considerable solids residue generation. This combined with the high ash content of the waste may lead to an increase in solids residue and ash management may become problematic.

The physical nature of the solids wastes affects the combustion behaviour of the wastes. The combustion pattern of fine solid wastes is somewhat like a liquid in that the solids are so fine that they follow the path of the gas rather that of the bulk bed solids. In this manner, they behave more like a liquid fuel than a coarse solid fuel. Incineration of solid wastes with coarser particle size resulted in lower CO emissions as compared to the same waste with finer particle size because of the longer overall residence time the coarser particles spend in the incineration system.

The UBC pilot CFB achieved high combustion efficiencies, greater than 99.9 %, for the incineration of Alcan solid organic wastes, although the CO emissions were high. The UBC pilot CFB provides good initial combustion of the wastes. The high CO emissions could be reduced by adding an insulated afterburner chamber following the cyclone systems. High CO emissions do not pose a problem for full-scale units because of their longer residence times. A full-scale unit can be designed for any desired residence time after the cyclones to complete the combustion reactions.

A fundamental study shows that the hydrodynamics of the CFB system are very complex and that high destruction and removal efficiencies of organics can be achieved at a lower incineration temperature than in conventional incinerators. It is important to include the effects of secondary air injection nozzles, baffles effects such as those caused by heat transfer surfaces and reactor exit effects on the hydrodynamic behaviour of gases and solids in CFB risers. The riser may be divided into zones characterized by different mixing behaviour of gases and solids in order to obtain a more accurate representation of the hydrodynamic behaviour of gases and solids in the CFB riser.

The UBC pilot CFB system achieved DREs of 100 % and 97.05 % respectively for chloroform and SF_6. The use of SF_6 as a surrogate test burn compound generally results in a conservative prediction of the waste destruction capability of an incineration system because of the assumption that high temperatures are required for high degrees of organics destruction. The experimental results from this work show that organics are destroyed at temperatures lower than conventional incineration temperatures due to both unimolecular and bimolecular reactions. Consequently, the incineration temperature should not be the sole parameter used to ensure good combustion and destruction performance. More work is needed to understand the involvement of free radicals in the destruction of organics. The

presence of halogenated compounds in the waste feed stream also affects the combustion performance of an incinerator. Their presence contributes to high CO emissions due to halogen inhibition of CO oxidation. It is clear that the performance of an incineration system and its emissions are affected by the chemical and physical nature of the waste streams as well as by the operating conditions.

Nomenclature

Ar	Archimedes number, dimensionless
C	concentration of compound (mol/m^3)
C_A	concentration of compound in the annulus (mol/m^3)
C_C	concentration of compound in the core (mol/m^3)
C_{CO}	concentration of carbon monoxide in the exhaust emissions (ppm)
C_{CO2}	concentration of carbon dioxide in the exhaust emissions (ppm)
CE	combustion efficiency (%)
D	axial dispersion coefficient (m^2/s)
d	pipe diameter (m)
d_s	mean particle diameter (m)
DRE	destruction and removal efficiency (%)
E_A	activation energy (calorie/mole)
g	gravitational constant (9.8 m/s^2)
K_M	mass transfer (crossflow) coefficient (m/s)
K_R	reaction rate constant (1/s)
N_{Pea}	Peclet number, dimensionless
N_{Re}	Reynolds number, based on the pipe diameter and the average fluid velocity, dimensionless
P_{O2}	partial pressure of oxygen (mole fraction)
R	universal gas constant (1.987 calories/mol.K)
R_R	radius of the riser column (m)
$R(C)$	reaction rate (mol/m^3.s)
R_C	radius of the core (m)
T	incineration temperature (K)
U	average fluid velocity (m/s)
U_A	superficial gas velocity in the annulus (m/s)
U_C	superficial gas velocity in the core (m/s)
U_{mf}	minimum fluidization velocity (m/s)
V	frequency factor (1/s)
W_{IN}	mass feed rate of one POHC in the waste feed stream (kg/hr)
W_{OUT}	mass emission rate of the same POHC in the exhaust emissions (kg/hr)
z	height coordinate (m)

Greek Letters

ρ	fluid density (kg/m^3)
ρ_f	density of air (kg/m^3)
ρ_s	density of sand (kg/m^3)
μ	fluid viscosity (kg/ms)
μ_f	viscosity of air (kg/ms)

References

Alcan Smelters and Chemicals Ltd., personal communication with Mr. A. Mikkelsen, P.Eng., Senior Development Engineer, Kitimat, B.C.

Anderson, B.M. and R.G. Wilbourn, "Contaminated Soil Remediation by Circulating Bed Combustion, Demonstration Test Results", Ogden Environmental Services Inc., San Diego, California, November 1989.

Anthony, E.J., E.M. Bulewicz and F. Preto, "The Combustion of Halogenated Wastes in FBC Systems", 49th Annual Purdue Industrial Waste Conference, May, 1994.

Arato, C.I., "The Usage of Sulfur Hexafluoride in the Incineration Processes", B.A.Sc. Thesis, University of British Columbia, 1991.

Attalla, P., "Sulphide Precipitation For Industrial Wastewater Treatment", B.A.Sc. Thesis, University of British Columbia, 1991.

Battelle Laboratories, Columbus, Ohio, Fluidized-Bed Incineration of Selected Carbonaceous Industrial Wastes, Water Pollution Control Research Series, 12120 FYF 03/72, US EPA, 1972.

Bott, J.F. and T.A. Jacobs, "Shock-Tube Studies of Sulfur Hexafluoride", Journal of Chemical Physics, 50, pp. 3850 - 3855, 1969.

Brady, J.E. and G.E. Humiston, General Chemistry Principles and Structure, 3rd Edition, John Wiley & Sons, New York, pp. 501 - 502, 1982.

Brereton, C.M.H., "Fluid Mechanics of High Velocity Fluidised Beds", Ph.D. Thesis, University of British Columbia, 1987.

Brereton, C.M.H., J.R. Grace, C.J. Lim, J. Zhu, R. Legros, J.R. Muir, J. Zhao, R.C. Senior, A. Luckos, N. Inumaru, J. Zhang and I. Hwang, "Environmental Aspects, Control and Scale-up of Circulating Fluidized Bed Combustion for Application in Western Canada", Final Report prepared for Energy, Mines and Resources Canada, under contract 55SS 23440-8-9243, December, 1991.

Brereton, C.M.H., J.R. Grace and J. Yu, "Axial Gas Mixing in a Circulating Fluidized Bed", from Circulating Fluidized Bed Technology II, Eds. P. Basu and J.F. Large, Pergammon Press, Toronto, 1988.

Brereton, C.M.H., S. Julien, C.J. Lim and J.R. Grace, "Combustion of Three Petroleum Cokes in a Pilot Scale Circulating Fluidized Bed Combustor", A Report to ABB Combustion Engineering, Windsor, Connecticut, October, 1993.

Brunner, C.R., Handbook of Hazardous Waste Incineration, Tab Books Inc., Pennsylvania, 1989.

Brunner, C.R., Hazardous Air Emissions from Incineration, Chapman and Hall, New York, 1985.

Brunner, C.R., Incineration Systems Selection and Design, Van Nostrand Reinhold Company, New York, 1984.

Bulewicz, E.M., E. Janicka and S. Kandefer, "Halogen Inhibition of CO Oxidation During the Combustion of Coal in a Fluidized Bed", Proc. 10th Intl. Conf. on Fluidized Bed Combustion, San Francisco, pp. 163 - 168, 1989.

Burkell, J.J., J.R. Grace, J. Zhao and C.J. Lim, "Measurement of Solids Circulation Rates in Circulating Fluidized Beds", Circulating Fluidized Bed Technology II, Eds. P. Basu and J.F. Large, Pergammon Press, pp. 501 - 504, 1988.

Butler, J.N., Ionic Equilibrium A Mathematical Approach, Addison-Wesley Publishing Company Inc., Massachusetts, pp. 310 - 316, 1964.

Chang, D.P.Y., N.W. Sorbo, G.S. Murchison, R.C. Adrian and D.C. Simeroth, "Evaluation of a Pilot-Scale Circulating Bed Combustor as a Potential Hazardous Waste Incinerator", JAPCA, 37, pp. 266 - 274, March 1987.

Chang, W.D., S.B. Karra and S.M. Senkan, Combust. Sci. Technol., 49, p. 107, 1987.

Chang, W.D. and S.M. Senkan, Environ. Sci. Technol. 23, p.442, 1989.

Cheremisinoff, P.N., "Thermal Treatment Technologies for Hazardous Wastes", Pollution Engineering, pp. 50 - 55, August 1988.

Clark, W.D., J.F. LaFond, D.K. Moyeda, W.F. Richter, W.R. Seeker and C.C. Lee, "Engineering Analysis of Hazardous Waste Incineration: Failure Mode Analysis for Two Pilot-Scale Incinerators", Incinerating Hazardous Wastes, Ed. H.M. Freeman, Technomic Publishing, Lancaster, PA, pp. 349 - 356, 1988.

Clemente, S., "The Use of Stud Blast Fines for the Stabilization of Incinerator Ash", B.A.Sc. Thesis, University of British Columbia, 1994.

CRC Handbook of Chemistry and Physics, 68th Edition, CRC Press Inc., Florida, pp. B207 - 208, 1987.

de Iribarne, A.P., E.J. Anthony and J.R. Stephenson, "Analysis of Solids from Circulating Fluidized Bed Combustion", Canada Centre for Mineral and Energy Technology, Energy Research Laboratories, 1988.

Dellinger, B. and D.L. Hall, "The Viability of Using Surrogate Compounds for Monitoring the Effectiveness of Incineration Systems", JAPCA, 36, pp. 179 - 183, February 1986.

Dellinger, B., P. Taylor and C.C. Lee, "Full-Scale Evaluation of the Thermal Stability-Based Hazardous Organic Waste Incinerability Ranking", Journal of Air & Waste Management, 43, pp. 203 - 207, February 1993.

Dempsey, C.R. and E.T. Oppelt, "Incineration of Hazardous Waste: A Critical Review Update", Air & Waste, 43, pp. 25 - 73, January 1993.

de Nevers, N., Fluid Mechanics for Chemical Engineers, 2nd Edition, McGraw-Hill Inc., New York, 1991.

Encyclopedia of Chemical Reactions, Ed. C.A. Jacobson, Reinhold Publishing Corporation, New York, 1951.

Exner, J.H., Ed. Detoxication of Hazardous Waste, Ann Arbor Science Publishers, Michigan, 1982.

Freeman, H.M., "Hazardous Waste Destruction Processes", Environmental Progress, Volume 2, pp. 205 - 210, November 1983.

Glassman, I. Combustion, Academic Press, New York, 1977.

Gordon, A.L., H.S. Caram and N.R. Amundson, "Modelling of Fluidized Bed Reactors-V, Combustion of Carbon Particles - an Extension", Chemical Engineering Science, 33, pp. 713 - 722, 1978.

Grace, J.R., Chapter 8 in Handbook of Multiphase Systems, Ed. G. Hetsroni, Hemisphere Publishing Corporation, New York, 1982.

Grace, J.R., "Contacting Modes and Behaviour Classification of Gas-Solid and Other Two-Phase Suspensions", Can. J. Chem. Eng., 64, pp. 353 - 361, 1986.

Grace, J.R., "High-Velocity Fluidized Bed Reactors", Chemical Engineering Science, 45, pp. 1953 - 1966, 1990.

Grace, J.R., C.M.H. Brereton, C.J. Lim, R. Legros, J. Zhao, R.C. Senior, R.L. Wu, J.R. Muir and R. Engman, "Circulating Fluidized Bed Combustion of Western Canadian Fuels", final report for Energy Mines and Resources of Canada, under contract, 52SS.23440-7-9136, 1989.

Grace, J.R. and C.J. Lim, "Circulating Fluidized Bed Combustion of Coal, Wood wastes and Pitch", final Report for CANMET, under contract 52SS 23440-6-9007, 1987.

Graham, J.L., D.L. Hall and B. Dellinger, "Laboratory Investigation of Thermal Degradation of a Mixture of Hazardous Compounds", Environmental Science & Technology, 20, pp. 703 - 710, 1986.

Grjotheim, K. and B.J. Welch, Aluminium Smelter Technology A Pure and Applied Approach, Aluminium-Verlag GmbH, Dusseldorf, 1980.

Incropera, F.P. and D.P. Dewitt, Fundamentals of Heat and Mass Transfer, 2nd Edition, John Wiley & Sons, New York, 1985.

Incineration of Hazardous Waste Toxic Combustion By-products, Eds. W.M.R. Seeker and C.P. Koshland, Gordon and Breach Science Publishers, Philadelphia, 1992.

Interim Protocol for Delisting Special Wastes and Residues, British Columbia Ministry of Environment, Environmental Protection Division, July 13, 1990.

Jensen, D.D. and D.T. Young, "PCB-Contaminated Soil Treatment in a Transportable Circulating Bed Combustor", Ogden Environmental Services Inc., San Diego, California, 1986.

Kataoka, A., W. Nowak, T. Ihara, H. Matsuda and H. Hasatani, "Flammability and Temperature Distributions in a Circulating Fluidized Bed Combustor", Journal of Chemical Engineering of Japan, 26, pp. 733 - 737, 1993.

Kakabadse, G., Ed. Chemistry of Effluent Treatment, Applied Science Publishers Ltd., London, pp. 60 -61, 1979.

Khare, V., "The Breakdown of Sulfur Hexafluoride in a Hot Gas Stream", B.A.Sc. Thesis, University of British Columbia, 1989.

Kiang, Y.H. and A.A. Metry, Hazardous Waste Processing Technology, Ann Arbor Science, Michigan, 1982.

Kirk-Othmer Encyclopedia of Chemical Technology, 2nd Edition, 12, Interscience Publishers, New York, 1963.

Lanford, C.E., "Trace Minerals Affect Stream Ecology", Oil & Gas Journal, 67, pp. 82 - 84, March/April 1969.

Lee, C.C., G.L. Huffman and S.M. Sasseville, "Incinerability Ranking Systems for RCRA Hazardous Constituents", Hazardous Waste & Hazardous Materials, 7, pp. 385 - 415, 1990.

Lee, K.C., "Incineration of Hazardous Waste: Critical Review Discussion Papers", JAPCA, 9, pp. 1011 - 1024, September 1987.

Levenspiel, O., Chemical Reaction Engineering, 2nd Edition, John Wiley & Sons, New York, 1972.

Loehr, R. and J.F. Malina Jr., Eds. Land Treatment A Hazardous Waste Management Alternative, Water Resources Symposium, Number 13, Center for Research in Water Resources, The University of Texas in Austin, 1986.

Lyman, J.L., "A Model for Unimolecular Reaction of Sulfur Hexafluoride", Journal Chemical Physics, 67, pp. 1868 - 1876, September 1977.

Manahan, S.E., Hazardous Waste Chemistry, Toxicology and Treatment, Lewis Publishers, Michigan, pp. 290 - 292, 1990.

Mournighan, R.E. and R.A. Olexsey, "Surrogate Compounds as Indicators of Hazardous Waste Incinerator Performance", Hazardous Waste Engineering Research Laboratory, Office of Research and Development, US EPA, EPA/600/D-85/140, 1985.

National Guidelines for Hazardous Waste Incineration Facilities: Design and Operating Criteria, Vol. 1 and 2, Canadian Council of Ministers of the Environment, 1992.

Oppelt, E.T., "Incineration of Hazardous Waste: A Critical Review", JAPCA, 37, pp. 558 - 586, May 1987.

Padma, D.K. and A.R.V. Murthy, "Thermal Decomposition of Sulphur Hexafluoride", Journal Fluorine Chemistry, 5, pp. 181 - 184, 1975.

Park, D., O. Levenspiel and T.J. Fitzgerald, "A Model for Large Scale Atmospheric Fluidized Bed Combustors", AIChE Symposium Series, 77, pp. 116 - 126, 1981.

Pauling, L., General Chemistry : An Introduction to Descriptive Chemistry and Modern Chemical Theory, 2nd Edition, W.H. Freeman and Company, pp. 541 - 542, 1958.

Perry, R.H. and D. Green, Perry's Chemical Engineers Handbook, 6th Edition, McGraw-Hill, New York, 1984.

"Plastics Are Safe to Burn, Given the Right Conditions", Chemical Engineering, 100, p.17, August 1993.

Proctor II, C.L., M.C. Berger, D.L. Fournier Jr. and S. Roychoudhury, "Sulfur Hexafluoride as a Tracer for the Verification of Waste Destruction Levels in an Incineration Process", University of Florida, Combustion Laboratory, Final Report, April 1987.

Rajan, R.R. and C.Y. Wen, "A Comprehensive Model for Fluidized Bed Coal Combustors", AIChE Journal, 26, pp. 642 - 655, 1980.

Reider, D.M., "Modelling of PCB Destruction Using SF6", B.A.Sc. Thesis, University of British Columbia, 1990.

Rhodes, M., Ed. Principles of Powder Technology, John Wiley & Sons, New York, 1990.

Rickman, W.S., "Circulating Bed Combustion of Spent Potliners", Ogden Environmental Services Inc., San Diego, California, 1988.

Roesler, J.F., R.A. Yetter and F.L. Dryer, "The Inhibition of the CO/H2O/O2 Reaction by Trace Quantities of HCl", Combustion Science and Technology, 82, pp. 87 - 100, 1992.

Ross, L.W., Removal of Heavy Metals from Mine Drainage by Precipitation, Environmental Protection Technology Series, EPA - 670/2-73-080, September 1973.

Rouse, J.V., "Removal of Heavy Metals from Industrial Effluents", Journal Environmental Engineering Division, Proceedings American Society of Civil Engineers, 102, pp. 929 - 936, October 1976.

Senior, R., "Circulating Fluidised Bed Fluid and Particle Mechanics: Modelling and Experimental Studies with Application to Combustion", Ph.D. Thesis, University of British Columbia, 1992.

Senser, D.W., V.A. Cundy and J.S. Morse, Combust. Sci. Technol.. 51, 209, 1986.

Sethumadhavan R., R. Vasudevan, D.K. Sahasrabudhe, and D.K. Biswas, "Incineration of Industrial Toxic Wastes: An Efficient Method of Waste Disposal", Fluidized Bed Combustion, ASME 1991, pp. 1111 - 1119.

Sevon, D.W. and D.J. Cooper, "Experimental Investigation of Combustion Efficiency in a Circulating Fluidized Bed Organic Waste Incinerator", Trans IChemE., 68, pp. 277 - 285, November 1990.

Smoot, D.L., "Modelling of Coal-Combustion Processes", Prog. Energy Combustion Science, 10, pp. 229 - 272, 1984.

Taylor, P.H. and J.F. Chadbourne, "Sulfur Hexafluoride as a Surrogate for Monitoring Hazardous Waste Incinerator Performance", JAPCA, 37, pp. 729 - 731, 1987.

Taylor, P.H., B. Dellinger, and C.C. Lee, "Development of a Thermal Stability Based Ranking of Hazardous Organic Compound Incinerability", Environmental Science Technology, 24, pp. 316 - 328, 1990.

Test Methods for Evaluating Solid Waste, Vol. 1A through 1C and Vol. 2 Field Manual Physical/Chemical Methods, EPA Report: EPA/SW-846, U.S. Environmental Protection Agency, Washington D.C., September 1986.

Theodore, L. and J. Reynolds, Introduction to Hazardous Waste Incineration, John Wiley and Sons, Toronto, 1987.

Tillman, D.A., A.J. Rossi and K.M. Vick, Incineration of Municipal and Hazardous Solid Wastes, Academic Press Inc., San Diego, California, 1989.

Tomita, M., T. Hirama and T. Adachi, "A Mathematical Model Simulation of Fluidized Bed Coal Combustion", Government Industrial Development Laboratory, Hokkaido, Japan.

Vrable, D.L., D.R. Engler and W.S. Rickman, "Application of Transportable Circulating Bed Combustor for Incineration of Hazardous Waste", Ogden Environmental Services Ltd., San Diego, California, December 1985.

Vural, H., P.M. Walsh, A.F. Sarofim and J.M. Beer, "Destruction of Tar During Oxidative and Nonoxidative Pyrolysis of Bituminous Coal in a Fluidized Bed", Combustion Science and Technology, 63, pp. 229 - 246, 1989.

Waste Management Act of B.C.: Special Waste Regulations, B.C. Reg. 63/88.

Weissman, M. and S.W. Benson, Int. J. Chem. Kinet., 16, p. 307, 1984.

Wells, J.W., P. Krishnan and C.E. Bell, " A Mathematical Model for Simulation of AFBC Systems", Jaro Stromberg, Studsvik, Sweden.

Wen, C.Y. and L.T. Fan, Models for Flow Systems and Chemical Reactors, Marcel Dekker, Inc., New York, 1975.

White, M.L., W.S. Rickman and H.R. Diot, "Transportable Circulating Bed Hazardous Waste Incinerator for Thermal Treatment of Soils, Sludges and Oils", Ogden Environmental Services Ltd., San Diego, California, 1987.

Wilbourn, R.G., S.A. Sterling and D.L. Vrable, "Destruction of Hazardous Refinery Wastes by means of Circulating Bed Combustion", Ogden Environmental Services Ltd., San Diego, California, 1986.

Wilkings, R.L., "Thermodynamics of SF6 and Its Decomposition and Oxidation Products", J. Chem. & Physics, 51, pp. 853 - 854, 1969.

Wolbach, C.D. and A.R. Garman, "Destruction of Hazardous Wastes Cofired in Industrial Boilers: Pilot-Scale Parametrics Testing", US EPA Research and Development, Hazardous Waste Engineering Research Laboratory, Cincinnati Ohio, EPA/600/S2-85/097, December 1985.

Zhao, J., "Nitric Oxides Emission from Circulating Fluidized Bed Combustion", Ph.D. Thesis, University of British Columbia, 1992.

1991 Annual Book of ASTM Standards, Section 5 Petroleum Products, Lubricants, and Fossil Fuels, Volume 05.05 Gaseous Fuels: Coal and Coke.

Appendix A Program Code and Results of CFB Incineration Model

Computer Code and Simulation Results with the Assumption that SF6 Decomposition is Dependent on Oxygen Concentration in CFB

```
C     program SF6
C
C     This program uses Finite Difference and Richardson
C     Extrapolation methods in the subroutine FDRE to solve the
C     problem for the term project to a prescribed accuracy.
C
C     The core-annulus model is used to determine the concentration
C     of SF6 in the core and the annulus as a function of the
C     riser height.
C
C     This program only considers the case where there is no gas
C     flow through the annulus (e.g. a stagnant annulus).
C
C
C     The boundary conditions are specified by the user in
C     subroutine BOUND
C
C
C     XO     = the bottom of the riser (m)
C     XF     = the top of the riser (m)
C     N      = the number of points along the height of the riser
C     EPS    = the desired accuracy of the solution
C     CIN    = the initial SF6 concentration upstream of the
C                  riser (mol/m3)
C     SF6IN  = the initial SF6 concentration upstream of the
C                  riser (ppm)
C     R      = the radius of the riser (m)
C     RC     = the radius of the core (m)
C     RE     = the Reynold's number
C     PEC    = the Pecklet number
C     DISP   = the dispersion coefficient (m2/s)
C     KM     = the mass transfer (crossflow) coefficient (m/s)
C     UC     = the average superficial gas velocity in the core (m/s)
C     TEMP   = the incineration temperature (deg. Celsius)
C     DENS   = the density of air at the incineration temp. (kg/m3)
C     VISC   = the viscosity of air at the incineration temp. (N.s/m2)
C     KR     = the reaction rate of SF6 (1/s)
C     FLAG   = 0  a converged solution cannot be obtained in the
C                  Richardson Extrapolation section of the program
C            = 1  a converged solution which satisfies the desired
C                  accuracy criteria is achieved
C     X      = 1-D array which stores the different heights of the
C                riser
C     YC     = 1-D array which stores the corresponding concentration
C                of SF6 in the core (mol/m3)
C     YA     = 1-D array which stores the corresponding concentration
C                of SF6 in the annulus (mol/m3)
C     MC     = 1-D array which stores the corresponding concentration
C                of SF6 in the core (ppm)
C     MA     = 1-D array which stores the corresponding concentration
C                of SF6 in the annulus (ppm)
C     DREC   = Destruction and removal efficiency of SF6 in the CFB
C                core region (%)
C     DREA   = Destruction and removal efficiency of SF6 in the CFB
C                annulus region (%)
C     Main Program
C
      IMPLICIT REAL*8(A-H,K,O-Z)
      COMMON/BLKB/CIN,C1,C2,C3,C4,C5
      DIMENSION X(21),YC(21),YA(21),MC(21),MA(21),A(21),B(21)
      DIMENSION C(21),D(21)
      EXTERNAL FUNC1,FUNC2
      OPEN(UNIT=6, FILE='sfout')
C
```

```
      XO=0.D0
      XF=7.3D0
      N=21
      EPS=1.D-7
      SF6IN=210.D0
      CIN=SF6IN/(0.08206D0*293.15D0*1000.D0)
      R=0.076D0
      RC=0.059D0
      KM=0.08D0
      UC=8.27D0
      TEMP=1200.D0
C
C     The combustion gas in the riser is assumed to have the
C     properties of air at the incineration temperature.  If TEMP is
C     changed, then the values for DENS and viscosity must also be
C     changed accordingly.
C
      DENS=0.2367D0
      VISC=550.D-7
C
C     Calculate the Reynold's number
C     Laminar flow: RE < 2000
C     Transition: 2000 < RE < 4000
C     Turbulent flow: RE > 4000
C
      RE=DENS*UC*2.D0*R/VISC
C
C     The Axial Dispersion Coeff. is determined from a correlation
C     based on single phase flow of fluids through an empty tube
C     or pipe and Reynold's number greater 2000
C
      IF (RE.LT.2000.D0) THEN
      WRITE (6,10)
 10   FORMAT(5X,'REYNOLDS NUMBER < 2000. PROGRAM STOPS')
      STOP
      ENDIF
C
C     Calculate the Pecklet number as a function of Reynold's number
C
      PEC=1.D0/(3.0D7*(RE**(-2.1D0))+1.35D0*(RE**-0.125D0))
      DISP=UC*2.D0*R/PEC
c
C     The partial pressure of oxygen at a given height in the riser
C     is used in the reaction rate term in the differential equations
C     representing the core and annulus.
C
C     The reaction rate constant is of the form:
C           k = A*exp(-E/RT)
C     where
C           A = Arrhenius factor (1/s)
C           E = activation energy (cal/gmole)
C           R = universal gas constant (cal/gmole.K)
C           T = temperature (K)
C
      KR=1.2D15*EXP(-92000.D0/(1.987D0*(TEMP+273.15)))
      C1=UC/DISP
      C2=KR/DISP
      C3=(2.D0*KM)/(DISP*RC)
      C4=(2.D0*KM*RC)/(R*R-RC*RC)
      C5=C3*C4
      NM=N-1
      DX=(XF-XO)/NM
      DO 20 I=1,N
         X(I)=XO+(I-1)*DX
```

```
 20   CONTINUE
C
      CALL FDRE(FUNC1,FUNC2,XO,XF,N,EPS,X,YC,NFUN,FLAG)
      IF (FLAG.EQ.0) THEN
         WRITE (6,30)
 30      FORMAT(1X,'NOTE: CONVERGED SOLUTION NOT OBTAINED')
      ELSE
         DO 40 I=1,N
            PAI=FUNC2(X(I))
            YA(I)=(C4*YC(I))/(C4+KR*PAI)
            MC(I)=INT(YC(I)*0.08206D0*293.15D0*1000.D0)
            MA(I)=INT(YA(I)*0.08206D0*293.15D0*1000.D0)
 40      CONTINUE
         DREC=(1.D0-(MC(N)/SF6IN))*100.D0
         DREA=(1.D0-(MA(N)/SF6IN))*100.D0
         WRITE (6,45)
 45      FORMAT(5X,'FIRST ORDER REACTION WITH RESPECT TO OXYGEN')
         WRITE (6,50) TEMP
 50      FORMAT(5X,'INCINERATION TEMP. (C) =',F8.1)
         WRITE (6,60) UC
 60      FORMAT(5X,'SUPERFICIAL GAS VELOCITY (m/s) =',F8.1)
         WRITE (6,70) RE
 70      FORMAT(5X,'REYNOLDS NUMBER =',F8.1)
         WRITE (6,80) PEC
 80      FORMAT(5X,'PECKLET NUMBER =',F8.2)
         WRITE (6,90) DISP
 90      FORMAT(5X,'AXIAL DISPERSION COEFF. (m2/s) =',F8.2)
         WRITE (6,100) KM
 100     FORMAT(5X,'CROSSFLOW COEFF. (m/s) =',F8.2)
         WRITE (6,110) SF6IN
 110     FORMAT(5X,'INLET SF6 CONC. (ppm) =',F8.1)
         WRITE (6,120)
 120     FORMAT(5X,'RISER HT.',2X,'CORE SF6',5X,'ANNULUS SF6')
         WRITE (6,130)
 130     FORMAT(6X,'(m)',7X,'CONC. (ppm)',2X,'CONC. (ppm)')
         WRITE (6,140) (X(I),MC(I),MA(I), I=1,N)
 140     FORMAT(5X,F6.4,5X,I6,7X,I6)
         WRITE (6,150) DREC
 150     FORMAT(5X,'DRE OF SF6 IN CORE (%) =',F6.2)
         WRITE (6,160) DREA
 160     FORMAT(5X,'DRE OF SF6 IN ANNULUS %) =',F6.2)
      ENDIF
      STOP
      END
C
C     end of MAIN PROGRAM
C
      DOUBLE PRECISION FUNCTION FUNC1(U)
      IMPLICIT REAL*8(A-H,K,O-Z)
C
C     This function calculates the percentage of oxygen in the
C     core as a function of the riser height.
C
C     This function is based on oxygen profile for Run #16, Minto Coal
C     Run conditions: T=895 C, U=7.6 m/s, Ca:S=3, O2=3 % and P:S=1
C
      FUNC1=(-1.5D0*U+17.275D0)/100.D0
      RETURN
      END
C
C     end of function FUNC1
C
      DOUBLE PRECISION FUNCTION FUNC2(U)
      IMPLICIT REAL*8(A-H,K,O-Z)
```

```
C
C     This function,based on the same run conditions as in FUNC1,
C     calculates the percentage of oxygen in the annulus as a
C     function of the riser height.
C
      FUNC2=(-0.784D0*U+6.150822D0)/100.D0
      RETURN
      END
C
C     end of function FUNC2
C
      SUBROUTINE BOUND(F1,F2,XO,XF,DX,DX2)
C
C     This subroutine sets the boundary conditions at the entrance
C     and the exit of the riser.
C
      IMPLICIT REAL*8(A-H,K,O-Z)
      COMMON/BLKA/A(6401),B(6401),C(6401),D(6401),X(6401),N
      COMMON/BLKB/CIN,C1,C2,C3,C4,C5
      COMMON/BLKC/KR
C
      A(1)=0.D0
      PC1=F1(XO)
      PA1=F2(XO)
      B(1)=(-C3+(C5/(C4+KR*PA1))-(C2*PC1)-(2.D0*C1/DX)-(2.D0/DX2)
     +       -(C1*C1))
      C(1)=2.D0/DX2
      D(1)=-C1*CIN*(2.D0/DX+C1)
C
      A(N)=2.D0/DX2
      PCN=F1(XF)
      PAN=F2(XF)
      B(N)=-A(N)-C3+(C5/(C4+KR*PAN))-(C2*PCN)
      C(N)=0.D0
      D(N)=0.D0
C
      RETURN
      END
C
C     end of subroutine BOUND
C
      SUBROUTINE FDRE(F1,F2,XO,XF,N,EPS,X,Y,NFUN,FLAG)
C
C     This subroutine uses the Thomas algorithm and the Richarson
C     Extrapolation method to solve the problem to the prescribed
C     accuracy.
C
      IMPLICIT REAL*8(A-H,K,O-Z)
      INTEGER FLAG
      COMMON/BLKA/A(6401),B(6401),C(6401),D(6401),YY(6401),NINTP
      COMMON/BLKB/CIN,C1,C2,C3,C4,C5
      COMMON/BLKC/KR
      DIMENSION X(51),Y(51),YR(8,8,51)
      EXTERNAL F1,F2
      FLAG=1
      NINT=N-1
      NFUN=0
      DO 10 I=1,8
C
C     F.D. approximation using N-1, 2(N-1), 4(N-1) ... subintervals
C
         IM=I-1
         II=2**IM
         IIM=II-1
```

```
            NFUN=NFUN+NINT-1
            NINTP=NINT+1
            DX=(XF-XO)/NINT
            DX2=DX*DX
            YDIFM=0.D0
            CALL BOUND(F1,F2,XO,XF,DX,DX2)
            DO 20 L=2,NINT
               XX=XO+(L-1)*DX
               A(L)=1.D0+C1*DX/2.D0
               PCX=F1(XX)
               PAX=F2(XX)
               B(L)=-(2.D0+(C3+(-C5/(C4+KR*PAX))+(C2*PCX))*DX2)
               C(L)=2.D0-A(L)
               D(L)=0.D0
 20         CONTINUE
C
            CALL TDMA
            DO 30 L=1,N
               YR(I,1,L)=YY(II*L-IIM)
 30         CONTINUE
            IF (I.GT.1) THEN
C
C           Richardson Extrapolation
C
            DO 40 L=1,N
               MULT=1
               DO 50 J=2,I
                  JM=J-1
                  MULT=4*MULT
                  YR(I,J,L)=(MULT*YR(I,JM,L)-YR(IM,JM,L))/(MULT-1)
 50            CONTINUE
               YDIFM=DMAX1(YDIFM,DABS(YR(I,I,L)-YR(IM,IM,L)))
 40         CONTINUE
               IF (YDIFM.LT.EPS) THEN
C
C              Final solution
C
                  DX=(XF-XO)/(N-1)
                  DO 60 L=1,N
                     X(L)=XO+(L-1)*DX
                     Y(L)=YR(I,I,L)
 60               CONTINUE
                  RETURN
               ENDIF
            ENDIF
            NINT=2*NINT
 10      CONTINUE
         FLAG=0
         RETURN
         END
C
C        end of subroutine FDRE
C
         SUBROUTINE TDMA
         IMPLICIT REAL*8(A-H,K,O-Z)
         COMMON/BLKA/A(6401),B(6401),C(6401),D(6401),X(6401),N
         DIMENSION P(6401),Q(6401)
C
         NM=N-1
         P(1)=-C(1)/B(1)
         Q(1)=D(1)/B(1)
         DO 10 I=2,N
            IM=I-1
            DEN=A(I)*P(IM)+B(I)
```

```
         P(I)=-C(I)/DEN
         Q(I)=(D(I)-A(I)*Q(IM))/DEN
 10    CONTINUE
C
       X(N)=Q(N)
       DO 20 I=N-1,1,-1
         X(I)=P(I)*X(I+1)+Q(I)
 20    CONTINUE
       RETURN
       END
C
C      end of subroutine TDMA
C
```

FIRST ORDER REACTION WITH RESPECT TO OXYGEN
INCINERATION TEMP. (C) = 915.0
SUPERFICIAL GAS VELOCITY (m/s) = 8.3
REYNOLDS NUMBER = 5409.8
PECKLET NUMBER = 1.12
AXIAL DISPERSION COEFF. (m2/s) = 1.12
CROSSFLOW COEFF. (m/s) = 0.08
INLET SF6 CONC. (ppm) = 210.0

RISER HT. (m)	CORE SF6 CONC. (ppm)	ANNULUS SF6 CONC. (ppm)
0.0000	209	209
0.3650	209	209
0.7300	209	209
1.0950	209	209
1.4600	209	209
1.8250	209	209
2.1900	209	209
2.5550	209	209
2.9200	209	209
3.2850	209	209
3.6500	209	209
4.0150	209	209
4.3800	209	209
4.7450	209	209
5.1100	209	209
5.4750	209	209
5.8400	209	209
6.2050	209	209
6.5700	209	209
6.9350	209	209
7.3000	209	209

DRE OF SF6 IN CORE (%) = 0.48
DRE OF SF6 IN ANNULUS %) = 0.48

FIRST ORDER REACTION WITH RESPECT TO OXYGEN
INCINERATION TEMP. (C) = 1200.0
SUPERFICIAL GAS VELOCITY (m/s) = 8.3
REYNOLDS NUMBER = 5409.8
PECKLET NUMBER = 1.12
AXIAL DISPERSION COEFF. (m2/s) = 1.12
CROSSFLOW COEFF. (m/s) = 0.08
INLET SF6 CONC. (ppm) = 210.0

RISER HT. (m)	CORE SF6 CONC. (ppm)	ANNULUS SF6 CONC. (ppm)
0.0000	196	139
0.3650	162	117
0.7300	135	99
1.0950	114	84
1.4600	96	72
1.8250	81	62
2.1900	69	54
2.5550	59	47
2.9200	51	41
3.2850	45	36
3.6500	39	32
4.0150	34	28
4.3800	30	26
4.7450	27	23
5.1100	24	21
5.4750	22	19
5.8400	19	18
6.2050	18	16
6.5700	16	15
6.9350	15	14
7.3000	14	14

DRE OF SF6 IN CORE (%) = 93.33
DRE OF SF6 IN ANNULUS %) = 93.33

Computer Code and Simulation Results with the Assumption that SF6 Decomposition is Independent of Oxygen Concentration in CFB

```
C     program SF6
C
C     This program uses Finite Difference and Richardson
C     Extrapolation methods in the subroutine FDRE to solve the
C     problem for the term project to a prescribed accuracy.
C
C     The core-annulus model is used to determine the concentration
C     of SF6 in the core and the annulus as a function of the
C     riser height.
C
C     This program only considers the case where there is no gas
C     flow through the annulus (e.g. a stagnant annulus).
C
C
C     The boundary conditions are specified by the user in
C     subroutine BOUND
C
C     The kinetic rate of decomposition of SF6 is assumed to be
C     independent of the local oxygen concentration in the riser.
C     Hence the sections of the program which calculates the partial
C     pressure of oxygen as a function of riser height will be ignored.
C     Also, the partial pressure terms in the differential equations
C     will not be used in solving the concentration of SF6 as a
C     function of the riser height.
C
C
C     XO     = the bottom of the riser (m)
C     XF     = the top of the riser (m)
C     N      = the number of points along the height of the riser
C     EPS    = the desired accuracy of the solution
C     CIN    = the initial SF6 concentration upstream of the
C              riser (mol/m3)
C     SF6IN = the initial SF6 concentration upstream of the
C              riser (ppm)
C     R      = the radius of the riser (m)
C     RC     = the radius of the core (m)
C     RE     = the Reynold's number
C     PEC    = the Pecklet number
C     DISP   = the dispersion coefficient (m2/s)
C     KM     = the mass transfer (crossflow) coefficient (m/s)
C     UC     = the average superficial gas velocity in the core (m/s)
C     TEMP   = the incineration temperature (deg. Celsius)
C     DENS   = the density of air at the incineration temp. (kg/m3)
C     VISC   = the viscosity of air at the incineration temp. (N.s/m2)
C     KR     = the reaction rate of SF6 (1/s)
C     FLAG   = 0  a converged solution cannot be obtained in the
C                 Richardson Extrapolation section of the program
C            = 1  a converged solution which satisfies the desired
C                 accuracy criteria is achieved
C     X      = 1-D array which stores the different heights of the
C              riser
C     YC     = 1-D array which stores the corresponding concentration
C              of SF6 in the core (mol/m3)
C     YA     = 1-D array which stores the corresponding concentration
C              of SF6 in the annulus (mol/m3)
C     MC     = 1-D array which stores the corresponding concentration
C              of SF6 in the core (ppm)
C     MA     = 1-D array which stores the corresponding concentration
C              of SF6 in the annulus (ppm)
C     DREC   = Destruction and removal efficiency of SF6 in the CFB
C              core region (%)
C     DREA   = Destruction and removal efficiency of SF6 in the CFB
C              annulus region (%)
C     Main Program
```

```
C
      IMPLICIT REAL*8(A-H,K,O-Z)
      COMMON/BLKB/CIN,C1,C2,C3,C4,C5
      DIMENSION X(21),YC(21),YA(21),MC(21),MA(21),A(21),B(21)
      DIMENSION C(21),D(21)
C     EXTERNAL FUNC1,FUNC2
      OPEN(UNIT=6, FILE='sfnout')
C
      XO=0.D0
      XF=7.3D0
      N=21
      EPS=1.D-7
      SF6IN=210.D0
      CIN=SF6IN/(0.08206D0*293.15D0*1000.D0)
      R=0.076D0
      RC=0.059D0
      KM=0.08D0
      UC=8.27D0
      TEMP=1200.D0
C
C     The combustion gas in the riser is assumed to have the
C     properties of air at the incineration temperature.  If TEMP is
C     changed, then the values for DENS and viscosity must also be
C     changed accordingly.
C
      DENS=0.2367D0
      VISC=550.D-7
C
C     Calculate the Reynold's number
C     Laminar flow: RE < 2000
C     Transition: 2000 < RE < 4000
C     Turbulent flow: RE > 4000
C
      RE=DENS*UC*2.D0*R/VISC
C
C     The Axial Dispersion Coeff. is determined from a correlation
C     based on single phase flow of fluids through an empty tube
C     or pipe and Reynold's number greater 2000
C
      IF (RE.LT.2000.D0) THEN
      WRITE (6,10)
 10   FORMAT(5X,'REYNOLDS NUMBER < 2000. PROGRAM STOPS')
      STOP
      ENDIF
C
C     Calculate the Pecklet number as a function of Reynold's number
C
      PEC=1.D0/(3.0D7*(RE**(-2.1D0))+1.35D0*(RE**-0.125D0))
      DISP=UC*2.D0*R/PEC
C
C     The thermal decomposition rate is independent of Oxygen
C
C
C     The thermal decompostion rate constant is of the form:
C           k = A*exp(-E/RT)
C     where
C           A = Arrhenius factor (1/s)
C           E = activation energy (cal/gmole)
C           R = universal gas constant (cal/gmole.K)
C           T = temperature (K)
C
      KR=1.2D15*EXP(-92000.D0/(1.987D0*(TEMP+273.15)))
      C1=UC/DISP
      C2=KR/DISP
```

```
      C3=(2.D0*KM)/(DISP*RC)
      C4=(2.D0*KM*RC)/(R*R-RC*RC)
      C5=C3*C4
      NM=N-1
      DX=(XF-XO)/NM
      DO 20 I=1,N
         X(I)=XO+(I-1)*DX
 20   CONTINUE
C
C     CALL FDRE(FUNC1,FUNC2,XO,XF,N,EPS,X,YC,NFUN,FLAG)
      CALL FDRE(XO,XF,N,EPS,X,YC,NFUN,FLAG)
      IF (FLAG.EQ.0) THEN
         WRITE (6,30)
 30      FORMAT(1X,'NOTE: CONVERGED SOLUTION NOT OBTAINED')
      ELSE
         DO 40 I=1,N
C           PAI=FUNC2(X(I))
C           YA(I)=(C4*YC(I))/(C4+KR*PAI)
            YA(I)=(C4*YC(I))/(C4+KR)
            MC(I)=INT(YC(I)*0.08206D0*293.15D0*1000.D0)
            MA(I)=INT(YA(I)*0.08206D0*293.15D0*1000.D0)
 40      CONTINUE
         DREC=(1.D0-(MC(N)/SF6IN))*100.D0
         DREA=(1.D0-(MA(N)/SF6IN))*100.D0
         WRITE (6,45)
 45      FORMAT(5X,'REACTION IS INDEPENDENT OF OXYGEN CONC.')
         WRITE (6,50) TEMP
 50      FORMAT(5X,'INCINERATION TEMP. (C) =',F8.1)
         WRITE (6,60) UC
 60      FORMAT(5X,'SUPERFICIAL GAS VELOCITY (m/s) =',F8.1)
         WRITE (6,70) RE
 70      FORMAT(5X,'REYNOLDS NUMBER =',F8.1)
         WRITE (6,80) PEC
 80      FORMAT(5X,'PECKLET NUMBER =',F8.2)
         WRITE (6,90) DISP
 90      FORMAT(5X,'AXIAL DISPERSION COEFF. (m2/s) =',F8.2)
         WRITE (6,100) KM
 100     FORMAT(5X,'CROSSFLOW COEFF. (m/s) =',F8.2)
         WRITE (6,110) SF6IN
 110     FORMAT(5X,'INLET SF6 CONC. (ppm) =',F8.1)
         WRITE (6,120)
 120     FORMAT(5X,'RISER HT.',2X,'CORE SF6',5X,'ANNULUS SF6')
         WRITE (6,130)
 130     FORMAT(6X,'(m)',7X,'CONC. (ppm)',2X,'CONC. (ppm)')
         WRITE (6,140) (X(I),MC(I),MA(I), I=1,N)
 140     FORMAT(5X,F6.4,5X,I6,7X,I6)
         WRITE (6,150) DREC
 150     FORMAT(5X,'DRE OF SF6 IN CORE (%) =',F6.2)
         WRITE (6,160) DREA
 160     FORMAT(5X,'DRE OF SF6 IN ANNULUS %) =',F6.2)
      ENDIF
      STOP
      END
C
C     end of MAIN PROGRAM
C
C      DOUBLE PRECISION FUNCTION FUNC1(U)
C      IMPLICIT REAL*8(A-H,K,O-Z)
C
C     This function calculates the percentage of oxygen in the
C     core as a function of the riser height.
C
C      FUNC1=(-1.5D0*U+17.275D0)/100.D0
C      RETURN
```

```
C       END
C
C      end of function FUNC1
C
C       DOUBLE PRECISION FUNCTION FUNC2(U)
C       IMPLICIT REAL*8(A-H,K,O-Z)
C
C      This function calculates the percentage of oxygen in the
C      annulus as a function of the riser height.
C
C       FUNC2=(-0.784D0*U+6.150822D0)/100.D0
C       RETURN
C       END
C
C      end of function FUNC2
C
C       SUBROUTINE BOUND(F1,F2,XO,XF,DX,DX2)
       SUBROUTINE BOUND(XO,XF,DX,DX2)
C
C      This subroutine sets the boundary conditions at the entrance
C      and the exit of the riser.
C
       IMPLICIT REAL*8(A-H,K,O-Z)
       COMMON/BLKA/A(6401),B(6401),C(6401),D(6401),X(6401),N
       COMMON/BLKB/CIN,C1,C2,C3,C4,C5
       COMMON/BLKC/KR
C
       A(1)=0.D0
C       PC1=F1(XO)
C       PA1=F2(XO)
C       B(1)=(-C3+(C5/(C4+KR*PA1))-(C2*PC1)-(2.D0*C1/DX)-(2.D0/DX2)
C      +        -(C1*C1))
       B(1)=(-C3+(C5/(C4+KR))-C2-(2.D0*C1/DX)-(2.D0/DX2)-(C1*C1))
       C(1)=2.D0/DX2
       D(1)=-C1*CIN*(2.D0/DX+C1)
C
       A(N)=2.D0/DX2
C       PCN=F1(XF)
C       PAN=F2(XF)
C       B(N)=-A(N)-C3+(C5/(C4+KR*PAN))-(C2*PCN)
       B(N)=-A(N)-C3+(C5/(C4+KR))-C2
       C(N)=0.D0
       D(N)=0.D0
C
       RETURN
       END
C
C      end of subroutine BOUND
C
C       SUBROUTINE FDRE(F1,F2,XO,XF,N,EPS,X,Y,NFUN,FLAG)
       SUBROUTINE FDRE(XO,XF,N,EPS,X,Y,NFUN,FLAG)
C
C      This subroutine uses the Thomas algorithm and the Richarson
C      Extrapolation method to solve the problem to the prescribed
C      accuracy.
C
       IMPLICIT REAL*8(A-H,K,O-Z)
       INTEGER FLAG
       COMMON/BLKA/A(6401),B(6401),C(6401),D(6401),YY(6401),NINTP
       COMMON/BLKB/CIN,C1,C2,C3,C4,C5
       COMMON/BLKC/KR
       DIMENSION X(51),Y(51),YR(8,8,51)
C       EXTERNAL F1,F2
       FLAG=1
```

```
      NINT=N-1
      NFUN=0
      DO 10 I=1,8
C
C     F.D. approximation using N-1, 2(N-1), 4(N-1) ... subintervals
C
         IM=I-1
         II=2**IM
         IIM=II-1
         NFUN=NFUN+NINT-1
         NINTP=NINT+1
         DX=(XF-XO)/NINT
         DX2=DX*DX
         YDIFM=0.D0
C         CALL BOUND(F1,F2,XO,XF,DX,DX2)
         CALL BOUND(XO,XF,DX,DX2)
         DO 20 L=2,NINT
            XX=XO+(L-1)*DX
            A(L)=1.D0+C1*DX/2.D0
C            PCX=F1(XX)
C            PAX=F2(XX)
C            B(L)=-(2.D0+(C3+(-C5/(C4+KR*PAX))+(C2*PCX))*DX2)
            B(L)=-(2.D0+(C3+(-C5/(C4+KR))+C2)*DX2)
            C(L)=2.D0-A(L)
            D(L)=0.D0
 20      CONTINUE
C
         CALL TDMA
         DO 30 L=1,N
            YR(I,1,L)=YY(II*L-IIM)
 30      CONTINUE
         IF (I.GT.1) THEN
C
C        Richardson Extrapolation
C
         DO 40 L=1,N
            MULT=1
            DO 50 J=2,I
               JM=J-1
               MULT=4*MULT
               YR(I,J,L)=(MULT*YR(I,JM,L)-YR(IM,JM,L))/(MULT-1)
 50         CONTINUE
            YDIFM=DMAX1(YDIFM,DABS(YR(I,I,L)-YR(IM,IM,L)))
 40      CONTINUE
            IF (YDIFM.LT.EPS) THEN
C
C           Final solution
C
               DX=(XF-XO)/(N-1)
               DO 60 L=1,N
                  X(L)=XO+(L-1)*DX
                  Y(L)=YR(I,I,L)
 60               CONTINUE
                  RETURN
               ENDIF
            ENDIF
            NINT=2*NINT
 10   CONTINUE
      FLAG=0
      RETURN
      END
C
C     end of subroutine FDRE
C
```

```
      SUBROUTINE TDMA
      IMPLICIT REAL*8(A-H,K,O-Z)
      COMMON/BLKA/A(6401),B(6401),C(6401),D(6401),X(6401),N
      DIMENSION P(6401),Q(6401)
C
      NM=N-1
      P(1)=-C(1)/B(1)
      Q(1)=D(1)/B(1)
      DO 10 I=2,N
         IM=I-1
         DENOM=A(I)*P(IM)+B(I)
         P(I)=-C(I)/DENOM
         Q(I)=(D(I)-A(I)*Q(IM))/DENOM
 10   CONTINUE
C
      X(N)=Q(N)
      DO 20 I=N-1,1,-1
         X(I)=P(I)*X(I+1)+Q(I)
 20   CONTINUE
      RETURN
      END
C
C     end of subroutine TDMA
C
```

REACTION IS INDEPENDENT OF OXYGEN CONC.
INCINERATION TEMP. (C) = 915.0
SUPERFICIAL GAS VELOCITY (m/s) = 8.3
REYNOLDS NUMBER = 5409.8
PECKLET NUMBER = 1.12
AXIAL DISPERSION COEFF. (m2/s) = 1.12
CROSSFLOW COEFF. (m/s) = 0.08
INLET SF6 CONC. (ppm) = 210.0

RISER HT. (m)	CORE SF6 CONC. (ppm)	ANNULUS SF6 CONC. (ppm)
0.0000	209	209
0.3650	209	209
0.7300	209	208
1.0950	209	208
1.4600	209	208
1.8250	209	208
2.1900	209	208
2.5550	209	208
2.9200	208	208
3.2850	208	208
3.6500	208	207
4.0150	208	207
4.3800	208	207
4.7450	208	207
5.1100	208	207
5.4750	207	207
5.8400	207	207
6.2050	207	206
6.5700	207	206
6.9350	207	206
7.3000	207	206

DRE OF SF6 IN CORE (%) = 1.43
DRE OF SF6 IN ANNULUS %) = 1.90

REACTION IS INDEPENDENT OF OXYGEN CONC.
INCINERATION TEMP. (C) = 1200.0
SUPERFICIAL GAS VELOCITY (m/s) = 8.3
REYNOLDS NUMBER = 5409.8
PECKLET NUMBER = 1.12
AXIAL DISPERSION COEFF. (m2/s) = 1.12
CROSSFLOW COEFF. (m/s) = 0.08
INLET SF6 CONC. (ppm) = 210.0

RISER HT. (m)	CORE SF6 CONC. (ppm)	ANNULUS SF6 CONC. (ppm)
0.0000	157	20
0.3650	64	8
0.7300	26	3
1.0950	10	1
1.4600	4	0
1.8250	1	0
2.1900	0	0
2.5550	0	0
2.9200	0	0
3.2850	0	0
3.6500	0	0
4.0150	0	0
4.3800	0	0
4.7450	0	0
5.1100	0	0
5.4750	0	0
5.8400	0	0
6.2050	0	0
6.5700	0	0
6.9350	0	0
7.3000	0	0

DRE OF SF6 IN CORE (%) =100.00
DRE OF SF6 IN ANNULUS %) =100.00

Appendix B Calibration Curves for Flowmeters Used in the Pnuematic Transport of Alcan Solid Fuel Feed

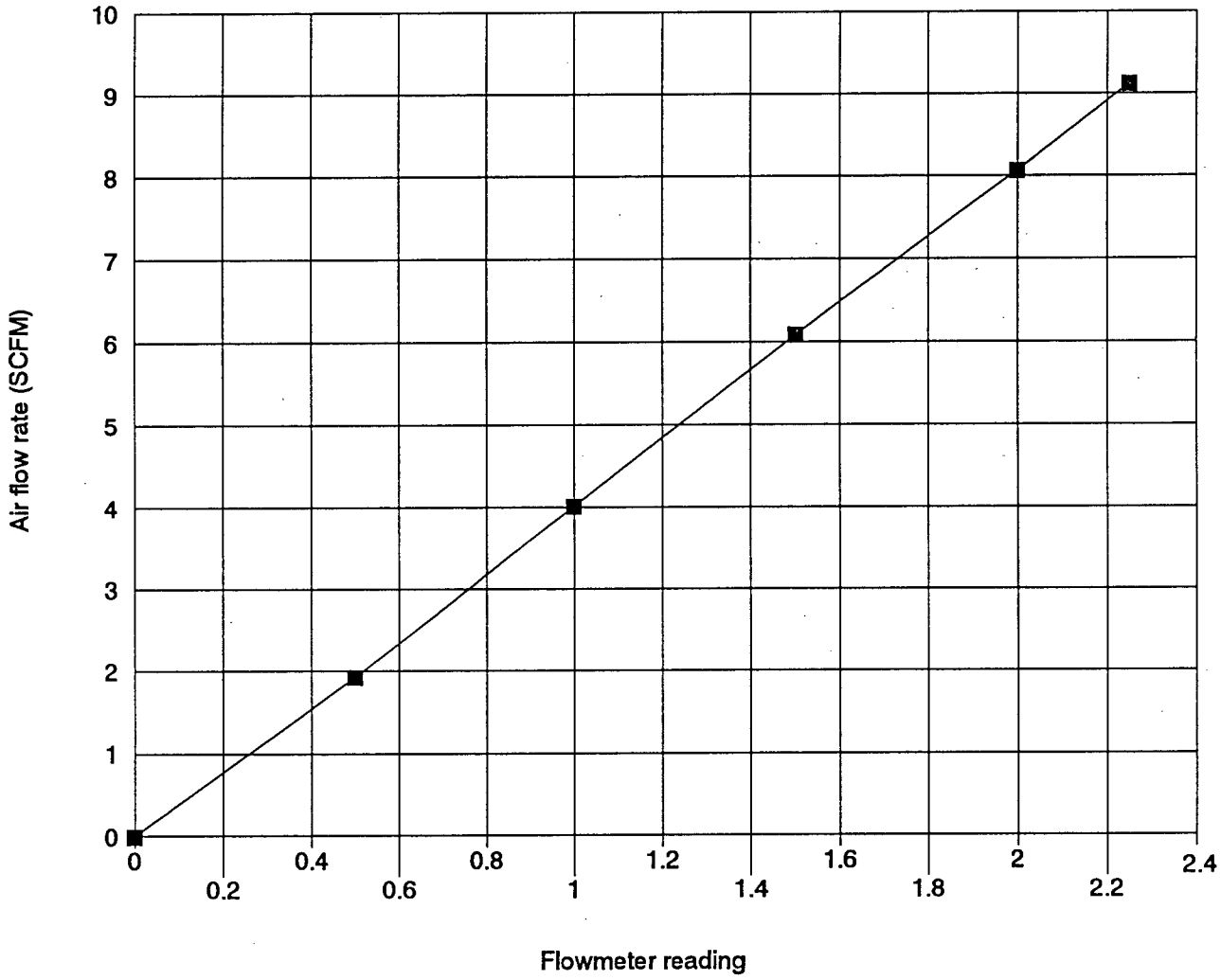

Figure B1 Calibration Curve for Flowmeter A

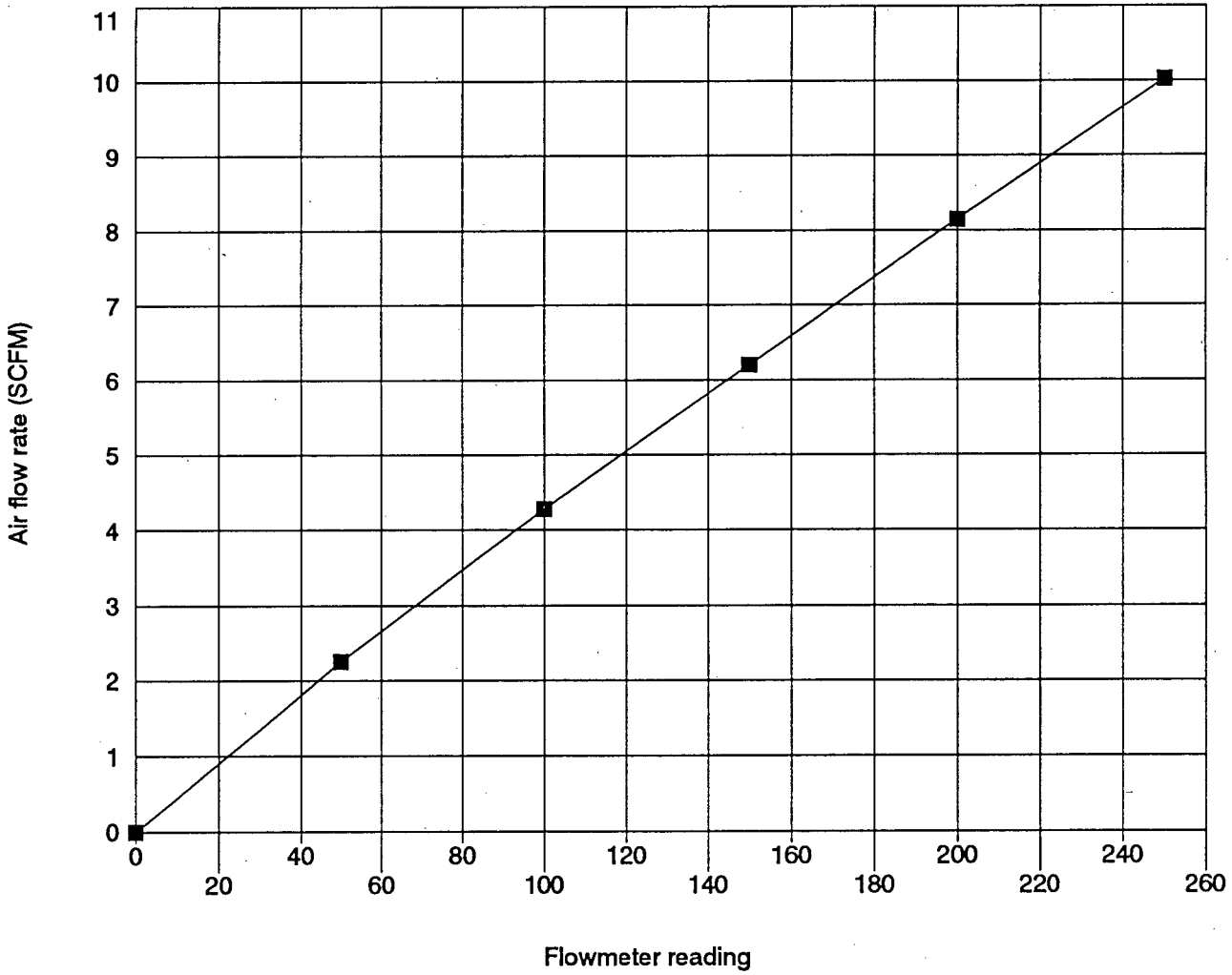

Figure B2 Calibration Curve for Flowmeter D

Appendix C Metal Analysis of Alcan Solid Fuels

Table C1 Metal Analysis of Alcan Solid Fuels

ACME ANALYTICAL LABORATORIES LTD. 852 E. HASTINGS ST. VANCOUVER B.C. V6A 1R6 PHONE(604)253-3158 FAX(604)253-1716

GEOCHEMICAL ANALYSIS CERTIFICATE

The University of British Columbia File # 92-2490

Dept. of Chemical Engineering, Vancouver BC V6T 1Z4 Submitted by: POLLY WONG

SAMPLE#	Mo ppm	Cu ppm	Pb ppm	Zn ppm	Ag ppm	Ni ppm	Co ppm	Mn ppm	Fe %	As ppm	U ppm	Au ppm	Th ppm	Sr ppm	Cd ppm	Sb ppm	Bi ppm	V ppm	Ca %	P %	La ppm	Cr ppm	Mg %	Ba ppm	Ti %	Al %	Na %	K %	W ppm	Zr ppm	Sn ppm	Y ppm	Nb ppm	Be ppm	Sc ppm	ASH gm	SAMPLE gm
PITCH COMES	301	573	8816	14568	6.2	4607	511	617	6.59	325	5	ND	15	760	581.2	38	1097	1043	1.90	.214	51	563	.52	1255	.61	18.05	1.68	.83	72	193	240	37	19	8	20.1	.26	25
PITCH DUST	222	431	19295	30066	.2	23310	307	1706	18.99	691	5	ND	1	834	1220.1	22	2555	45287	2.12	.206	63	1059	.57	1214	.65	9.46	2.82	.65	2	254	674	50	196	15	23.2	.07	25
VACUUM DUST	53	392	154	408	.2	2769	45	1045	33.71	25	5	ND	1	14	11.9	2	6	2519	.17	.060	2	608	.05	45	.04	12.20	.41	.02	8	10	6	2	1	1	.2	3.36	25
STUD BLAST FINES	155	1343	321	188	.2	865	46	3402	68.21	67	5	ND	1	4	1.7	2	75	419	.03	.010	2	686	.03	12	.02	1.25	.28	.04	4	1	23	3	1	4	.2	11.94	25
MISC. PASTE WASTE	46	103	2216	3379	.6	5188	53	892	6.75	99	5	ND	2	460	137.5	2	342	9311	3.00	.126	19	148	1.31	435	.47	7.38	3.06	1.02	2	51	74	19	13	3	17.2	.44	26
STANDARD HFC	22	64	39	138	7.3	93	46	1235	4.52	42	21	7	36	61	21.0	17	19	79	.55	.123	40	63	.99	236	.08	2.08	.10	.17	12	4	16	8	1	1	5.6	-	-

ICP - .500 GRAM SAMPLE IS DIGESTED WITH 10ML HCLO4-HNO3-HCL-HF AT 200 DEG. C TO FUMING AND IS DILUTED TO 10 ML WITH DILUTED AQUA REGIA. THIS LEACH IS PARTIAL FOR MAGNETITE, CHROMITE, BARITE, OXIDES OF AL, ZR & MN AND MASSIVE SULFIDE SAMPLES. AU DETECTION LIMIT BY ICP IS 3 PPM.
AS, CR, SB SUBJECT TO THE LOST OF VOLATILIZATION DURING HCLO4 FUMING.
- SAMPLE TYPE: COAL

DATE RECEIVED: AUG 11 1992 DATE REPORT MAILED: Aug 25/92 SIGNED BY .....C.L.....D.TOYE, C.LEONG, J.WANG; CERTIFIED B.C. ASSAYERS

P.002

IU 8226005

Appendix D Mass Balances for the Incineration of Solid Fuels at Different Operating Conditions

For each steady state, the inputs into the mass balance spreadsheet included: the average incineration temperature, the measured flow rates of primary, secondary and pneumatic air, the moisture content of the waste, the ultimate analysis of the wastes, the limestone feed rate if applicable, and the combustion efficiency. The combustion efficiencies used in the mass balances are based on flue gas emissions. The waste feed rate is adjusted until the oxygen content in the flue gas matches the experimentally measured flue gas oxygen content. This calculated waste feed rate satisfies the mass balance in which the air flows and ultimate analysis are assumed to be measured correctly. The "measured" waste feed rate is determined by loss in weight on the feed hopper load cells and is somewhat sensitive to e.g. combustor vibration, and drift slightly from calibration values. Generally, the measured and calculated values will agree within approximately 10 %. The calculated waste feed rate, based on accurate air flow measurements is used for calculation purposes. The waste feed rates reported in this work are the calculated waste feed rate.

Stud Blast Fines

Fuel Feed Rate (kg/hr):	24.4
Moisture % :	0.6
Dry feed rate (kg/hr) :	24.2536
Limestone Feed Rate(kg/hr):	0
% CaCO3 :	95.5
CaCO3 Feed Rate(kg/hr) :	0

Combustion Eff % :	99.3
Sulphur Capt % :	0
Ca:S ratio :	0
P:S Air Split:	2.102824965

Ash Flow (kg/hr) :

CaO	0
CaSO4	0
C	0.079488749
Ash	9.61412704
Total	9.693615789

Dry Flue Gas Analysis:

	kgmol/hr	mol%/ppm
N2	5.089287673	79.6674504
O2	0.26726982	4.183828169
CO2	0.939670564	14.70955522
SO2	0.091936303	14391.66204
Cl2	0.00003416	0.000534739
H2O		
Tot	6.38816436	

Wet Flue Gas Analysis:

	kgmol/hr	mol%/ppm
N2	5.089287673	78.27463574
O2	0.26726982	4.110682899
CO2	0.939670564	14.45239017
SO2	0.091936303	14140.05466
Cl2	0.00003416	0.00052539
H2O	0.113636493	1.747760334
Tot	6.501835013	

Air Rates

1'Rot	1'P(psig)	F(scfm)	F(kg/hr)
23.06	3	40.54669644	88.63681715
2'Rot	2'P(psig)		
28.45	3	27.36637494	59.82406915
P nozzle (psig)			
50		17	37.162729

Rot A	(psig)	F(scfm)	F(kg/hr)
0	1	0	0
Rot D	(psig)	F(scfm)	F(kg/hr)
0	1	0	0

Total Air(scfm) :	84.91307139	
Tot.Air(kgmol/hr):	6.43632508	

T base (C) :	861
T top (C) :	861
V base (m/s) :	4.969298652
V top (m/s) :	7.332452378

Assume Ash = SiO2

Ultimate Analysis (Dry basis)

C	46.82
H	0.87
S	12.13
O	0
Cl	0.01
Ash	39.64
N	0.53
	100

Combustion Calculations (one hour basis)

	kg In	kgmol In		kgmol Out	kg Out
C	11.35553552	0.946294627	CO2	0.939670564	41.34550483
H	0.21100632	0.21100632	H2O	0.113636493	2.04545688
S	2.94196168	0.091936303	SO2	0.091936303	5.88392336
O	43.25210454	2.703256534	N2	5.089287673	142.5000548
Cl	0.00242536	0.00006832	CaO	0	0
N	142.5000548	10.17857535	CaSO4	0	0
Ash	9.61412704	0.160235451	Ash	0.160235451	9.61412704
CaCO3	0	0	C	0.006624062	0.079488749
H2O	0.1464	0.008133333	O2	0.26726982	8.55263424
			Cl2	0.00003416	0.00242536
Total	210.0236153				210.0236153

Mass Balance Check:

Fuel	24.4
Lime	0
Air	185.6236153
	210.0236153

Alcan Stud Blast Fines (with limestone addition)

Fuel Feed Rate (kg/hr):	23.4
Moisture % :	0.6
Dry feed rate (kg/hr) :	23.2596
Limestone Feed Rate(kg/hr):	18.5
% CaCO3 :	95.5
CaCO3 Feed Rate(kg/hr) :	17.6675

Ash Flow (kg/hr) :

CaO	5.20323999
CaSO4	11.39136003
C	0.076231013
Ash	10.05260544
Total	26.72343647

Air Rates

1'Rot	1'P(psig)	F(scfm)	F(kg/hr)
23.06	3	40.54669644	88.63681715
2'Rot	2'P(psig)		
28.45	3	27.36637494	59.82406915
P nozzle (psig)			
50		17	37.162729

Rot A	(psig)	F(scfm)	F(kg/hr)
0	1	0	0
Rot D	(psig)	F(scfm)	F(kg/hr)
0	1	0	0

Total Air(scfm) :	84.91307139
Tot.Air(kgmol/hr):	6.43632508

Ultimate Analysis (Dry basis)

C	46.82
H	0.87
S	12.13
O	0
Cl	0.01
Ash	39.64
N	0.53
	100

Combustion Eff % :	99.3
Sulphur Capt % :	95
Ca:S ratio :	2.003835358
P:S Air Split:	2.102824965

Dry Flue Gas Analysis:			Wet Flue Gas Analysis:		
	kgmol/hr	mol%/ppm		kgmol/hr	mol%/ppm
N2	5.089099523	79.00889166	N2	5.089099523	77.69397938
O2	0.26983074	4.189155192	O2	0.26983074	4.119436817
CO2	1.077834476	16.73351188	CO2	1.077834476	16.45502297
SO2	0.004408421	684.4127542	SO2	0.004408421	673.0223561
Cl2	0.00003276	0.000508603	Cl2	0.00003276	0.000500139
H2O			H2O	0.10897926	1.663758459
Tot	6.44117316		Tot	6.55018518	

T base (C) :	861
T top (C) :	861
V base (m/s) :	5.006252283
V top (m/s) :	7.386979337

Assume Ash = SiO2

Combustion Calculations (one hour basis)

	kg In	kgmol In		kgmol Out	kg Out
C	10.89014472	0.90751206	CO2	1.077834476	47.42471693
H	0.20235852	0.20235852	H2O	0.10897926	1.96162668
S	2.82138948	0.088168421	SO2	0.004408421	0.282138948
O	43.25210454	2.703256534	N2	5.089099523	142.4947866
Cl	0.00232596	0.00006552	CaO	0.092915	5.20323999
N	142.4947866	10.17819905	CaSO4	0.08376	11.39136003
Ash	10.05260544	0.167543424	Ash	0.167543424	10.05260544
CaCO3	17.6675	0.176675	C	0.006352584	0.076231013
H2O	0.1404	0.0078	O2	0.26983074	8.634583675
			Cl2	0.00003276	0.00232596
Total	227.5236153				227.5236153

Mass Balance Check:

Fuel	23.4
Lime	18.5
Air	185.6236153
	227.5236153

Alcan Pitch Cones : Preliminary Test Condition # 1

Fuel Feed Rate (kg/hr):	10.3
Moisture % :	0.37
Dry feed rate (kg/hr) :	10.26189
Limestone Feed Rate(kg/hr):	0
% CaCO3 :	95.5
CaCO3 Feed Rate(kg/hr) :	0

Combustion Eff % :	99.88
Sulphur Capt % :	0
Ca:S ratio :	0
P:S Air Split:	2.051046252

Ash Flow (kg/hr) :

CaO	0
CaSO4	0
C	0.011526155
Ash	0.108776034
Total	0.120302189

Dry Flue Gas Analysis:

	kgmol/hr	mol%/ppm
N2	4.74551634	80.00051839
O2	0.38527032	6.494936083
CO2	0.799466907	13.47751486
SO2	0.00160342	270.3066368
Cl2	1.44534E-05	0.000243657
H2O		
Tot	5.931856988	

Wet Flue Gas Analysis:

	kgmol/hr	mol%/ppm
N2	4.74551634	77.97604161
O2	0.38527032	6.330576557
CO2	0.799466907	13.13645562
SO2	0.00160342	263.4663123
Cl2	1.44534E-05	0.000237491
H2O	0.153993194	2.530342087
Tot	6.085864635	

Air Rates

1'Rot	1'P(psig)	F(scfm)	F(kg/hr)
14.9	3	26.07664621	57.00466683
2'Rot	2'P(psig)		
27	3	25.94944463	56.72659873
P nozzle (psig)			
50		17	37.162729

Rot A	(psig)	F(scfm)	F(kg/hr)
1.2	1	5.012665377	10.95790147
Rot D	(psig)	F(scfm)	F(kg/hr)
120	1	5.13419957	11.22358043

Total Air(scfm) :	79.17295579
Tot.Air(kgmol/hr):	6.001230113

T base (C) :	897
T top (C) :	900
V base (m/s) :	4.76028875
V top (m/s) :	7.099350895

Ultimate Analysis (Dry basis)

C	93.6
H	2.96
S	0.5
O	0.63
Cl	0.01
Ash	1.06
N	1.24
	100

Assume Ash = SiO2

Combustion Calculations (one hour basis)

	kg In	kgmol In		kgmol Out	kg Out
C	9.60512904	0.80042742	CO2	0.799466907	35.17654391
H	0.303751944	0.303751944	H2O	0.153993194	2.771877496
S	0.05130945	0.00160342	SO2	0.00160342	0.1026189
O	40.39291627	2.524557267	N2	4.74551634	132.8744575
Cl	0.001026189	2.89067E-05	CaO	0	0
N	132.8744575	9.491032681	CaSO4	0	0
Ash	0.108776034	0.001812934	Ash	0.001812934	0.108776034
CaCO3	0	0	C	0.000960513	0.011526155
H2O	0.03811	0.002117222	O2	0.38527032	12.32865024
			Cl2	1.44534E-05	0.001026189
Total	183.3754765				183.3754765

Mass Balance Check:

Fuel	10.3
Lime	0
Air	173.0754765
	183.3754765

Alcan Pitch Cones : Preliminary Test Condition # 2

Fuel Feed Rate (kg/hr):	10.4
Moisture % :	0.37
Dry feed rate (kg/hr) :	10.36152
Limestone Feed Rate(kg/hr):	0
% CaCO3 :	95.5
CaCO3 Feed Rate(kg/hr) :	0

Combustion Eff % :	99.86
Sulphur Capt % :	0
Ca:S ratio :	0
P:S Air Split:	1.137195438

Ash Flow (kg/hr) :

CaO	0
CaSO4	0
C	0.013577736
Ash	0.109832112
Total	0.123409848

Dry Flue Gas Analysis:

	kgmol/hr	mol%/ppm
N2	4.767120909	80.00571917
O2	0.382668188	6.422250285
CO2	0.807067082	13.54485937
SO2	0.001618988	271.7117139
Cl2	1.45937E-05	0.000244923
H2O		
Tot	5.958475167	

Wet Flue Gas Analysis:

	kgmol/hr	mol%/ppm
N2	4.767120909	77.97085436
O2	0.382668188	6.258906823
CO2	0.807067082	13.20035953
SO2	0.001618988	264.8010004
Cl2	1.45937E-05	0.000238694
H2O	0.155488274	2.543160491
Tot	6.113978034	

Air Rates

1'Rot	1'P(psig)	F(scfm)	F(kg/hr)
8.5	3	15.17241663	33.16755338
2'Rot	2'P(psig)		
38.3	3	37.21372788	81.35080494
P nozzle (psig)			
50		17	37.162729

Rot A	(psig)	F(scfm)	F(kg/hr)
1.2	1	5.012665377	10.95790147
Rot D	(psig)	F(scfm)	F(kg/hr)
120	1	5.13419957	11.22358043

Total Air(scfm) :	79.53300945
Tot.Air(kgmol/hr):	6.028521817

T base (C) :	893
T top (C) :	893
V base (m/s) :	3.772349914
V top (m/s) :	7.089589667

Assume Ash = SiO2

Ultimate Analysis (Dry basis)

C	93.6
H	2.96
S	0.5
O	0.63
Cl	0.01
Ash	1.06
N	1.24
	100

Combustion Calculations (one hour basis)

	kg In	kgmol In		kgmol Out	kg Out
C	9.69838272	0.80819856	CO2	0.807067082	35.51095161
H	0.306700992	0.306700992	H2O	0.155488274	2.798788928
S	0.0518076	0.001618988	SO2	0.001618988	0.1036152
O	40.57694419	2.536059012	N2	4.767120909	133.4793854
Cl	0.001036152	2.91874E-05	CaO	0	0
N	133.4793854	9.534241818	CaSO4	0	0
Ash	0.109832112	0.001830535	Ash	0.001830535	0.109832112
CaCO3	0	0	C	0.001131478	0.013577736
H2O	0.03848	0.002137778	O2	0.382668188	12.24538203
			Cl2	1.45937E-05	0.001036152
Total	184.2625692				184.2625692

Mass Balance Check:

Fuel	10.4
Lime	0
Air	173.8625692
	184.2625692

Alcan Pitch Cones : Steady State # 1

Fuel Feed Rate (kg/hr):	11.3
Moisture % :	0.37
Dry feed rate (kg/hr) :	11.25819
Limestone Feed Rate(kg/hr):	0
% CaCO3 :	95.5
CaCO3 Feed Rate(kg/hr) :	0

Combustion Eff % :	99.91
Sulphur Capt % :	0
Ca:S ratio :	0
P:S Air Split:	2.011387067

Ash Flow (kg/hr) :

CaO	0
CaSO4	0
C	0.009483899
Ash	0.119336814
Total	0.128820713

Dry Flue Gas Analysis:

	kgmol/hr	mol%/ppm
N2	5.090324485	80.02359835
O2	0.391597162	6.156191828
CO2	0.877348495	13.79255562
SO2	0.001759092	276.5420693
Cl2	1.58566E-05	0.000249277
H2O		
Tot	6.361029234	

Wet Flue Gas Analysis:

	kgmol/hr	mol%/ppm
N2	5.090324485	77.95303211
O2	0.391597162	5.996903778
CO2	0.877348495	13.43568089
SO2	0.001759092	269.3866966
Cl2	1.58566E-05	0.000242827
H2O	0.16894399	2.58720172
Tot	6.52998908	

Air Rates

1'Rot	1'P(psig)	F(scfm)	F(kg/hr)
15.7	3	27.46717123	60.04441416
2'Rot	2'P(psig)		
29.3	3	28.20088853	61.64835164
P nozzle (psig)			
50		17	37.162729

Rot A	(psig)	F(scfm)	F(kg/hr)
1.5	1	6.265831722	13.69737684
Rot D	(psig)	F(scfm)	F(kg/hr)
140	1	5.989899498	13.09417716

Total Air(scfm) :	84.92379098	
Tot.Air(kgmol/hr):	6.437137614	

T base (C) :	900
T top (C) :	900
V base (m/s) :	5.087891969
V top (m/s) :	7.617435911

Assume Ash = SiO2

Ultimate Analysis (Dry basis)

C	93.6
H	2.96
S	0.5
O	0.63
Cl	0.01
Ash	1.06
N	1.24
	100

Combustion Calculations (one hour basis)

	kg In	kgmol In		kgmol Out	kg Out
C	10.53766584	0.87813882	CO2	0.877348495	38.60333378
H	0.333242424	0.333242424	H2O	0.16894399	3.040991816
S	0.05629095	0.001759092	SO2	0.001759092	0.1125819
O	43.32849136	2.70803071	N2	5.090324485	142.5290856
Cl	0.001125819	3.17132E-05	CaO	0	0
N	142.5290856	10.18064897	CaSO4	0	0
Ash	0.119336814	0.001988947	Ash	0.001988947	0.119336814
CaCO3	0	0	C	0.000790325	0.009483899
H2O	0.04181	0.002322778	O2	0.391597162	12.53110918
			Cl2	1.58566E-05	0.001125819
	Total	196.9470488			196.9470488

Mass Balance Check:

Fuel	11.3
Lime	0
Air	185.6470488
	196.9470488

Alcan Pitch Cones: Steady State # 2

Fuel Feed Rate (kg/hr):	11.9
Moisture % :	0.37
Dry feed rate (kg/hr) :	11.85597
Limestone Feed Rate(kg/hr):	0
% CaCO3 :	95.5
CaCO3 Feed Rate(kg/hr) :	0

Ash Flow (kg/hr) :

CaO	0
CaSO4	0
C	0.017755501
Ash	0.125673282
Total	0.143428783

Air Rates

1'Rot	1'P(psig)	F(scfm)	F(kg/hr)
15.72	3	27.50201264	60.12057898
2'Rot	2'P(psig)		
30.07	3	28.95934761	63.30637571
P nozzle (psig)			
50		17	37.162729

Rot A	(psig)	F(scfm)	F(kg/hr)
1.5	1	6.265831722	13.69737684
Rot D	(psig)	F(scfm)	F(kg/hr)
140	1	5.989899498	13.09417716

Total Air(scfm) :	85.71709147
Tot.Air(kgmol/hr):	6.49726899

Ultimate Analysis (Dry basis)

C	93.6
H	2.96
S	0.5
O	0.63
Cl	0.01
Ash	1.06
N	1.24
	100

Combustion Eff % :	99.84
Sulphur Capt % :	0
Ca:S ratio :	0
P:S Air Split:	1.959910998

	Dry Flue Gas Analysis: kgmol/hr	mol%/ppm		Wet Flue Gas Analysis: kgmol/hr	mol%/ppm
N2	5.138093003	80.06852666	N2	5.138093003	77.90831787
O2	0.353887924	5.514747328	O2	0.353887924	5.365962205
CO2	0.923286035	14.387858	CO2	0.923286035	13.99968079
SO2	0.001852495	288.6801975	SO2	0.001852495	280.8917502
Cl2	1.66985E-05	0.000260219	Cl2	1.66985E-05	0.000253198
H2O			H2O	0.177914467	2.697696762
Tot	6.417119458		Tot	6.595050623	

T base (C) :	856
T top (C) :	856
V base (m/s) :	4.903094672
V top (m/s) :	7.404787186

Assume Ash = SiO2

Combustion Calculations (one hour basis)

	kg In	kgmol In		kgmol Out	kg Out
C	11.09718792	0.92476566	CO2	0.923286035	40.62458554
H	0.350936712	0.350936712	H2O	0.177914467	3.202460408
S	0.05927985	0.001852495	SO2	0.001852495	0.1185597
O	43.73634023	2.733521264	N2	5.138093003	143.8666041
Cl	0.001185597	3.33971E-05	CaO	0	0
N	143.8666041	10.27618601	CaSO4	0	0
Ash	0.125673282	0.002094555	Ash	0.002094555	0.125673282
CaCO3	0	0	C	0.001479625	0.017755501
H2O	0.04403	0.002446111	O2	0.353887924	11.32441356
			Cl2	1.66985E-05	0.001185597
Total	199.2812377				199.2812377

Mass Balance Check:

Fuel	11.9
Lime	0
Air	187.3812377
	199.2812377

Alcan Pitch Cones: Steady State # 3

Fuel Feed Rate (kg/hr):	12
Moisture % :	0.37
Dry feed rate (kg/hr) :	11.9556
Limestone Feed Rate(kg/hr):	0
% CaCO3 :	95.5
CaCO3 Feed Rate(kg/hr) :	0

Ash Flow (kg/hr) :

CaO	0
CaSO4	0
C	0.027976104
Ash	0.12672936
Total	0.154705464

Air Rates

1'Rot	1'P(psig)	F(scfm)	F(kg/hr)
15.35	3	26.85806468	58.71288112
2'Rot	2'P(psig)		
29.75	3	28.64385663	62.61669889
P nozzle (psig)			
50		17	37.162729

Rot A	(psig)	F(scfm)	F(kg/hr)
1.5	1	6.265831722	13.69737684
Rot D	(psig)	F(scfm)	F(kg/hr)
140	1	5.989899498	13.09417716

Total Air(scfm) :	84.75765253
Tot.Air(kgmol/hr):	6.424544487

Ultimate Analysis (Dry basis)

C	93.6
H	2.96
S	0.5
O	0.63
Cl	0.01
Ash	1.06
N	1.24
	100

Combustion Eff % :	99.75
Sulphur Capt % :	0
Ca:S ratio :	0
P:S Air Split:	1.959016784

	Dry Flue Gas Analysis: kgmol/hr	mol%/ppm		Wet Flue Gas Analysis: kgmol/hr	mol%/ppm
N2	5.080684768	80.08997281	N2	5.080684768	77.88700965
O2	0.330963141	5.217176452	O2	0.330963141	5.073672251
CO2	0.930205458	14.66340331	CO2	0.930205458	14.26007021
SO2	0.001868063	294.4742327	SO2	0.001868063	286.3743937
Cl2	1.68389E-05	0.000265442	Cl2	1.68389E-05	0.00025814
H2O			H2O	0.179409547	2.750352311
Tot	6.343721429		Tot	6.523147814	

T base (C) :	833
T top (C) :	833
V base (m/s) :	4.750122183
V top (m/s) :	7.174870262

Assume Ash = SiO2

Combustion Calculations (one hour basis)

	kg In	kgmol In		kgmol Out	kg Out
C	11.1904416	0.9325368	CO2	0.930205458	40.92904015
H	0.35388576	0.35388576	H2O	0.179409547	3.22937184
S	0.059778	0.001868063	SO2	0.001868063	0.119556
O	43.24825923	2.703016202	N2	5.080684768	142.2591735
Cl	0.00119556	3.36777E-05	CaO	0	0
N	142.2591735	10.16136954	CaSO4	0	0
Ash	0.12672936	0.002112156	Ash	0.002112156	0.12672936
CaCO3	0	0	C	0.002331342	0.027976104
H2O	0.0444	0.002466667	O2	0.330963141	10.5908205
			Cl2	1.68389E-05	0.00119556
Total	197.283863				197.283863

Mass Balance Check:

Fuel	12
Lime	0
Air	185.283863
	197.283863

Alcan Pitch Cones: Steady State # 4

Fuel Feed Rate (kg/hr):	12.3
Moisture % :	0.37
Dry feed rate (kg/hr) :	12.25449
Limestone Feed Rate(kg/hr):	0
% CaCO3 :	95.5
CaCO3 Feed Rate(kg/hr) :	0

Ash Flow (kg/hr) :	
CaO	0
CaSO4	0
C	0.009176162
Ash	0.129897594
Total	0.139073756

Air Rates

1'Rot	1'P(psig)	F(scfm)	F(kg/hr)
10.67	3	18.825814	41.1540367
2'Rot	2'P(psig)		
38.84	3	37.76477315	82.55541353
P nozzle (psig)			
50		17	37.162729

Rot A	(psig)	F(scfm)	F(kg/hr)
1.5	1	6.265831722	13.69737684
Rot D	(psig)	F(scfm)	F(kg/hr)
140	1	5.989899498	13.09417716

Total Air(scfm) :	85.84631837
Tot.Air(kgmol/hr):	6.507064259

Ultimate Analysis (Dry basis)

C	93.6
H	2.96
S	0.5
O	0.63
Cl	0.01
Ash	1.06
N	1.24
	100

Combustion Eff % :	99.92
Sulphur Capt % :	0
Ca:S ratio :	0
P:S Air Split:	1.273185067

	Dry Flue Gas Analysis: kgmol/hr	mol%/ppm		Wet Flue Gas Analysis: kgmol/hr	mol%/ppm
N2	5.146007753	80.1032227	N2	5.146007753	77.87385651
O2	0.321212567	5.000023909	O2	0.321212567	4.860867407
CO2	0.95508554	14.866948	CO2	0.95508554	14.45318349
SO2	0.001914764	298.053908	SO2	0.001914764	289.7587198
Cl2	1.72598E-05	0.000268668	Cl2	1.72598E-05	0.000261191
H2O			H2O	0.183894785	2.782855529
Tot	6.424220624		Tot	6.608132669	

T base (C) :	887
T top (C) :	887
V base (m/s) :	4.269651701
V top (m/s) :	7.623171792

Assume Ash = SiO2

Combustion Calculations (one hour basis)

	kg In	kgmol In		kgmol Out	kg Out
C	11.47020264	0.95585022	CO2	0.95508554	42.02376375
H	0.362732904	0.362732904	H2O	0.183894785	3.310106136
S	0.06127245	0.001914764	SO2	0.001914764	0.1225449
O	43.8046751	2.737792194	N2	5.146007753	144.0882171
Cl	0.001225449	3.45197E-05	CaO	0	0
N	144.0882171	10.29201551	CaSO4	0	0
Ash	0.129897594	0.00216496	Ash	0.00216496	0.129897594
CaCO3	0	0	C	0.00076468	0.009176162
H2O	0.04551	0.002528333	O2	0.321212567	10.27880215
			Cl2	1.72598E-05	0.001225449
Total	199.9637332				199.9637332

Mass Balance Check:

Fuel	12.3
Lime	0
Air	187.6637332
	199.9637332

Alcan Pitch Cones: Steady State # 5

Fuel Feed Rate (kg/hr):	12
Moisture % :	0.37
Dry feed rate (kg/hr) :	11.9556
Limestone Feed Rate(kg/hr):	0
% CaCO3 :	95.5
CaCO3 Feed Rate(kg/hr) :	0

Combustion Eff % :	99.9
Sulphur Capt % :	0
Ca:S ratio :	0
P:S Air Split:	1.956594266

Ash Flow (kg/hr) :

CaO	0
CaSO4	0
C	0.011190442
Ash	0.12672936
Total	0.137919802

Dry Flue Gas Analysis:

	kgmol/hr	mol%/ppm
N2	5.156845217	80.07365644
O2	0.349809518	5.431717647
CO2	0.931604263	14.4656193
SO2	0.001868063	290.0660938
Cl2	1.68389E-05	0.000261468
H2O		
Tot	6.440127061	

Wet Flue Gas Analysis:

	kgmol/hr	mol%/ppm
N2	5.156845217	77.90321898
O2	0.349809518	5.284488159
CO2	0.931604263	14.07352128
SO2	0.001868063	282.2037038
Cl2	1.68389E-05	0.000254381
H2O	0.179409547	2.710296822
Tot	6.619553446	

Air Rates

1'Rot	1'P(psig)	F(scfm)	F(kg/hr)
15.82	3	27.676277	60.50152833
2'Rot	2'P(psig)		
30.21	3	29.09750336	63.6083901
P nozzle (psig)			
50		17	37.162729

Rot A	(psig)	F(scfm)	F(kg/hr)
1.5	1	6.265831722	13.69737684
Rot D	(psig)	F(scfm)	F(kg/hr)
140	1	5.989899498	13.09417716

Total Air(scfm) :	86.02951158	
Tot.Air(kgmol/hr):	6.520950119	

T base (C) :	887
T top (C) :	887
V base (m/s) :	5.053528188
V top (m/s) :	7.636346853

Ultimate Analysis (Dry basis)

C	93.6
H	2.96
S	0.5
O	0.63
Cl	0.01
Ash	1.06
N	1.24
	100

Assume Ash = SiO2

Combustion Calculations (one hour basis)

	kg In	kgmol In		kgmol Out	kg Out
C	11.1904416	0.9325368	CO2	0.931604263	40.99058758
H	0.35388576	0.35388576	H2O	0.179409547	3.22937184
S	0.059778	0.001868063	SO2	0.001868063	0.119556
O	43.89610508	2.743506567	N2	5.156845217	144.3916661
Cl	0.00119556	3.36777E-05	CaO	0	0
N	144.3916661	10.31369043	CaSO4	0	0
Ash	0.12672936	0.002112156	Ash	0.002112156	0.12672936
CaCO3	0	0	C	0.000932537	0.011190442
H2O	0.0444	0.002466667	O2	0.349809518	11.19390458
			Cl2	1.68389E-05	0.00119556
Total	200.0642014				200.0642014

Mass Balance Check:

Fuel	12
Lime	0
Air	188.0642014
	200.0642014

Alcan Pitch Cones: Steady State # 6

Fuel Feed Rate (kg/hr):	13.6
Moisture % :	0.37
Dry feed rate (kg/hr) :	13.54968
Limestone Feed Rate(kg/hr):	0
% CaCO3 :	95.5
CaCO3 Feed Rate(kg/hr) :	0

Combustion Eff % :	99.85
Sulphur Capt % :	0
Ca:S ratio :	0
P:S Air Split:	1.94912224

Ash Flow (kg/hr) :

CaO	0
CaSO4	0
C	0.019023751
Ash	0.143626608
Total	0.162650359

Dry Flue Gas Analysis:

	kgmol/hr	mol%/ppm
N2	5.13581684	80.22408815
O2	0.208615142	3.258675315
CO2	1.055289727	16.48416576
SO2	0.002117138	330.7077155
Cl2	1.90841E-05	0.000298103
H2O		
Tot	6.401838848	

Wet Flue Gas Analysis:

	kgmol/hr	mol%/ppm
N2	5.13581684	77.75427825
O2	0.208615142	3.158352472
CO2	1.055289727	15.97667784
SO2	0.002117138	320.5264194
Cl2	1.90841E-05	0.000288925
H2O	0.20333082	3.078349873
Tot	6.605188751	

Air Rates

1'Rot	1'P(psig)	F(scfm)	F(kg/hr)
15.64	3	27.3626699	59.81596978
2'Rot	2'P(psig)		
30.16	3	29.04815304	63.5005082
P nozzle (psig)			
50		17	37.162729

Rot A	(psig)	F(scfm)	F(kg/hr)
1.5	1	6.265831722	13.69737684

Rot D	(psig)	F(scfm)	F(kg/hr)
140	1	5.989899498	13.09417716

Total Air(scfm) :		85.66655417
Tot.Air(kgmol/hr):		6.493438314

T base (C) :	889
T top (C) :	889
V base (m/s) :	5.044713779
V top (m/s) :	7.632911521

Assume Ash = SiO2

Ultimate Analysis (Dry basis)

C	93.6
H	2.96
S	0.5
O	0.63
Cl	0.01
Ash	1.06
N	1.24
	100

Combustion Calculations (one hour basis)

	kg In	kgmol In		kgmol Out	kg Out
C	12.68250048	1.05687504	CO2	1.055289727	46.43274801
H	0.401070528	0.401070528	H2O	0.20333082	3.659954752
S	0.0677484	0.002117138	SO2	0.002117138	0.1354968
O	43.72126845	2.732579278	N2	5.13581684	143.8028715
Cl	0.001354968	3.81681E-05	CaO	0	0
N	143.8028715	10.27163368	CaSO4	0	0
Ash	0.143626608	0.002393777	Ash	0.002393777	0.143626608
CaCO3	0	0	C	0.001585313	0.019023751
H2O	0.05032	0.002795556	O2	0.208615142	6.675684551
			Cl2	1.90841E-05	0.001354968
Total	200.870761				200.870761

Mass Balance Check:

Fuel	13.6
Lime	0
Air	187.270761
	200.870761

Alcan Pitch Cones: Steady State # 6 (with limestone addition)

Fuel Feed Rate (kg/hr):	13.6
Moisture % :	0.37
Dry feed rate (kg/hr) :	13.54968
Limestone Feed Rate(kg/hr):	0.15
% CaCO3 :	95.5
CaCO3 Feed Rate(kg/hr) :	0.14325

Combustion Eff % :	99.85
Sulphur Capt % :	63
Ca:S ratio :	0.676621145
P:S Air Split:	1.94912224

Ash Flow (kg/hr) :

CaO	0.005527389
CaSO4	0.181396341
C	0.019023751
Ash	0.150376608
Total	0.356324089

Air Rates

1'Rot	1'P(psig)	F(scfm)	F(kg/hr)
15.64	3	27.3626699	59.81596978
2'Rot	2'P(psig)		
30.16	3	29.04815304	63.5005082
P nozzle (psig)			
50		17	37.162729

Rot A	(psig)	F(scfm)	F(kg/hr)
1.5	1	6.265831722	13.69737684
Rot D	(psig)	F(scfm)	F(kg/hr)
140	1	5.989899498	13.09417716

Total Air(scfm) :	85.66655417	
Tot.Air(kgmol/hr):	6.493438314	

Ultimate Analysis (Dry basis)

C	93.6
H	2.96
S	0.5
O	0.63
Cl	0.01
Ash	1.06
N	1.24
	100

Dry Flue Gas Analysis:

	kgmol/hr	mol%/ppm
N2	5.13581684	80.23120907
O2	0.207948244	3.248546346
CO2	1.056722227	16.50800731
SO2	0.000783341	122.3727159
Cl2	0.000019084	0.000298129
H2O		
Tot	6.401270653	

Wet Flue Gas Analysis:

	kgmol/hr	mol%/ppm
N2	5.13581684	77.76096744
O2	0.207948244	3.148526734
CO2	1.056722227	15.99974167
SO2	0.000783341	118.6049779
Cl2	0.000019084	0.00028895
H2O	0.20333082	3.078614703
Tot	6.604620556	

T base (C) :	889
T top (C) :	889
V base (m/s) :	5.044279821
V top (m/s) :	7.632254919

Assume Ash = SiO2

Combustion Calculations (one hour basis)

	kg In	kgmol In		kgmol Out	kg Out
C	12.68250048	1.05687504	CO2	1.056722227	46.49577801
H	0.401070528	0.401070528	H2O	0.20333082	3.659954752
S	0.0677484	0.002117138	SO2	0.000783341	0.050133816
O	43.72126845	2.732579278	N2	5.13581684	143.8028715
Cl	0.001354968	0.000038168	CaO	0.000098703	0.005527389
N	143.8028715	10.27163368	CaSO4	0.001333797	0.181396341
Ash	0.150376608	0.002506277	Ash	0.002506277	0.150376608
CaCO3	0.14325	0.0014325	C	0.001585313	0.019023751
H2O	0.05032	0.002795556	O2	0.207948244	6.654343805
			Cl2	0.000019084	0.001354968
Total	201.020761				201.020761

Mass Balance Check:

Fuel	13.6
Lime	0.15
Air	187.270761
	201.020761

Alcan Pitch Cones: Steady State # 7

Fuel Feed Rate (kg/hr):	10.4
Moisture % :	0.37
Dry feed rate (kg/hr) :	10.36152
Limestone Feed Rate(kg/hr):	0
% CaCO3 :	95.5
CaCO3 Feed Rate(kg/hr) :	0

Combustion Eff % :	99.91
Sulphur Capt % :	0
Ca:S ratio :	0
P:S Air Split:	2.020032643

Ash Flow (kg/hr) :

CaO	0
CaSO4	0
C	0.008728544
Ash	0.109832112
Total	0.118560656

Dry Flue Gas Analysis:

	kgmol/hr	mol%/ppm
N2	4.339430648	80.10622993
O2	0.268574273	4.957902133
CO2	0.807471181	14.9059813
SO2	0.001618988	298.8663616
Cl2	1.45937E-05	0.000269401
H2O		
Tot	5.41709509	

Wet Flue Gas Analysis:

	kgmol/hr	mol%/ppm
N2	4.339430648	77.87087246
O2	0.268574273	4.8195523
CO2	0.807471181	14.49003117
SO2	0.001618988	290.5265214
Cl2	1.45937E-05	0.000261883
H2O	0.155488274	2.79022953
Tot	5.572597958	

Air Rates

1'Rot	1'P(psig)	F(scfm)	F(kg/hr)
10.87	3	19.16479537	41.89506451
2'Rot	2'P(psig)		
24.96	3	23.97017036	52.3998203
P nozzle (psig)			
50		17	37.162729

Rot A	(psig)	F(scfm)	F(kg/hr)
1.5	1	6.265831722	13.69737684
Rot D	(psig)	F(scfm)	F(kg/hr)
140	1	5.989899498	13.09417716

Total Air(scfm) :	72.39069695	
Tot.Air(kgmol/hr):	5.487141741	

T base (C) :	890
T top (C) :	890
V base (m/s) :	4.311049364
V top (m/s) :	6.44519773

Assume Ash = SiO2

Ultimate Analysis (Dry basis)

C	93.6
H	2.96
S	0.5
O	0.63
Cl	0.01
Ash	1.06
N	1.24
	100

Combustion Calculations (one hour basis)

	kg In	kgmol In		kgmol Out	kg Out
C	9.69838272	0.80819856	CO2	0.807471181	35.52873198
H	0.306700992	0.306700992	H2O	0.155488274	2.798788928
S	0.0518076	0.001618988	SO2	0.001618988	0.1036152
O	36.93887007	2.30867938	N2	4.339430648	121.5040582
Cl	0.001036152	2.91874E-05	CaO	0	0
N	121.5040582	8.678861297	CaSO4	0	0
Ash	0.109832112	0.001830535	Ash	0.001830535	0.109832112
CaCO3	0	0	C	0.000727379	0.008728544
H2O	0.03848	0.002137778	O2	0.268574273	8.594376737
			Cl2	1.45937E-05	0.001036152
Total	168.6491678				168.6491678

Mass Balance Check:

Fuel	10.4
Lime	0
Air	158.2491678
	168.6491678

Alcan Misc. Paste Waste : Steady State # 1

Fuel Feed Rate (kg/hr):	13.2
Moisture % :	0.35
Dry feed rate (kg/hr) :	13.1538
Limestone Feed Rate(kg/hr):	0
% CaCO3 :	95.5
CaCO3 Feed Rate(kg/hr) :	0

Ash Flow (kg/hr) :	
CaO	0
CaSO4	0
C	0.011082076
Ash	1.25487252
Total	1.265954597

Air Rates

1'Rot	1'P(psig)	F(scfm)	F(kg/hr)
15.75	3	27.55428193	60.23484187
2'Rot	2'P(psig)		
30.07	3	28.95934761	63.30637571
P nozzle (psig)			
50		17	37.162729

Rot A	(psig)	F(scfm)	F(kg/hr)
1.5	1	6.265831722	13.69737684
Rot D	(psig)	F(scfm)	F(kg/hr)
140	1	5.989899498	13.09417716

Total Air(scfm) :	85.76936075	
Tot.Air(kgmol/hr):	6.501230949	

Ultimate Analysis (Dry basis)

C	84.25
H	2.48
S	1.34
O	1.34
Cl	0
Ash	9.54
N	1.05
	100

Combustion Eff % :	99.9
Sulphur Capt % :	0
Ca:S ratio :	0
P:S Air Split:	1.961715917

	Dry Flue Gas Analysis: kgmol/hr	mol%/ppm		Wet Flue Gas Analysis: kgmol/hr	mol%/ppm
N2	5.140905125	79.95039828	N2	5.140905125	77.94219589
O2	0.361122071	5.616103133	O2	0.361122071	5.475037273
CO2	0.922582869	14.34783681	CO2	0.922582869	13.98744636
SO2	0.005508154	856.6178044	SO2	0.005508154	835.1011897
Cl2	0	0	Cl2	0	0
H2O			H2O	0.165673787	2.511810357
Tot	6.430118218		Tot	6.595792005	

T base (C) :	877
T top (C) :	877
V base (m/s) :	4.996397256
V top (m/s) :	7.543349755

Assume Ash = SiO2

Combustion Calculations (one hour basis)

	kg in	kgmol In		kgmol Out	kg Out
C	11.0820765	0.923506375	CO2	0.922582869	40.59364622
H	0.32621424	0.32621424	H2O	0.165673787	2.98212816
S	0.17626092	0.005508154	SO2	0.005508154	0.35252184
O	43.8645329	2.741533306	N2	5.140905125	143.9453435
Cl	0	0	CaO	0	0
N	143.9453435	10.28181025	CaSO4	0	0
Ash	1.25487252	0.020914542	Ash	0.020914542	1.25487252
CaCO3	0	0	C	0.000923506	0.011082076
H2O	0.0462	0.002566667	O2	0.361122071	11.55590626
			Cl2	0	0
Total	200.6955006				200.6955006

Mass Balance Check:

Fuel	13.2
Lime	0
Air	187.4955006
	200.6955006

Alcan Misc. Paste Waste : Steady State # 2

Fuel Feed Rate (kg/hr):	13.5
Moisture % :	0.35
Dry feed rate (kg/hr) :	13.45275
Limestone Feed Rate(kg/hr):	0
% CaCO3 :	95.5
CaCO3 Feed Rate(kg/hr) :	0

Ash Flow (kg/hr) :	
CaO	0
CaSO4	0
C	0.023801278
Ash	1.28339235
Total	1.307193628

Air Rates

1'Rot	1'P(psig)	F(scfm)	F(kg/hr)
15.75	3	27.55428193	60.23484187
2'Rot	2'P(psig)		
30.07	3	28.95934761	63.30637571
P nozzle (psig)			
50		17	37.162729

Rot A	(psig)	F(scfm)	F(kg/hr)
1.5	1	6.265831722	13.69737684
Rot D	(psig)	F(scfm)	F(kg/hr)
140	1	5.989899498	13.09417716

Total Air(scfm) :	85.76936075	
Tot.Air(kgmol/hr):	6.501230949	

Ultimate Analysis (Dry basis)

C	84.25
H	2.48
S	1.34
O	1.34
Cl	0
Ash	9.54
N	1.05
	100

Combustion Eff % :	99.79
Sulphur Capt % :	0
Ca:S ratio :	0
P:S Air Split:	1.961715917

	Dry Flue Gas Analysis: kgmol/hr	mol%/ppm		Wet Flue Gas Analysis: kgmol/hr	mol%/ppm
N2	5.141017231	79.97224261	N2	5.141017231	77.91850727
O2	0.339339733	5.278675061	O2	0.339339733	5.143115508
CO2	0.942511716	14.66145167	CO2	0.942511716	14.28493676
SO2	0.005633339	876.3066489	SO2	0.005633339	853.8025667
Cl2	0	0	Cl2	0	0
H2O			H2O	0.1694391	2.568060201
Tot	6.42850202		Tot	6.59794112	

T base (C) :	819
T top (C) :	819
V base (m/s) :	4.745983797
V top (m/s) :	7.165286081

Assume Ash = SiO2

Combustion Calculations (one hour basis)

	kg In	kgmol In		kgmol Out	kg Out
C	11.33394188	0.944495156	CO2	0.942511716	41.47051552
H	0.3336282	0.3336282	H2O	0.1694391	3.0499038
S	0.18026685	0.005633339	SO2	0.005633339	0.3605337
O	43.86853883	2.741783677	N2	5.141017231	143.9484825
Cl	0	0	CaO	0	0
N	143.9484825	10.28203446	CaSO4	0	0
Ash	1.28339235	0.021389873	Ash	0.021389873	1.28339235
CaCO3	0	0	C	0.00198344	0.023801278
H2O	0.04725	0.002625	O2	0.339339733	10.85887145
			Cl2	0	0
Total	200.9955006				200.9955006

Mass Balance Check:

Fuel	13.5
Lime	0
Air	187.4955006
	200.9955006

Alcan Misc. Paste Waste : Steady State # 3

Fuel Feed Rate (kg/hr):	13.6
Moisture % :	0.35
Dry feed rate (kg/hr) :	13.5524
Limestone Feed Rate(kg/hr):	0
% CaCO3 :	95.5
CaCO3 Feed Rate(kg/hr) :	0

Ash Flow (kg/hr) :	
CaO	0
CaSO4	0
C	0.011417897
Ash	1.29289896
Total	1.304316857

Air Rates

1'Rot	1'P(psig)	F(scfm)	F(kg/hr)
15.77	3	27.58913289	60.31102757
2'Rot	2'P(psig)		
30.07	3	28.95934761	63.30637571
P nozzle (psig)			
50		17	37.162729

Rot A	(psig)	F(scfm)	F(kg/hr)
1.5	1	6.265831722	13.69737684

Rot D	(psig)	F(scfm)	F(kg/hr)
140	1	5.989899498	13.09417716

Total Air(scfm) :	85.80421171	
Tot.Air(kgmol/hr):	6.503872617	

Ultimate Analysis (Dry basis)

C	84.25
H	2.48
S	1.34
O	1.34
Cl	0
Ash	9.54
N	1.05
	100

Combustion Eff % :	99.9
Sulphur Capt % :	0
Ca:S ratio :	0
P:S Air Split:	1.962919361

	Dry Flue Gas Analysis: kgmol/hr	mol%/ppm
N2	5.143141517	79.97912411
O2	0.331248444	5.151124142
CO2	0.950539925	14.78150084
SO2	0.005675068	882.509117
Cl2	0	0
H2O		
Tot	6.430604954	

	Wet Flue Gas Analysis: kgmol/hr	mol%/ppm
N2	5.143141517	77.91105044
O2	0.331248444	5.017928082
CO2	0.950539925	14.39928569
SO2	0.005675068	859.6894889
Cl2	0	0
H2O	0.170694204	2.585766837
Tot	6.601299159	

T base (C) :	870
T top (C) :	870
V base (m/s) :	4.971163774
V top (m/s) :	7.503699686

Assume Ash = SiO2

Combustion Calculations (one hour basis)

	kg In	kgmol In		kgmol Out	kg Out
C	11.417897	0.951491417	CO2	0.950539925	41.82375671
H	0.33609952	0.33609952	H2O	0.170694204	3.07249568
S	0.18160216	0.005675068	SO2	0.005675068	0.36320432
O	43.88762615	2.742976634	N2	5.143141517	144.0079625
Cl	0	0	CaO	0	0
N	144.0079625	10.28628303	CaSO4	0	0
Ash	1.29289896	0.021548316	Ash	0.021548316	1.29289896
CaCO3	0	0	C	0.000951491	0.011417897
H2O	0.0476	0.002644444	O2	0.331248444	10.59995022
			Cl2	0	0
Total	201.1716863				201.1716863

Mass Balance Check:

Fuel	13.6
Lime	0
Air	187.5716863
	201.1716863

Alcan Misc. Paste Waste : Steady State # 4

Fuel Feed Rate (kg/hr):	13.5
Moisture % :	0.35
Dry feed rate (kg/hr) :	13.45275
Limestone Feed Rate(kg/hr):	1.44
% CaCO3 :	98
CaCO3 Feed Rate(kg/hr) :	1.4112

Combustion Eff % :	99.94
Sulphur Capt % :	87
Ca:S ratio :	2.50508621
P:S Air Split:	1.961715917

Ash Flow (kg/hr) :

CaO	0.515815721
CaSO4	0.666536678
C	0.006800365
Ash	1.31219235
Total	2.501345114

Dry Flue Gas Analysis:

	kgmol/hr	mol%/ppm
N2	5.141017231	79.88822867
O2	0.335472488	5.213035009
CO2	0.958040459	14.8873563
SO2	0.000732334	113.8001871
Cl2	0	0
H2O		
Tot	6.435262512	

Wet Flue Gas Analysis:

	kgmol/hr	mol%/ppm
N2	5.141017231	77.83875083
O2	0.335472488	5.079298164
CO2	0.958040459	14.50543136
SO2	0.000732334	110.8807212
Cl2	0	0
H2O	0.1694391	2.565431566
Tot	6.604701612	

Air Rates

1'Rot	1'P(psig)	F(scfm)	F(kg/hr)
15.75	3	27.55428193	60.23484187
2'Rot	2'P(psig)		
30.07	3	28.95934761	63.30637571
P nozzle (psig)			
50		17	37.162729

Rot A	(psig)	F(scfm)	F(kg/hr)
1.5	1	6.265831722	13.69737684
Rot D	(psig)	F(scfm)	F(kg/hr)
140	1	5.989899498	13.09417716

Total Air(scfm) :	85.76936075
Tot.Air(kgmol/hr):	6.501230949

T base (C) :	871
T top (C) :	871
V base (m/s) :	4.97704643
V top (m/s) :	7.514134695

Ultimate Analysis (Dry basis)

C	84.25
H	2.48
S	1.34
O	1.34
Cl	0
Ash	9.54
N	1.05
	100

Assume Ash = SiO2

Combustion Calculations (one hour basis)

	kg In	kgmol In		kgmol Out	kg Out
C	11.33394188	0.944495156	CO2	0.958040459	42.1537802
H	0.3336282	0.3336282	H2O	0.1694391	3.0499038
S	0.18026685	0.005633339	SO2	0.000732334	0.046869381
O	43.86853883	2.741783677	N2	5.141017231	143.9484825
Cl	0	0	CaO	0.009210995	0.515815721
N	143.9484825	10.28203446	CaSO4	0.004901005	0.666536678
Ash	1.31219235	0.021869873	Ash	0.021869873	1.31219235
CaCO3	1.4112	0.014112	C	0.000566697	0.006800365
H2O	0.04725	0.002625	O2	0.335472488	10.73511961
			Cl2	0	0
Total	202.4355006				202.4355006

Mass Balance Check:

Fuel	13.5
Lime	1.44
Air	187.4955006
	202.4355006

Appendix E Sample Calculations for Correction of Flue Gas and Baghouse Emissions and Emission Graphs for the Incineration of Stud Blast Fines, Pitch Cones and Miscellaneous Paste Wastes at Different Operating Conditions

Sample Calculations for Correction of Flue Gas and Baghouse Emissions to 11 % O_2, 20 ^{o}C, 760 mmHg, dry basis

Sample Calculations

Operating Condition: Pitch Cones: Steady State 1, (See Tables, 7.6 to 7.9)

(1) Correction of flue gas emissions

All the gas emissions are on a volume basis, e.g. % by volume or ppm by volume.

Raw flue gas emissions:
6.1 % O_2
14.6 % CO_2
0.0010 % CH_4
137 ppm CO
150 ppm NO_x
149 ppm SO_2
75 ppm N_2O

Molecular weights of CH_4 = 16.04 kg/kgmole
CO = 28.01 kg/kgmole
NO_x = 64.06 kg/kgmole
N_2O = 44.01 kg/kgmole

Assumption: The gas analyzers measure the emissions at 20 ^oC and 1 atm.

T = 20 ^oC = 293.15 K
P = 1 atm
R = 0.08206 m^3atm/kgmoleK

General Form of Correction Expression:

$$\frac{x_i * (1cm^3/m^3)}{(10E6cm^3/m^3)} \left(\frac{21\%O2 - 11\%O2}{21\%O2 - y\%O2}\right) \frac{MW_i P * 10E6(mg/kg)}{RT}$$

where

x_i = concentration of species *i* in flue gas (ppm, cm^3/m^3)
y = concentration of oxygen in flue gas or in baghouse (%)
MW_i = molecular weight of species *i* in flue gas
P = operating pressure of gas analyzers (atm)
R = universal gas constant (m^3atm/kgmoleK)
T = operating temperature of gas analyzers (K)

(i) Corrected CH_4 emission (mg/m^3)

$$1\,ppm = \frac{1cm^3}{m^3}\left(\frac{m^3}{10E6cm^3}\right)*100\,\%$$

$$= 0.0001\ \%\ \text{by volume}$$

Therefore, 0.0010 % CH_4 = 10 ppm

$$CH_4 = \frac{10}{10E6}\left(\frac{21-11}{21-6.1}\right)\frac{16.04(1)*10E6(mg/kg)}{(0.08206*293.15)}$$

$$= 4\ mg/m^3$$

(ii) Corrected CO emission (mg/m^3)

$$CO = \frac{137}{10E6}\left(\frac{21-11}{21-6.1}\right)\frac{28.01(1)*10E6(mg/kg)}{(0.08206*293.15)}$$

$$= 107\ mg/m^3$$

(iii) Corrected NO_x emission (mg/m^3)

$$NO_x = \frac{150}{10E6}\left(\frac{21-11}{21-6.1}\right)\frac{46.01(1)*10E6(mg/kg)}{(0.08206*293.15)}$$

$$= 193\ mg/m^3$$

(iv) Corrected SO_2 emission (mg/m^3)

$$SO_2 = \frac{149}{10E6}\left(\frac{21-11}{21-6.1}\right)\frac{64.04(1)*10E6(mg/kg)}{(0.08206*293.15)}$$

$$= 266\ mg/m^3$$

(v) Corrected N_2O emission (mg/m^3)

$$N_2O = \frac{75}{10E6}\left(\frac{21-11}{21-6.1}\right)\frac{44.01(1)*10E6(mg/kg)}{(0.08206*293.15)}$$

$$= 92\ mg/m^3$$

(vi) Corrected CO_2 emission (%), at 11 % O_2

$$CO_2 = 14.6\left(\frac{21-11}{21-6.1}\right)$$

$$= 9.8\ \%$$

(2) Correction of baghouse emissions

Raw baghouse emissions:
15.2 % O_2
7 % CO_2
0 % CH_4
47 ppm CO
60 ppm NO_x
75 ppm SO_2
28 ppm N_2O

(i) Corrected CH_4 emission (mg/m^3)

$$CH_4 = 0\ mg/m^3$$

(ii) Corrected CO emission (mg/m^3)

$$CO = \frac{47}{10E6}\left(\frac{21-11}{21-15.2}\right)\frac{28.01(1)*10E6(mg/kg)}{(0.08206*293.15)}$$

$$= 94\ mg/m^3$$

(iii) Corrected NO_x emission (mg/m^3)

$$NO_x = \frac{60}{10E6}\left(\frac{21-11}{21-15.2}\right)\frac{46.01(1)*10E6(mg/kg)}{(0.08206*293.15)}$$

$$= 198\ mg/m^3$$

(iv) Corrected SO_2 emission (mg/m^3)

$$SO_2 = \frac{75}{10E6}\left(\frac{21-11}{21-15.2}\right)\frac{64.04(1)*10E6(mg/kg)}{(0.08206*293.15)}$$

$$= 344\ mg/m^3$$

(v) Corrected N_2O emission (mg/m^3)

$$N_2O = \frac{28}{10E6}\left(\frac{21-11}{21-15.2}\right)\frac{44.01(1)*10E6(mg/kg)}{(0.08206*293.15)}$$

$$= 88\ mg/m^3$$

(vi) Corrected CO_2 emission (%), at 11 % O_2

$$CO_2 = 7\left(\frac{21-11}{21-15.2}\right)$$

$$= 12.1\ \%$$

Emission Plots for Stud Blast Fines

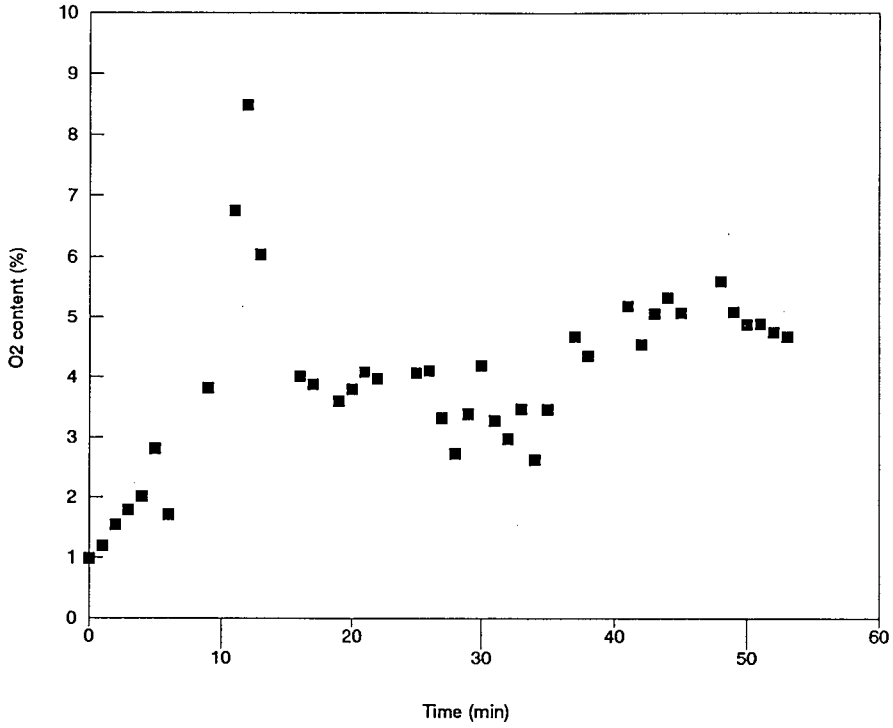

Figure E1 Flue Gas O2 Content for Stud Blast Fines

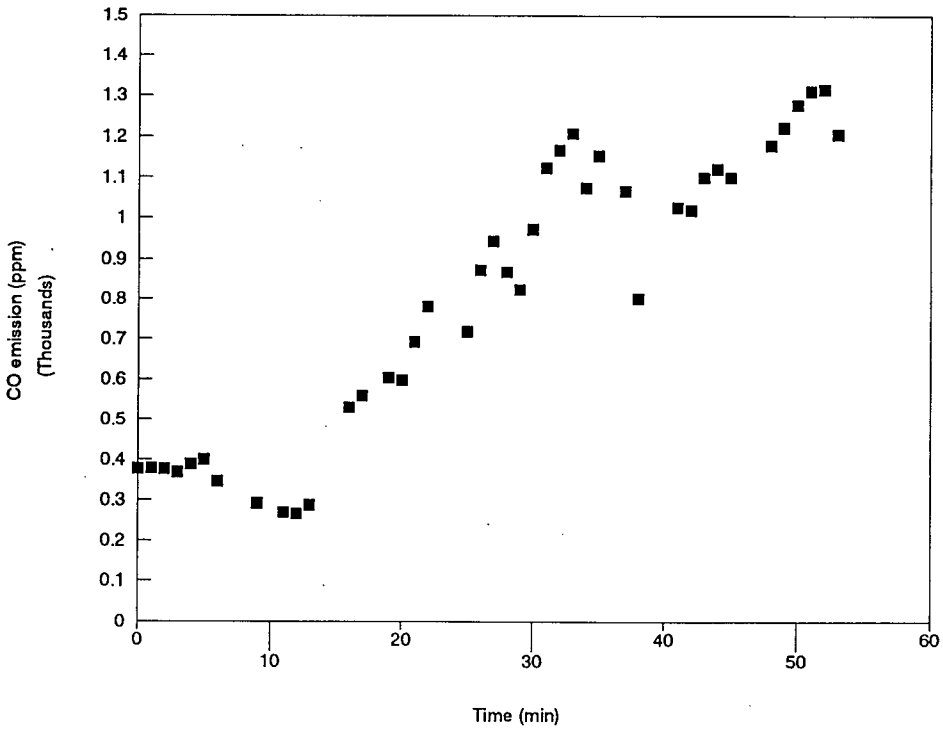

Figure E2 Flue Gas CO Emission for Stud Blast Fines

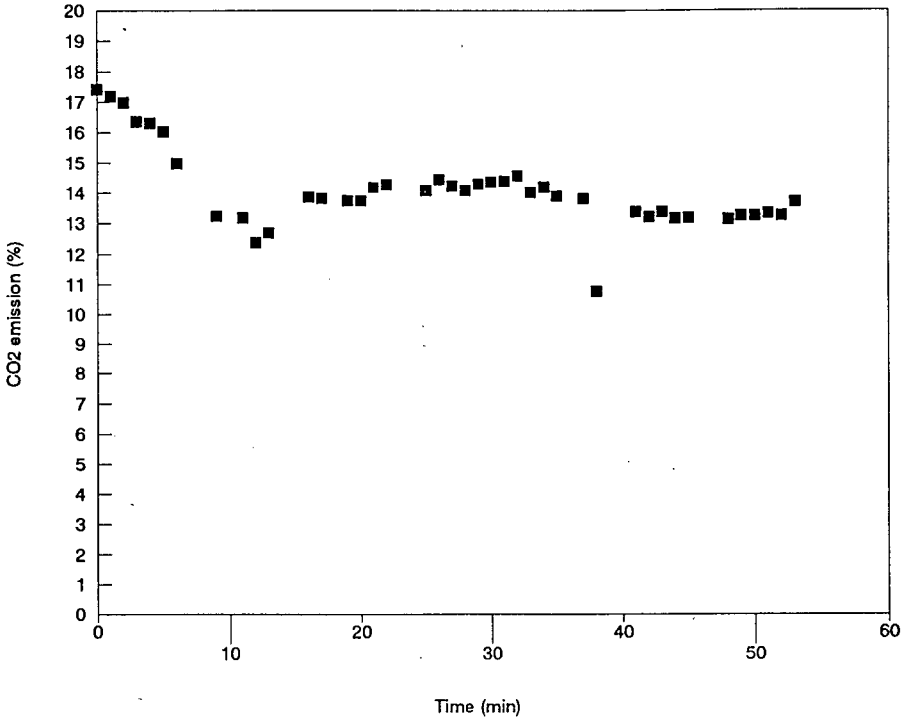

Figure E3 Flue Gas CO2 Emission for Stud Blast Fines

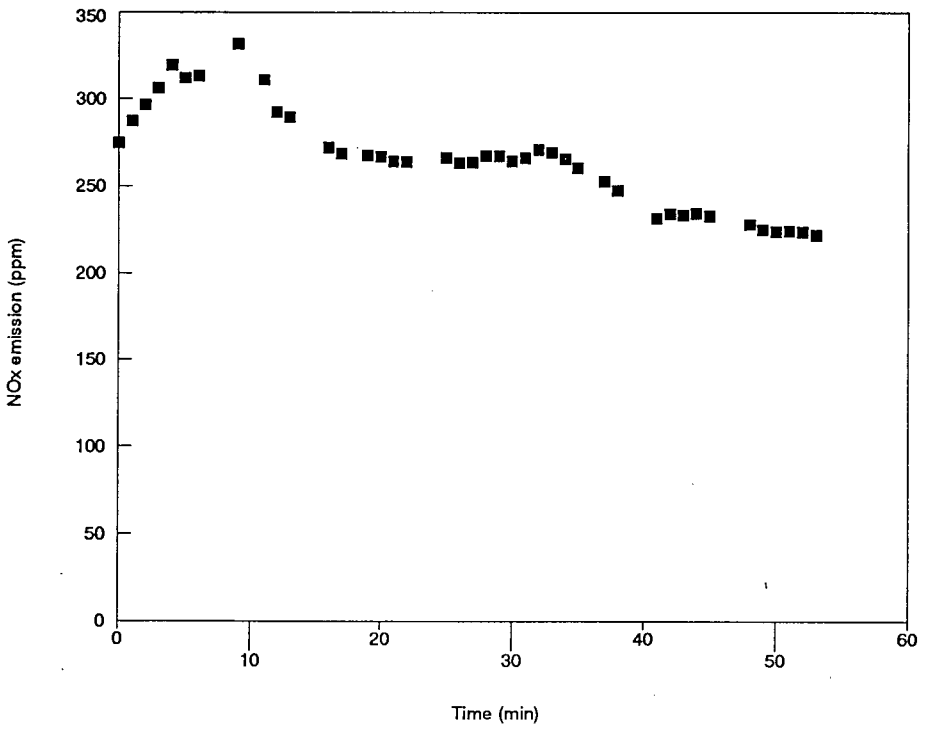

Figure E4 Flue Gas NOx Emission for Stud Blast Fines

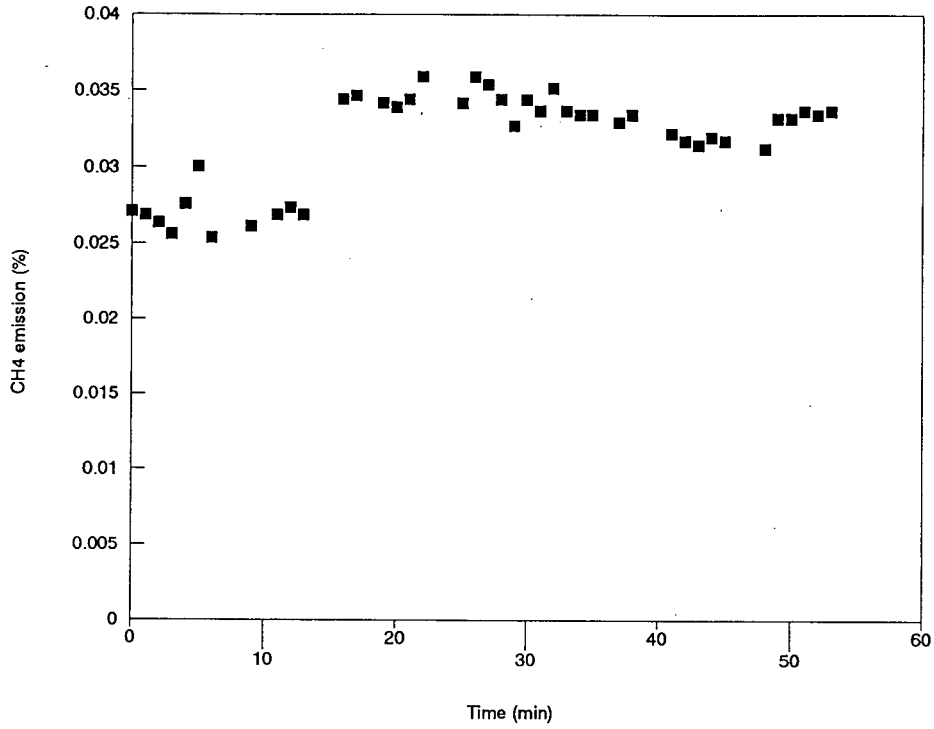

Figure E5 Flue Gas CH4 Emission for Stud Blast Fines

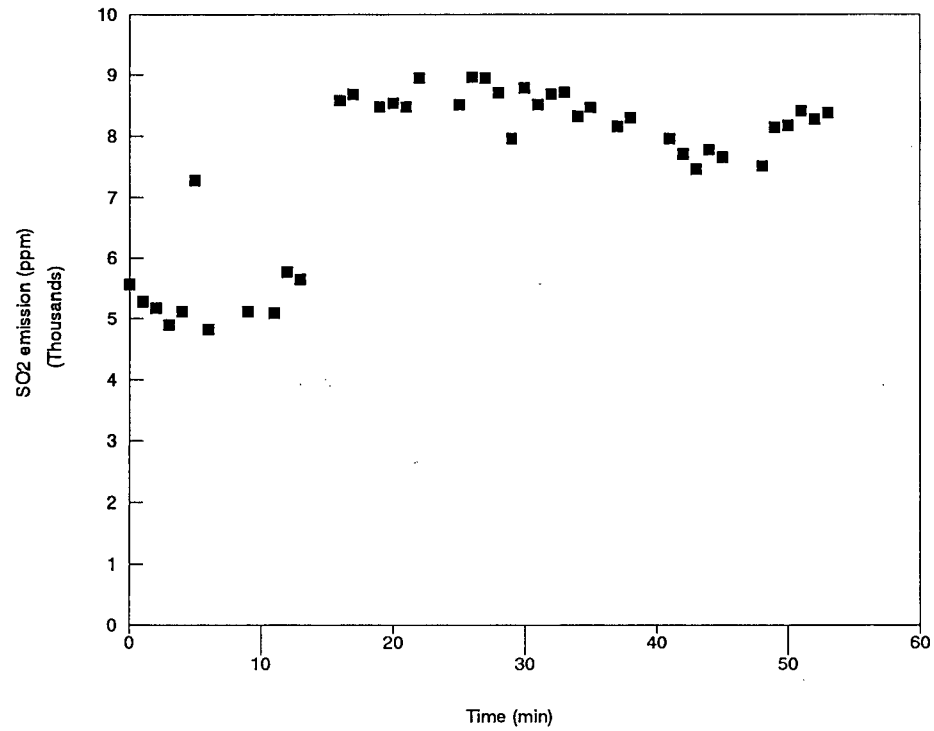

Figure E6 Flue Gas SO2 Emission for Stud Blast Fines

Emission Plots for Pitch Cones: Steady State 1

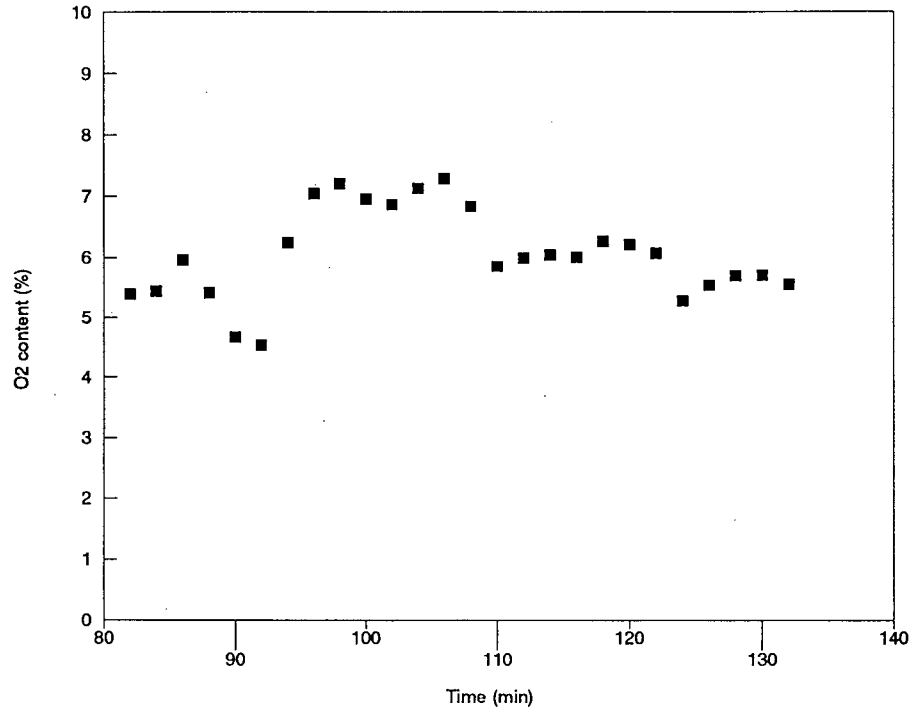

Figure E7 Flue Gas O2 Content for Pitch Cones : Steady State 1

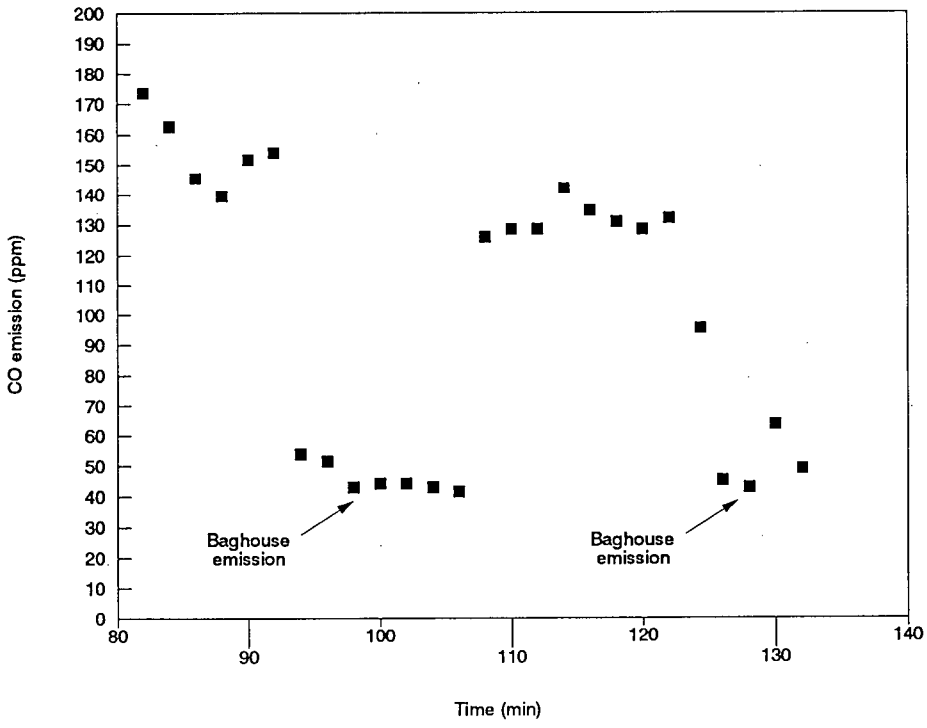

Figure E8 Flue Gas CO Emission for Pitch Cones : Steady State 1

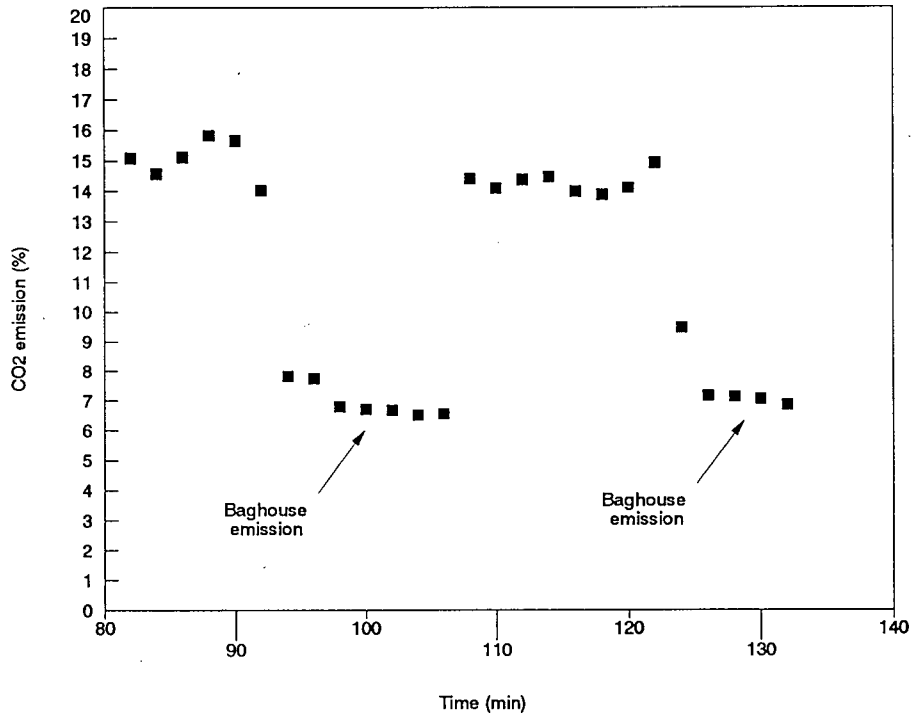

Figure E9 Flue Gas CO2 Emission for Pitch Cones : Steady State 1

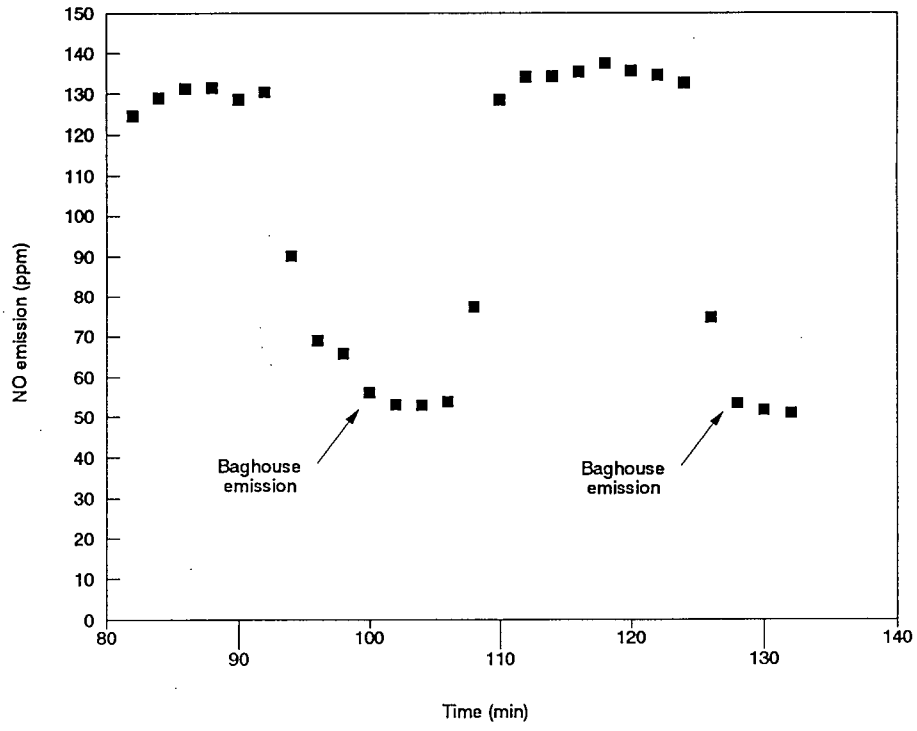

Figure E10 Flue Gas NO Emission for Pitch Cones : Steady State 1

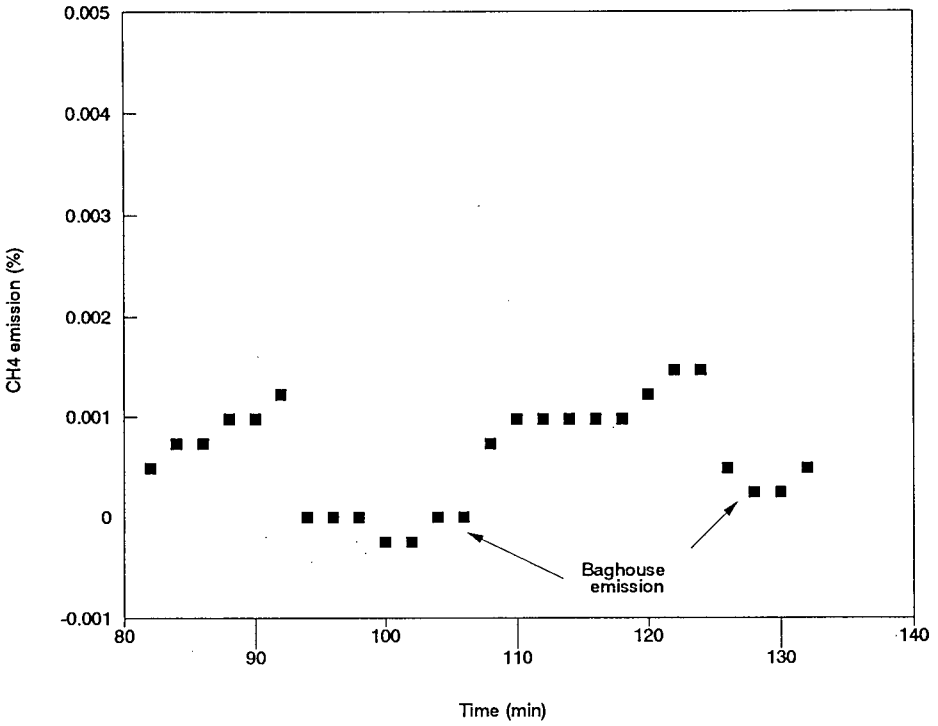

Figure E11 Flue Gas CH4 Emission for Pitch Cones : Steady State 1

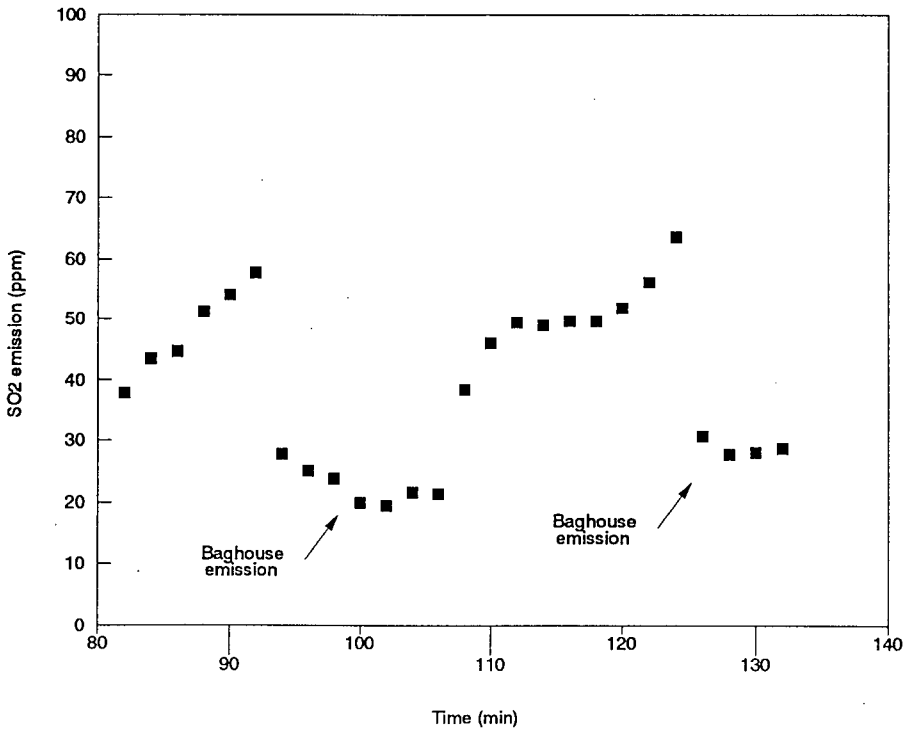

Figure E12 Flue Gas SO2 Emission for Pitch Cones : Steady State 1

Emission Plots for Pitch Cones: Steady State 2

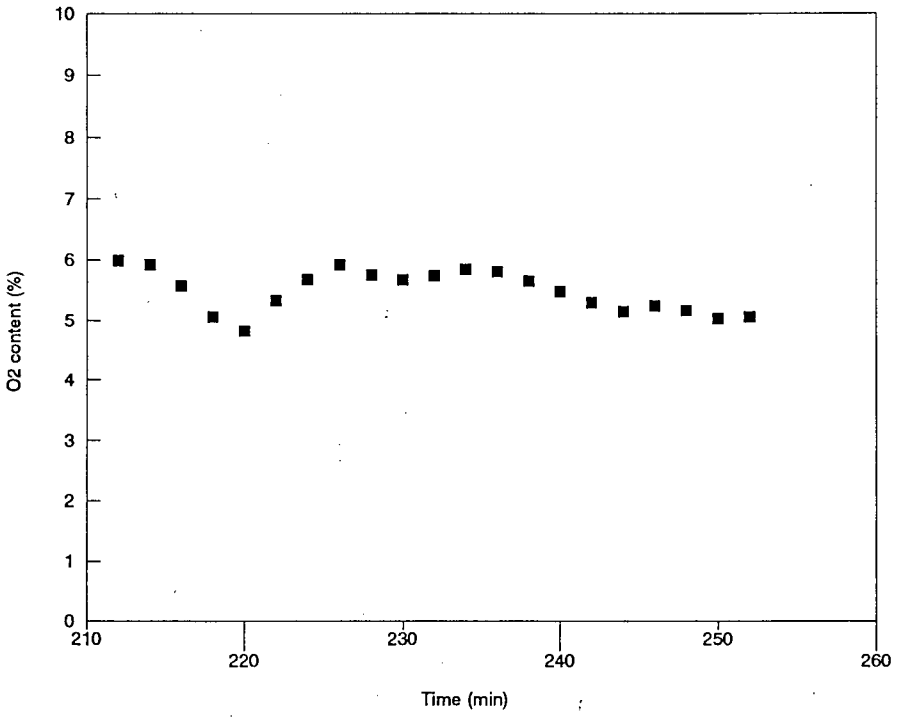

Figure E13 Flue Gas O2 Content for Pitch Cones : Steady State 2

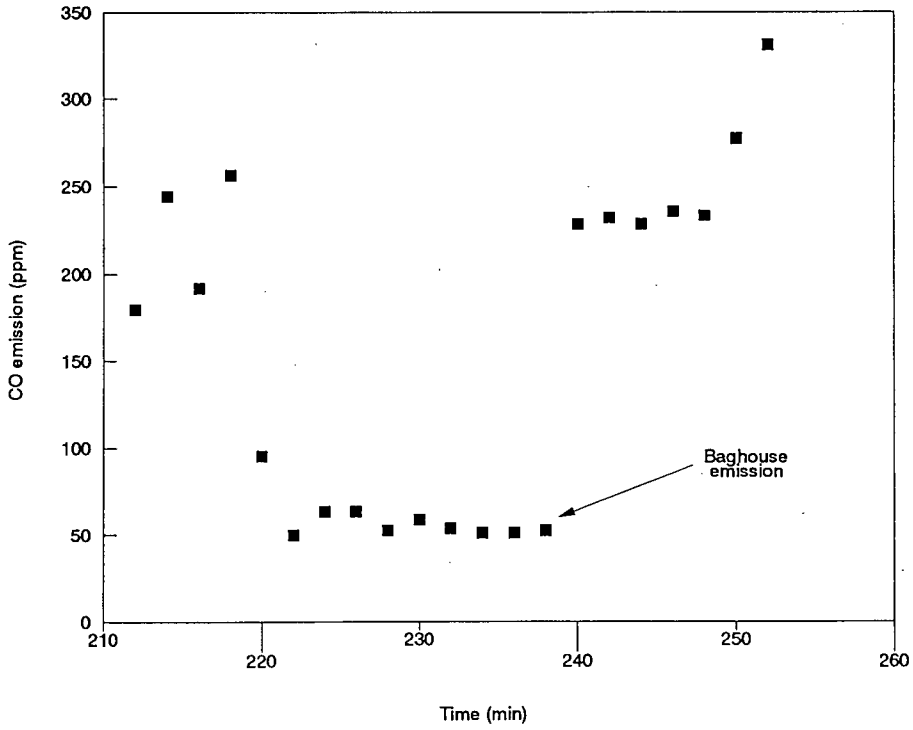

Figure E14 Flue Gas CO Emission for Pitch Cones : Steady State 2

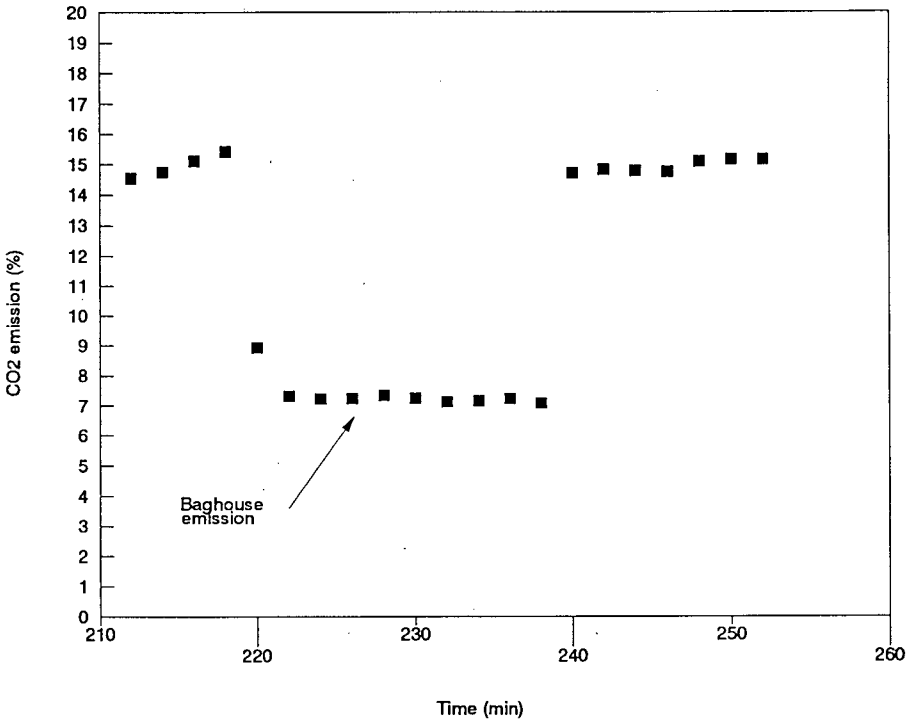

Figure E15 Flue Gas CO2 Emission for Pitch Cones : Steady State 2

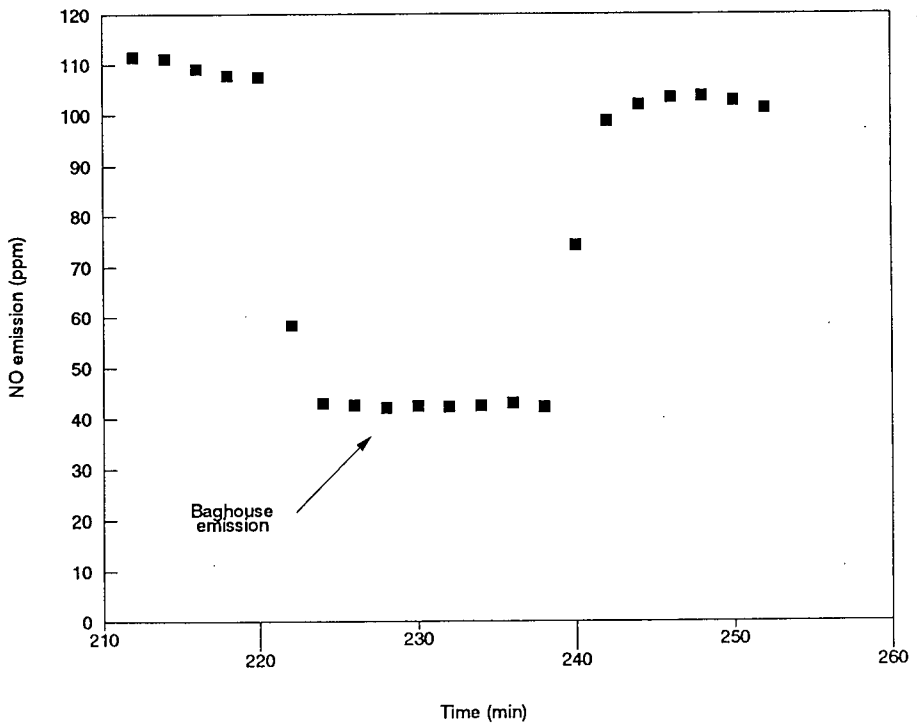

Figure E16 Flue Gas NO Emission for Pitch Cones : Steady State 2

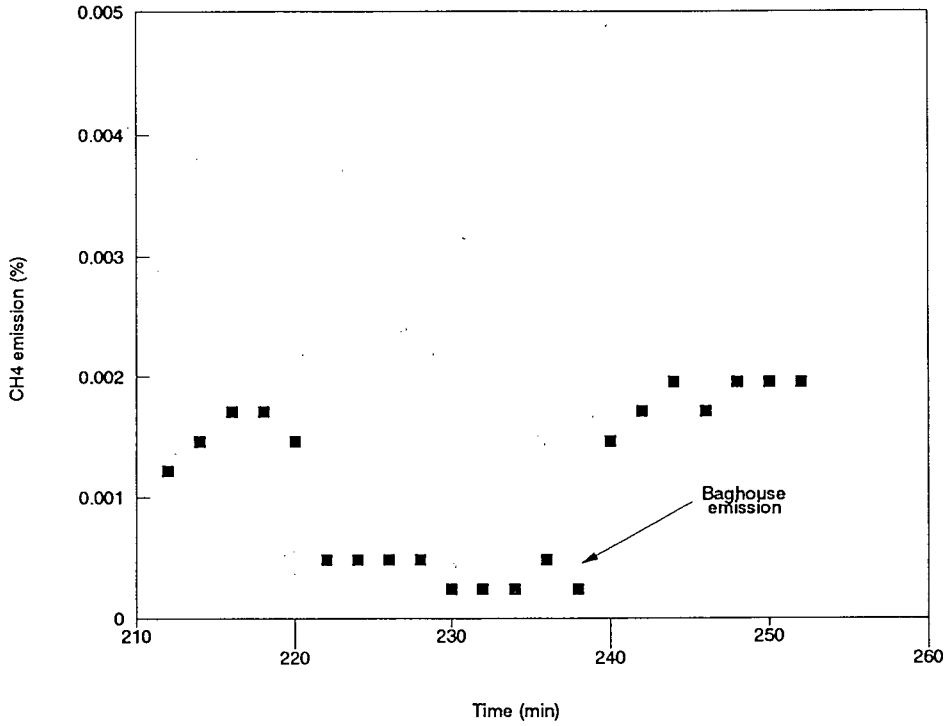

Figure E17 Flue Gas CH4 Emission for Pitch Cones : Steady State 2

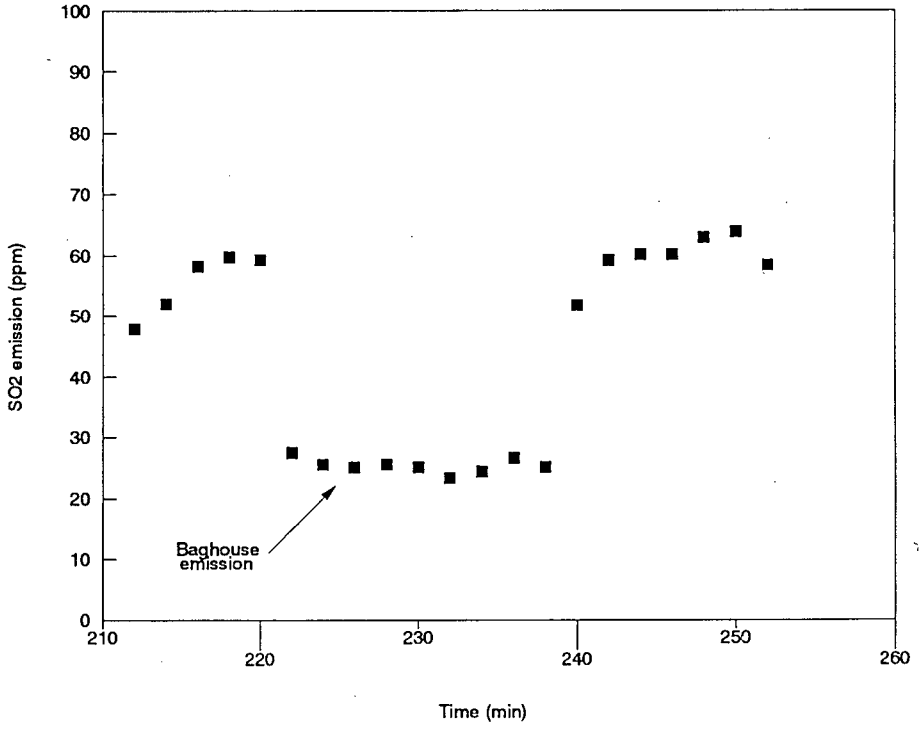

Figure E18 Flue Gas SO2 Emission for Pitch Cones : Steady State 2

Emission Plots for Pitch Cones: Steady State 3

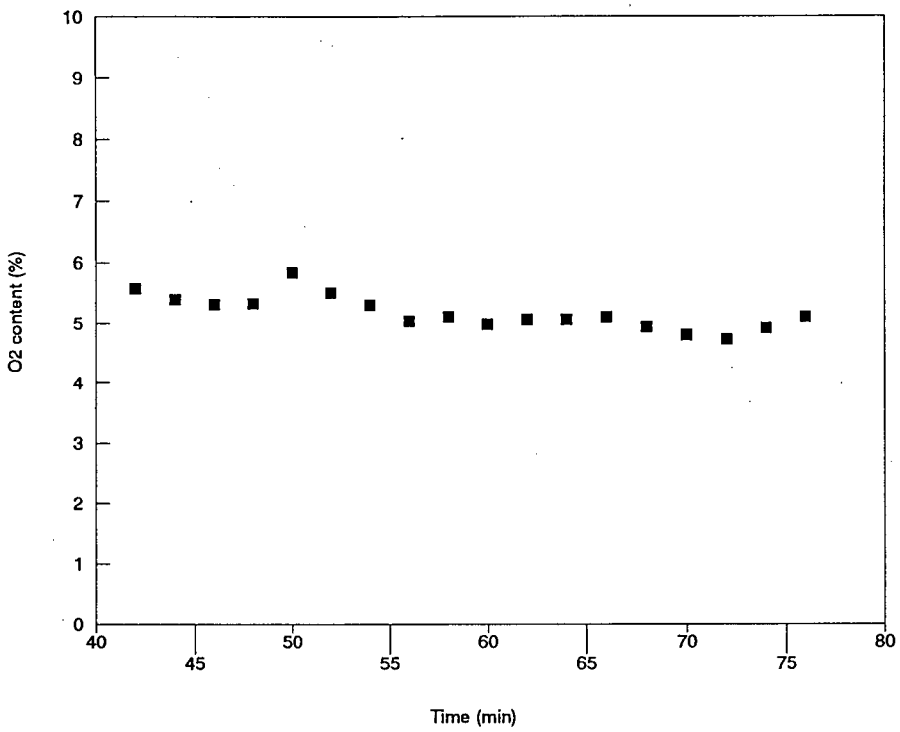

Figure E19 Flue Gas O2 Content for Pitch Cones : Steady State 3

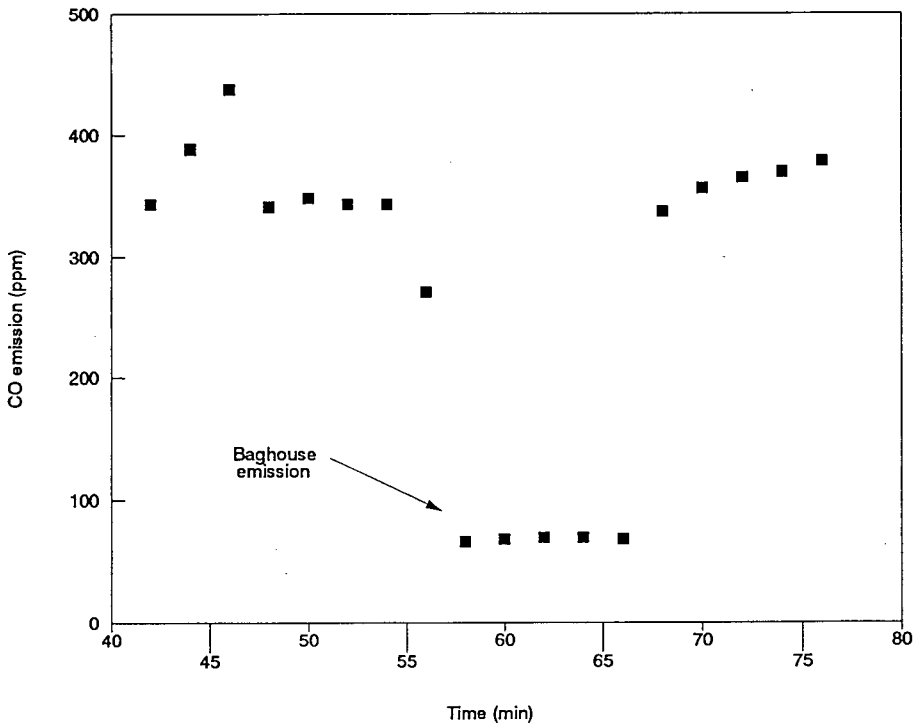

Figure E20 Flue Gas CO Emission for Pitch Cones : Steady State 3

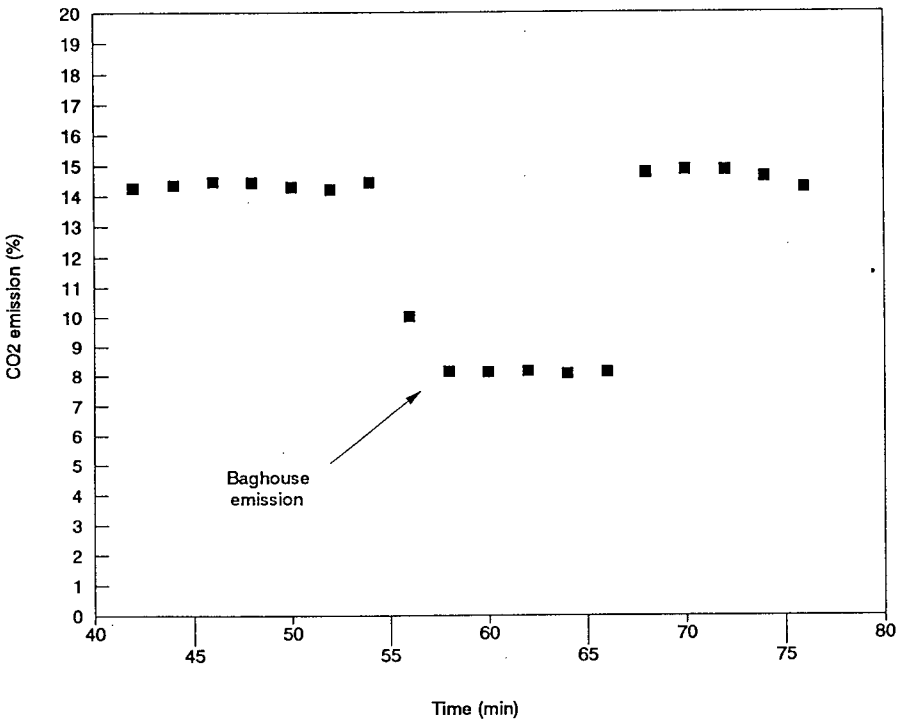

Figure E21 Flue Gas CO2 Emission for Pitch Cones : Steady State 3

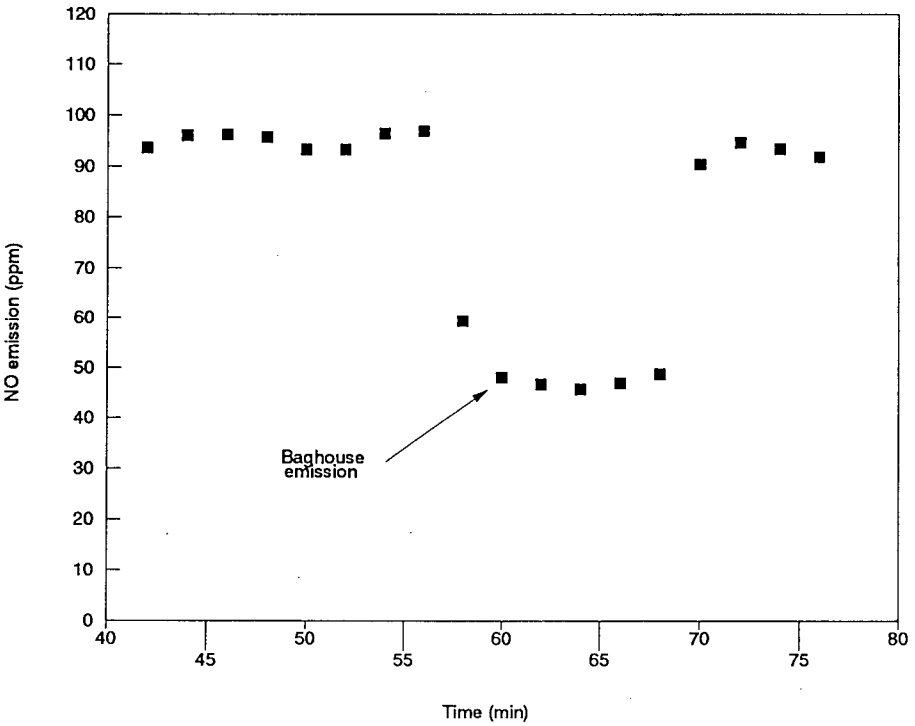

Figure E22 Flue Gas NO Emission for Pitch Cones : Steady State 3

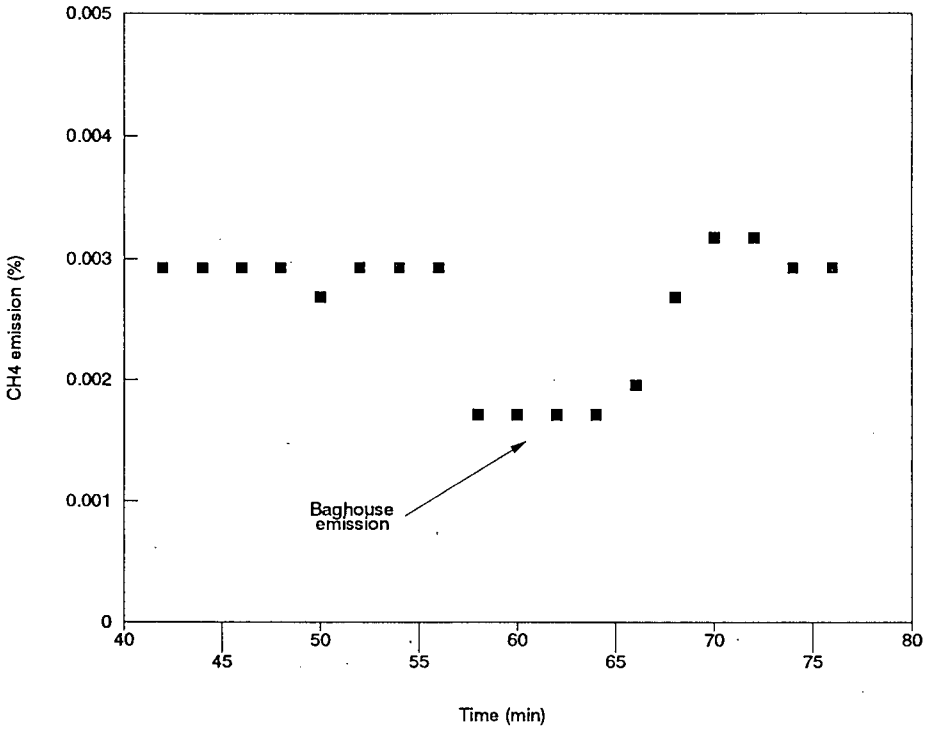

Figure E23 Flue Gas CH4 Emission for Pitch Cones : Steady State 3

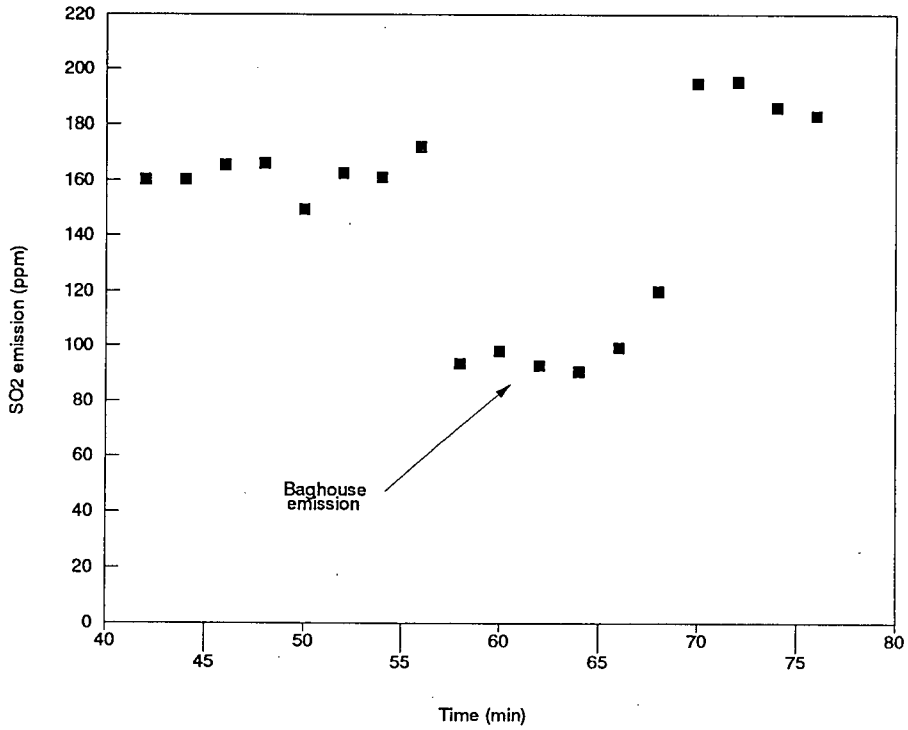

Figure E24 Flue Gas SO2 Emission for Pitch Cones : Steady State 3

Emission Plots for Pitch Cones: Steady State 4

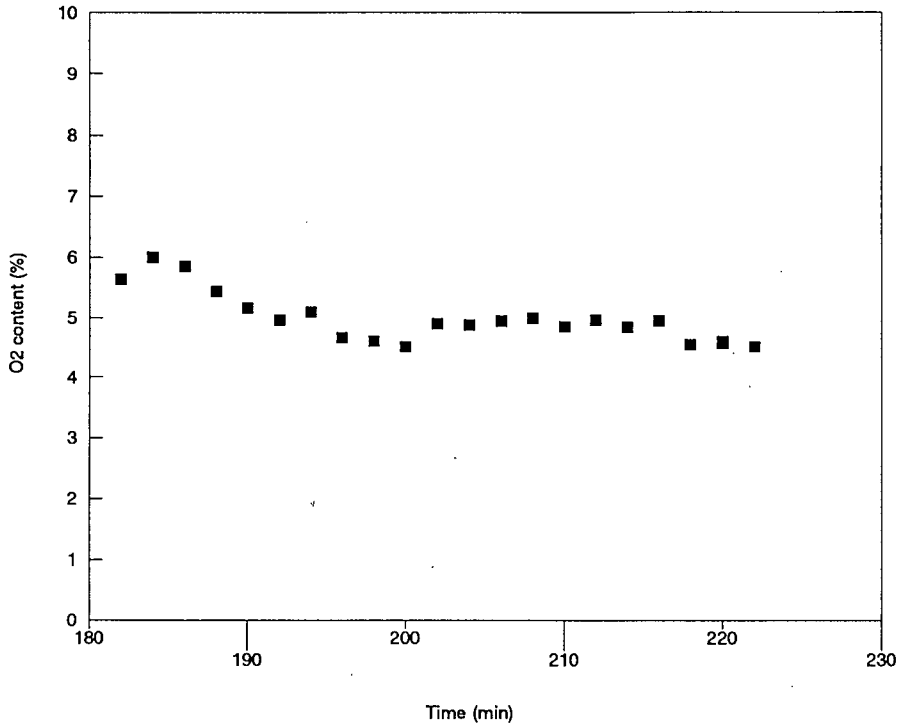

Figure E25 Flue Gas O2 Content for Pitch Cones : Steady State 4

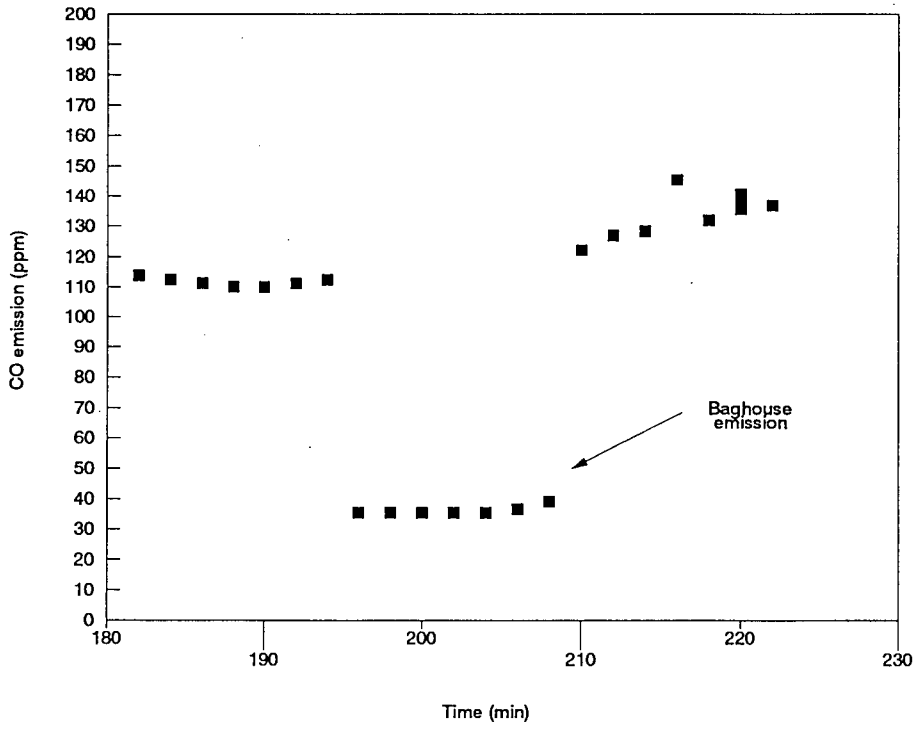

Figure E26 Flue Gas CO Emission for Pitch Cones : Steady State 4

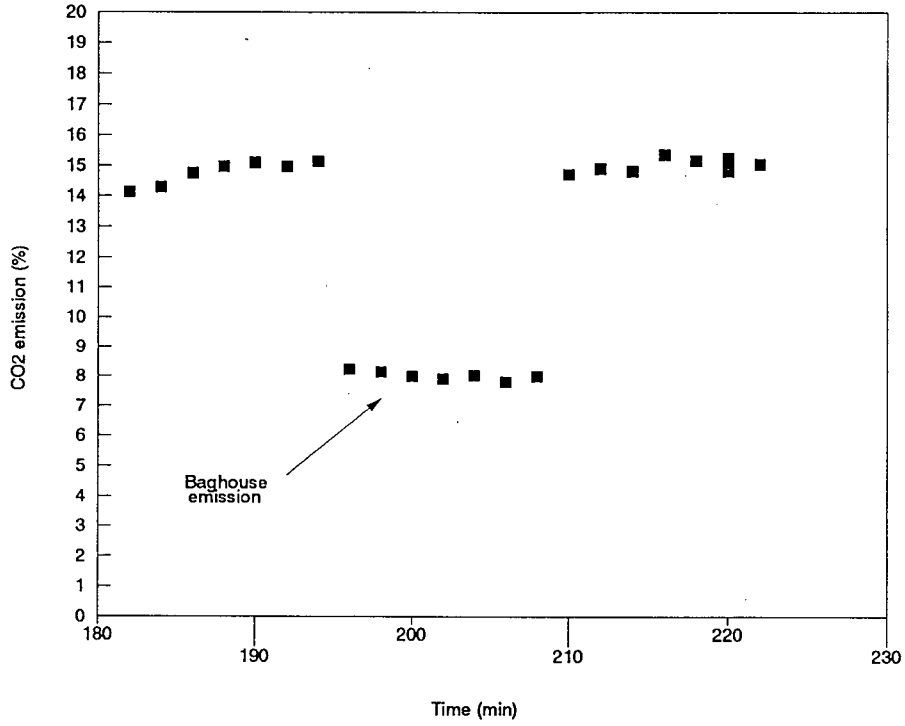

Figure E27 Flue Gas CO2 Emission for Pitch Cones : Steady State 4

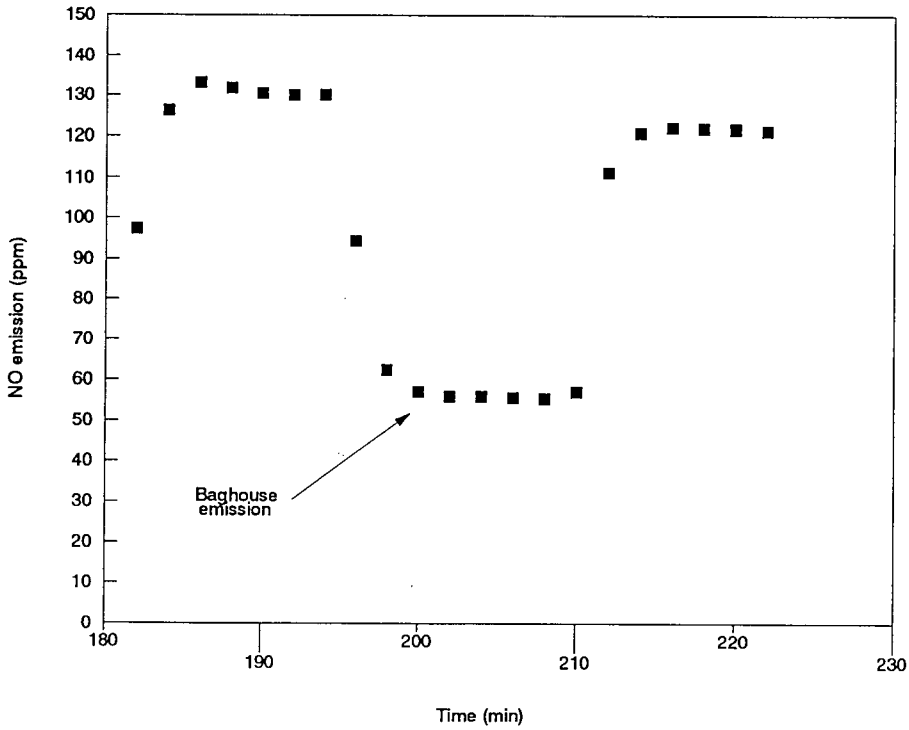

Figure E28 Flue Gas NO Emission for Pitch Cones : Steady State 4

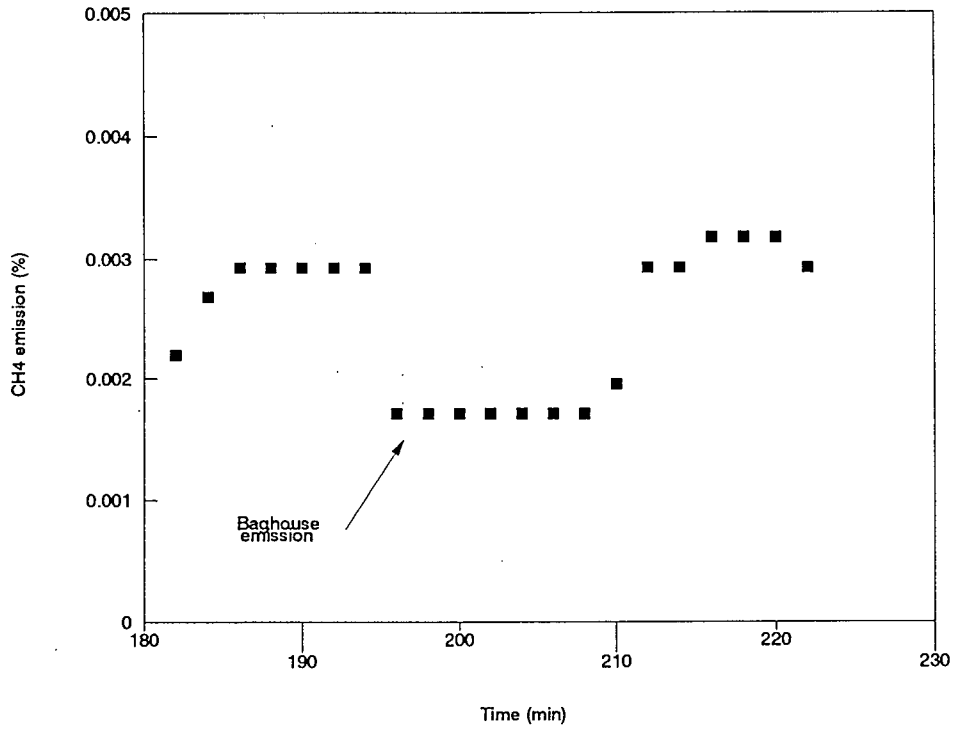

Figure E29 Flue Gas CH4 Emission for Pitch Cones : Steady State 4

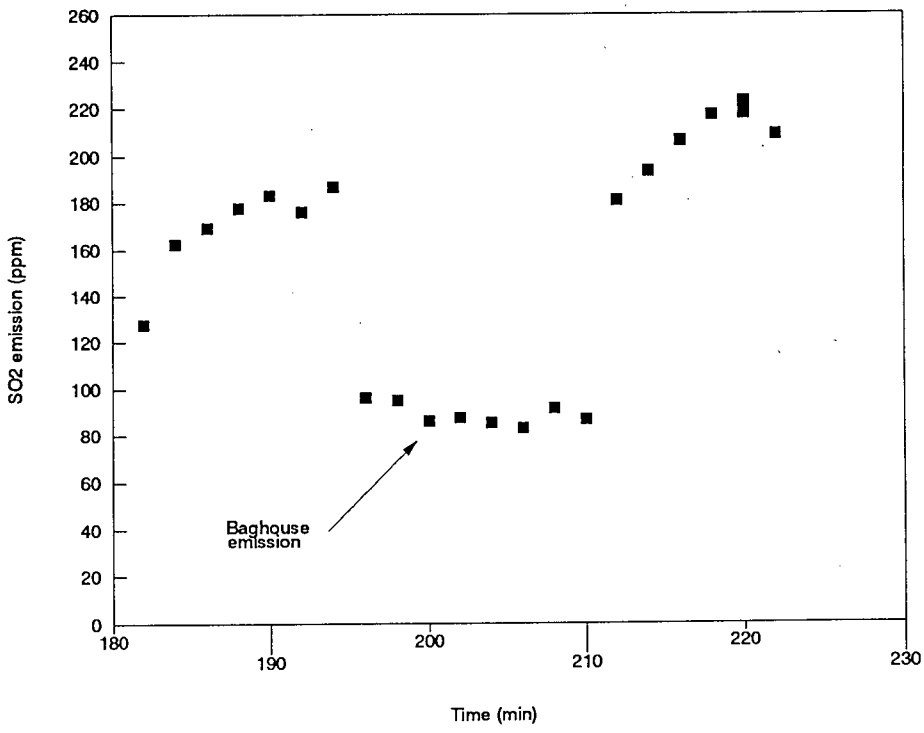

Figure E30 Flue Gas SO2 Emission for Pitch Cones : Steady State 4

Emission Plots for Pitch Cones: Steady State 5

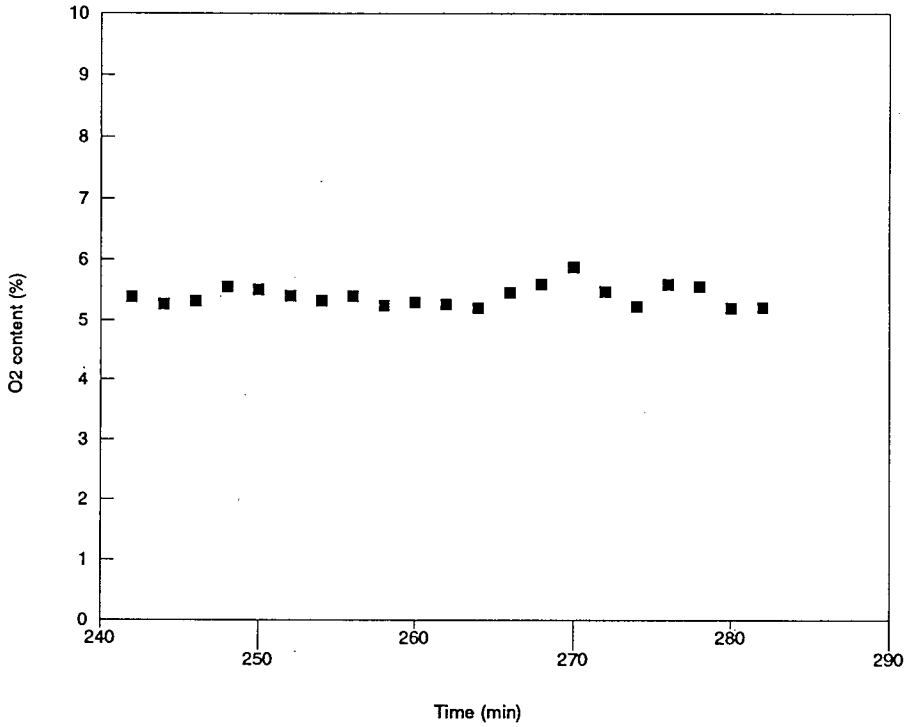

Figure E31 Flue Gas O2 Content for Pitch Cones : Steady State 5

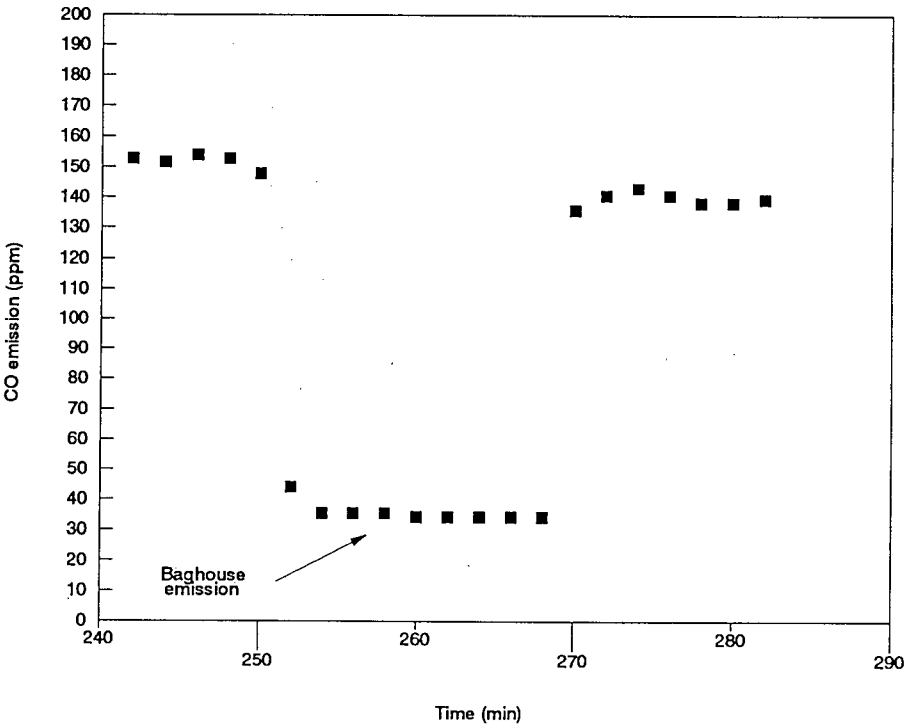

Figure E32 Flue Gas CO Emission for Pitch Cones : Steady State 5

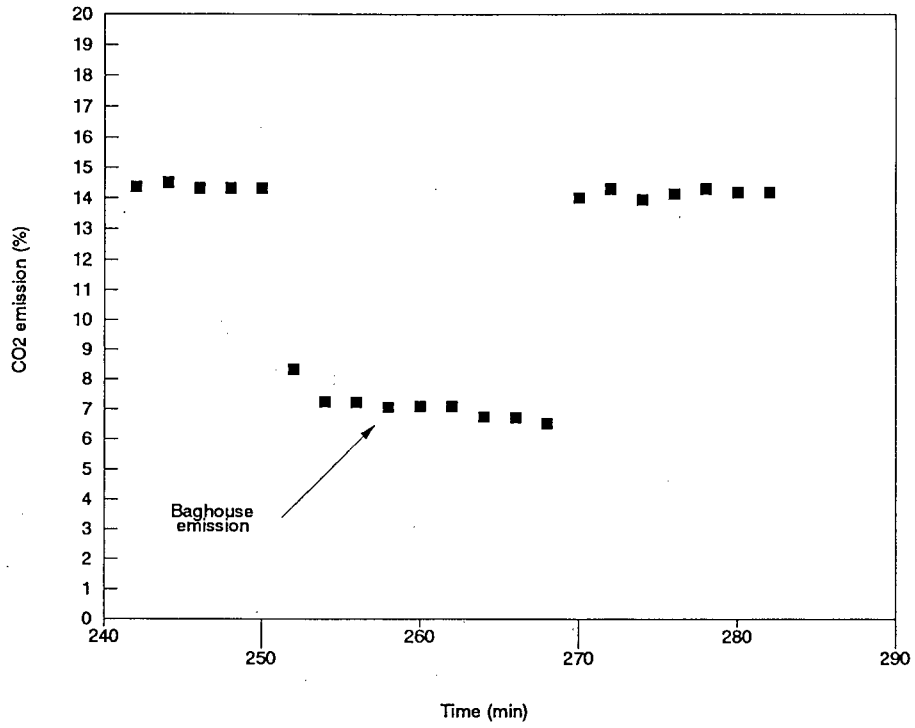

Figure E33 Flue Gas CO2 Emission for Pitch Cones : Steady State 5

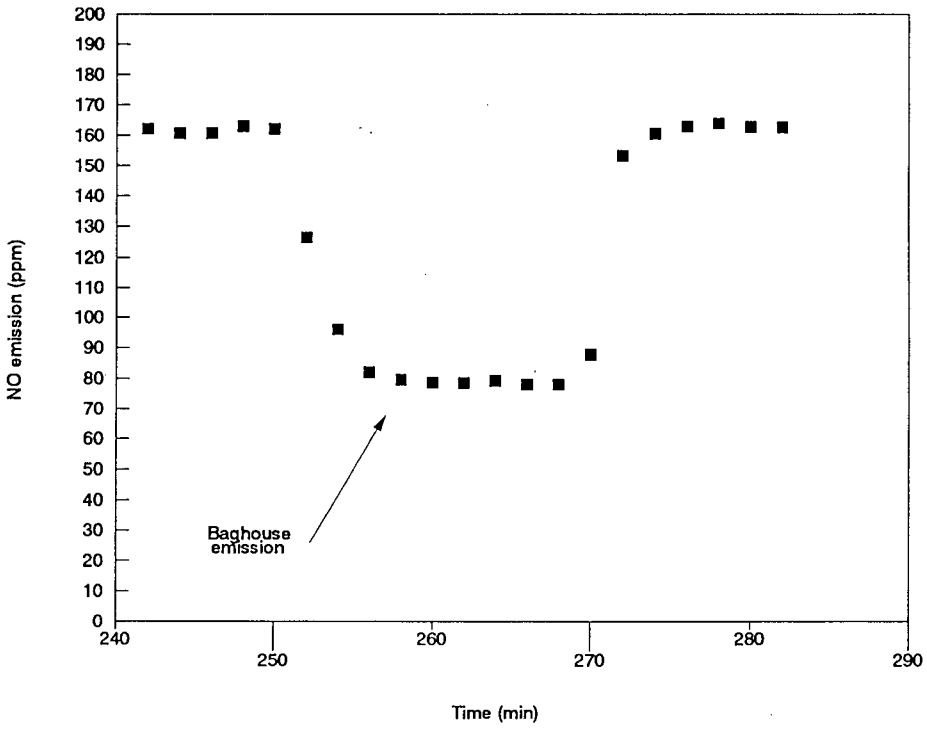

Figure E34 Flue Gas NO Emission for Pitch Cones : Steady State 5

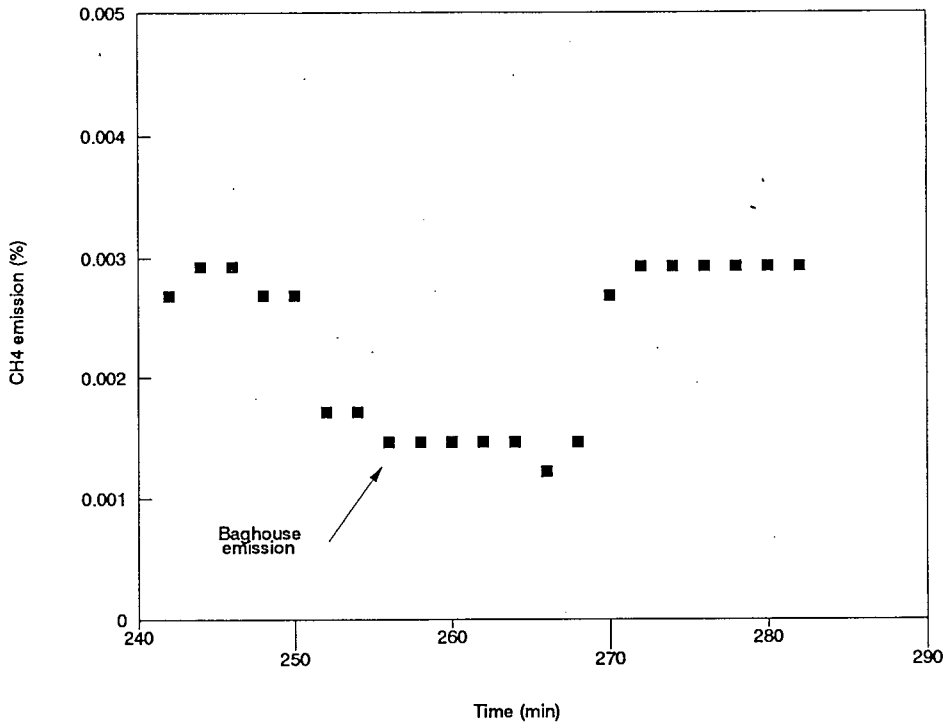

Figure E35 Flue Gas CH4 Emission for Pitch Cones : Steady State 5

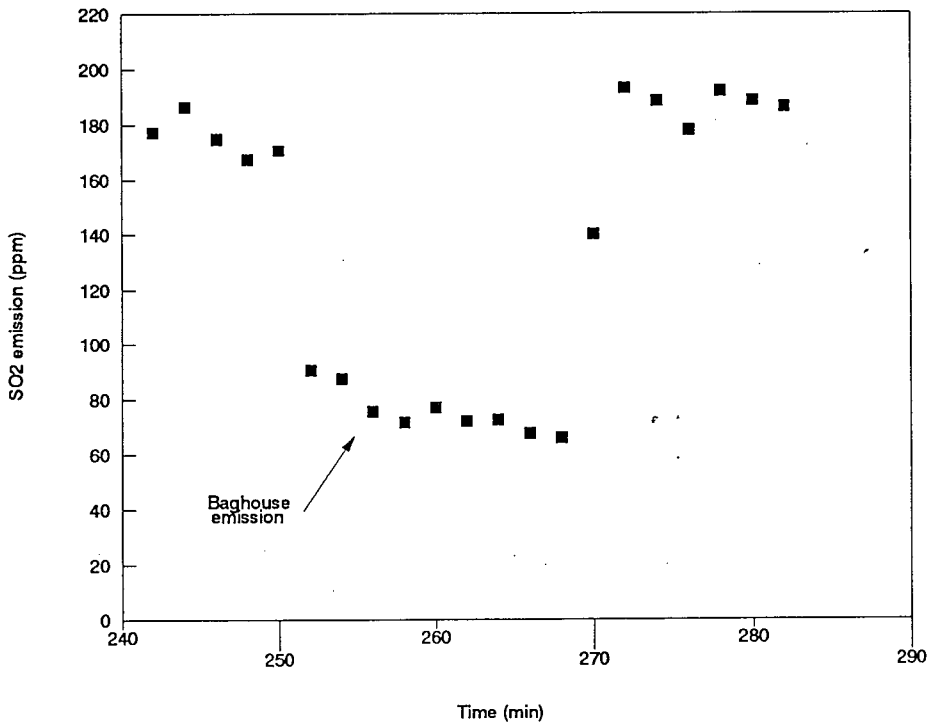

Figure E36 Flue Gas SO2 Emission for Pitch Cones : Steady State 5

Emission Plots for Pitch Cones: Steady State 6

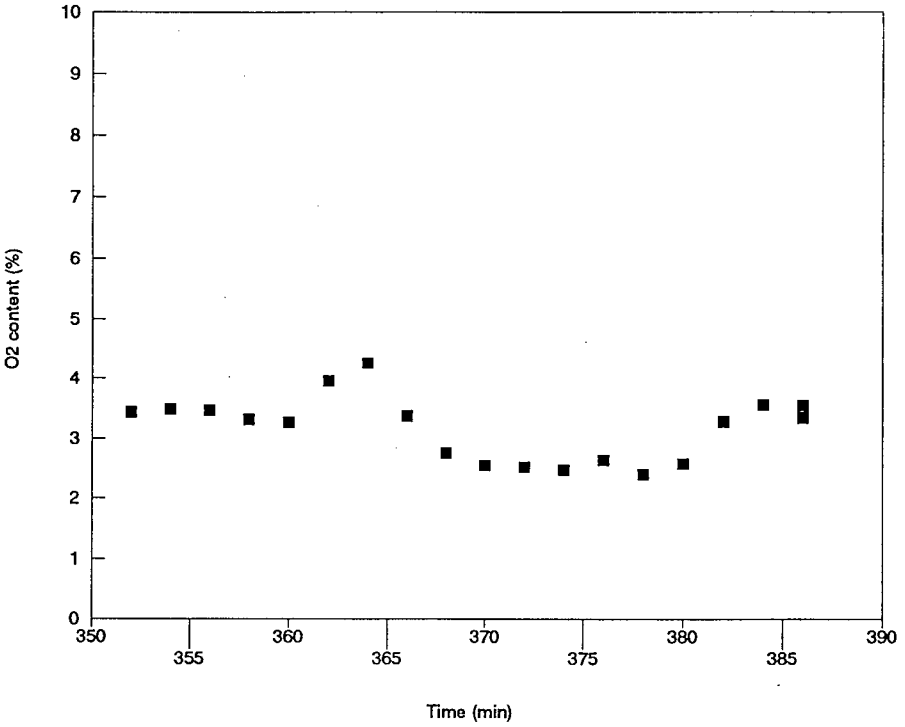

Figure E37 Flue Gas O2 Content for Pitch Cones : Steady State 6

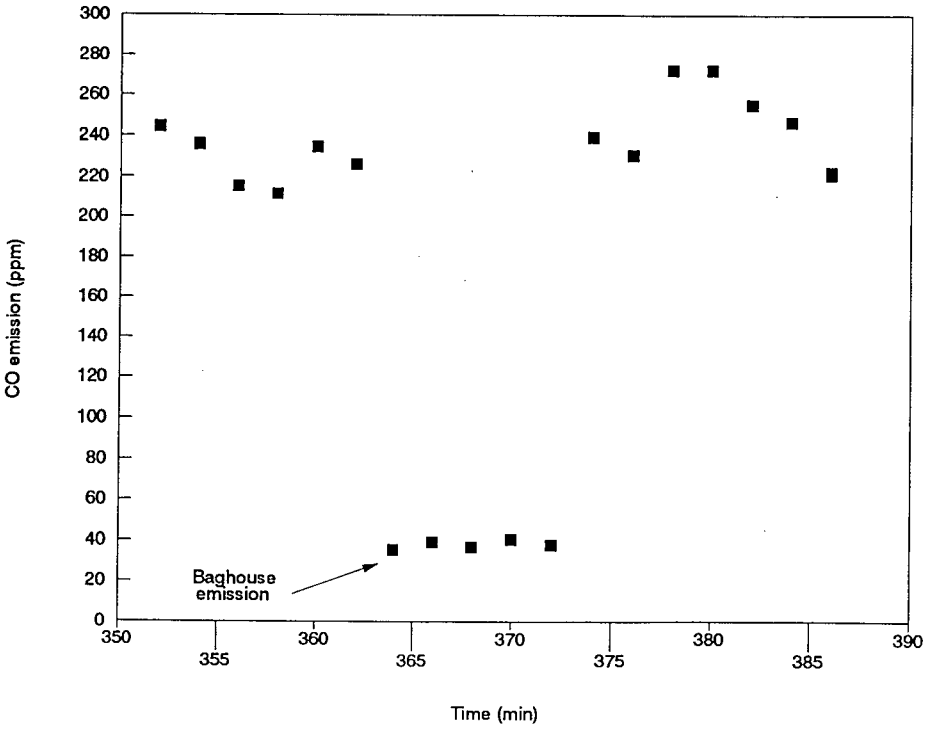

Figure E38 Flue Gas CO Emission for Pitch Cones : Steady State 6

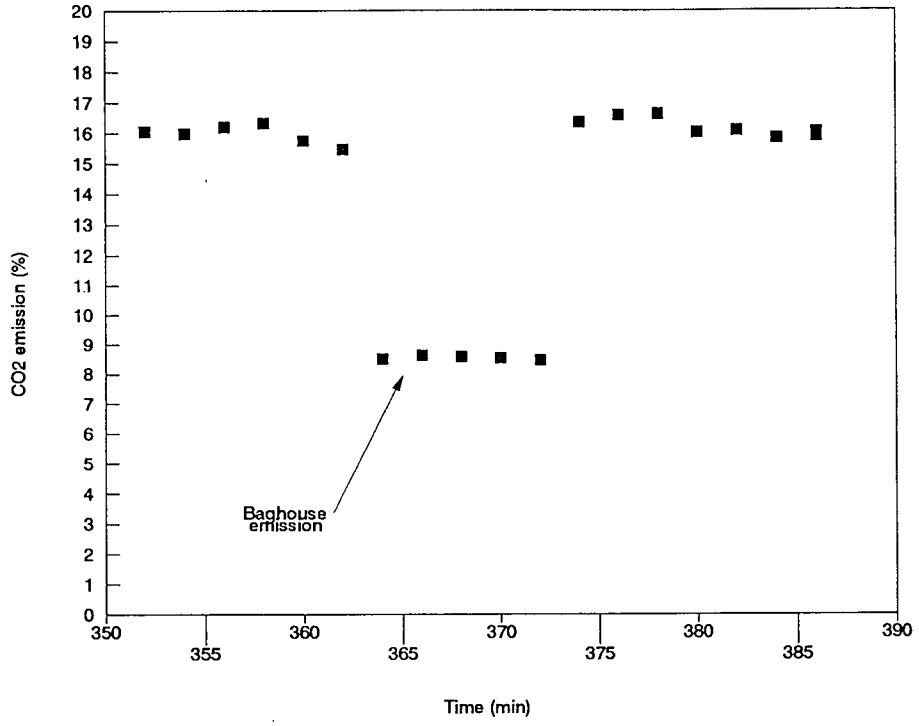

Figure E39 Flue Gas CO2 Emission for Pitch Cones : Steady State 6

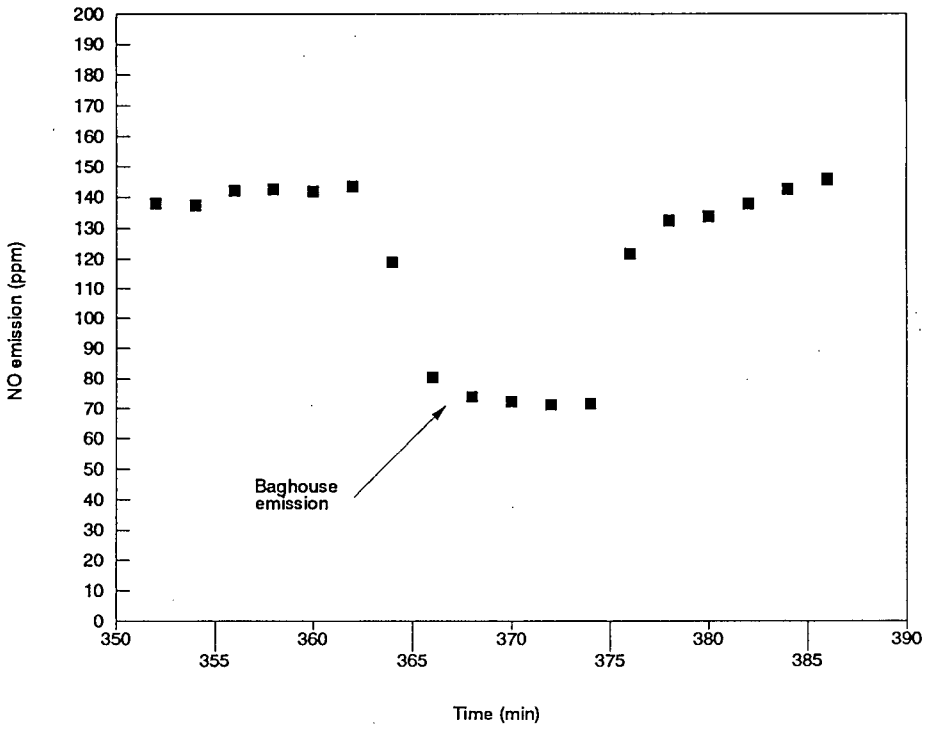

Figure E40 Flue Gas NO Emission for Pitch Cones : Steady State 6

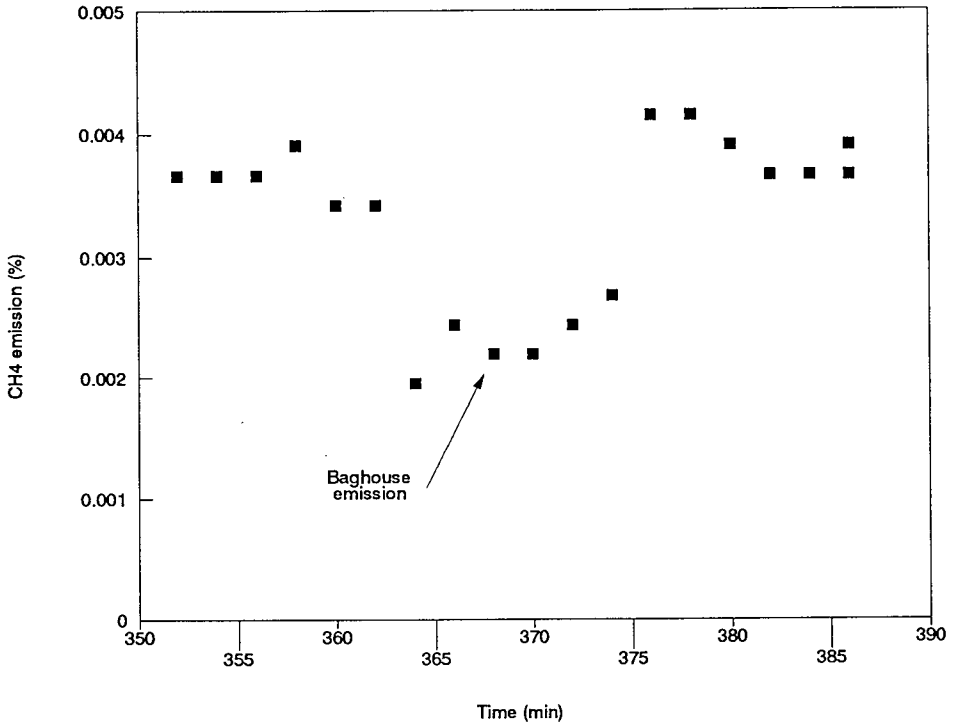

Figure E41 Flue Gas CH4 Emission for Pitch Cones : Steady State 6

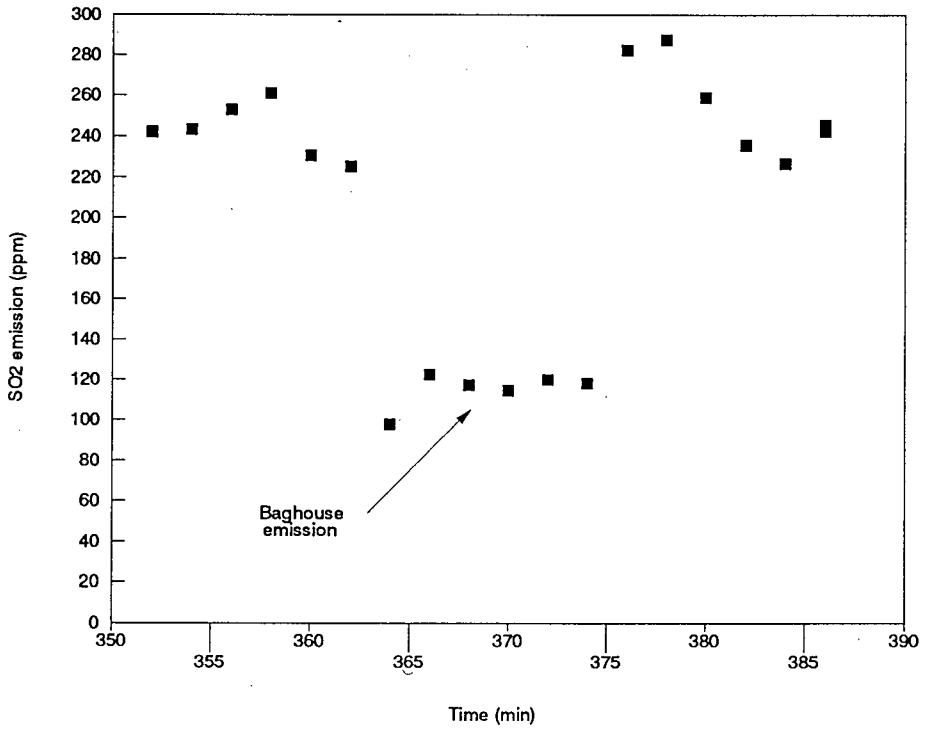

Figure E42 Flue Gas SO2 Emission for Pitch Cones : Steady State 6

Emission Plots for Pitch Cones: Steady State 7

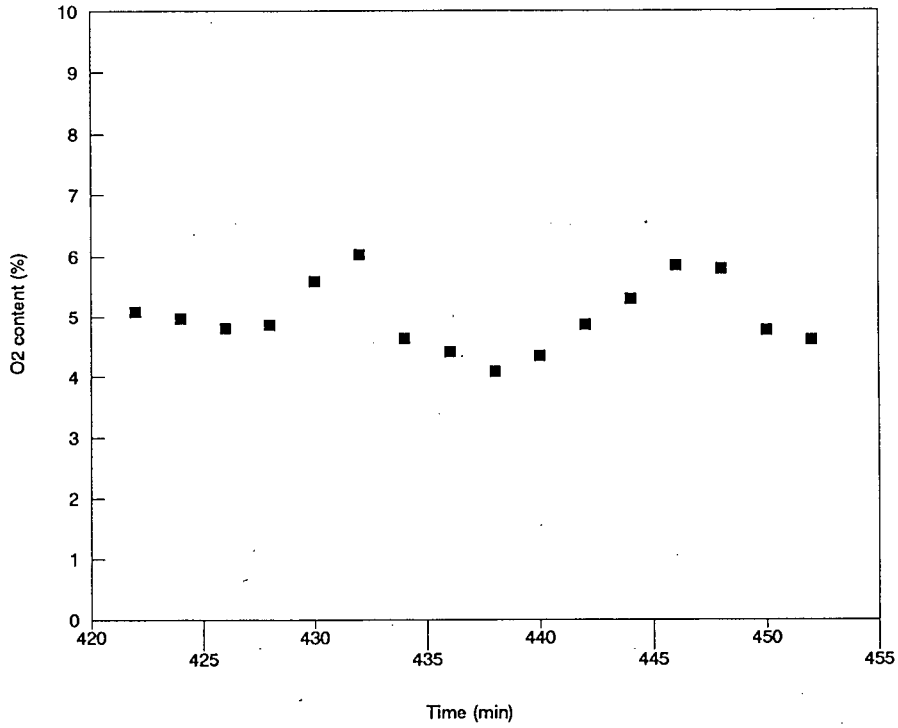

Figure E43 Flue Gas O2 Content for Pitch Cones : Steady State 7

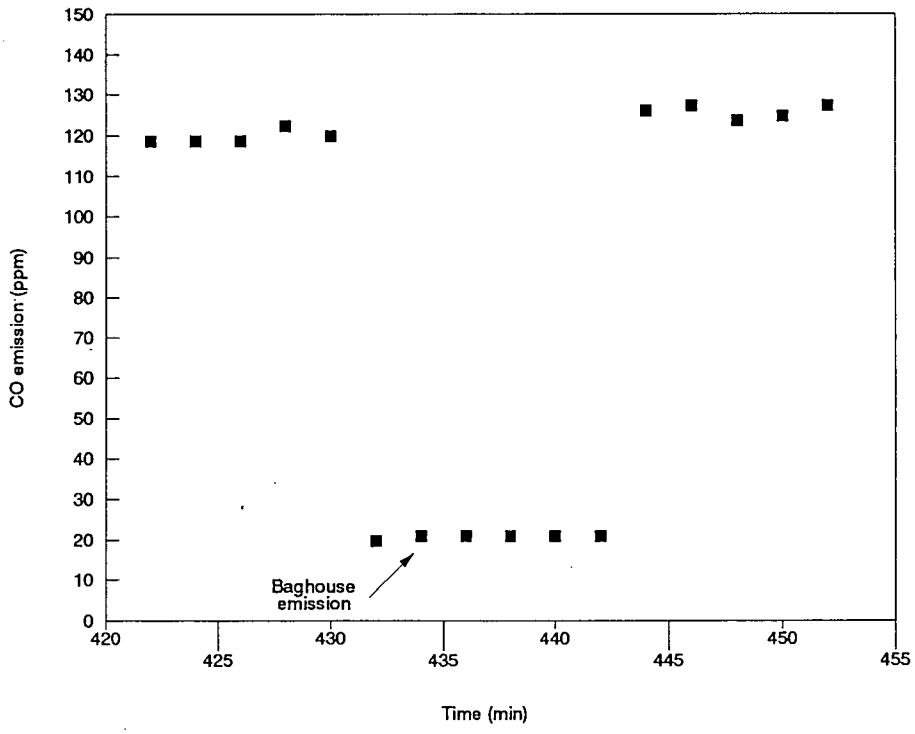

Figure E44 Flue Gas CO Emission for Pitch Cones : Steady State 7

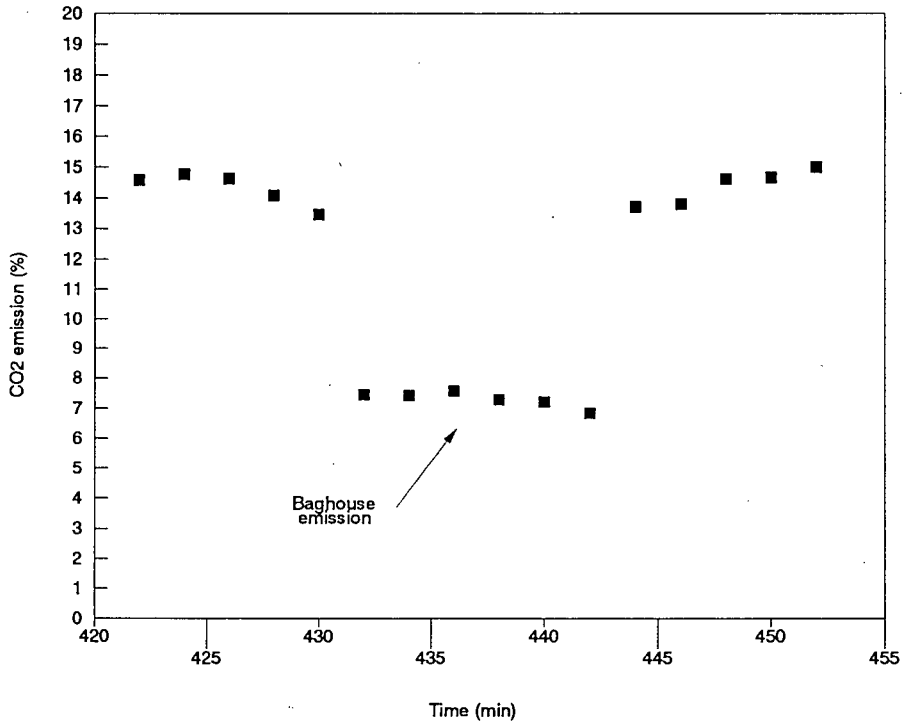

Figure E45 Flue Gas CO2 Emission for Pitch Cones : Steady State 7

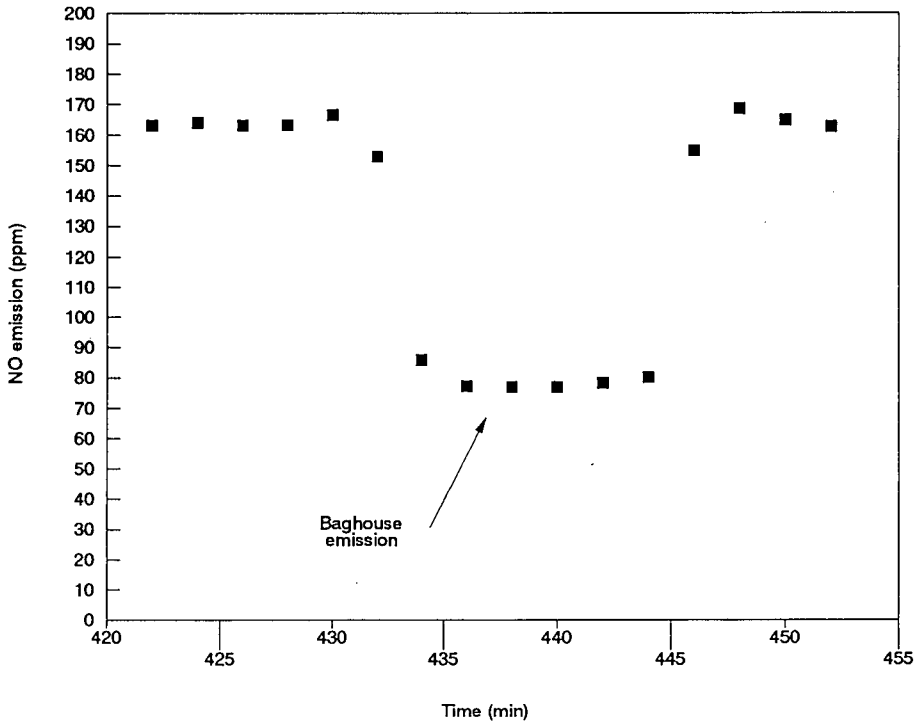

Figure E46 Flue Gas NO Emission for Pitch Cones : Steady State 7

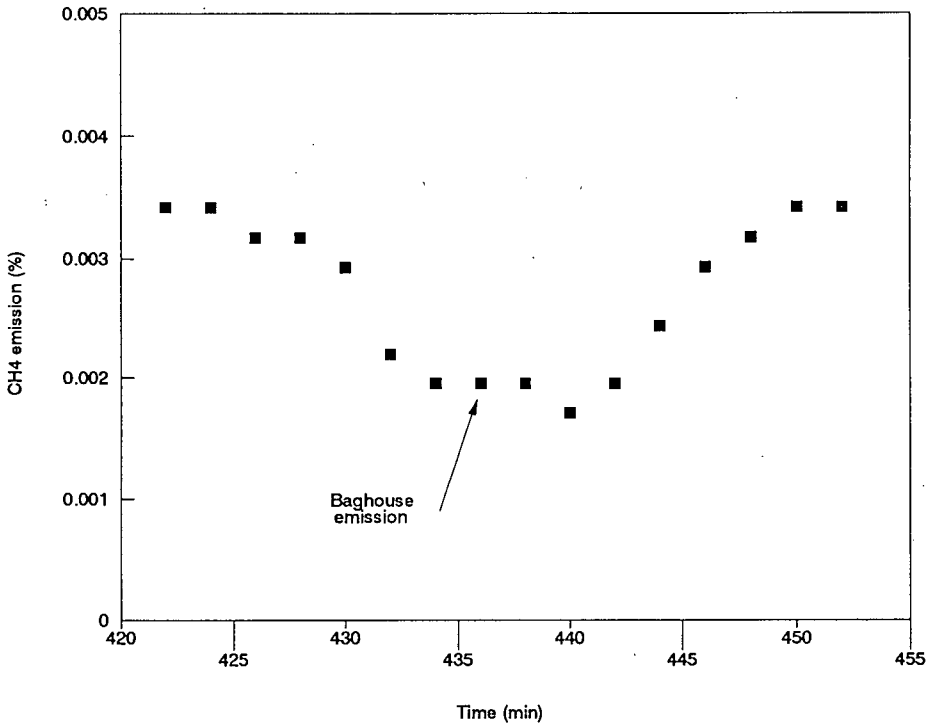

Figure E47 Flue Gas CH4 Emission for Pitch Cones : Steady State 7

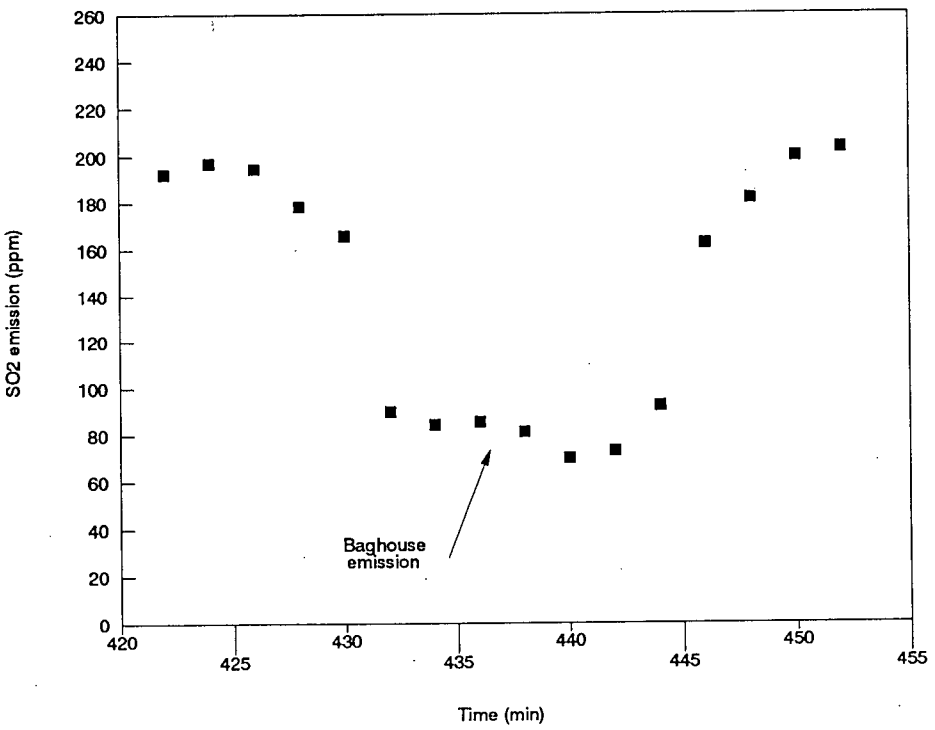

Figure E48 Flue Gas SO2 Emission for Pitch Cones : Steady State 7

Emission Plots for Misc. Paste Waste: Steady State 1

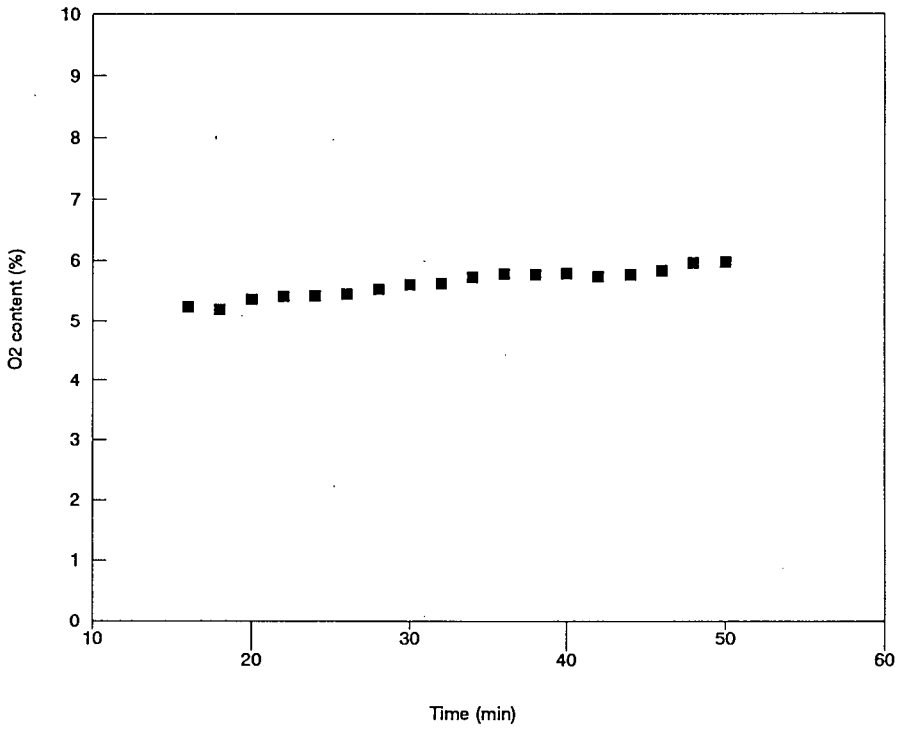

Figure E49 Flue Gas O2 Content for Misc. Paste Waste : Steady State 1

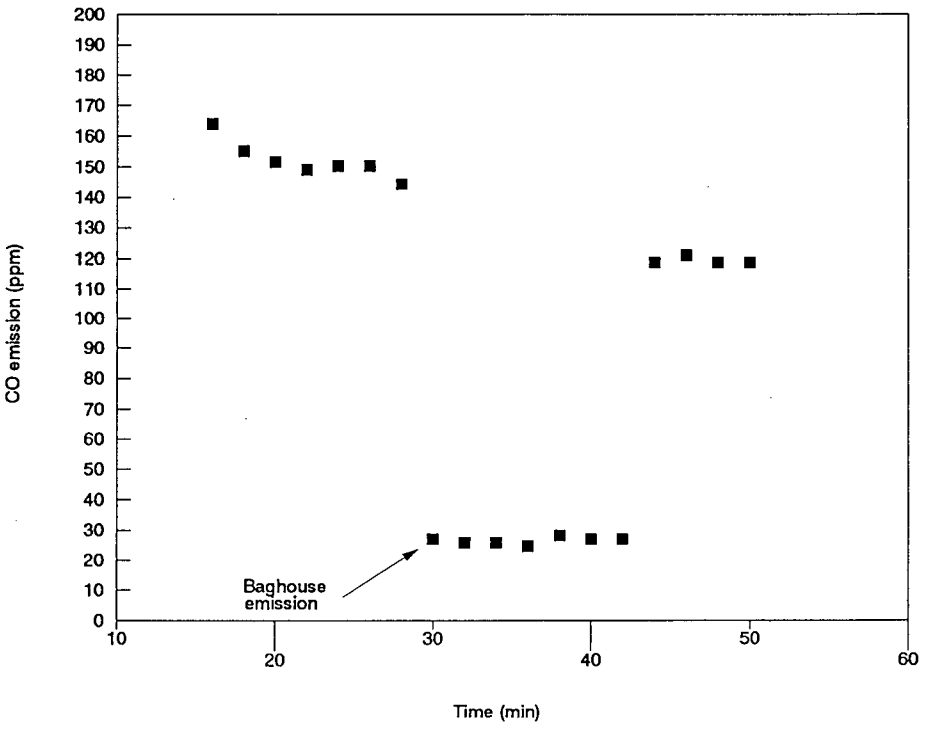

Figure E50 Flue Gas CO Emission for Misc. Paste Waste : Steady State 1

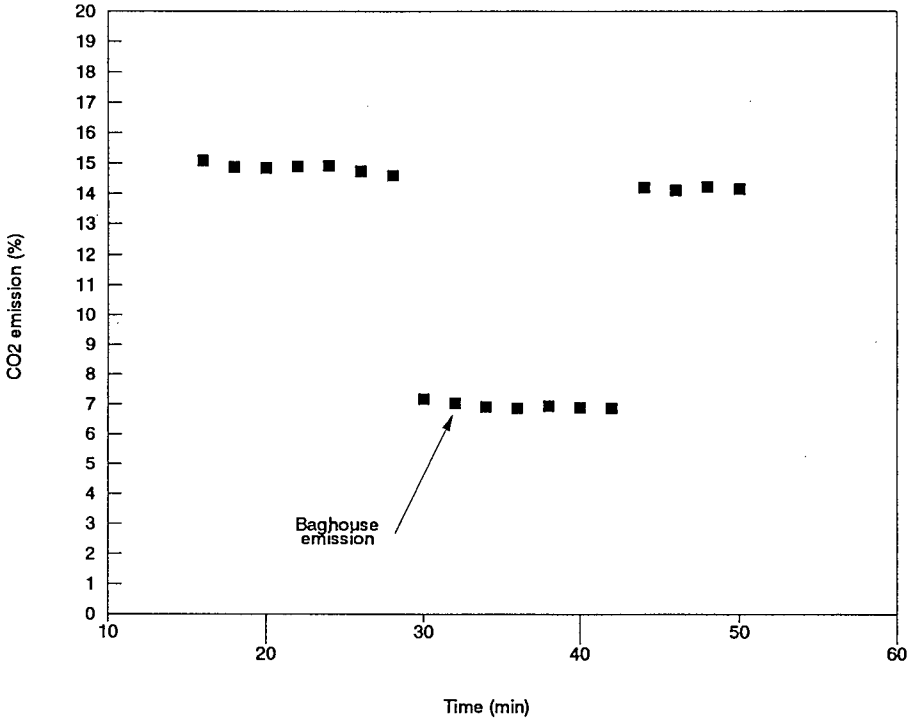

Figure E51 Flue Gas CO2 Emission for Misc. Paste Waste : Steady State 1

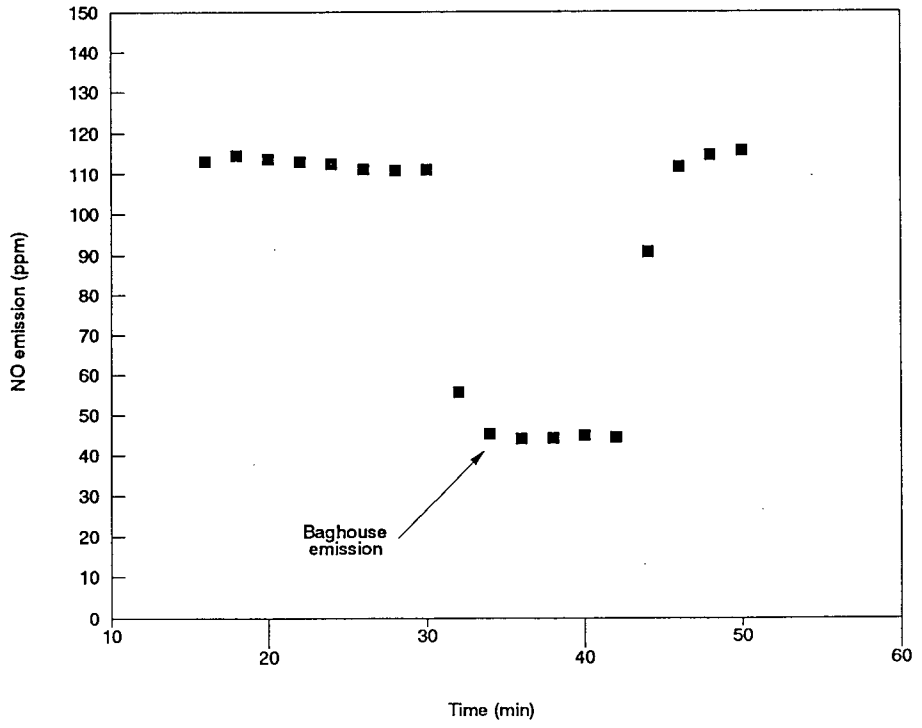

Figure E52 Flue Gas NO Emission for Misc. Paste Waste : Steady State 1

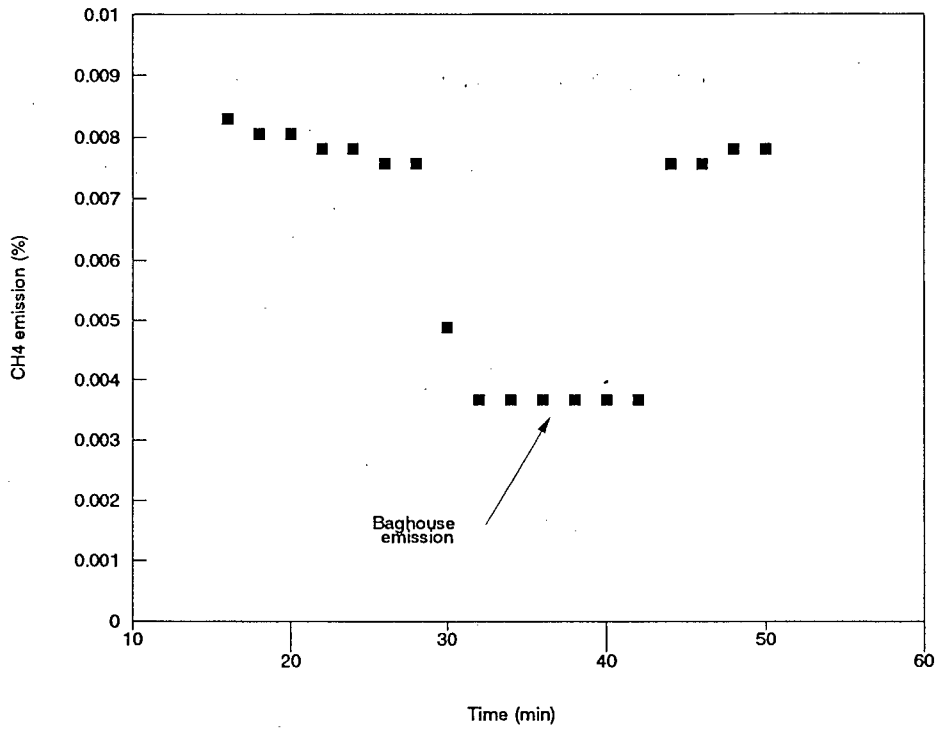

Figure E53 Flue Gas CH4 Emission for Misc. Paste Waste : Steady State 1

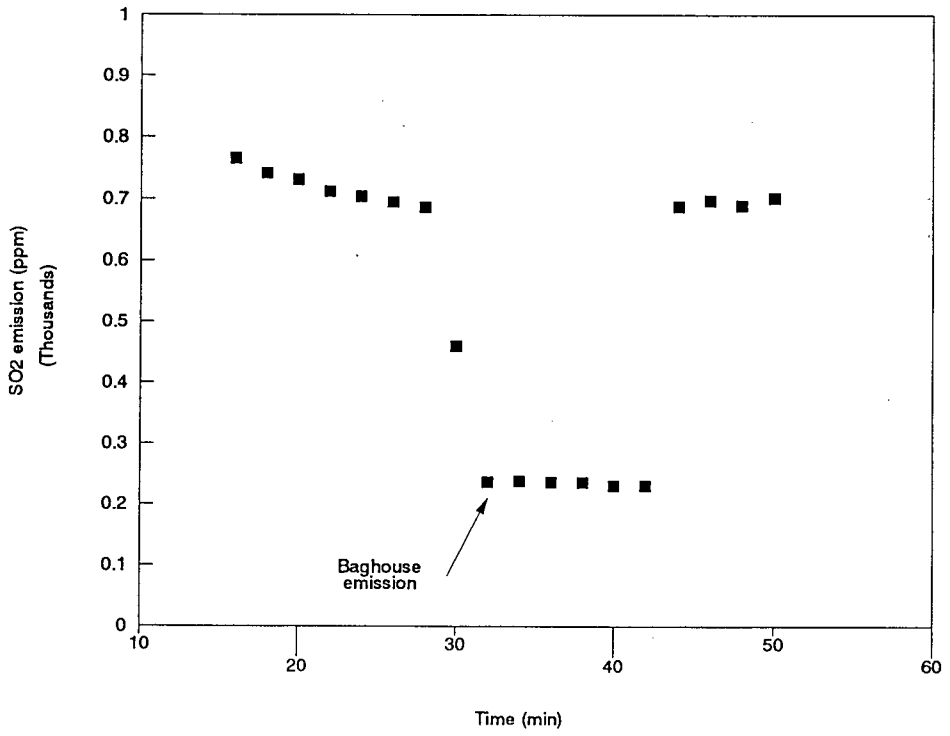

Figure E54 Flue Gas SO2 Emission for Misc. Paste Waste : Steady State 1

Emission Plots for Misc. Paste Waste: Steady State 2

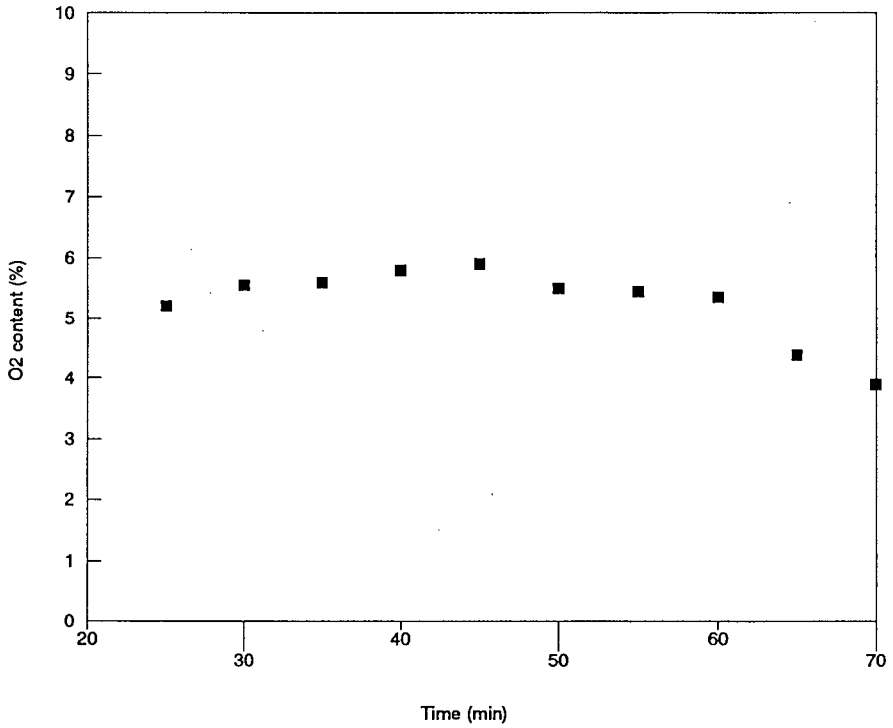

Figure E55 Flue Gas O2 Content for Misc. Paste Waste : Steady State 2

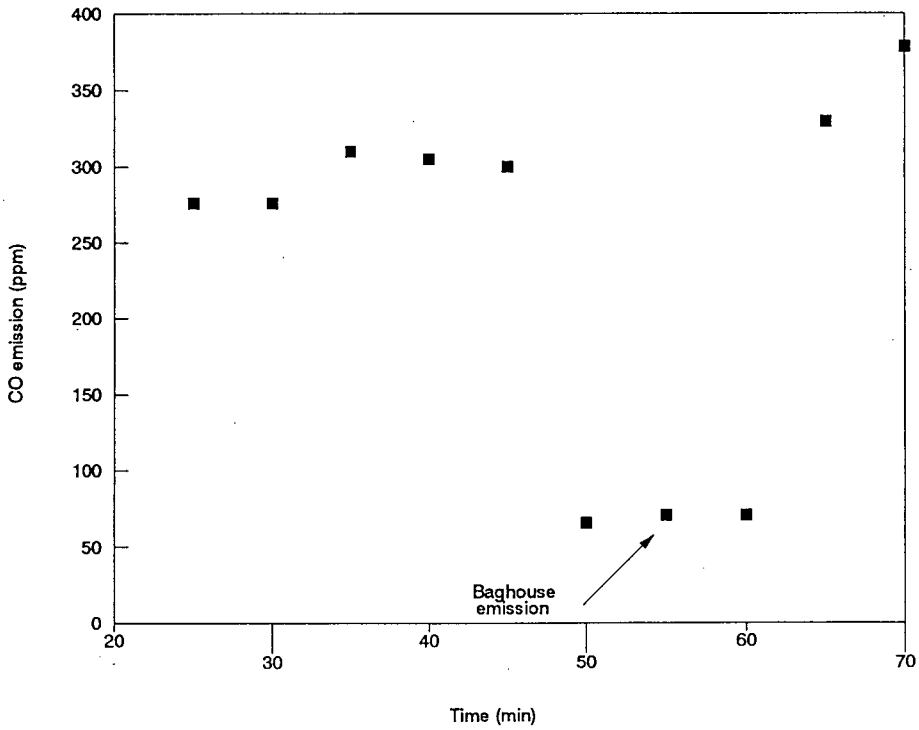

Figure E56 Flue Gas CO Emission for Misc. Paste Waste : Steady State 2

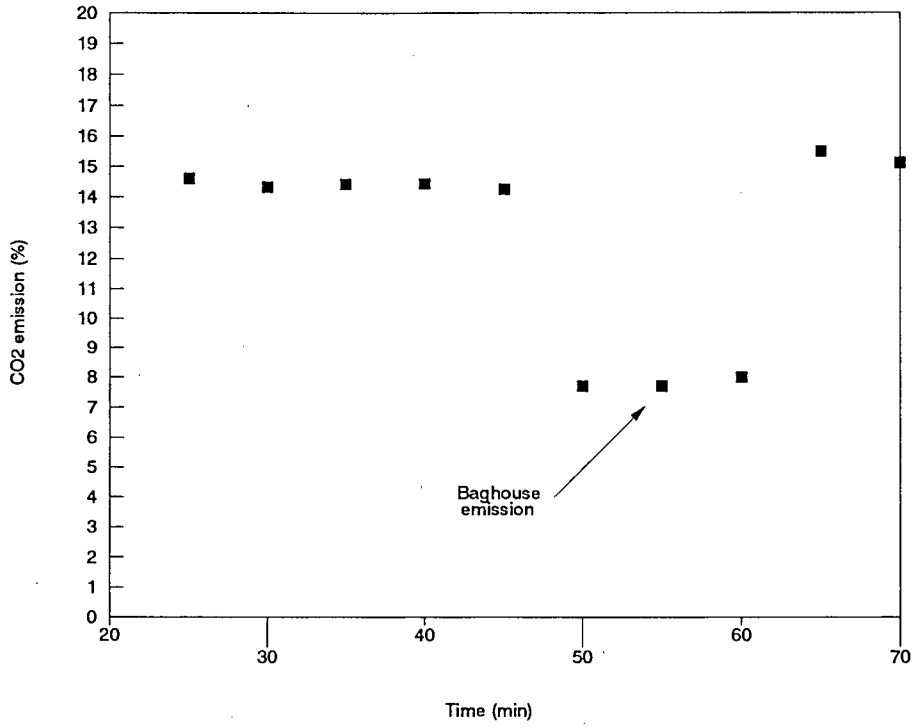

Figure E57 Flue Gas CO2 Emission for Misc. Paste Waste : Steady State 2

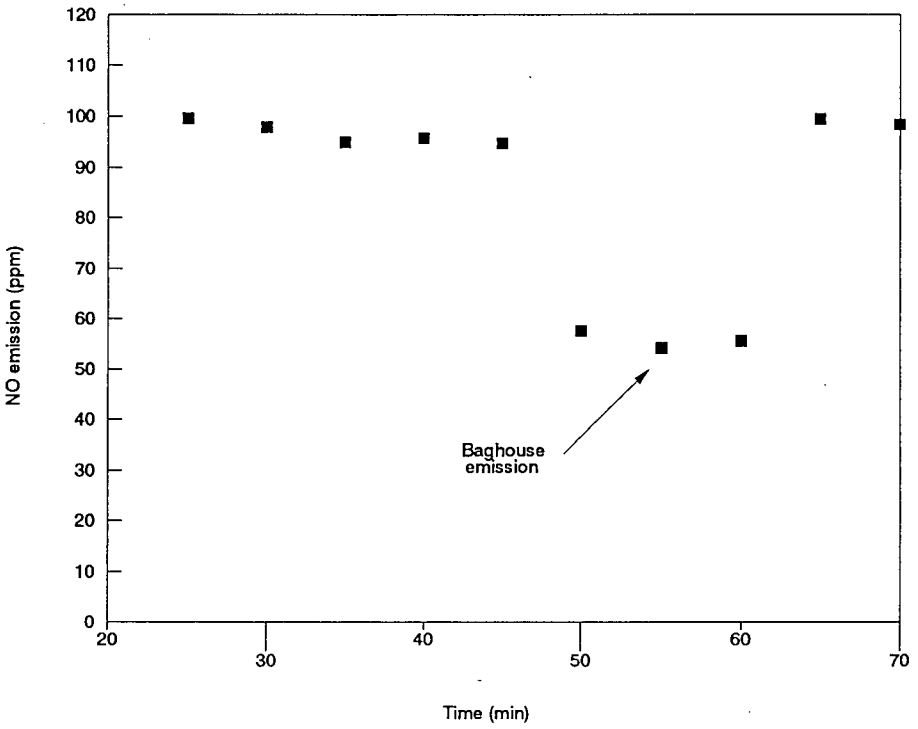

Figure E58 Flue Gas NO Emission for Misc. Paste Waste : Steady State 2

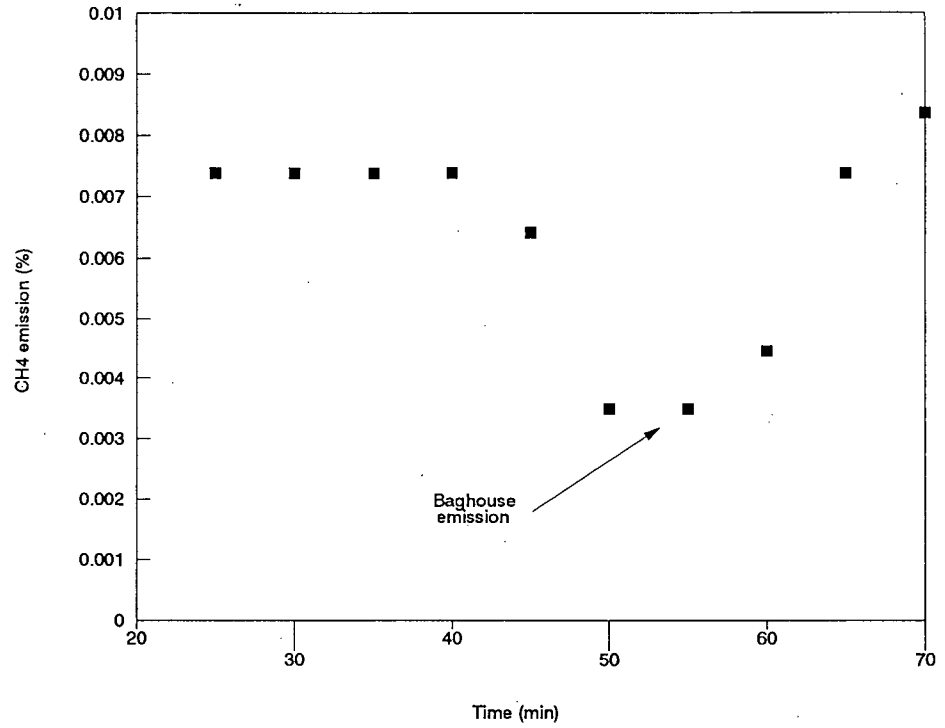

Figure E59 Flue Gas CH4 Emission for Misc. Paste Waste : Steady State 2

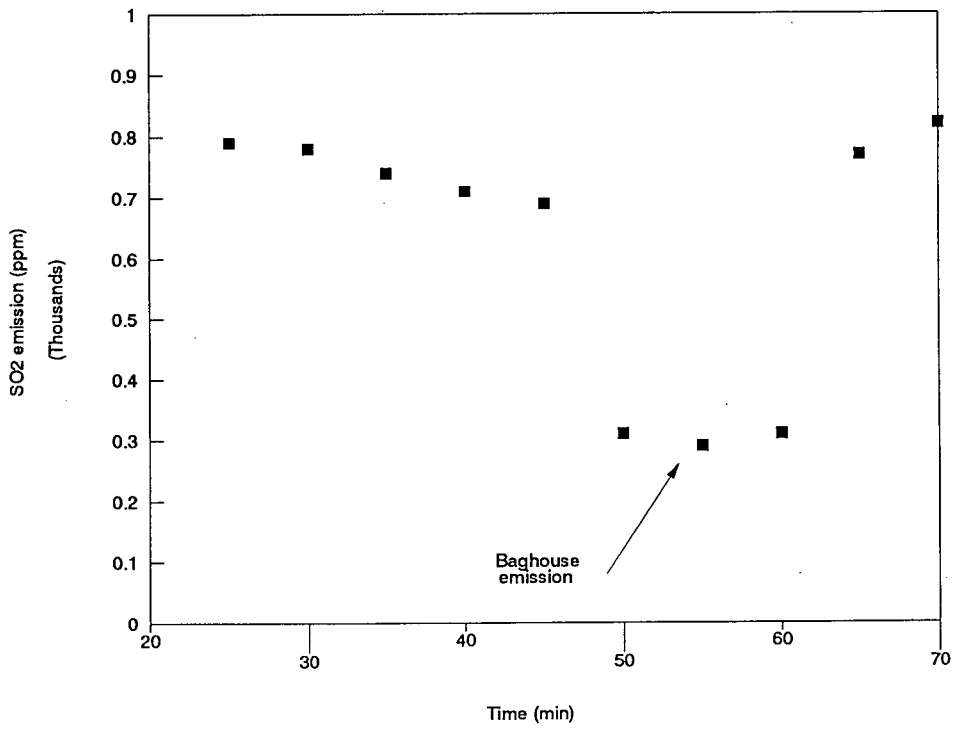

Figure E60 Flue Gas SO2 Emission for Misc. Paste Waste : Steady State 2

Appendix F Temperature Profiles for the Incineration of Stud Blast Fines, Pitch Cones and Miscellaneous Paste Wastes at Different Operating Conditions

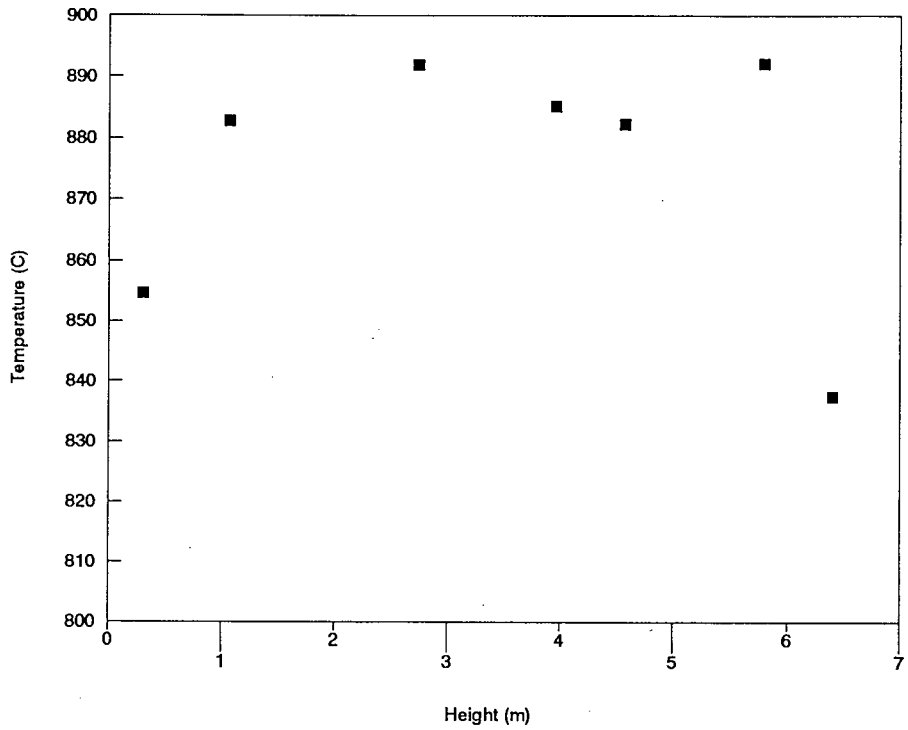

Figure F1 Axial Temperature Profile for Stud Blast Fines

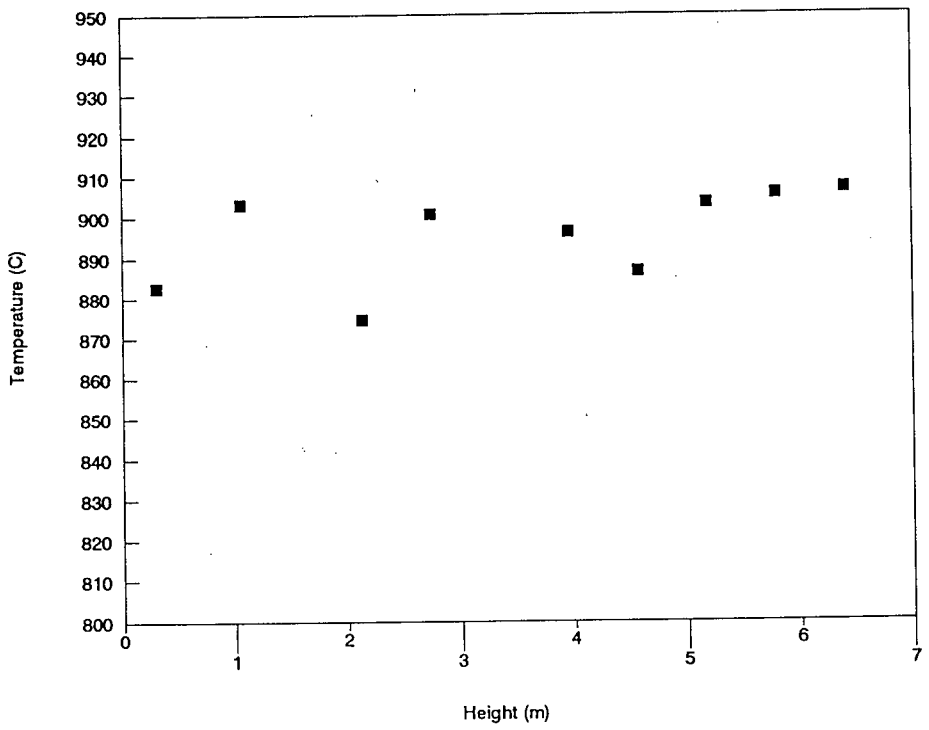

Figure F2 Axial Temperature Profile for Pitch Cones : Steady State 1

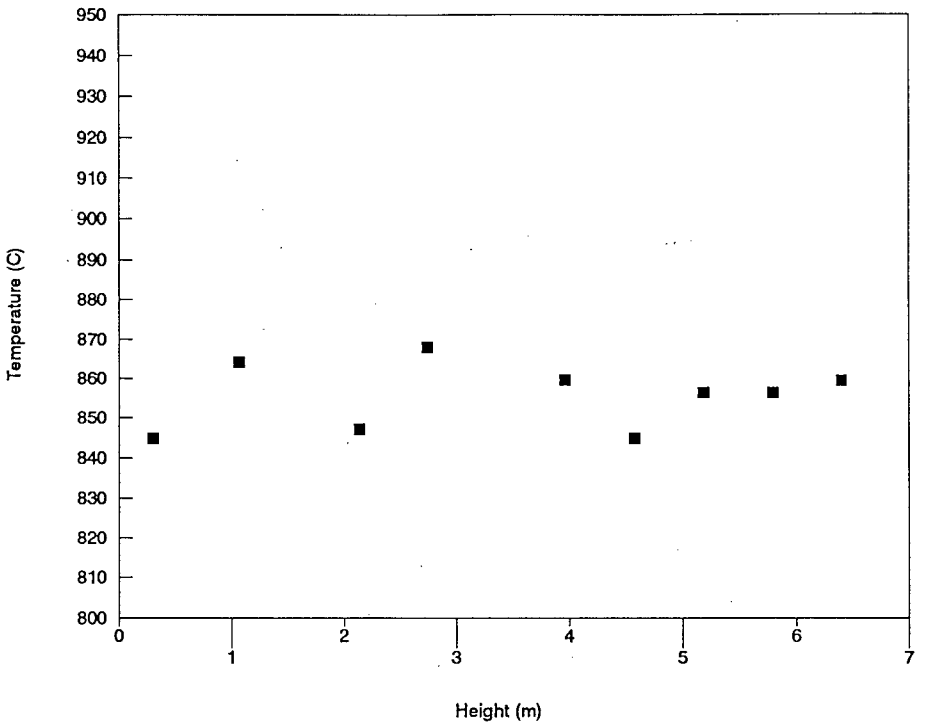

Figure F3 Axial Temperature Profile for Pitch Cones : Steady State 2

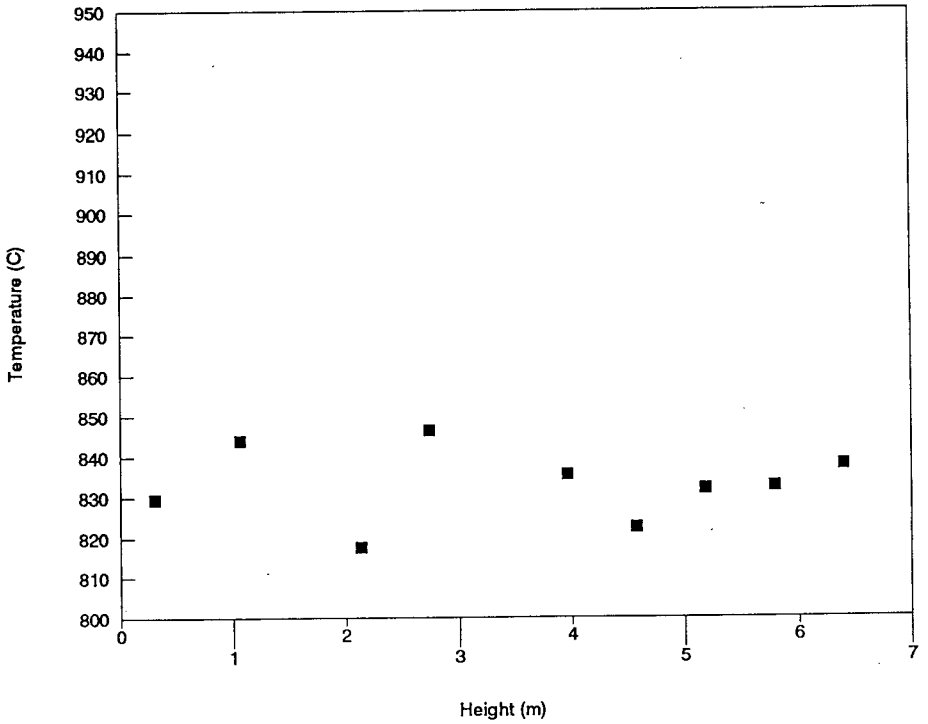

Figure F4 Axial Temperature Profile for Pitch Cones : Steady State 3

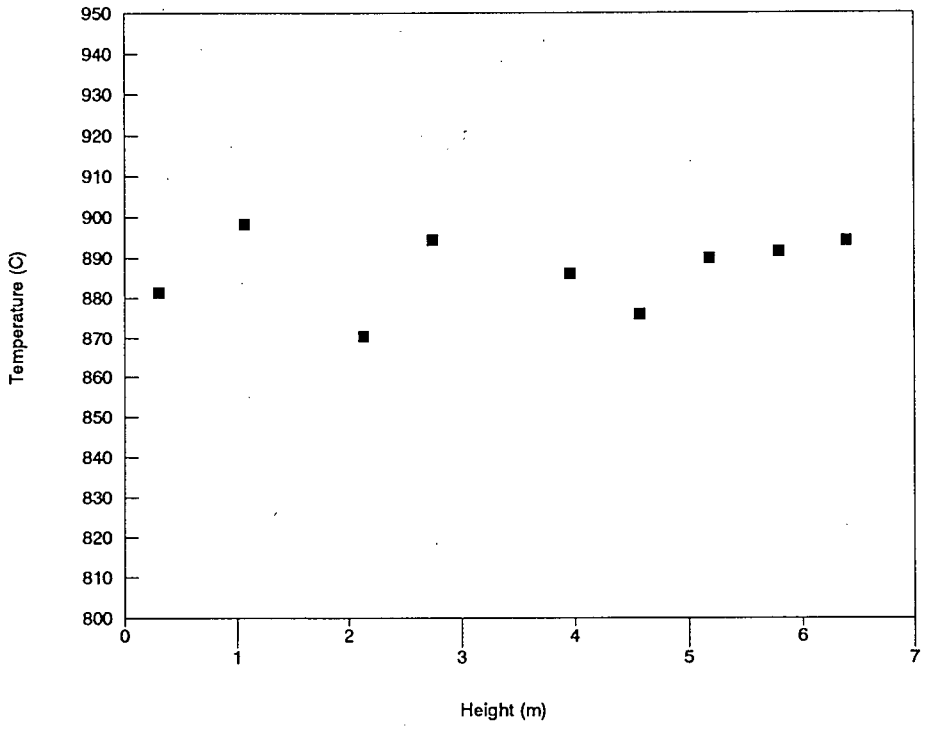

Figure F5 Axial Temperature Profile for Pitch Cones : Steady State 4

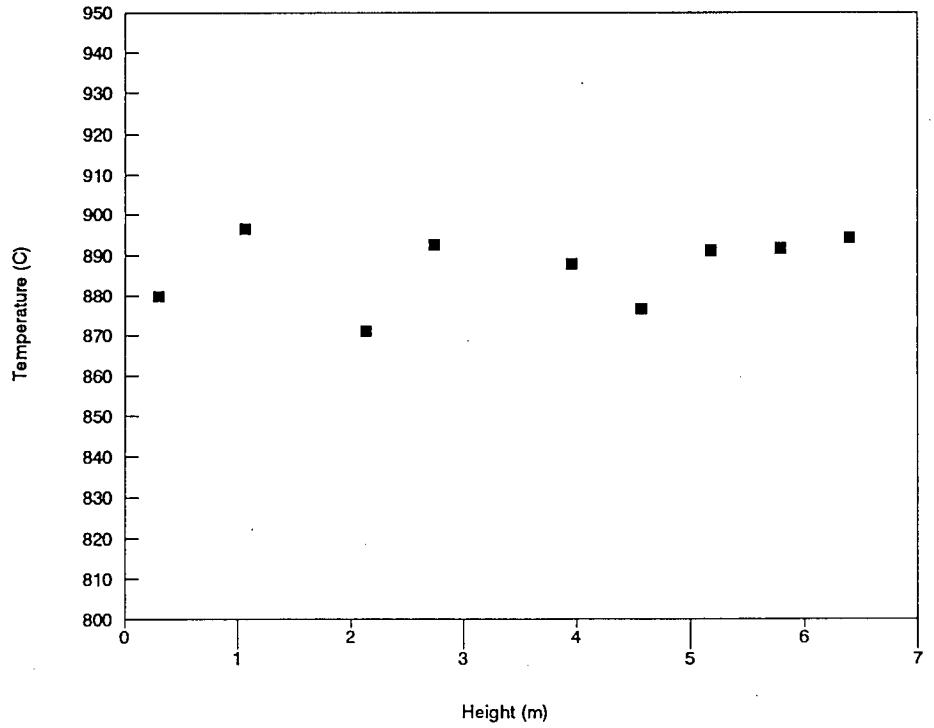

Figure F6 Axial Temperature Profile for Pitch Cones : Steady State 5

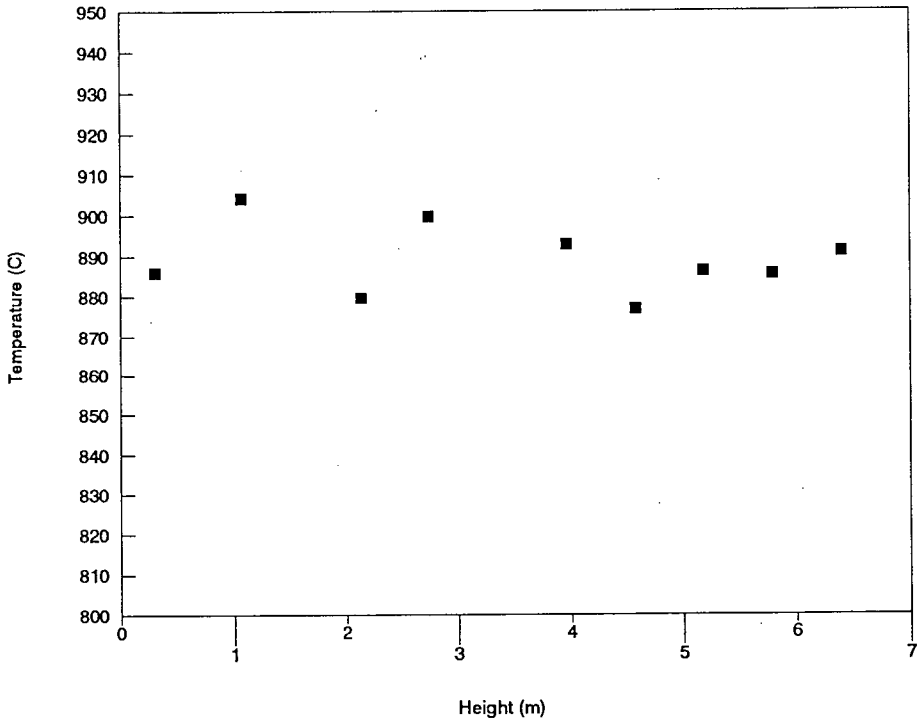

Figure F7 Axial Temperature Profile for Pitch Cones : Steady State 6

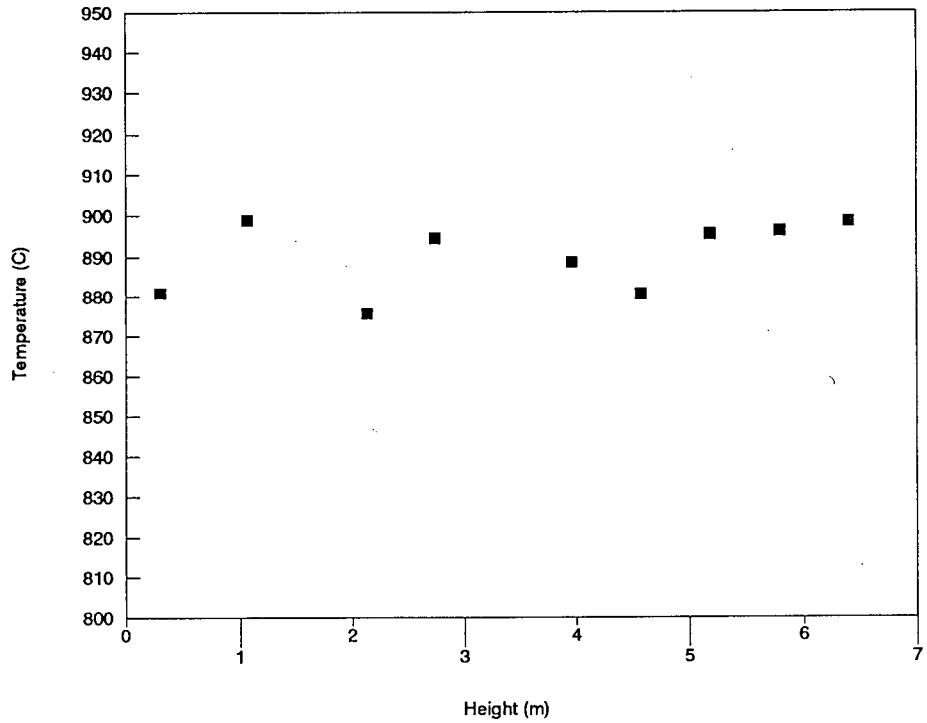

Figure F8 Axial Temperature Profile for Pitch Cones : Steady State 7

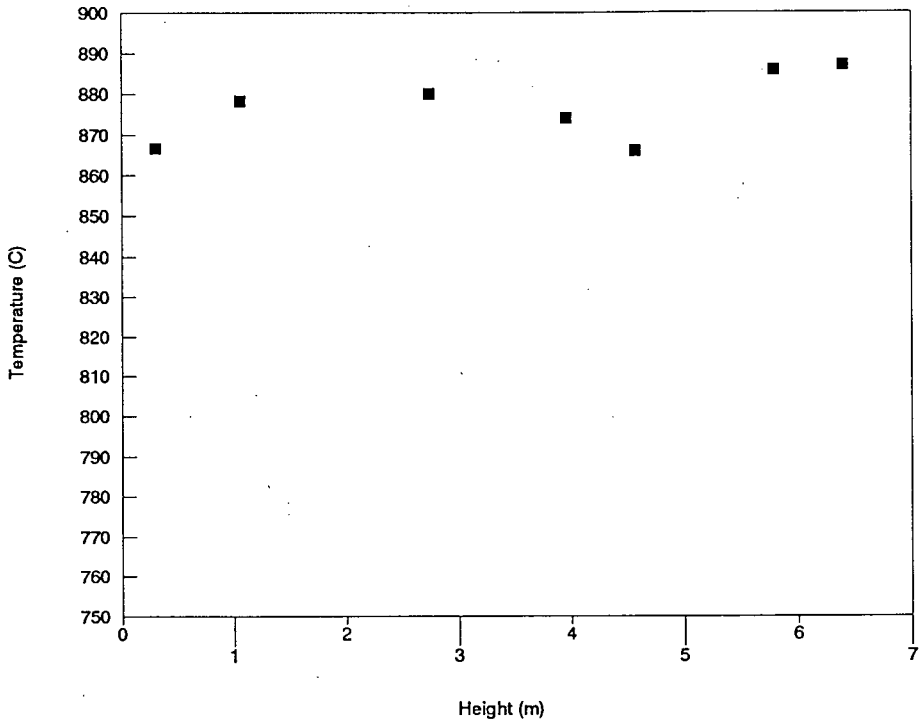

Figure F9 Axial Temperature Profile for Misc. Paste Waste : Steady State 1

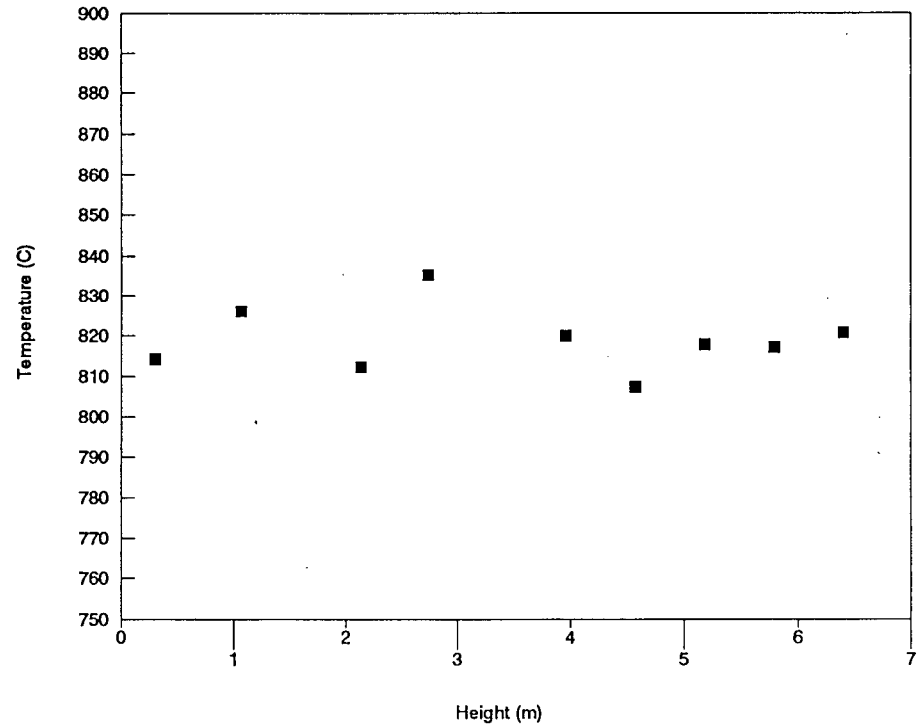

Figure F10 Axial Temperature Profile for Misc. Paste Waste : Steady State 2

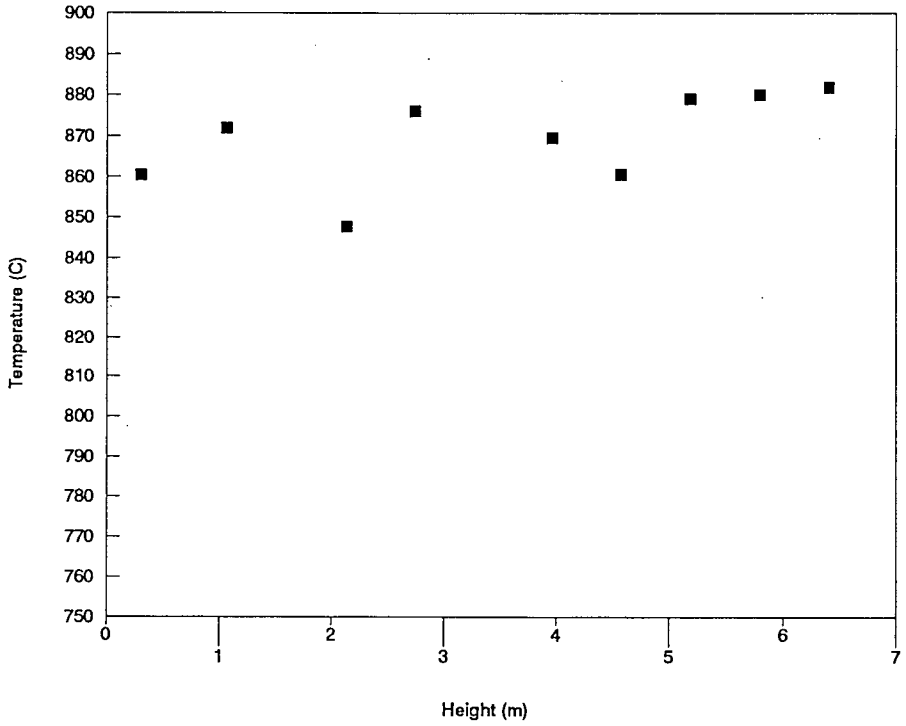

Figure F11 Axial Temperature Profile for Misc. Paste Waste : Steady State 3

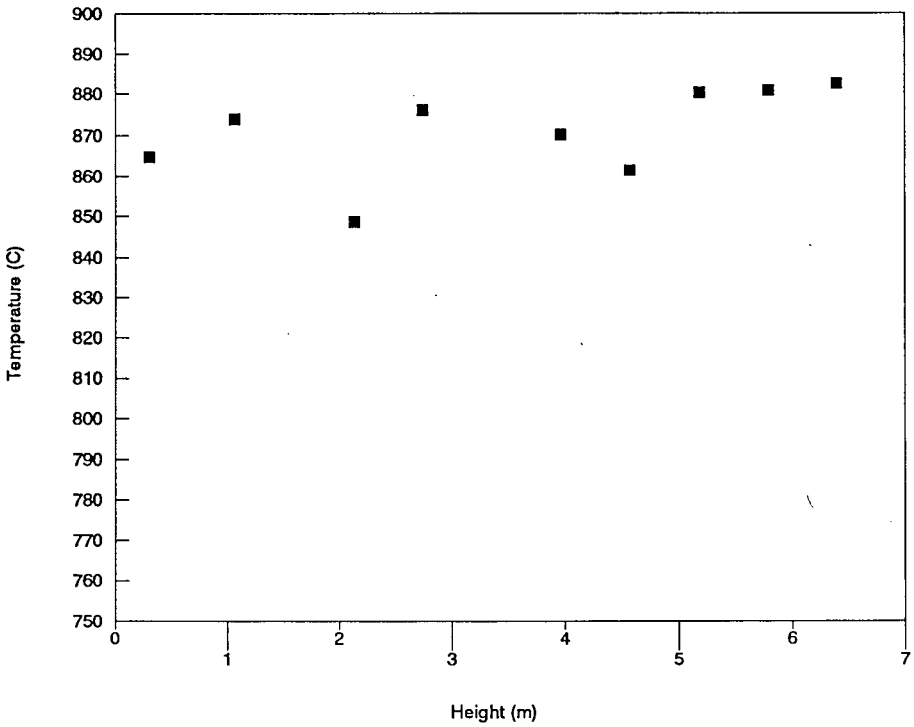

Figure F12 Axial Temperature Profile for Misc. Paste Waste : Steady State 4

Appendix G Momentum Calculations

Order of Magnitude Momentum Flux Calculations

Assumptions: 1) thickness of solids layer at the wall = A = 0.005 m

2) downwards velocity of solids layer = B = 1 m/s

3) density of solids layer = C = density of sand * voidage
= 2650 kg/m^3 * 0.4
= 1060 kg/m^3

4) temperature of secondary air stream = 200 ^oC = 473 K

Given: 1) width of air jet = D = 1.61 inch = 0.04 m

2) mass flow rate of secondary air = 61 kg/h = 0.0169 kg/s

3) cross-sectional area of tube = Area= [pi * $(0.04m)^2$]/4
= 0.00126 m^2

4) density of air at 298 K = 1.2 kg/m^3

Consider a time interval of 1 second

Solids mass flow rate = A* B * C * D
= 0.212 kg/s

Momentum flux of solids = solids mass flow rate * solids velocity
= 0.212 kg/s * 1 m/s
= **0.212 kg.m/s^2**

Air velocity = mass flow rate of secondary air / (Area * density of air * 298 K/473 K)
= 17.8 m/s

This air velocity is based on all the secondary air passing through a single port. Since there are two ports, the air velocity is halved to 8.9 m/s. Similarly, the mass flow rate of air at each port is 0.5 * 0.0169 kg/s = 0.00845 kg/s.

Momentum flux of air (at each port) = 0.00845 kg/s * 8.9 m/s
= **0.0752 kg.m/s^2**

The air stream momentum is clearly less than the downward flowing solids momentum. Therefore, penetration by the air stream will not be very high and the air will preferentially channel up the wall.

Appendix H Sulphide Determination

Sulphide Determination (adapted from de Iribarne et al., 1988)

Total sulphides were determined by treating the sample with HCl acid and absorbing the evolved H_2S in appropriate solutions for its volumetric determination by iodometry.

Indirect Iodometric Method:

A measured volume of standard iodine solution was used to absorb the hydrogen sulphide evolved from the sample by treatment with acid. The excess iodine was back titrated with standard sodium thiosulphate solution and starch as an indicator.

Reagents:

Hydrochloric acid:	6 N HCl
Iodine solution:	0.1 N I_2
Potassium iodine:	KI
Sodium thiosulphate:	0.1 N $Na_2S_2O_3$
Starch	

(Note: I_2 was first dissolved in concentrated KI and diluted to volume. The solution of I^{2+} KI was made acidic to prevent oxidation of S^{2-}, which may occur in alkaline solution).

Procedure:

The apparatus used is shown in Figure H.1. The reaction flask was previously dried and flushed with nitrogen. Approximately 0.25 gram of sample dried and weighed with analytical balance was placed into flask B which was connected to the two absorption impingers, each

containing 20 mL of acidified (with 1 mL of 1 M HCl) iodine and 40 mL of distilled water. 50 mL of HCl solution placed in container A was slowly introduced to the flask B. When the addition was almost completed, the stopcock was closed and the flask was heated with occasional stirring until gentle boiling. The solution was then cooled for 15 minutes while nitrogen was introduced through the 3-way stopcock to sweep out the residual hydrogen sulphide in the flask. Care was taken such that the N_2 was introduced as soon as the heating was stopped; otherwise, the solution in the impingers may be sucked by the pressure reduction accompanying the cooling of the gas and vapour contained in flask B.

The gas coming out of the reaction flask B through the vapour condenser, bubbled through the two impingers in series. The H_2S reacts with I_2 according to:

$$H_2S + I_2 = S^o + 2\,I^- + 2\,H^+ \qquad (1)$$

The I_2 solution from the two impingers was then back titrated with $Na_2S_2O_3$ using starch as indicator. The wt. % of S^{2-} is calculated as follows:

$$C_{IR} = C_{IO} - C_I \qquad (2)$$

where

C_{IR} = concentration of I_2 reacted (N)

C_{IO} = initial concentration of I_2 in the impingers (N)

C_I = concentration of I_2 solution after reaction (N)

$$I_2 + 2\,e^- \rightarrow 2\,I^- \quad \text{(reduction)} \qquad (3)$$

$$S^{2-} \rightarrow S^o + 2\,e^- \quad \text{(oxidation)} \qquad (4)$$

From reaction (3), 1 mole of I_2 consumes 2 moles of e^-.

1 mole of I_2	=	2 eq. I_2
1 mole/L I_2	=	2 eq/L I_2
1 M I_2	=	2 N I_2
1 N I_2	=	0.5 M I_2

From reaction (1), 1 mole of S produces 1 mole of H_2S which reacts with 1 mole of I_2.

$$wt.\%S = \left(\frac{C_{IR} * 0.5 * MWs}{m}\right) * 100\%$$

where

MWs	=	molecular weight of sulphur (32.06g/mole)
m	=	mass of sample used (g)

Ferrous Sulphide Determination

There is approximately 68. wt % Fe in the ash analysis of the stud blast fines, sbf. It is believed that the sulphide is present in a form of iron sulphide. In order to determine the form of iron sulphide, ferrous sulphide or ferric sulphide, 6 N HCl was added to the stud blast fines sample and a green solution resulted. According to Pauling (1958), the form of iron, ferrous or ferric can be identified by the following reactions:

sbf	+	HCl	→	$FeCl_2$ (green soln.)	+	H_2S	(5)
sbf	+	HCl	→	$FeCl_3$ (reddish brown soln.)	+	H_2S	(6)

Consequently, the iron sulphide present in the stud blast fines is in the form of ferrous sulphide.

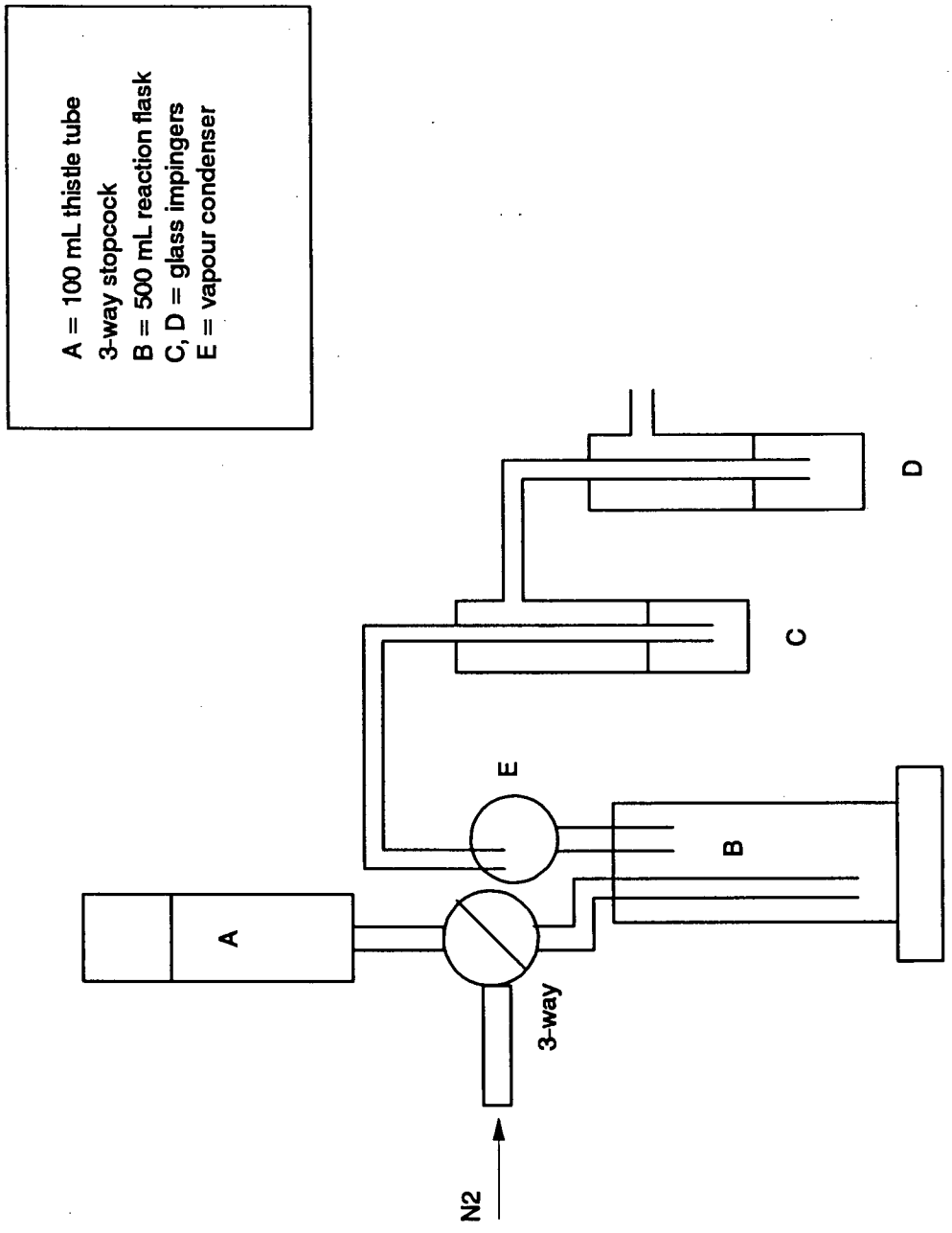

Figure H.1 Apparatus for Sulphide Determination